OCS Study
BOEM 2024-075

Scenarios for Replacing Conventional Energy With Offshore Renewable Energy Along the Central California Coast

U.S. Department of the Interior
Bureau of Ocean Energy Management
Pacific OCS Region, Camarillo, CA

BOEM
BUREAU OF OCEAN ENERGY MANAGEMENT

OCS Study
BOEM 2024-075

Scenarios for Replacing Conventional Energy With Offshore Renewable Energy Along the Central California Coast

December 2024

Authors:
Benjamin Ruttenberg
Yi-Hui Wang
Ryan Walter
Crow White

Prepared under M16AC00023
By
Cal Poly State University, San Luis Obispo
1 Grand Ave, San Luis Obispo, CA 93407

U.S. Department of the Interior
Bureau of Ocean Energy Management
Pacific OCS Region, Camarillo, CA

BOEM
BUREAU OF OCEAN ENERGY MANAGEMENT

DISCLAIMER

Study collaboration and funding were provided by the U.S. Department of the Interior, Bureau of Ocean Energy Management (BOEM), Environmental Studies Program, Washington, DC, under Agreement Number M16AC00023. This report has been technically reviewed by BOEM, and it has been approved for publication. The views and conclusions contained in this document are those of the authors and should not be interpreted as representing the opinions or policies of BOEM, nor does mention of trade names or commercial products constitute endorsement or recommendation for use.

REPORT AVAILABILITY

To download a PDF file of this report, go to the U.S. Department of the Interior, Bureau of Ocean Energy Management Data and Information Systems webpage (http://www.boem.gov/Environmental-Studies-EnvData/), click on the link for the Environmental Studies Program Information System (ESPIS), and search on 2024-075. The report is also available at the National Technical Reports Library at https://ntrl.ntis.gov/NTRL/.

CITATION

Ruttenberg BI, Wang, YH, Walter RK, White C. (California Polytechnic State University, San Luis Obispo, CA). 2024. Scenarios for replacing conventional energy with offshore renewable energy along the Central California Coast. Camarillo, CA: U.S. Department of the Interior, Bureau of Ocean Energy Management. 181 p. Report No.: OCS Study BOEM 2024-075. Contract No.: M16AC00023.

ABOUT THE COVER

Photo of a floating offshore wind turbine, Hywind Scotland. Photo Credit: Ben Ruttenberg

ACKNOWLEDGMENTS

Chapter 2: Data used in this chapter are publicly available at the respective links in the manuscript. The WRF regional model data were obtained from Dong et al. 2017. This chapter was originally published as:

Wang Y-H, Walter Ryan K., White C, Farr H, Ruttenberg BI. 2019. Assessment of surface wind datasets for estimating offshore wind energy along the Central California Coast. Renewable Energy. 133:343–353. doi:10.1016/j.renene.2018.10.008.

Chapter 3: Data used in this study are publicly available at the respective links in the manuscript. This chapter was originally published as:

Wang Y-H, Walter Ryan K, White C, Kehrli MD, Hamilton SF, Soper PH, Ruttenberg BI. 2019. Spatial and temporal variation of offshore wind power and its value along the Central California Coast. Environ Res Commun. 1(12):121001. doi:10.1088/2515-7620/ab4ee1.

Chapter 4: We acknowledge support from The William and Linda Frost Fund. We thank two anonymous reviewers for their comments that improved the manuscript. The WIND Toolkit data used in this study are publicly available at https://www.nrel.gov/grid/wind-toolkit.html. This chapter was originally published as:

Wang YH, Walter RK, White C, Kehrli MD, Ruttenberg B. 2022. Scenarios for offshore wind power production for Central California Call Areas. Wind Energy. 25(1):23-33.

Chapter 5: We acknowledge support from The William and Linda Frost Fund for the data synthesis phase of this work. This chapter was originally published as:

Farr H, Ruttenberg B, Walter RK, Wang YH, White C. 2021. Potential environmental effects of deepwater floating offshore wind energy facilities. Ocean & Coastal Management. 207:105611.

Chapter 6: We thank the California Department of Fish and Wildlife (CDFW) for providing landings data. CDFW acquires data from its own fisheries management activities and from mandatory reporting requirements on the commercial and recreational fishery pursuant to the Fish and Game Code and the California Code of Regulations. These data are constantly being updated, and datasets are constantly modified. CDFW may provide data upon request, but, unless otherwise stated, does not endorse any particular analytical methods, interpretations, or conclusions based upon the data it provides. This chapter was originally published as:

Wang Y, Walter RK, White C, Ruttenberg BI. 2022. Spatial and Temporal Characteristics of California Commercial Fisheries from 2005 to 2019 and Potential Overlap with Offshore Wind Energy Development. Mar Coast Fish. 14(4):e10215. doi:10.1002/mcf2.10215.

Chapter 7: Additional funding was provided the California Ocean Protection Council (OPC). We are indebted to Brian Owens, Todd Neahr, and Paulo Serpa at the California Department of Fish and Wildlife (CDFW) for providing access to and sharing insights about CDFW landings data. CDFW acquires data from its own fisheries management activities and from mandatory reporting requirements on the commercial and recreational fishery pursuant to the Fish and Game Code and the California Code of Regulations. These data are constantly being updated, and datasets are constantly modified. CDFW may provide data upon request, but, unless otherwise stated, does not endorse any particular analytical methods, interpretations, or conclusions based upon the data it provides. We also thank Kelly Spaulding in the National Marine Fisheries Service Office of Law Enforcement for providing access to Vessel Monitoring System Data.

This chapter was originally published as:

Wang YH, Ruttenberg BI, Walter RK, Pendleton F, Samhouri J, Liu O, White C. 2024. High resolution assessment of commercial fisheries activity along the US West Coast using Vessel Monitoring System data with a case study using California groundfish fisheries. PLoS ONE 19(6): e0298868. https://doi.org/10.1371/journal.pone.0298868

Contents

List of Figures

List of Tables

List of Abbreviations and Acronyms

AC	Alternating current
ASCAT	Advanced SCATterometer
BOEM	Bureau of Ocean Energy Management
CAISO	California Independent System Operator
CCLME	California Current Large Marine Ecosystem
CCMP	Cross Calibrated Multi-Platform
CDFW	California Department of Fish and Wildlife
CEC	California Energy Commission
CPS	Coastal Pelagic Species
DCNPP	Diablo Canyon Nuclear Power Plant
DOI	Department of the Interior
EEZ	Exclusive Economic Zone
EIA	Energy Information Administration
EMF	Electromagnetic Field
ENSO	El Niño Southern Oscillation
HVDC	High voltage direct current
IFQ	Individual Fishing Quota
LE	Limited Entry
MERRA	Modern Era Retrospective Analysis
MHW	Marine heatwaves
MMS	Meteorological Measurement System
MRE	Marine Renewable Energy
NARR	North American Regional Reanalysis
NDBC	National Data Buoy Center
NDL	No depth limit
NERL	National Renewable Energy Laboratory
NMFS	National Marine Fisheries Service
NOAA	National Oceanic and Atmospheric Administration
OA	Open Access
ODFW	Oregon Department of Fish and Wildlife
OLE	Office of Law Enforcement
OWF	Offshore Wind Farm
PacFIN	Pacific Fisheries Information Network
PV	Photovoltaic
RMSE	Root Mean Square Error
RSA	Rockfish Conservation Area
SAR	Satellite synthetic aperture radar
VMS	Vessel Monitoring System
WEA	Wind Energy Area
WRF	Weather Research and Forecast

1 Executive Summary

Over the last few decades, renewable energy sources have become increasingly important components of broader energy portfolios and renewable energy targets globally. In the United States (U.S.), California has set aggressive goals to reduce greenhouse gas emissions, seeking to generate 100% of the state's electricity from renewables by 2045. To achieve this ambitious goal, California will need to develop and expand a range of renewable energy sources.

Deployment of renewable energy projects in California has expanded over the last decade, from generating just over 20% of the state's power production in 2013 to nearly 38% in 2021, with the energy coming mainly from land-based wind turbines and photovoltaics (i.e., solar). While these sources will continue to grow, demand for electricity continues to rise, and California will need to both expand and diversify its renewable energy portfolio. Arrays of offshore wind turbines (i.e., wind farms) have the potential to generate large amounts of renewable energy, while also addressing the some of the challenges of intermittency and base-load associated with other renewables such as solar and land-based wind power. Recognizing the potential importance of offshore wind power in the mix of renewables, California has set offshore wind energy production goals of 5 GW by 2030 and 25 GW by 2050. This report explores comprehensive scenarios for offshore wind energy on the Central California Coast, emphasizing the critical need for science to guide the evaluation processes.

Developing offshore wind energy farms in the marine environment at a commercial scale can be challenging, and even more so in areas where wind power will likely be developed. In Europe and along the U.S. East Coast, most of the offshore wind industry is or will be developed as turbines mounted on pylons affixed to the seafloor in relatively shallow waters, given the water depths and wind resources available in those shallow waters. However, along the U.S. West Coast, given the deeper bathymetry and available wind resources, areas that are going to be prioritized for offshore wind development will be in water depths of 1000 m or more that require floating turbines that are moored to the seafloor. Understanding the potential renewable energy benefits and the environmental and socioeconomic impacts of offshore wind energy development in these deeper waters is critical to planning optimal locations to maximize power production while minimizing environmental impacts.

The Central California Coast presents a wealth of opportunities for offshore wind energy development, as well as some challenges. There are two potential grid connections in the area, the now-closed Dynegy Power Plant in Morro Bay, and the still-operating Diablo Canyon Nuclear Power Plant at Point Buchon. These existing facilities provide critical infrastructure not available in many other locations, making the Central Coast region attractive for offshore wind energy development. At the same time, the region is largely rural, with little industrial base and no major ports, such that other infrastructure and the workforce for supporting offshore wind energy will need to be developed.

In response to the growing interest in offshore wind, the U.S. Bureau of Ocean Energy Management (BOEM) received an unsolicited commercial lease request in 2016, which initiated the planning process to develop offshore wind in California. BOEM then delineated Call Areas for potential leasing in 2018, defined Wind Energy Areas (WEAs) in 2021, and completed a lease sale auction in late 2022 for the northern and central California WEAs. Work for this report was ongoing during this entire process, initially focusing on issues and scenarios for offshore wind energy development on the Central California Coast, and ultimately expanding to explore issues across the entire State and the U.S. West Coast as the leasing process progressed. This report explores key findings from diverse studies on the region, including the evaluation of wind datasets along Central California, the analysis of spatiotemporal variability potential wind power in Central California, scenarios for power production in the two Central California Call Areas, potential environmental impacts of deepwater wind facilities, an assessment of

catch and value from California's commercial fisheries, and an overview of fishing effort across the entire U.S. West Coast. The results provide information that can guide detailed assessments of offshore wind development over the Central California Coast and offer a transferable framework for similar evaluations in other regions, including the U.S. West Coast.

1.1 Evaluation of Surface Wind Datasets in Central California

The first study provides a comprehensive evaluation of near-surface wind datasets in Central California, including satellite-based observations (QuikSCAT, ASCAT, and CCMP V2.0), atmospheric reanalysis products (NARR and MERRA), and regional atmospheric models (Weather Research and Forecast (WRF) and WIND Toolkit). The research highlights spatiotemporal variations in dataset performance, with the WIND Toolkit identified as the most suitable for the region. The framework developed for assessing offshore wind datasets serves as a valuable tool applicable to other regions exploring offshore wind energy.

1.2 Spatiotemporal Variability of Wind Power

The second study addresses the limited understanding of spatiotemporal variability in wind power during the planning stage of offshore wind farms. By investigating potential offshore wind power along the Central California Coast over daily and seasonal time scales, the study reveals that peak offshore wind energy production is expected to align well with peak energy demand. Importantly, results suggest that offshore wind energy production will increase as other renewables (e.g., land-based wind, solar) decrease in the evening hours, such that offshore wind may fill the gap left by other renewables and provide substantial value in broader renewable energy portfolios. The research emphasizes the importance of considering spatiotemporal variability in wind power for accurate predictions and underscores the potential value of offshore wind in filling the supply gap during high demand periods.

1.3 Characterization of Central California Call Areas

The third study comprehensively characterizes and compares offshore wind power potential within the two Central California Call Areas (Diablo Canyon and Morro Bay) using different turbine types, inter-turbine spacing, and wind farm sizes. The results provide guidance on offshore wind development in this region, with combined power production from the Call Areas having the potential to contribute to a significant portion of California's annual power production.

1.4 Environmental Impacts of Deepwater Floating Wind Facilities

The fourth study explores the potential environmental impacts of deepwater, floating offshore wind energy facilities. At the time of this work, only limited floating wind turbines had been deployed globally, so there were very few field-based datasets to evaluate the environmental effects of these facilities. The study conducts a qualitative systematic review, evaluating potential effects and mitigation measures. The synthesis suggests that, with appropriate strategies, the potential environmental risks of deepwater, floating OWFs can be mitigated. This study provides a reference document for stakeholders and policymakers tasked with evaluating and minimizing the environmental impacts of floating offshore wind energy development.

1.5 California's Changing Commercial Fisheries

The fifth study shifts focus to California's commercial fisheries. As climate change accelerates and fisheries management evolves, the dynamics of California's fisheries are changing. Analyzing commercial landings receipts, the study characterizes temporal and spatial variation in landing and value of key fisheries groups. Results indicate a shift toward lower-biomass, higher-value species, providing valuable insights for informing fisheries management and marine spatial planning. The study also assesses fisheries landings and values in the Northern and Central California WEAs.

1.6 Spatial and Temporal Dynamics of West Coast Fisheries

The final study addresses the spatial and temporal dynamics of commercial fisheries along the entire U.S. West Coast. Using vessel tracking data, the research generates high-resolution spatiotemporal estimates of fishing effort. The study highlights the complexity of U.S. West Coast fisheries, providing crucial information for sustainable spatial fisheries management and informing the coordination of diverse ocean activities, including offshore renewable energy planning.

1.7 Conclusion

These studies collectively contribute to a comprehensive understanding of offshore wind energy scenarios on the Central California Coast and beyond. From wind dataset evaluation to environmental impacts, potential leasing areas, and fisheries dynamics, the findings underscore the multidimensional considerations required for offshore wind energy development. As California—and the U.S. more broadly—strives toward a sustainable and diverse energy future, the methods and findings of these studies can serve as a guide for policymakers, industry stakeholders, and researchers involved in shaping the State's offshore wind landscape.

2 Assessment of surface wind datasets for estimating offshore wind energy along the Central California Coast

2.1 Introduction

Over the last few decades, renewable energy sources have become an increasingly important component of broader energy portfolios. Costs of renewable energy have decreased substantially, and more governments recognize the importance of reducing greenhouse gas emissions. As a result, governments at many levels have set targets for increasing renewable energy generation. For example, across the European Union, the European Parliament and Council has set a target of 20% for energy consumption from renewables by the year 2020 (2020 Climate & Energy Package). Additionally, many states within the United States have adopted increased renewable energy portfolio targets. This includes California, which has set a goal to supply 60% of energy through renewable sources by the year 2030 (SB350-Clean Energy and Pollution Reduction Act of 2015).

In response to governmental initiatives and decreases in costs, deployment of renewable energy projects has been increasing rapidly, with an emphasis on photovoltaic solar and land-based wind turbines (Graabak and Korpås 2016). Offshore wind turbines also have received considerable interest and investment, particularly in Europe (Sun et al. 2012). Offshore wind energy has several advantages over solar and land-based energy sources since offshore winds tend to be stronger and more consistent than land-based winds (Carvalho et al. 2017) and are less likely to directly conflict with other land-use activities (while acknowledging that there may be some marine space-use conflicts). Additionally, offshore wind energy production may be able to reduce discrepancies in production and demand that are difficult to alleviate with solar output because of its diurnal cycle.

To best guide the evaluation and planning of offshore wind energy in a particular area, accurate wind datasets with sufficient temporal and spatial resolution are needed. Offshore winds typically exhibit temporal variability on interannual, seasonal, synoptic, and diurnal time scales. Furthermore, wind power is proportional to the cube of the wind speed, meaning that small changes in wind speed (e.g., over the course of the day or with different seasons) can lead to drastic differences in power output. Also, for power generation to be most valuable, it will need to match grid demands and base load needs, which vary daily and seasonally. Thus, wind datasets long enough to capture interannual variability and with sufficient temporal resolution to resolve diurnal variability are required for estimating wind energy power production and value. In addition, understanding spatial variation in offshore wind power can help support site planning and assessment by highlighting areas with the greatest potential to generate power and therefore areas with the greatest potential value. Despite the importance of understanding temporal and spatial variations in offshore winds for assessing this renewable energy resource, previous work has rarely resolved both daily and seasonally cycles at multiple sites and/or over a large area. Moreover, the utilization of temporally-averaged (mean) wind speeds over an annual cycle can lead to large errors and mismatches in grid demand and production estimates over shorter (seasonal and daily) time scales.

The lack of detailed assessments across a range of time scales and over broad spatial domains is mainly attributable to the absence of a single perfect offshore wind dataset with the appropriate temporal and spatial resolution. In-situ near-surface wind measurements from moored buoys are often available over long time periods (decades) with a very high temporal resolution (hourly or better), but these buoys are usually sparse (often > 10 to 100 km apart). Remote sensing measurements of near-surface winds obtained from satellites equipped with scatterometers can measure vector wind fields across large areas that are more spatially resolved than buoy platforms, but the measurements are only available during satellite passes, at most several times per day (Liu and Xie 2006). Reanalysis products, which objectively combine both observations and numerical models, often have consistent temporal resolution over decades

and contain winds at various vertical levels above the surface, but have coarser spatial resolution compared to satellite-derived data. Finally, regional atmospheric models have some of the highest spatial and temporal resolution, including data aloft at various vertical levels; however, they often experience substantial error relative to in-situ observations and are sensitive to local parameterizations (Carvalho et al. 2012).

Previous studies have evaluated the performance of various wind datasets in different regions (see Carvalho et al. 2017 and the references therein). Pickett et al. (Pickett et al. 2003) and Tang et al. (Tang et al. 2004) assessed the performance of QuickSCAT satellite observations relative to local buoys along the West Coast of the United States, but they did not assess other datasets. Carvalho et al. (Carvalho et al. 2014) conducted a comprehensive comparison of satellite-based observations, reanalysis products, and the WRF regional model with five buoys in the Iberian Peninsula coast. Carvalho et al. (Carvalho et al. 2017) extended the analyses of Carvalho et al. (Carvalho et al. 2014) by including newer scatterometers (e.g., ASCAT). However, these studies focused on error metrics over one year and did not consider longer time periods or seasonal and diurnal variability. Alvarez et al. (Alvarez et al. 2014) used a longer time period (10 years) to evaluate satellite-based products and reanalysis products against in-situ buoy measurements in the southern Bay of Biscay. They found that QuikSCAT had the lowest bias in wind speed and wind direction and the Cross-Calibrated Multi-Platform (CCMP, blended satellite product) had the lowest error, but they did not include an analysis of the diurnal signal.

Collectively, these studies and others (see Carvalho et al. 2017 and references therein), also suggest that the performance of different wind products varies by study region, indicating the need for site-specific analyses. The majority of site-specific evaluations of offshore wind data have focused on coastal waters along Europe, typically in association with existing or planned offshore wind farms (e.g., Carvalho et al. 2017, Carvalho et al. 2014, Sharp et al. 2015). To date, all but one of the world's offshore wind farms in operation consist of fixed-bottom wind turbines located in shallow waters of less than 100 m. Yet, as technology advances, the cost of building floating wind turbines in water greater than 100 m deep may be less than that of fixed-bottom platforms by 2030 (Beiter et al. 2016). The first MW-scale floating turbine was successfully deployed in the North Sea in 2009 (Prachi 2009). In 2017, the world's first floating offshore wind farm was successfully launched with the Hywind project in Scotland, paving the way for future wind farms in deeper waters further from the coast (Frith 2017). With improvements in floating turbine technology, deployment of offshore wind farms is likely to increase in the future, particularly in areas with deeper shelf waters. Understanding wind patterns (both spatially and temporally) in these environments will be key to guiding and assessing marine renewable energy production.

Along the West Coast of the United States, the continental shelf is narrow, such that waters are often > 100 m deep only a few kilometers from shore. As a result, the majority of the ocean area with the potential for wind power production is located in deep waters where floating turbines would be necessary (Musial et al. 2016). The Central California region considered in this study, spanning from south of Monterey Bay to Point Conception is characterized by moderately strong winds throughout the year (e.g., Fewings et al. 2016; Figure 2.1). Additionally, this region is located in the vicinity of several existing connections to the State's electrical grid, including the Morro Bay power plant (closed in 2014) and the Diablo Canyon nuclear power plant (California's last remaining nuclear power plant slated to close in 2025). Finally, the study domain is outside of National Marine Sanctuary areas, where restrictions on disturbance to the seabed will likely preclude floating turbine deployment. Attracted by these features, private industry has shown great interest in pursuing permits from government agencies for the development of deep water, floating offshore wind farms (BOEM: https://boem.gov/California/).Therefore, a detailed analysis of the available wind products in this region is needed. However, aside from a few simple analyses of winds (e.g., Jiang et al. 2008), there are no comprehensive assessments of long-range, high-resolution wind products in this region. Without this information, it is difficult to accurately evaluate the power production potential of this region.

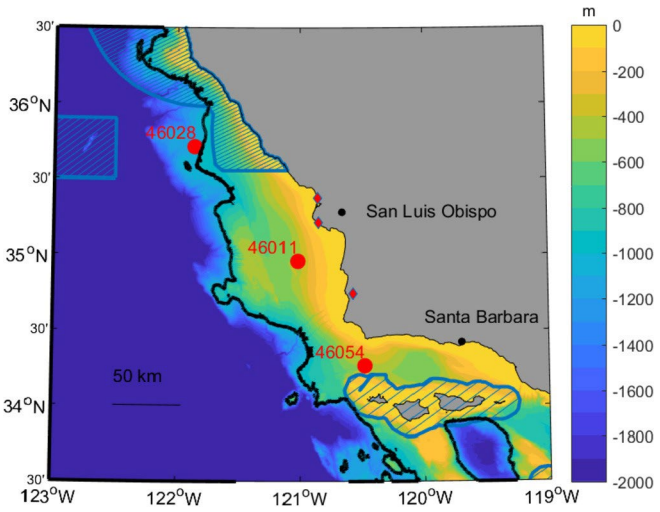

Figure 2.1. Bathymetry of the Central California Coast.
Note: Highlighting the locations of buoy platforms (red circles, representing buoys 46028, 46011, 46054 from north to south), existing state electrical grid connections (red diamonds), National Marine Sanctuaries (dashed blue lines; Monterey Bay Sanctuary to the north and Channel Islands Sanctuary to the south), and the 1000 m isobath (solid black line). The state electrical grid connections from north to south are the Morro Bay power plant, Diablo Canyon nuclear power plant, and Vandenberg Air Force Base.

To address this knowledge gap, we conducted a comprehensive evaluation of near-surface winds from various datasets (satellite-based, model, reanalysis) and compared them to local buoy measurements. We used these datasets, which span nearly a decade and with up to 2-km spatial resolution, to assess error metrics (bias and root-mean-square-error) over seasonal and diurnal time scales. Using the results of these point-to-point comparisons, and consideration of the spatiotemporal resolution of each dataset and whether it provides data aloft, we examined tradeoffs between various dataset attributes (e.g., bias, error, spatial and temporal resolution, availability of data aloft) to identify the best dataset for offshore wind energy application. We then explored characteristics of the chosen dataset to reveal temporal changes in near-surface wind speeds across the domain along the Central Coast of California. The framework we developed to evaluate the various products is readily applicable to other regions where similar analyses are needed, and the wind dynamics we reveal for the Central Coast can be used to support the generation of accurate and detailed estimates of potential power production in the region.

2.2 Data and methods

2.2.1 Study domain

The Central Coast of California is located along the eastern boundary of the Pacific Ocean and features steeply sloping bathymetry. In this study, we considered the domain bounded by the Monterey Bay National Marine Sanctuary to the north, the Channel Islands National Marine Sanctuary to the south, and the 1000 m isobath in the offshore direction, generally west (Figure 2.1). The offshore limit is the maximum water depth for offshore wind turbine installation based on current technology and industry experience (Musial et al. 2016). Along this stretch of coastline, there are three existing connections to the State's electrical grid: the Morro Bay power plant (closed in 2014), the Diablo Canyon nuclear plant (slated to close in 2025), and Vandenberg Air Force Base. This region is characterized by moderately strong and consistently equatorward winds throughout much of the year, particularly for the region north of Point Conception (e.g., Fewings et al. 2016, Walter et al. 2018). A previous study suggested that the annual average of wind speed at hub height exceeds 7 m s^{-1}, highlighting the potential for offshore wind farms (Musial et al. 2016).

2.2.2 Wind datasets

2.2.2.1 Buoy observations

Near-surface winds in this study domain were obtained from moored buoys measuring winds at 5 m above the surface and reporting an average wind speed every 10 min (i.e., the National Data Buoy Center (NDBC) continuous wind product, http://www.ndbc.noaa.gov/). We employed buoy data as a reference to represent true characteristics of near-surface winds, as is commonly done in the existing literature (e.g., Pensieri et al. 2010). While buoy measurements are the best available in-situ data, buoy measurements may be less reliable under strong winds (Taylor et al. 1999), but these measurements are still likely the best estimates of true wind speeds. Among all datasets considered, the buoy dataset is the only to output near-surface winds at 5 m above the sea surface, with the other datasets outputting near-surface winds at 10 m above the sea surface. Thus, to enable a direct comparison, we converted the buoy-measured wind speeds from 5 m to 10 m assuming a neutrally stable atmosphere following the method of Liu and Tang 1996. This is a reasonable assumption given that calculated atmospheric stabilities show a neutrally stable atmosphere during most seasons and hours of the day. Potential errors in 10-m winds speeds when atmospheric stability deviates slightly from neutral conditions are expected to be small (Capps and Zender 2009). Buoys 46028 and 46011 are located north of Point Conception, and buoy 46054 is located just to the south of Point Conception, at the western edge of the Santa Barbara Channel (red dots in Figure 2.1).

2.2.2.2 Satellite-based observations

We evaluated two scatterometers, which measure surface wind stress by sending microwave signals and then recording the back-scattered signal in response to ocean roughness (e.g., Liu and Tang 1996). Surface wind stress is converted to equivalent neutral winds 10 m above grounds based on the assumption of a nearly neutral atmosphere (Liu and Tang 1996). Vector wind fields are produced at approximately the same geographical location during ascending and descending passes of the satellite (i.e., twice per day). Here, we opted to use the swath data with 12.5 km spatial resolution because this high-resolution product can contain small-scale features (Verhoef and Stoffelen 2009). We downloaded both scatterometer-derived datasets from the NASA's Jet Propulsion Laboratory Physical Oceanography Distributed Active Archive Center site (https://podaac.jpl.nasa.gov).

The first scatterometer dataset we evaluated was QuikSCAT, which measures the backscattered signal using the Ku-band frequency and passes through our study domain around 5 and 18 h every day. QuikSCAT data were available from June 1999 to November 2009. This widely-used product has been validated for accuracy against in-situ buoy observations over various forcing regimes (e.g., Ebuchi et al. 2002). We adopted the latest version of the Level 2 product (QuikSCAT Level 2B Version 3), which uses the improved geophysical model function and corrected rain contaminated wind speeds with a neural network approach (Physical Oceanography Distributed Active Archive Center 2013).

The second scatterometer dataset we evaluated was ASCAT, which is a new-generation scatterometer launched in October 2006. It agrees well with QuikSCAT especially when wind speeds range between 3 m s^{-1} and 20 m s^{-1} (Bentamy et al. 2008). ASCAT passes a local point around 9 and 20 h and uses the C-band frequency operation, which is less sensitive to rain contamination than the Ku-band frequency operation (Weissman et al. 2002). Because of its narrower swath width,

ASCAT is limited to approximately 60% of the coverage of QuikSCAT during the same period (Kako et al. 2011). The ASCAT Level 2-Coastal product applies a boxcar filtering to yield more wind data close to the coast (Osi 2016). We used the Level 2 product's Climate Data Record version, which was reprocessed using consistent calibration from January 2007 to March 2014.

The last satellite-based product we assessed was the Cross-Calibrated Multi-Platform Version 2 (CCMP V2.0, a continuation of CCMP Version 1.1) (Atlas et al. 2011). We obtained this dataset from Remote Sensing Systems (http://www.remss.com/). This blended product combines satellite-derived wind fields from microwave radiometers and scatterometers, with moored buoys and ERA-Interim model data using a Variational Analysis Method. It provides global and gap-free wind fields on a 0.250 grid four times per day from 1987 to the present. Previous studies in the southern Bay of Biscay (Alvarez et al. 2014) and the Iberian Peninsula coast (Carvalho et al. 2017 and Carvalho et al. 2014) demonstrated that CCMP accurately captured offshore winds.

2.2.2.3 Reanalysis datasets

We also assessed two reanalysis products, which combine in-situ observations with numerical models: 1) Modern-Era Retrospective Analysis (MERRA, http://disc.sci.gsfc.nasa.gov/mdisc/), a global reanalysis product (Reinecker et al. 2011), and 2) North American Regional Reanalysis (NARR, https://www.esrl.noaa.gov/psd/), a regional reanalysis product (Mesinger et al. 2006). MERRA is a commonly-used global reanalysis product for wind resource evaluations (e.g., Draxl et al. 2015). It provides hourly data on a grid of 2/30 by 1/20 from 1979 to 2016. NARR outputs data every 3 h (since 1979) and has a spatial resolution of 32 km. Both products yield wind data at various pressure levels above the surface. In part because it assimilates more observations into its model, NARR data yield more accurate results relative to global reanalysis products (Mesinger et al. 2006). Previous studies in other regions have also shown good agreement between NARR and in-situ measurements near the surface and aloft (e.g., Bylhouwer et al. 2013, Li et al. 2010 and Moore et al. 2008).

2.2.2.4 Regional atmospheric model simulations

We analyzed simulated near-surface wind speeds from two regional model datasets. The first dataset covers the entire U.S. West Coast and was carried out using WRF model version 3.6 (Skamarock et al. 2008 and Renault et al. 2016), which is initialized and forced at boundaries with the Climate Forecast System Reanalysis. The model is configured with two nested grids, where the outer domain has a horizontal resolution of 18 km, and the inner domain has a resolution of 6 km. It is set up with a full set of parameterization schemes including the Mellor-Yamada-Nakanishi-Niino planetary boundary layer scheme (Nakanishi and Niino 2006), which is one of the best planetary boundary layer schemes to simulate realistic cloud cover and wind. More details can be found in Renault et al. 2016. Hourly 10-m wind fields above the ground level are available from 2004 to 2013 and used for this study.

The second regional model dataset is from the WIND Toolkit (https://www.nrel.gov/grid/wind-toolkit.html), developed by the National Renewable Energy Laboratory (NREL) for the purpose of wind power application (Draxl et al. 2015). The results were generated by the WRF model version 3.4.1, which is initialized and forced at boundaries by the European Center for Medium-Range Weather Forecasts Interim Reanalysis. This model uses three nested grids with resolutions of 18 km, 6 km, and 2 km, respectively, with the inner 2 km grid covering the entire contiguous United States. The optimal model configuration is the best one from the eight model configurations tested by NREL. This configuration outputs simulations with small overall bias and in complex terrain, realistic hourly and diurnal wind variations, and highly resolved wind fields near the surface. More details can be found in Draxl et al. 2015a and 2015b). We analyzed hourly 10-m wind fields (2007–2013). In addition to near-surface wind fields, wind data at higher altitudes up to 200 m are also available.

2.2.3 Comparisons and statistics

In order to compare the various datasets to the buoy observations, we obtained the closest point in space and time from each wind dataset relative to each of the three buoys. We included observations only if they met our collocation criteria with buoy data: measurements must have been recorded within 30 min of

a buoy measurement and no more than 12.5-km from the buoy for all datasets except WIND Toolkit. We use a more restrictive spatial criterion of 2 km for WIND Toolkit because of its higher resolution of 2 km. Unlike gridded datasets, the closest swath point of the scatterometer data to a local buoy is not fixed and its measurement time is slightly different each day. In line with previous studies (e.g., Pickett et al. 2003), we found no connection between the separation distance and the bias in QuikSCAT/ASCAT relative to a local buoy. Between 2000 and 2008 (time period used for comparison in this study), the mean separation distance between the closest QuikSCAT point and buoy was 5.59, 4.45, and 4.93 km for buoy sites 46028, 46011, and 46054, respectively. Between 2007 and 2013, the mean separation distance between the closest ASCAT point and buoy was 4.91, 3.55, and 3.77 km. The distance between a local buoy and the closest point of a comparative gridded dataset is shown in Table 2.2.

We evaluated the seven aforementioned wind datasets in relation to buoy measurements using the collocation criteria described above. To summarize the performance of each wind data, we utilized the statistical metrics of the bias and the root-mean-square-error (RMSE) between one dataset and buoy measurements. To illustrate the relationship between two variables, we fitted the paired data to a linear regression line and provided its intercept, its slope, and the coefficient of determination (R^2) of the model fit in Tables 2.2–2.4.

Complete annual data were available for at least 7 years for all datasets (see Table 2.1 for details), thereby reducing the impact of interannual variability on our analysis. To display climatological characteristics of near-surface winds, we used buoy data from 1998 to 2016 and compared these winds between the buoys and other datasets for each year of overlap.

2.2.4 Tradeoff analysis

To evaluate the relative merits of the datasets and identify the best dataset for offshore wind power applications, we applied a tradeoff analysis to our results. Tradeoff analysis is a useful graphical tool for comparing the relative performance of a set of options in relation to multiple objectives (Lester et al. 2013). We considered five key objectives, or factors, in the tradeoff analysis of the seven wind datasets: temporal and spatial resolution (higher better), the absolute value of bias and RMSE (lower better), and availability of wind speed data aloft (better). We then conducted visual inspection of pairwise tradeoff plots of the seven datasets in relation to the five factors in order to compare and contrast the relative merits of the datasets and identify the most appropriate one(s) for offshore wind power applications.

Table 2.1. Characteristics of wind datasets considered for comparison with buoy observations

Dataset	Type of dataset	Spatial resolution	Temporal resolutions	Times used in this study
QuikSCAT	Satellite (Swath)	12.5 km	2 times per day	2000–2008
ASCAT	Satellite (Swath)	12.5 km	2 times per day	2007–2013
CCMP V2	Satellites and analyses	0.25olat/lon	4 times per day	2004–2013
NARR	Regional reanalysis	32 km	8 times per day	2004–2013
MERRA	Global reanalysis	1/2olat-2/3olon	Hourly	2004–2013
WRF	Regional model	6 km	Hourly	2004–2013
WIND Toolkit	Regional model	2 km	Hourly	2007–2013

Table 2.2. Statistical metrics from the linear regression between buoy data and each of the comparison datasets

Buoy	Dataset	Slope	Intercept	R^2	Distance from buoy (km)	Number of valid pairs
46028	QuikSCAT	0.90	1.01	0.92	5.59	5654
	ASCAT	0.94	0.25	0.94	4.91	2153
	CCMP V2	0.68	1.37	0.77	9.80	13013
	NARR	0.76	1.59	0.75	9.07	26018
	MERRA	0.59	1.69	0.74	26.85	78014
	WRF	0.38	4.88	0.15	3.64	78012
	WIND	0.79	1.13	0.83	0.62	55957
46011	QuikSCAT	0.85	1.56	0.84	4.45	5449
	ASCAT	0.89	1.02	0.84	3.55	2241
	CCMP V2	0.75	2.00	0.67	13.22	12368
	NARR	0.72	1.40	0.69	7.62	24695
	MERRA	0.62	2.04	0.64	29.07	74049
	WRF	0.39	4.77	0.14	3.24	74046
	WIND	0.77	1.65	0.73	0.89	51953
46054	QuikSCAT	0.68	2.23	0.82	4.93	3875
	ASCAT	0.81	1.16	0.88	3.77	1670
	CCMP V2	0.53	1.66	0.62	15.41	7928
	NARR	0.49	1.13	0.53	7.62	15754
	MERRA	0.40	1.76	0.58	31.41	47392
	WRF	0.37	4.91	0.16	2.10	47385
	WIND	0.80	1.45	0.79	0.99	34001

Table 2.3. Statistics from the comparison between the buoy data and comparison datasets, including error metrics (bias and RMSE), as well as outputs (slope, intercept, coefficient of determination) from the linear regression between the wind speed difference and the buoy wind speed

Buoy	Dataset	Bias	RMSE	Slope	Intercept	R^2 46028
QuikSCAT	0.26	1.22	-0.10	1.01		0.12
	ASCAT	-0.18	1.03	-0.06	0.25	0.06
	CCMP V2	-0.94	2.20	-0.32	1.37	0.42
	NARR	-0.15	2.03	-0.24	1.59	0.23
	MERRA	-1.28	2.54	-0.41	1.69	0.58
	WRF	0.41	4.47	-0.62	4.88	0.32
	WIND	-0.43	1.76	-0.21	1.13	0.26
46011	QuikSCAT	0.67	1.50	-0.15	1.56	0.14
	ASCAT	0.38	1.40	-0.11	1.02	0.08
	CCMP V2	0.52	2.02	-0.25	2.00	0.19
	NARR	-0.29	1.90	-0.28	1.40	0.26
	MERRA	-0.21	2.04	-0.38	2.04	0.40
	WRF	1.17	4.07	-0.61	4.77	0.28
	WIND	0.28	1.82	-0.23	1.65	0.18
46054	QuikSCAT	-0.49	2.03	-0.32	2.23	0.50
	ASCAT	-0.33	1.47	-0.19	1.16	0.31
	CCMP V2	-1.99	3.29	-0.47	1.66	0.57
	NARR	-2.78	4.00	-0.51	1.13	0.55
	MERRA	-2.87	4.08	-0.60	1.76	0.75
	WRF	0.04	4.43	-0.63	4.91	0.36
	WIND	-0.07	1.90	-0.20	1.45	0.19

Table 2.4. Statistical metrics of wind direction (º) from paired data. A positive bias indicates a clockwise bias

Buoy	Dataset	Bias	RMSE
46028	QuikSCAT	6.74	38.74
	ASCAT	1.49	37.36
	CCMP V2	6.51	41.86
	NARR	3.77	40.85
	MERRA	5.95	41.98
	WRF	7.10	68.88
	WIND	3.84	36.76
46011	QuikSCAT	0.44	45.83
	ASCAT	-3.09	47.30
	CCMP V2	2.02	44.47
	NARR	0.26	41.96
	MERRA	0.28	44.49
	WRF	14.50	68.05
	WIND	0.99	39.97
46054	QuikSCAT	1.39	46.85
	ASCAT	-3.86	46.73
	CCMP V2	7.78	42.85
	NARR	-8.32	45.03
	MERRA	11.12	45.30
	WRF	14.18	69.37
	WIND	2.70	38.65

2.3 Results

2.3.1 Buoy climatology

Climatological characteristics of buoy winds are shown in Figure 2.2. Each curve represents the composite day average wind speed for a particular month (i.e., average wind speed calculated using data over all years from a particular hour during each month). All times referenced are Pacific Standard Time (PST).

The three different buoy sites display similar diurnal structure with daily minimums in the late morning and peaks in the early evening (Figure 2.2). There is also a slight seasonality in both the timing of the daily minimums and peaks, as well as the daily range. During months with stronger wind forcing (e.g., spring/summer upwelling months, cf. Walter et al. 2018), the daily peaks arrived slightly later compared to during other months. For example, at 46028, wind speed peaks around 20 h in May and at 18 h in

January. Notably, the diurnal variability is comparable to that of the seasonal variability. There is also considerable buoy-to-buoy (i.e., spatial) variability at various time scales. Among the three sites, buoy 46054 displayed the strongest diurnal variations in wind speed with differences as large as 3 m s^{-1} between the daily minimum and maximum in some months.

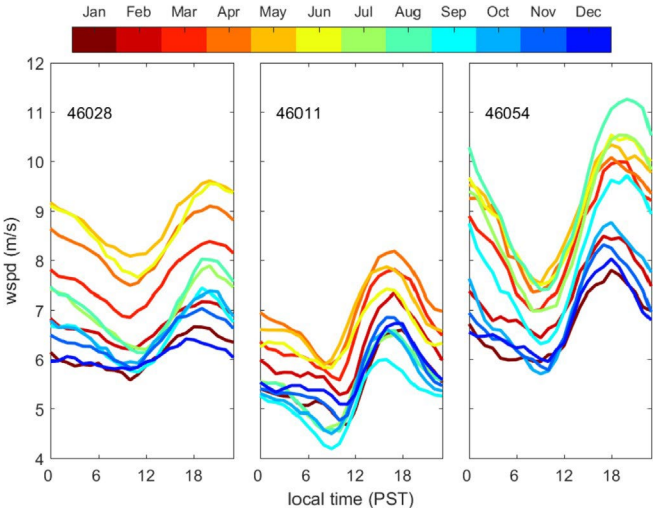

Figure 2.2. Composite day average buoy wind speed for a particular month (colors) using data calculated over all years (1998–2016) for each buoy (46028, 46011, and 46054 from left to right).

Seasonal cycles also varied among buoys. The 10-m wind speeds at buoys 46028 and 46011 reached their maxima in spring, whereas the 10-m wind speed at buoy 46054 reached its maximum in the summer (see Walter et al. 2018 for a discussion of the seasonality at buoy 46011). This seasonal variation is closely connected to large-scale pressure systems, which fluctuate seasonally, but tend to produce equatorward winds near the surface along the coastline (see Fewings et al. 2016 for a detailed description). Among the three sites, buoy 46054 had the strongest and most variable winds, which is strongly impacted by the interaction between the marine boundary layer and coastal capes (i.e., Point Conception) (Fewings et al. 2016).

2.3.2 Paired comparisons with buoy measurements

Direct comparison between the wind speed calculated from each buoy at each site and each respective dataset were made using all data available over the selected time period for all points in each dataset that met collocation criteria. Figure 2.3 shows scatter plots and the linear regression line between each wind product's wind speed and the buoy site's wind speed. Statistics from the linear regression and collocation criteria are shown in Table 2.2. The error metrics (bias and RMSE) are displayed in Table 2.3.

Based on the performance of the linear regression (Table 2.2, Figure 2.3) and the error metrics (Table 2.3), ASCAT had the lowest bias and RMSE, and the largest coefficient of regression with buoy-based site measurements, slightly outperforming the other scatterometer-based observation, QuikSCAT. This is not surprising, given previous validations of the product in other regions (e.g., Carvalho et al. 2017). We note, however, that the scatterometers (particularly ASCAT) have the smallest number of points used for comparison with the buoy data because of the temporal resolution (typically only two measurements per day) and a shorter time period relative to other datasets. Following scatterometer-based observations, the WIND Toolkit showed the best correspondence with buoy data; this dataset even outperformed the scatterometers slightly with respect to bias at buoys 46011 and 46054 and had relatively low error as well (Table 2.3). We note that the WIND Toolkit is also the most spatially (2 km) and temporally (1 h)

resolved dataset, and it contains wind data at various levels about the sea surface. While the WIND Toolkit, a version of the WRF regional model, displayed some of the best results, the other WRF model considered (denoted WRF here, a model developed for the West Coast of the United States) showed the worst correspondence to local buoys in this region. Given the sensitivity of the performance of the WRF model in wind simulation to various configurations and parameterizations, (e.g., Carvalho et al. 2012), it is possible that the better performance of the WIND Toolkit than its counterparts is associated with its configuration particularly optimized for simulating wind for wind energy applications. The largest error (RMSE) among the three sites is generally found at buoy 46054, which is located just south of Point Conception, highlighting the difficulty of resolving the wind field near complex land topography. Among these seven wind datasets, five (ASCAT, QuikSCAT, CCMP, NARR, and MERRA) display the worst correspondence at buoy 46054, while model simulations (WRF and WIND Toolkit) show relatively consistent correspondence across all buoys. The greater biases in the reanalysis datasets at buoy 46054 are likely due to their coarser spatial resolution, which is not able to accurately capture small-scale coastal orography near Point Conception and its impact on the velocity field.

To further investigate the differences between the various datasets and the local buoys, we examined the wind speed difference between a particular dataset and the local buoy as a function of the buoy wind speed (Figure 2.4). In general, data products over-estimated winds relative to the buoy at low wind speeds and underestimated at high wind speeds, with varying degrees of magnitude. This feature and negative relationship is consistent with the findings of previous studies using less than two years of data (Carvalho et al. 2017, Pickett et al. 2003 and Tang et al. 2004). Statistics of the linear regression between wind speed difference and buoy wind speed are shown in Table 2.3. Both scatterometer-based observations (ASCAT and QuikSCAT) and WIND Toolkit exhibit smaller slopes among the three local buoys, indicating less functional dependence of the errors on wind speed relative to other datasets. We note that at the lowest and highest wind speeds, wind speed differences are less important for estimating wind power production due to turbine mechanical constraints that require cut-in and cut-out wind speed restrictions at low and high wind speeds, respectively.

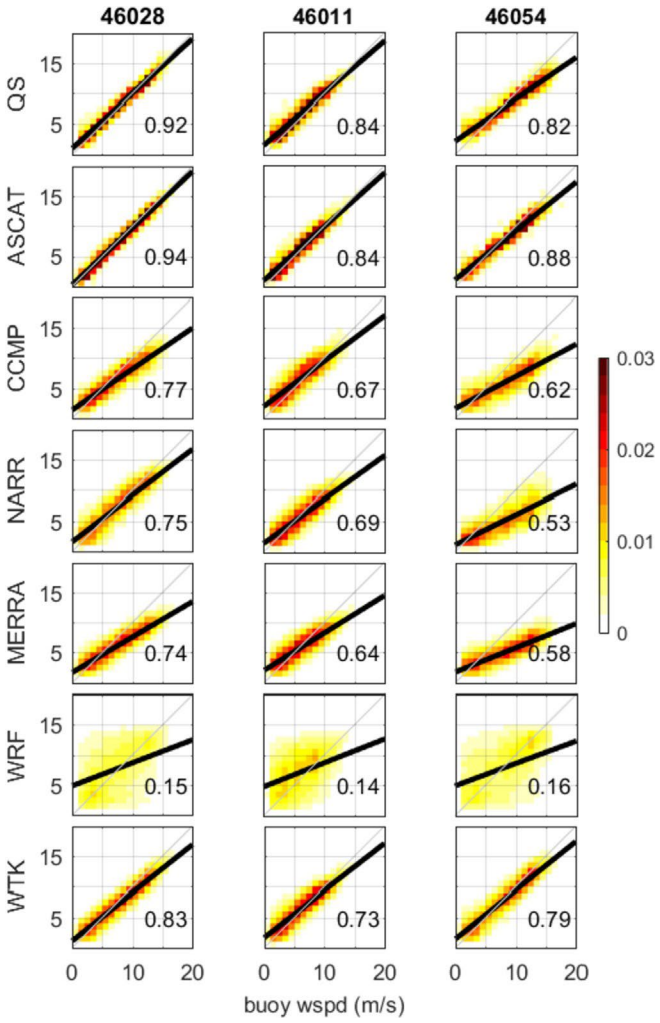

Figure 2.3. Comparisons of wind speed between the buoy measurements and each respective dataset (all in m s^{-1}).

Note: The value on each subplot shows the coefficient of determination (R^2) from a linear regression model (fit shown as bold black line). The one-to-one line is also shown for reference (thin gray line). Wind speed is binned by 1m s -1 along both of the x-axis and y-axis, and then divided by the total number of data pairs to yield the frequency of data points in a particular bin (colors). The rows from the top to the bottom are QuikSCAT (QS), ASCAT, CCMP V2.0 (CCMP), NARR, MERRA, WRF, and WIND Toolkit (WTK). The columns from the left to the right represent the local buoy 46028, 46011, and 46054, respectively. Note that the time period used for analysis depends on data availability.

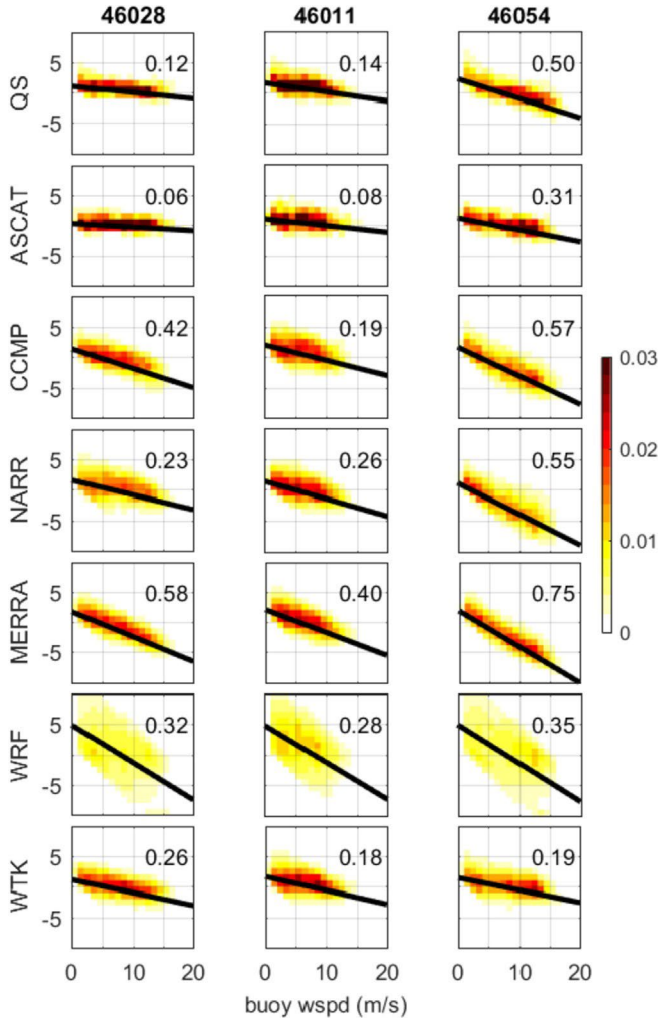

Figure 2.4. Differences in wind speed between the buoy and the other respective datasets as a function of the buoy wind speed (all in m s^{-1}).
Note: The value on each subplot shows the coefficient of determination (R^2) from a linear regression model (black line). Wind speed is binned by 1 m s-1 along both of the x-axis and the y-axis, and then divided by the total number of data pairs to yield the frequency of data points in a particular bin (colors). The rows from the top to the bottom are QuikSCAT (QS), ASCAT, CCMP V2.0 (CCMP), NARR, MERRA, WRF, and WIND Toolkit (WTK). The columns from the left to the right represent the local buoy 46028, 46011, and 46054, respectively. Note that the time period used for analysis depends on data availability.

2.3.3 Seasonal and diurnal bias

We examined the diurnal and seasonal dependence of bias and error (RMSE) as a function of both the time of day (i.e., diurnal signal) and month (i.e., seasonal signal) (bias: Figure 2.5; RMSE: Figure 2.6). To ensure that one dataset and reference buoy have the same sample size, we used paired data for the comparison analysis from Section 2.3.2. Here, a positive (negative) bias indicates that the respective dataset overestimates (underestimates) the buoy wind speed.

Overall, QuikSCAT and ASCAT show some of the smallest biases among the datasets, although there are only two hours per day for comparison. Generally, both datasets show different performance between the early morning and evening. While the bias is consistently low at 46028, the bias at 46011 is more positive

in the mornings, whereas the bias at 46054 is negative in the evenings. The other satellite-based product, CCMP, is more temporally resolved (6 h resolution), but shows much higher bias. Similar to QuikSCAT and ASCAT, CCMP tends to overestimate buoy-measured wind speeds near 46011. In contrast to 46011, CCMP underestimates wind speeds near 46028 and 46054.

The reanalysis product NARR exhibits consistently low biases at 46028 and 46011, yet strongly underestimates wind speed (i.e., negative bias) at 46054. Such low and homogeneous biases at the two northernmost buoy sites (46028 and 46011) are not seen in the other reanalysis product, MERRA, which displays weaker wind speeds compared to buoy measurements (i.e., negative bias) in the morning. The weaker winds in the morning, along with no difference (46028) or relatively higher wind speeds (46011) in the evening, particularly from May to September, lead to stronger predicted diurnal cycles than observed at the buoys.

Both atmospheric regional model simulations used in this study display lower biases at 46054, compared to other datasets. At 46028 and 46011, WRF overestimates wind speed throughout the day in summer months. For the WIND Toolkit, wind speed is underestimated (i.e., negative bias) close to buoy measurements at 46028. It tends to overestimate wind speed (i.e., positive bias) from 00:00 to 12:00 PST at 46011 in contrast to slight underestimates in the evening.

Overall, QuikSCAT, ASCAT, and WIND Toolkit are the best performing datasets with the lowest bias, and hence smallest discrepancies from local buoys. The bias appears to be tied to the RMSE in which the greater bias corresponds to the greater RMSE. Since the diurnal and seasonal patterns in bias (RMSE) are different across the three buoys, a simple correction of the underlying dataset is likely to lead to more uncertainties spatially.

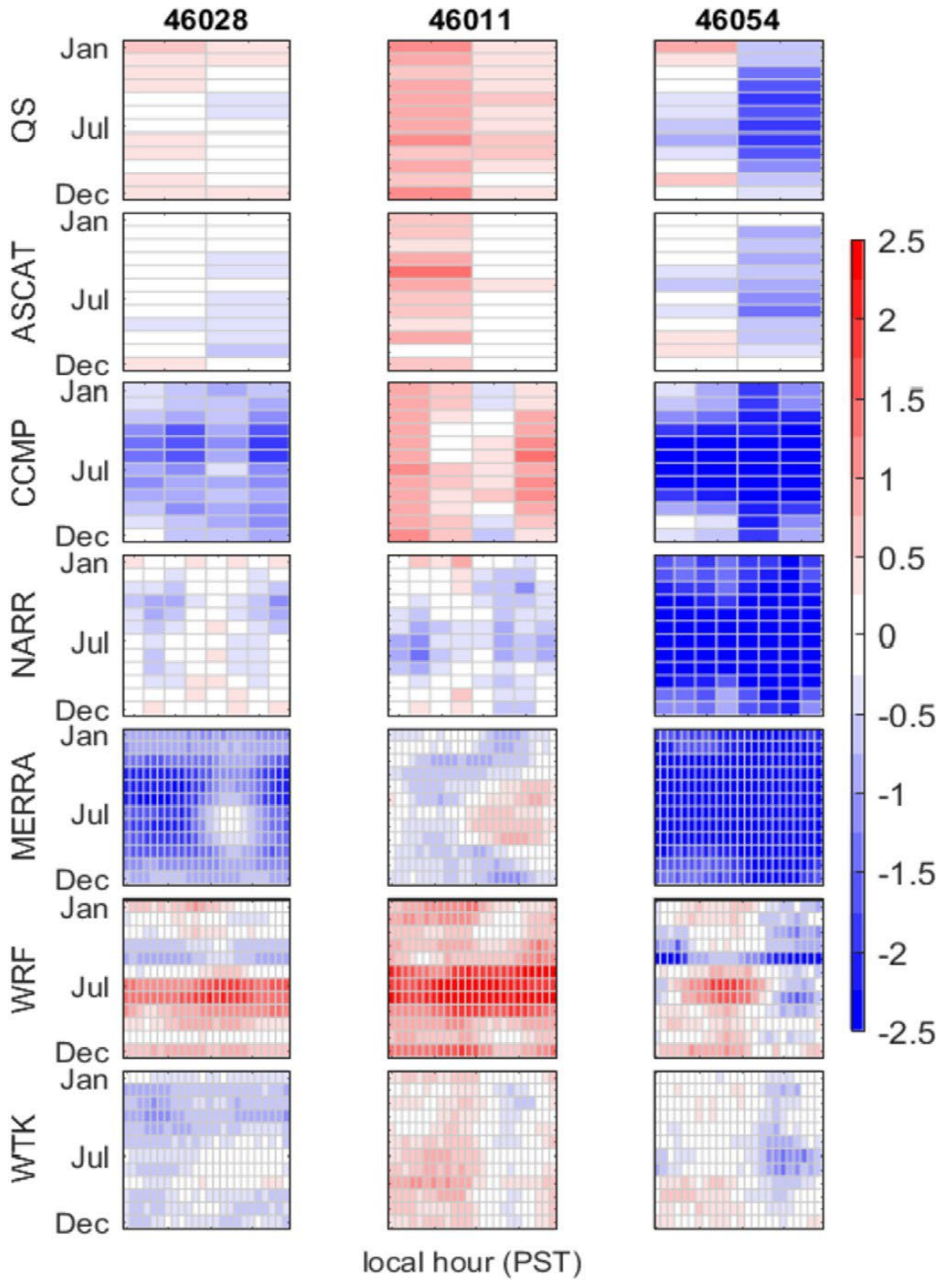

Figure 2.5. Bias (m s^{-1}) in the hourly near-surface wind speed in each month for all available paired data in relation to the buoy measurements at 46028 (left), 46011 (middle), and 46054 (right).
Note: A positive (negative) bias indicates that the respective dataset overestimates (underestimates) the buoy wind speed. The white color indicates zero bias. The rows from the top to the bottom are QuikSCAT (QS), ASCAT, CCMP V2.0 (CCMP), NARR, MERRA, WRF, and WIND Toolkit (WTK). The following hours (in PST) are shown for the respective dataset: QS (05 and 18); ASCAT (9 and 20); CCMP (04, 10, 16, and 22); NARR (01, 04, 07, 10, 13, 16, 19, and 22); and for MERRA, WRF, and WTF (hourly from 00 to 23). See Table 1 for the time period used for analysis of individual datasets.

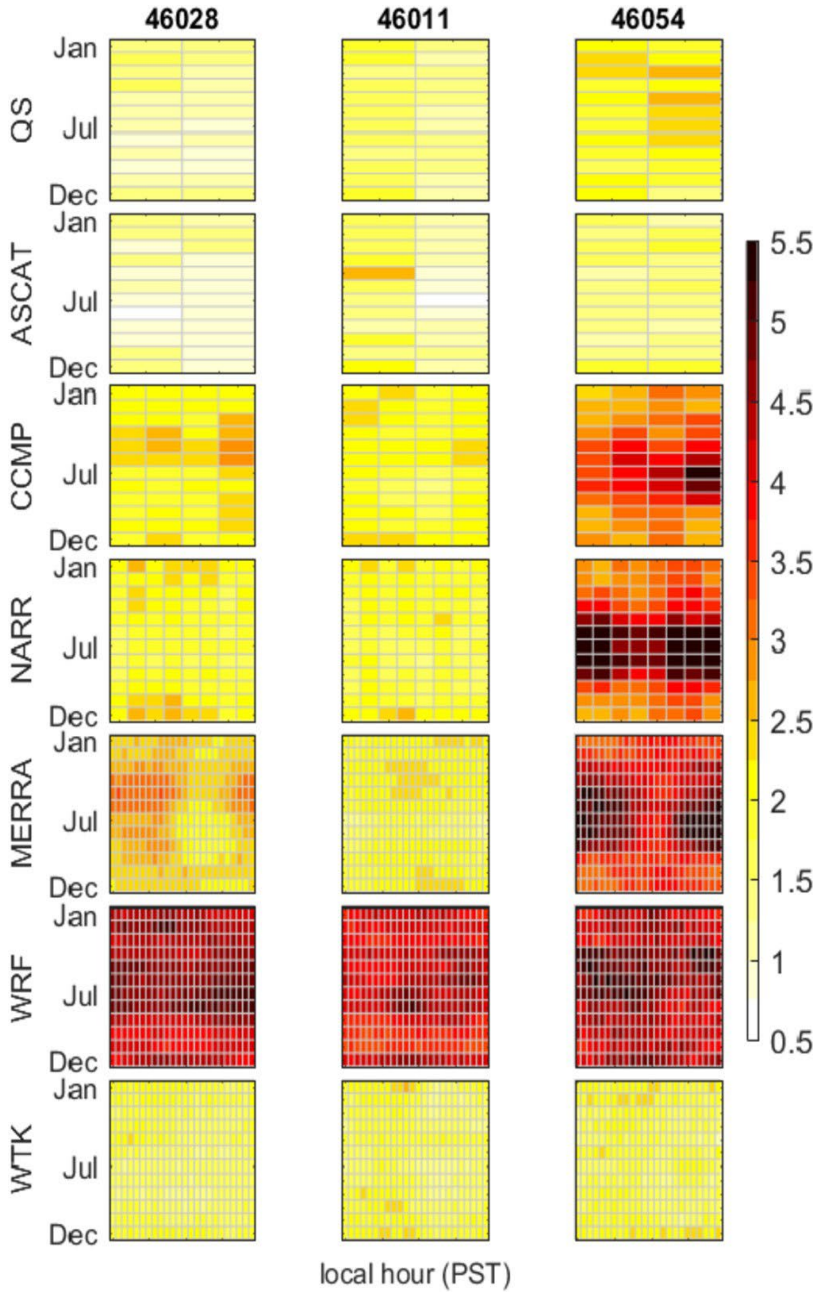

Figure 2.6. Similar to Figure 2.5, but for root-mean-squared error in the hourly near-surface wind speed in each month (m s^{-1}).

2.3.4 Tradeoff analysis for seven datasets

Although scatterometer-based observations were the best performing datasets relative to buoy measurements in this study domain, their temporal resolution is too coarse to fully resolve the diurnal cycle of near-surface winds. By contrast, the next performing dataset, WIND Toolkit, provides hourly wind fields with much higher spatial resolution. To evaluate the relative merits of the datasets and identify the best dataset for offshore wind power applications, we conducted tradeoff analysis to illustrate important differences in the characteristics of the seven datasets in relation to five factors: the absolute value of bias, RMSE, data availability aloft, temporal resolution, and spatial resolution. Here, we considered the overall performance (the absolute value of bias and RMSE) at the three local buoy sites in

this domain (Table 2.3), but the performance at individual sites can be obtained in a similar fashion. Figure 2.7a shows the mean bias and RMSE over the three buoy sites along with error bars representing one standard deviation from the mean. ASCAT, QuickScat, and WIND Toolkit all have similarly low levels of bias and RMSE, consistently at the three buoy sites; however, among these datasets, only WIND Toolkit contains data aloft (Figure 2.7a). Furthermore, WIND Toolkit contains a far superior spatial and temporal resolution, compared with ASCAT and QuickScat (Figure 2.7b). Only WRF contains spatial and temporal resolution comparable with that by the WIND Toolkit, but WRF is otherwise inferior because it has a much larger RMSE. Collectively, these tradeoff analysis results indicate that WIND Toolkit is the most appropriate dataset for supporting offshore wind power applications in this region.

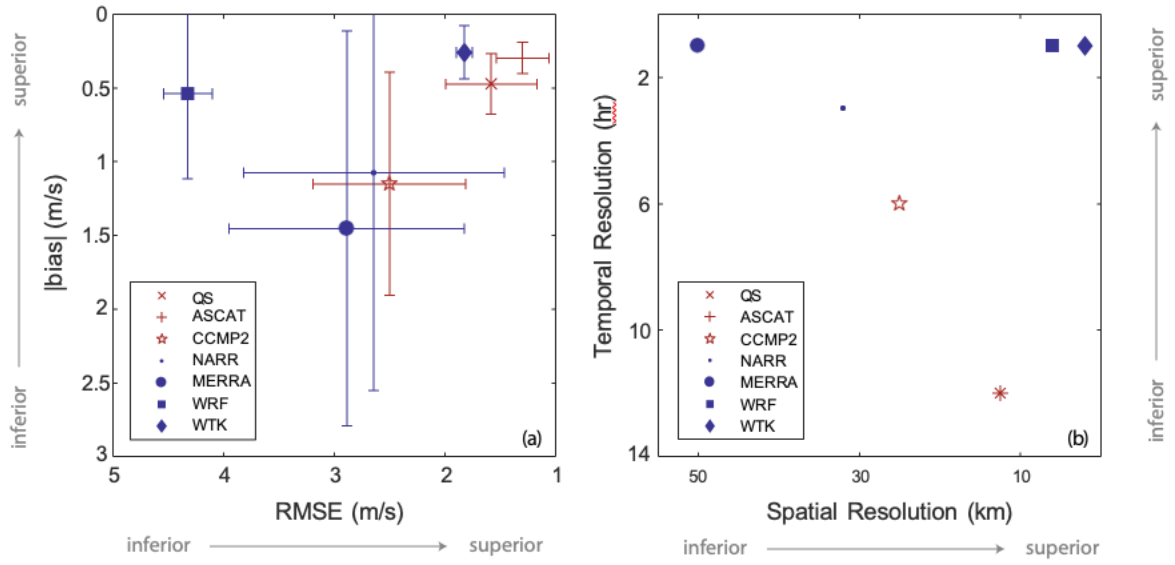

Figure 2.7. Pairwise tradeoffs in relation to different factors for seven datasets.
Note: Blue color represents the data availability aloft, while red color represents no data available aloft. (a, left panel) The absolute value of the bias and RMSE. The markers represent the mean and the error bars represent one standard deviation from the mean. (b, right panel) The temporal and spatial resolution. QS and ASCAT have the same temporal and spatial resolution so they are overlapping in the panel (b). For the MERRA data, we show the spatial resolution in the latitudinal direction (see Table 2.1).

2.3.5 Spatial and temporal variations of wind speed over a wide area

Based on the point-to-point comparison and the tradeoff analysis, the WIND Toolkit appears to be the best dataset for offshore wind power applications and can better estimate wind speeds daily and seasonally over a wide area. Figure 2.8 displays the average 10-m wind speeds at different hours and over four seasons from 2007 to 2013 using WIND Toolkit. Similar to the three buoy sites, other areas across the central California region are characterized by strong diurnal (weaker in the morning and stronger in the evening) and seasonal (stronger in spring and weaker in fall) variability in the wind speed. The diurnal cycle is enhanced during spring and summer months, relative to fall and winter months, consistent with data from the three buoy sites shown in Figure 2.2. Figure 2.8 also highlights the local maxima of wind speed near the complex topography of Point Conception.

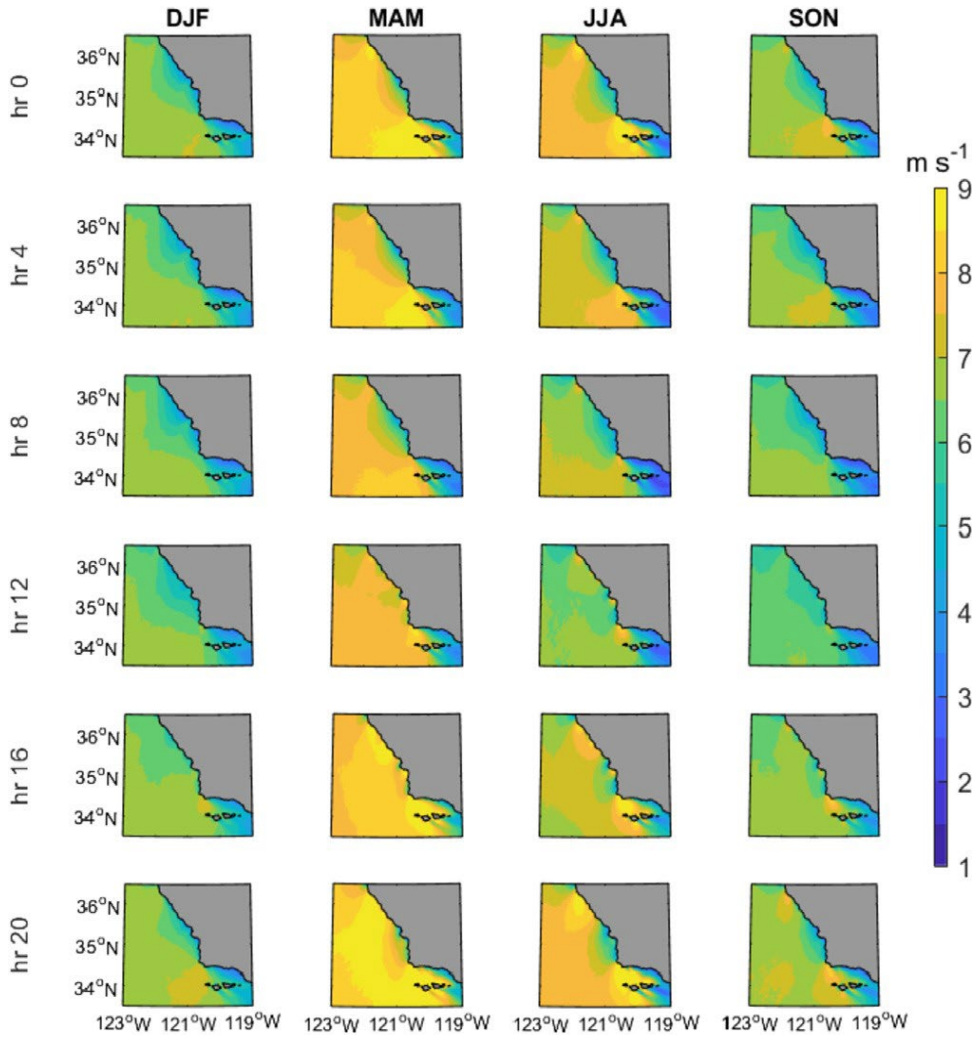

Figure 2.8. Averages of the hourly 10-m wind speed from WIND Toolkit over 2007–2013 at different hours and four seasons.

Note: Each column from the left to the right represents winter (December-January-February, DJF), spring (March-April-May, MAM), summer (June-July-August, JJA), and fall (September-October-November, SON). Each row from the top to the bottom represents 00 PST, 04 PST, 08 PST, 12 PST, 16 PST, and 20 PST.

2.3.6 Characteristics of wind direction

We also assessed the climatology of near-surface wind direction at the local buoys and in comparison with the other wind datasets. We present wind direction in terms of where the wind is coming from in degrees clockwise from true north (i.e., 0^0 wind direction indicates a wind coming from the north and blowing to the south). To account for the direction difference due to the discontinuity between 0^0 and 360^0, and to quantify the direction difference between -180^0 and 180^0, the wind direction from the respective dataset (q_O) relative to the buoy data (q_B) was modified following Pensieri et al. 2010. First, we computed the wind direction difference (q_O e q_B). When q_O e $q_B > 180^0$, q_O ¼ $q_O - 360^0$ and when q_O e $q_B < -180^0$, q_O ¼ q_O þ 360^0. With the modified q_O, the wind speed difference was calculated as q_O e q_B.

Based on the time period of 1998–2016, winds measured at the three buoys are predominately northwesterly (i.e., along-shore equatorward) (see wind rose histograms in Figure 2.9). Persistent, but variable in magnitude, northwesterly winds are closely linked to large-scale pressure systems and the interaction between air flows and topography along the coast (e.g., Fewings et al. 2016). At the site

46054, near- surface winds have more westerly components than the other two sites, resulting from steering by the adjacent coastline that is oriented in the E-W direction near the Santa Barbara Channel. Examination of the diurnal cycle shows a more northerly component in the early morning, followed by a more westerly component in the afternoon (not shown), consistent with local sea breezes along the Central Coast (e.g., Walter et al. 2017).

The error metrics (bias and RMSE) of wind direction from paired data are shown in Table 2.4. Most of the datasets reveal a positive (i.e., clockwise) bias, with the exception of ASCAT at 46011 and 46054 and NARR at 46054. Similar to the wind speed analysis, the two scatterometers (QuikSCAT and ASCAT) and WIND Toolkit display the best overall performance in terms of bias and RMSE for wind direction. QuikSCAT has the lowest bias in wind direction at 46011 and 46054. ASCAT has the lowest bias in wind direction and the second lowest RMSE at 46028. WIND Toolkit has the second lowest bias and the lowest RMSE at all three sites.

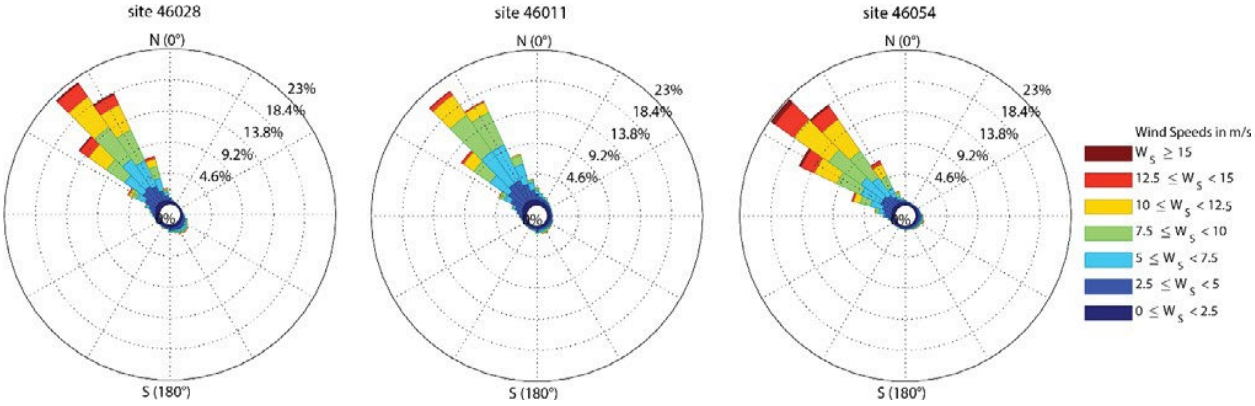

Figure 2.9. Wind rose histograms using data from 1998 to 2016 for the three buoys considered in this study (46028, 46011, and 46054 from left to right, respectively).
Note: The direction shown is the direction from which the wind is coming from in degrees clockwise from true north (i.e., 0^0 wind direction indicates a wind coming from the north and blowing to the south).

2.4 Discussion and conclusion

This study provides a comprehensive evaluation of near-surface wind datasets along the central region of the California coast, ranging from south of Monterey Bay to north of Point Conception. This particular region has received considerable interest in the development of offshore wind farms due to its strong, steady winds and existing connections to the State's electrical grid. This study provides the first known assessment of various wind datasets in this region over both seasonal and diurnal time scales, both of which are critical for accurate assessment of offshore wind power production but are seldom considered at the same time by previous studies. In addition, this study provides a framework by which to assess spatiotemporal variations among various datasets for a particular region, including comparison of error metrics over both seasonal and diurnal time scales and tradeoff analysis. This framework can be applied to other regions e using the five factors we focused on and possibly others of importance e where accurate estimates of wind speed are needed to evaluate wind energy potential as well as other needs.

We examined near-surface wind fields from seven datasets, including satellite observations, reanalysis products, and regional model output. For each dataset considered, we found no common pattern of bias and RMSE at all local buoy sites on certain hours of the day or months of the year. Overall, the two scatterometers, QuikSCAT and ASCAT, showed the best performance relative to the in-situ buoy measurements. However, the coarse temporal resolution (i.e., two measurements per day) and spatial

resolution (12.5 km) of these datasets limits their applicability for offshore wind power assessment, particularly since this region experiences strong diurnal wind forcing and strong spatial gradients in the wind field. On the other hand, WIND Toolkit was one of the most highly resolved datasets (1 h temporal and 2 km spatial resolution), and performed nearly as well as the scatterometers in the various error metrics we assessed. Moreover, the WIND Toolkit has wind data available above the surface and at potential turbine hub heights, which could obviate interpolation and extrapolation techniques needed with other data products (Carvalho et al. 2017). Site-specific assessments should consider tradeoffs between spatiotemporal resolution of the underlying dataset, error metrics relative to local buoy measurements, and the availability of data at hub height when assessing various data products for offshore wind energy assessments and power calculations. With consideration of these factors, the WIND Toolkit appears to be the best dataset for the central California region. Due to the lack of wind observations at altitudes greater than 5 or 10 m in this region, it is challenging to evaluate offshore wind power potential at hub height (i.e., heights of at least 100 m above the sea surface based on current technologies), which is a critical factor considered for future offshore wind siting and development. Since the surface wind distribution can provide the implications for wind distribution at hub height, future work will focus on the calculation of wind power generation at hub height from the WIND Toolkit under different scenarios both spatially and temporally.

Finally, tradeoff analysis is a useful graphical tool for comparing the relative performance of a set of options in relation to multiple objectives. Grounded in Portfolio Theory (maximize return, minimize risk of financial investments (Markowitz 1952)), we applied tradeoff analysis to factors important to offshore wind power applications. This analysis revealed the overall superior value of WIND Toolkit (in relation to the prescribed factors), and more generally demonstrated a framework that could be used for evaluating wind data-sets in other regions. Furthermore, the tradeoff analysis framework is adaptable, allowing for integration of additional factors important to offshore wind power applications, including potential impacts of wind energy development on the marine ecosystem (White et al. 2012 and Farr et al. 2017). In such cases the tradeoff analysis axes can be expanded to include these factors, and relative weights can be applied to the factors, in order to help identify development options that most effectively represent the socio-economic priorities in the system (Dong et al. 2017).

3 Spatial and temporal variation of offshore wind power and its value along the Central California Coast

3.1 Introduction

Renewable energy production has accelerated in recent years, representing a substantial proportion of broader energy portfolios (Graabak and Korpas 2016). Offshore wind energy in particular has grown significantly because it offers several advantages over land-based winds and solar energy, including stronger and more consistent winds over the ocean, and less likely to impact other land-use activities (Sun et al. 2012). To date, most wind farms are installed in relatively shallow waters (< 50 m) using fixed foundations (Musial et al. 2016). However, technology is rapidly advancing, and floating wind farms are being deployed worldwide in deeper waters (e.g., 120 m depth) farther from shore (GWEC 2018). In 2017, the first demonstration-scale floating offshore wind farm (Hywind) began operation off the Scotland coast (Equinor 2018). Several other deep, offshore floating wind farms are under development or in the planning phase in other regions of the world (GWEC 2018), including in the United States off the California Coast (BOEM 2019).

To guide the evaluation and optimal planning of offshore wind energy, it is critical to consider both spatial and temporal variability in energy production across a range of scales (Lee et al. 2018). Offshore winds, such as along the California Coast, vary on interannual, seasonal (peaks in the spring), synoptic, and daily time scales (peaks in the early evening), in addition to being spatially variable (Walter et al. 2018; Wang et al. 2019). This spatiotemporal variability becomes critical in estimating power production since the power produced by a turbine depends on the cube of the wind speed, a nonlinear relationship that amplifies the effects of small changes in wind speed. Moreover, temporal variability of wind power impacts its value within electricity markets (Fripp and Wiser 2008). For example, the economic value of offshore wind production along the East Coast of the United States varies with time and space, driven by electricity pricing and production fluctuations (Mills et al. 2018). The value of offshore wind to a broader energy portfolio (including both renewable and non-renewable sources) is driven by both the seasonal and daily variability in power production from wind and the other sources, as well as seasonal and daily variations in grid demand for power (Fripp and Wiser 2008; Sinden 2007; Wiser et al. 2017). Alignment between production and demand over seasonal and daily time scales is thus critical for reliability and functionality of the grid system (Shaner et al. 2018). However, these factors are not specifically considered by previous studies when assessing the value of power produced (e.g., Mills et al. 2018 and references therein).

Despite its importance, at the time of initial publication of this work, areas for offshore wind commercial development had been commonly identified based on annual wind speed, without considering temporal variability of the wind (Marine Scotland Science 2018). The approach of averaging higher-frequency temporal variability has the potential to lead to significantly biased power estimates (Karnaukas et al. 2018). Considering the role of seasonal and daily variations in power production in the grid system, spatial patterns of offshore wind speed across seasonal and daily time scales are documented by Wang et al. (2019); however, realistic power generation estimates are missing, making it difficult to assess their value. Previous studies that consider variations in offshore wind power generation either considered the spatial patterns of temporal variability on time scales longer than the diurnal cycle (e.g., Dvorak et al. 2012; He et al. 2014; Hong and Moller 2011) or the daily and seasonal variability subjected to specific spatial points like buoy sites or spatial aggregation over a domain (e.g., Musial et al. 2016; Stoutenburg et al. 2010). As more offshore wind projects are proposed, a comprehensive analysis of offshore wind power patterns over spatial, diurnal, and seasonal scales is needed.

This study aims to assess the spatial and temporal patterns of potential offshore wind power production along the Central California Coast. This region is ideal for offshore wind development because wind speeds are generally strong (albeit highly variable); there are existing nearby connections on land to the State's electrical grid; much of the coast is outside of currently-designated national marine sanctuaries where disturbance to the seabed is prohibited; and the region is between major population centers with high power demand in Northern and Southern California (see Figure A1 for geographic information/details). Consequently, the Central Coast contains two of three sites proposed by BOEM, the agency that manages lease requests in U.S. federal waters, for offshore wind development in California (BOEM 2019). Moreover, California has enacted laws mandating ambitious goals of providing 60% renewable energy by 2030 and 100% by 2045 (SB-100, California Renewables Portfolio Standard Program). These laws will require California to diversify its renewable energy portfolio, and offshore wind will likely be a part of this energy mix. A detailed study of the variability of offshore wind power will improve the accuracy of power estimates to inform decision makers and also provide a framework to assess power generation and its compatibility to meet grid demand with other energy resources in future projects.

This study shows how power production and its value varies seasonally and daily along the Central California Coast, and further highlights the added benefit of considering temporal variation in wind speeds by comparing power production estimates from hourly wind speed data with those calculated using annual mean wind speeds. We compare the diurnal and seasonal patterns of offshore wind power production to diurnal and seasonal patterns of power demand across the State of California, as well as to power production from other renewables such as solar and land-based wind. We use the relative alignment between the power production of the various renewables and demand to calculate a demand-based value. Finally, we consider daily and seasonal fluctuations in recent wholesale prices of power to generate an estimate of the wholesale dollar value of power produced. The framework by which we assess spatial and temporal patterns in offshore wind energy production and its value can be applied to other regions where offshore wind is being considered.

3.2 Data

WIND Toolkit is a simulated historic dataset for wind power application developed by the National Renewable Energy Laboratory (https://www.nrel.gov/grid/wind-toolkit.html). The model is based on a Weather Research Forecast regional model, details of which can be found in Draxl et al. (2015a; 2015b). The model's spatial resolution is 2 km and its availability spans from 2007 to 2013. WIND Toolkit provides hourly winds from 10 m to 160 m above sea level at approximately 20 m intervals, as well as other meteorological data (https://github.com/NREL/hsds-examples). WIND Toolkit's 10 m wind speed and direction data were validated against buoy measurements along the Central California Coast, and WIND Toolkit was determined to be the best dataset for offshore wind energy production estimates for the region (Wang et al. 2019).

Given the lack of observational datasets at altitude with an appropriate spatiotemporal resolution to assess error metrics, we assume that model performance aloft (i.e., at hub height) is comparable to the model performance near ocean surface (see Wang et al., 2019 for details on model validation). Because the WIND Toolkit does not provide hub-height air density, we used the North American Regional Reanalysis (NARR; https://www.esrl.noaa.gov/psd), which is available from the surface to top of the atmosphere over three decades and provides needed parameters for air density calculations, to help estimate hub-height air density (Appendix A).

For assessing electricity demand and power generation from other renewable sources, we obtained hourly-averaged historic data of power generation from every energy resource in California assessed by the California Independent System Operator (CAISO)

(http://www.caiso.com/market/Pages/ReportsBulletins/RenewablesReporting.aspx) (Supplemental Material). We calculated hourly demand by summing all of the sources of power production.

CAISO data also allows us to assess patterns of energy production from other renewables, including land-based wind, which typically have hub heights between 80 m and 100 m high (WINDExchange 2019), and solar production. Here, solar production includes both photovoltaic (PV) and thermal generation; they are grouped together in the CAISO data even though PV solar provides the vast majority of solar energy production. We note that there is a positive trend of solar production since 2012 due to growing development of commercial and residential PV solar in California (Figure A2). In comparison, development of land-based wind facilities has been relatively modest and no long-term trend is found for electricity demand in the State (Figure A2). The pronounced trend in solar production leads to biases when considering seasonal variations. To reduce long-term trends and to focus on current renewable production and demand, we use only the most recent year of CAISO data, 2018. We use power production data from CAISO rather than modeling onshore wind or solar production, since CAISO data provides accurate estimates of actual power produced over this time period.

3.3 Methods

3.3.1 Wind power production calculation

Although WIND Toolkit provides power estimates using a generic power curve with a rated power of 2.0 MW (e.g., King et al., 2014), this particular power curve does not capture recent advancements in turbine technology for offshore wind (Musial et al. 2016). For example, the proposed wind farms in California plan to use at least 10 MW turbines (Trident Winds 2016). Therefore, we estimated power using the power curve of the 10 MW turbine with the 125 m hub height from Musial et al. (2016) (Figure A3), which is the largest rated wind turbine in their study. The temporal and spatial patterns, as well as major conclusions, were similar using the 8 MW turbine (not shown).

We estimate wind speeds at the hub height of the 10 MW using a power law interpolation following Draxl et al. (2015a). We calculated the power law exponent at each spatial point each hour using wind speeds at two adjacent altitudes (120 m and 140 m), and then obtained the hub-height wind speed with the calculated power law exponent and the 120 m wind speed. Considering temporal and spatial changes in the exponent yields more accurate wind speeds than using a constant exponent value (Holt and Wang 2012).

To incorporate air density variations, we estimated air density at hub height using the NARR data and then used hub-height air density with the interpolated wind speed at hub height and the turbine reference density to obtain an effective wind speed at hub height following IEC (2005) (Supplemental Material). With the effective wind speed at hub height, we estimated power production using the 10 MW power curve.

3.3.2 Calculation of composite averages and demand-based relative value

To assess the daily and seasonal patterns of offshore wind, land-based wind, and solar power production, as well as power demand, we calculated composite averages of power ($power_{ij}$) for each respective source (offshore wind, onshore wind, and solar) and demand ($demand_{ij}$) over all hours (i) in a given month (j) (i.e., averages fixed to 24 hours over each of the 12 months). For offshore wind, we calculated these composite averages at every spatial point (2 km resolution) in our study domain. For the land-based wind, solar, and grid demand, we calculated this for the single time-series aggregated across the State of California. Note that the CAISO data (2018) and the WIND Toolkit data (2007–2013) are available during different time periods, but we assume that the offshore wind field composite averages created

using the seven years of available data are representative of typical offshore wind conditions and are less impacted by interannual variability.

We develop a demand-based measure of relative energy need, which quantifies the relative alignment of composite averages of production with those of demand, while still capturing seasonal and daily variability. This method does not consider absolute magnitudes of the various production sources and demand, but rather enables us to compare the temporal alignment between production and demand for different sources of production. This is particularly applicable in areas like the Central California Coast, where there is currently no offshore wind power production so the magnitude of production is unknown, and yet stakeholders need estimates of the value of offshore wind projects to evaluate their feasibility. To calculate the demand-based relative values, we first normalized composite averages of power ($\overline{power}_{ij}$) and demand ($\overline{demand}_{ij}$) by dividing each respective curve by the maximum over all months and hours of each respective curve, such that each respective curve varies between 0 and 1. Demand-based relative values at a given hour (i) and month (j) are then obtained by multiplying the respective normalized power by the normalized demand:

$$value_{ij} = \overline{power}_{ij} \; x \; \overline{demand}_{ij}. \quad (1)$$

When a normalized production composite aligns with the normalized demand composite at a given time of the day and month, then the demand-based relative value is high, and vice-versa.

3.3.3 Calculation of wholesale value

To assess the monetary value of offshore wind power, we match wholesale energy prices with the average hourly offshore wind power production over the seven-year dataset at every spatial point. Wholesale prices are based on hourly day-ahead prices for the ZP 26 Central California hub in 2018 from CAISO. We rely on 2018 wholesale prices for the most recent complete year of price data available. Given the recent trend in solar power development in California, diurnal wholesale prices have changed considerably in recent years toward a pattern with a more pronounced trough in mid-day energy prices, which makes 2018 prices appropriate for measuring the current value of offshore wind energy.

3.4 Results

3.4.1 Spatiotemporal variations in offshore wind power production

Offshore wind production along the Central California Coast peaks during the evening hours across all seasons and shows seasonal maximums during the spring and summer (Figure 3.1). This daily and seasonal variability is consistent with that of wind speeds at hub height (Figure 3.1, Figure A4). Spatial patterns show lower production close to the coastline where wind speeds are lower and higher production further from the coastline and in the region around Point Conception (cf. Fewings et al 2016).

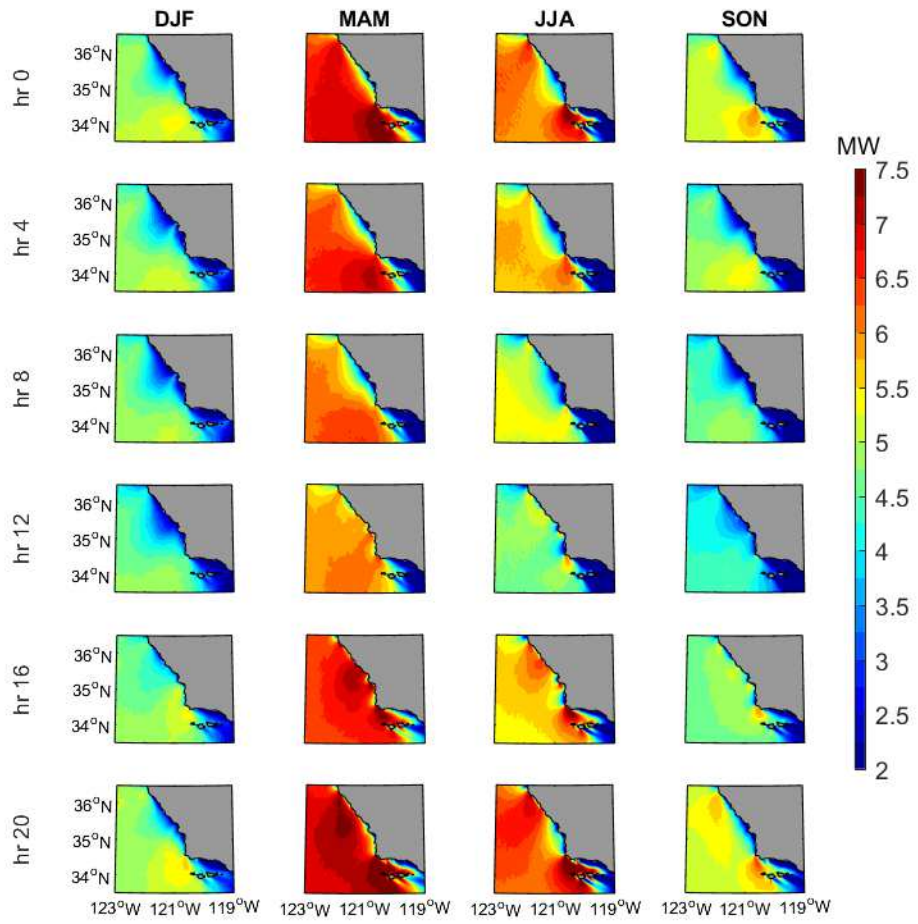

Figure 3.1. Averages of the hourly wind production based on the NREL's 10 MW wind turbine from WIND Toolkit over 2007–2013 at different hours and four seasons.
Note: Each column from the left to the right represents winter (December-January-February, DJF), spring (March-April-May, MAM), summer (June-July-August, JJA), and fall (September-October-November, SON). Each row from the top to the bottom represents 00 PST, 04 PST, 08 PST, 12 PST, 16 PST, and 20 PST.

3.4.2 Impact of using mean wind speed on production estimates

We average hourly power production at each spatial point to examine spatial variation in mean power production (Figure 3.2a); the magnitude of spatial variation at a given point in time is relatively modest compared to hourly or seasonal variation (Figure 3.2a and Figure 3.1). Although mean power production provides a general picture of power potential, the conventional approach to identify areas with abundant wind resources is based on mean wind speed, not energy production. To illustrate the impact of using mean wind speed, instead of a time series of wind speed, for estimating power production, we compared the power production using annual mean wind speed with the mean power production estimated from hourly wind speed (Figure 3.2b and Figure 3.2a). We found the conventional approach to underestimate power production by over 1 MW near the shore (Figure 3.2c), which is approximately 10% to 50% lower than the mean power production calculated from hourly wind speed (Figure 3.2d). Further offshore, the conventional approach overestimates power production by as much as 0.5 MW (~30% higher than the mean power production calculated from hourly wind speed).

The bias from using mean wind speed is magnified when the power production using annual mean wind speed is compared to averaged power production estimated from hourly wind speed during different hours and seasons (Figure A5). These results indicate that the mean wind speed is unable to characterize temporal variability of wind power production and can lead to both positive and negative biases in mean power estimates.

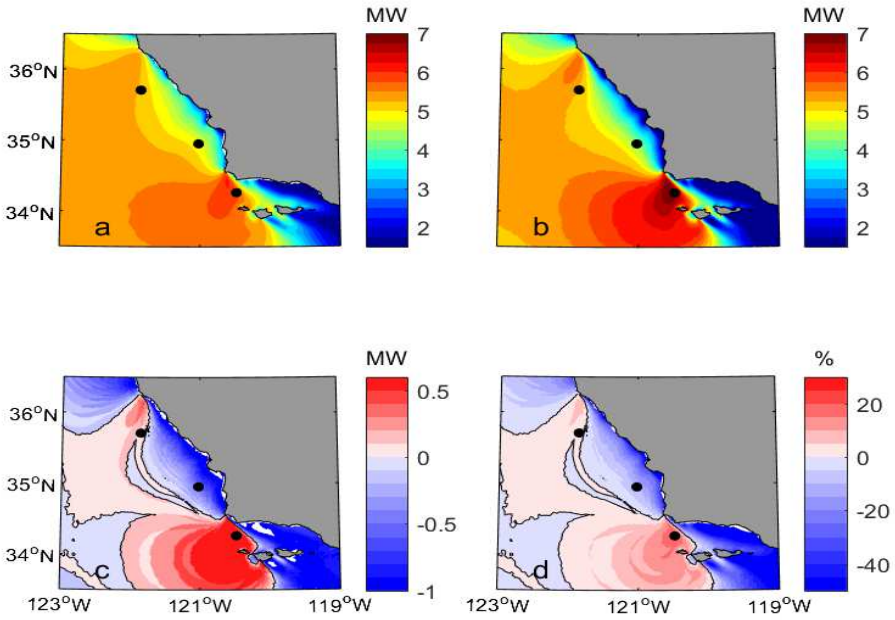

Figure 3.2. (a) Mean wind power production using hourly power production over the 2007–2013 period. (b) Wind power production calculated from mean wind speeds over the same period as (a). Both productions are based on the NREL's 10-MW power curve. (c) The absolute difference between (b) and (a) (b-a) in which 0 MW is marked by black contours. (d) The percent difference between (b) and (a) in relation to (a) [(b-a)/a] in which 0% is marked by black contours. Local buoy sites are displayed by black circles in all plots.

3.4.3 Temporal variation in electricity demand and production from renewable resources

To investigate the relationship between the temporal variability of offshore wind power, and other renewable sources, in relation to the temporal variability of demand, we displayed hourly composite averages in each month for electricity demand (black), production for statewide solar (red), statewide land-based wind (green), and offshore wind at the spatial point closest to the buoy site 46028 (blue) (Figure 3.3). The specific point is chosen for demonstration due to its proximity to the area where industry is pursuing development. The daily and seasonal patterns of wind power generation at this point are consistent with those aggregated over the entire study domain of interest (Figure A6). Each respective quantity has unique diurnal cycles, which evolve throughout the year (Figure 3.3). Overall, electricity demand is higher in the summer than the winter due to more air-conditioner use on high temperature days (CEC 2017).

While there are two high demand periods during the day in winter months, one that is relatively lower at around 8:00 am and a second that is relatively higher at around 7:00 pm, there is one peak around 6:00 pm in summer months (Figure 3.3). Like electricity demand, solar and land-based wind generation have their seasonal peak in the summer. For diurnal cycles, solar and land-based wind generation show opposite behaviors, particularly during non-winter months: solar peaks around noon, whereas land-based

wind peaks around midnight. Although solar and land-based wind are important contributors to supply electricity at different times of the day, neither of them peak in generation at a time of day coincident with peaks in demand. Conversely, offshore wind power generation aligns well with daily peak demand (i.e., daily peak at 7-8:00 pm, depending on the month). Note that the timing of daily peak offshore wind generation coincides with the evening hours when net demand (demand minus wind and solar production) ramps up quickly (Figure A7), highlighting the potential of offshore wind generation to accommodate high ramp rates and reduce solar curtailment.

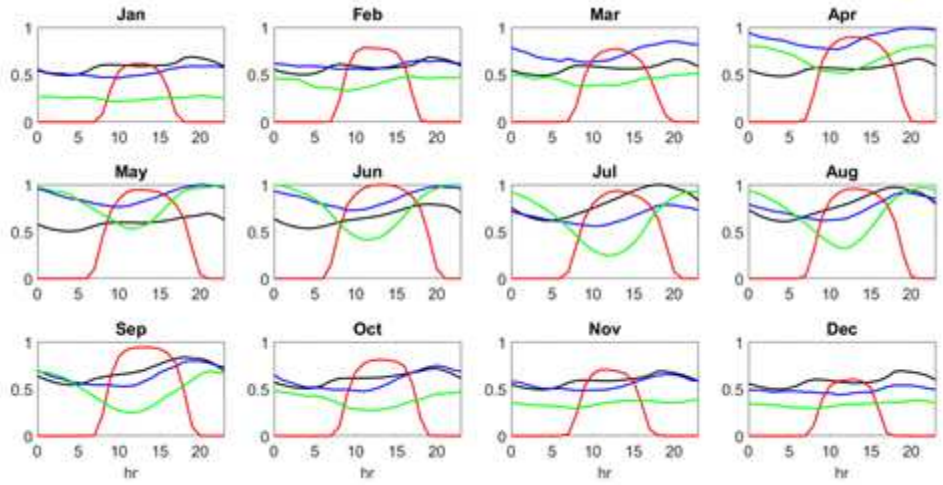

Figure 3.3. Daily composite averages of hourly California electricity demand (black), solar production (red), onshore wind production (green), and offshore wind production near 46028 (blue) in each month (see text for details).
Note: Composite averages are normalized by the maximum over all months and hours of each respective curve. Data from CAISO (http://www.caiso.com/market/Pages/ReportsBulletins/RenewablesReporting.aspx)

3.4.4 Temporal variation in demand-based value of offshore wind production

The value of a power source depends not only on its production, but also the relationship between power produced and electricity demand (Sinden 2007). To factor in temporal correspondence between power and demand, we calculate a demand-based relative value of energy at each hour in each month for each respective renewable energy source. This approach illustrates the relative value of power produced at various times during the day by giving more weight to power produced during high demand periods, and vice versa.

The demand-based relative value of each of the renewables considered showed a different daily and monthly pattern compared to its power production composite average (cf Figures 3.3 and 3.4). For example, peak solar generation occurs in June at noon, whereas its peak demand-based value occurs in July/August at 4 pm. Land-based wind also shifts, from peak generation in June at midnight to peak value in August at 10pm. Offshore wind also shifts, but mainly seasonally, from the spring to the summer. Of the three renewable energy sources considered, offshore wind demonstrates superior temporal alignment with demand and hence has the largest demand-based value.

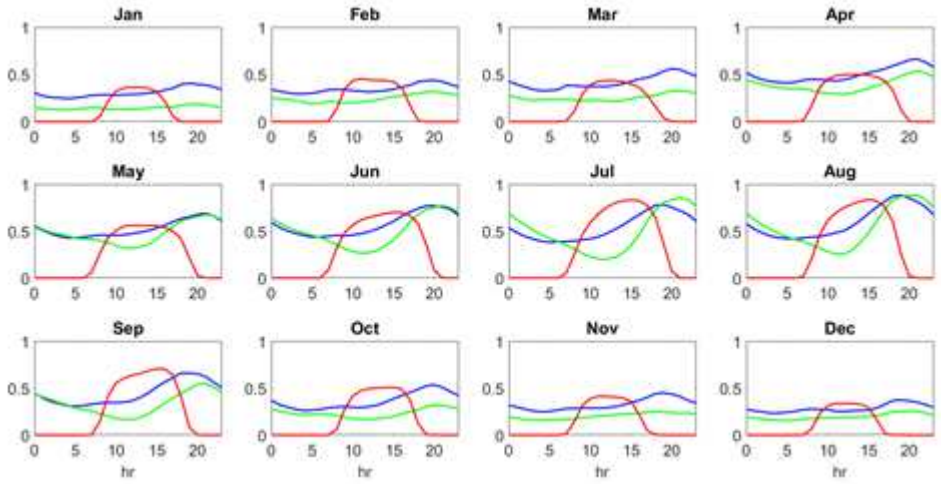

Figure 3.4. Hourly demand-based values (Equation 1) of solar production (red), onshore wind production (green), and offshore wind production near 46028 (blue) in each month.

To further understand the seasonal variations in demand-based values and their spatial dependence, we calculate monthly average demand-based values by averaging composite-average hourly values over a given month for each renewable. This monthly average demand-based value also represents the proportion of full-capacity power production that is perfectly aligned with full constant demand in a given month. Figure 3.5 shows maps of monthly average demand-based values of offshore wind generation along with that of solar (solid line) and land-based wind (dashed line) generation. Although the value of offshore wind generation displays monthly and spatial variability, it is higher than that of solar and land-based wind throughout the year. In winter months, offshore wind is two to four times more valuable than solar and land-based wind generation over most areas. Although solar and land-based wind have higher values in summer than winter, they are still smaller than offshore wind over most areas. In general, offshore wind power production along the Central California Coast is better suited to meet demand than existing major renewables.

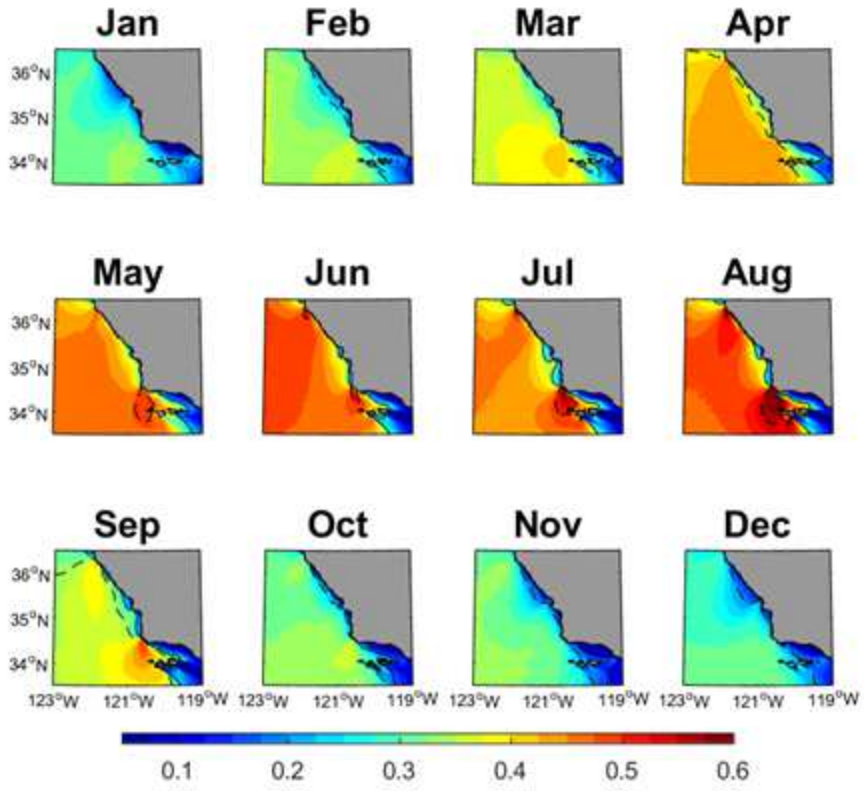

Figure 3.5. Monthly average demand-based values for offshore wind production shown in color (see text for details), for statewide solar production shown as solid contours and statewide land-based wind production shown as dashed contour (contours are typically very close to shore).

3.4.5 Temporal variation in wholesale value of offshore wind production

We also assess the relationship between power production variability and local pricing variability, the latter of which is influenced by a number of factors such as demand variability, outages of electrical facilities, and fluctuation of other forms of power generation (Woo et al. 2016 and references therein). Figure 3.6 shows the average of hourly wholesale value of offshore wind production at every spatial point over different hours and seasons. Due to strong variations in pricing, wholesale values of offshore wind show more extreme daily and seasonal changes than power production (cf Figure 3.1 and Figure 3.6). The wholesale value of power is close to zero on a typical spring noon driven by overgeneration from solar (e.g., Denholm et al. 2015), whereas it peaks during evening hours when solar generation is low and demand is high. Note that the diurnal and seasonal patterns of the wholesale value change quantitatively, but not qualitatively, using other years (Figure A8). This metric indicates the time-varying economic benefits of offshore wind that can inform stakeholders in offshore wind projects.

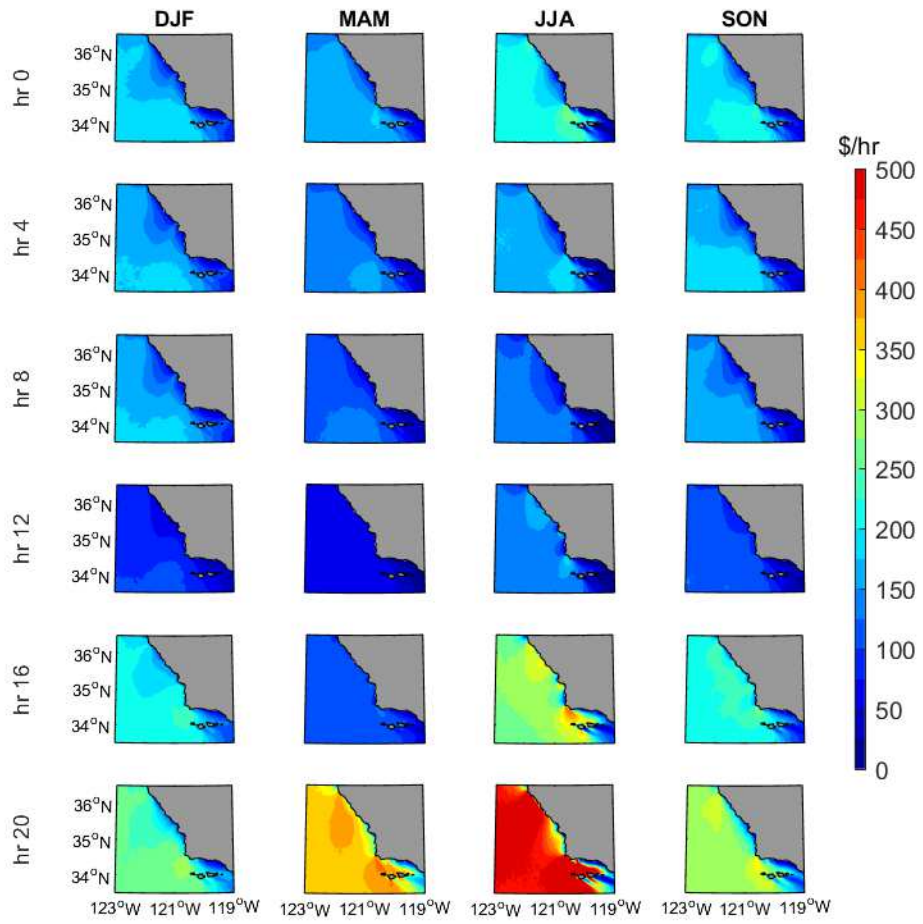

Figure 3.6. Similar to Figure 3.1, but for wholesale values of offshore wind power production using the pricing data in 2018.

3.5 Discussion and Conclusion

We calculate the diurnal and seasonal pattern of offshore wind power produced across the Central California Coast and the value of wind power based on future wind turbine specifications and current wholesale energy prices. Like wind speed, offshore wind power production increases during evening hours and is maximized in the spring and summer months. Power production is lower near the shore and higher further offshore.

We show that understanding the daily, seasonal, and spatial variations in offshore wind power can benefit planning and management of commercial development. We demonstrate that using annual mean wind speed for power production estimates leads to significant biases compared to using a time-varying wind speed for power production estimates. These biased wind resource assessments could mislead decision making in an offshore wind project and lead to suboptimal site choices. We also found the timing of daily peak offshore wind production across the Central California Coast to better align with daily peaks in State demand compared to statewide solar generation and land-based wind generation. This close temporal alignment between production of offshore wind and demand highlights the important role offshore wind

power could play in filling the supply gap when other forms of renewable generation are low and demand is high.

To quantify the value of power generation, we developed useful metrics from two contexts—a demand-based value which measures power production variability in relation to demand variability, and a wholescale value which measures power variability in relation to local wholesale pricing variability. Both metrics contextualize the value of offshore wind energy along the Central California Coast as the State of California works toward meeting its renewable energy portfolio target.

Due to the availability of certain data in certain years (see Methods), we use composite averages to yield robust diurnal and seasonal patterns of power and demand (Fripp and Wiser 2008) and to further obtain that of demand-based relative values. Yet, in real life, power systems balance electricity generation and demand instantly; thus, their simultaneous relationship at higher-frequency time scales (e.g., hour-to-hour variability) is important (e.g., Schill 2014; Brown et al., 2018; Koivisto et al., 2018) and should be considered in future work. Moreover, due to the lack of development of offshore renewable energy in California, the cost of offshore wind energy development remains largely uncertain. Hence, this study did not perform a full economic analysis, since we have no information about the cost involved in offshore wind farm construction and operation, policy incentives associated with siting locations, or losses caused by transmission and other reasons in our power estimation. Instead, we focused on the variability of offshore wind values in relation to the daily and seasonal variability of electricity demand and other primary renewable generation to highlight the revenue potential of offshore wind energy production at different time scales.

In summary, daily and seasonal variation in offshore wind power generation across space is of great importance and should be investigated in detail. While we focused on offshore wind power and its value along the Central California Coast in particular, this study also serves as a framework that is easily applicable to offshore wind development elsewhere. Our analysis of power production variability and metrics of values can be adopted separately and combined with other analyses.

4 Scenarios for offshore wind power production for Central California Call Areas

4.1 Introduction

California is taking a leading role in the U.S. to reduce greenhouse gas emissions and address the climate crisis by setting ambitious goals to provide 60% of its electricity from renewables by 2030, and 100% by 2045 (SB-100, California Renewables Portfolio Standard Program). To achieve these goals, the State has incentivized commercial and residential solar energy production, along with commercial onshore wind farms. However, these renewable energy sources alone may not be sufficient to meet California's growing electricity demand. For example, the daily peak in demand occurs in the evening as solar production wanes close to zero. Likewise, the trend toward electric heating (e.g., instead of gas) is expected to increase electricity demand in winter when there is less solar production (e.g., Denholm et al. 2015). To achieve the State's energy targets during all times of the day and throughout the year, California has begun exploring ways to diversify its energy portfolio, including using offshore wind (e.g., Collier et al. 2019).

Offshore wind deployment is increasing in many parts of the world, supplying up to 10-15% of electricity in locations such as the United Kingdom (U.K.) and Denmark (IEA 2019). Compared to Europe and China, the U.S. has developed offshore wind more slowly (e.g., deCastro et al. 2019), with only a single operating commercial offshore wind farm (Block Island in Rhode Island), several others in the planning stages on the East Coast, and none in California or the U.S. West Coast in 2021, in spite of abundant offshore wind resources in both the East and West Coast (e.g., Costoya et al. 2020). However, industry and policymakers are currently exploring the potential for offshore wind development in California, likely using floating wind turbines due to the steep bathymetry and higher potential wind power further offshore in waters too deep for fixed-platform turbines. The Central California Coast—defined here as the area north of Point Conception and south of the Monterey Bay National Marine Sanctuary, and from 3 nautical miles (nm) from the coast (i.e., federal waters) in the east to the 1200 m isobath in the west (i.e., current proposed upper limit for floating turbine technology at this time)—has received considerable interest in the development of offshore wind energy. The Central California Coast has relatively strong offshore winds that align with the peak electricity demand and complement power produced by solar and land-based wind (Wang et al. 2019a; DeCastro et al. 2019). Much of the area is both within a developable depth (< 1200 m) and outside National Marine Sanctuary zones that would likely legally preclude development. There are existing grid connections, at the retired Dynegy Power Plant in Morro Bay and at Diablo Canyon Nuclear Power Plant near Point Buchon, that may facilitate transmission and reduce the need for additional infrastructure (Beiter et al. 2020). The region also sits between major population centers in Southern California and the San Francisco Bay area with high electricity demand. Partly as a result of these reasons, BOEM, the federal agency responsible for permitting and leasing these types of projects, partnered with the State of California to delineate two 'Call Areas', the areas for commercial wind leases, off the Central California Coast for potential offshore wind energy development (Figure 4.1; BOEM 2020).

Recent work explored offshore wind energy resources along the Central California Coast, examining potential power production and the utility and value of that power. Dvorak et al. 2010 divided the coast in California into three geographical regions (i.e., Northern, Central, and Southern California) and assessed the annual energy production of each region. Musial et al. 2016 estimated the long-term offshore wind power produced by a hypothetical wind farm near the Morro Bay Call Area and in five other reference areas in California. Wang et al. 2019a assessed spatial and temporal patterns of wind speeds in the region over daily, seasonal, and annual time scales. Subsequently, Wang et al. 2019b quantified temporal variation in the potential power that could be extracted from those winds by offshore wind turbines, and

valuation of that power in relation to its alignment with statewide demand for power and wholesale value. Recently, Beiter et al. 2020 estimated offshore wind energy production across California's Call Areas by four turbine types, including the latest projected 15-MW turbine, and computed the cost of a large-scale (1000 MW) wind farm assuming a 7-rotor diameter by 7-rotor diameter (D) spacing. In the California Coast Call Areas, there have been proposals for pilot-scale, medium-scale, and commercial-scale projects, and thus the need for power production estimates for different wind farm sizes (Collier 2020). Additionally, no previous studies in the Central Coast Call Areas have combined detailed assessments of the temporal (daily and seasonal patterns) and spatial characteristics of power production while considering the latest turbine technology (i.e., hub height and power curve characteristics) different turbine spacing scenarios, and different wind farm size scenarios.

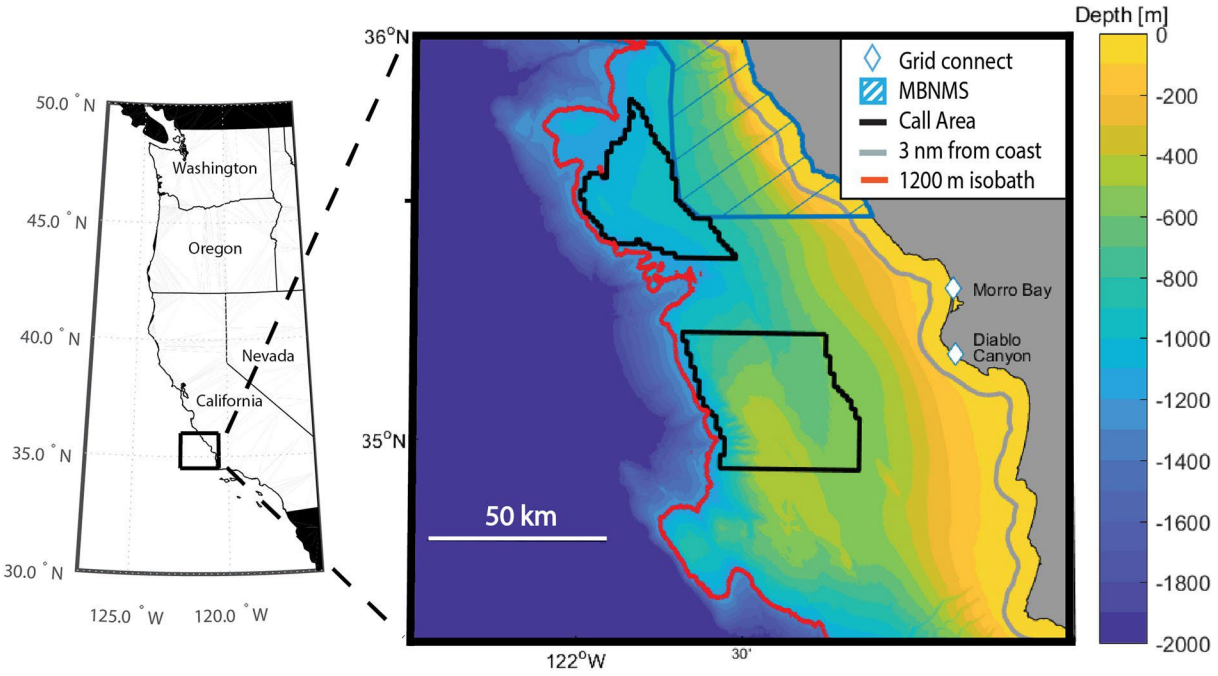

Figure 4.1. Bathymetry of the Central California Coast highlighting the two Call Areas.
Note: Black lines; Morro Bay Call Area to the north and Diablo Canyon Call Area to the south, the locations of existing state electrical grid connections (white diamonds, the Morro Bay Power Plant to the north and the DCNPP to the south), Monterey Bay National Marine Sanctuaries (MBNMS, dashed blue lines), and the 1200-m isobath (red line) and the 3-nm distance limit from the coast (gray line)

As technology and local interest from developers, regulators, and other stakeholders have increased, an updated and more comprehensive assessment of offshore wind resources within the Call Areas of the Central California Coast is needed. To meet this expanding need, this study aims to provide an accurate estimate of power production with reasonable future turbine design and spacing scenarios. We focused on the BOEM Central California Coast Call Areas ("Diablo Canyon" and "Morro Bay"; black polygons of Figure 1), since these are areas where offshore wind energy development is likely to occur. We evaluated a variety of scenarios for offshore renewable energy production and the potential ocean area occupied in the Call Areas using both 12 and 15 MW turbines, considering alternative wind farm sizes, different spacing scenarios, and daily and seasonal variations. These results will help inform potential stakeholders, policymakers, and citizens as to whether, how, and where to pursue offshore wind energy development in California.

4.2 Data and Methods

This study used the WIND Toolkit dataset, which provides hourly wind data during 2007–2013 from near surface to 160 m above the sea level in intervals of 20 m with a spatial resolution of 2 km between grid points (Draxl et al. 2015). The WIND Toolkit is among the best datasets for analysis in this region because of its high temporal (1 hr) and spatial (2 km) resolution, as well as its small error in comparison to buoy measurements along the Central California Coast (Wang et al. 2019a). While preparing this contribution, an updated wind resource dataset (CA 20) developed by NREL became available, which shows a 17.4% and 19.7% increase in the mean 100-m wind speed at the centroids of the Morro Bay and Diablo Canyon Call Area, respectively, from the WIND Toolkit (Optis et al. 2020). We chose the WIND Toolkit for analysis, because it was previously validated using a variety of statistical metrics against local Central California buoy measurements on different time scales, including daily and seasonal time scales, which have been shown to be critical for meeting grid demand and for the reliability and functioning of the grid system (Wang et al. 2019a; Wang et al. 2019b). Furthermore, a recently deployed (October 2020) offshore wind buoy in Central California equipped with LIDAR does not contain enough data, particularly over seasonal time scales, to validate hub-height wind speeds against the new dataset.

To estimate power generated by a wind turbine of interest, we interpolated wind speed to the hub height of the wind turbine, then adjusted the interpolated wind speed in relation to variation in air density, following Wang et al. 2019a. Finally, we converted wind speed to power production based on the respective power curve for turbine type. For more details regarding power generation calculation, see Wang et al. 2019b.

Since the wind energy industry expects to be deploying turbines with rated power between 12-15 MW within the next decade (Musial et al. 2019), we assessed power production using both 12 MW and 15 MW turbines (specifications shown in Table 4.1). Because engineering technology information of wind turbines for commercial development is proprietary, we used the power curves of 12 MW and 15 MW turbines estimated by the National Renewable Energy Laboratory (Figure 4.2) (Musial et al. 2019). These wind turbines generate no power when wind speed is below their cut-in wind speed, 3 m/s (5.8 kts). Power generation increases with wind speed from this cut-in speed until winds reach rated wind speed at 11 m/s (21 kts). Power generation remains at the rated level between the rated wind speed and cut-out wind speed at around 25 m/s (48.6 kts). When wind speed exceeds the cut-out wind speed, the wind turbines shut down to avoid damage and therefore produce no power. The power coefficient curve as a function of wind speed was plotted in Figure B1.

Table 4.1. Turbine specifications for 12 MW and 15MW turbines, adapted from Musial et al. 2019

Turbine Rated Power (MW)	12	15
Turbine Rotor Diameter (m)	222	248
Turbine Hub Height (m)	136	149

Following the evaluation of hub-height wind speed characteristics, we investigated temporal and spatial characteristics of potential power production in the BOEM Central Coast Call Areas. First, we explored spatial variation in mean power production and capacity factor across the entire Central Coast region. Capacity factor is defined as the ratio of actual power to the rated power that a turbine could produce in a given time period (e.g., He and Kammen 2014). The capacity factor of new offshore wind projects is expected to be around 50%.[3] In other words, a 12 MW turbine is expected to produce an average of about 6 MW of power over the course of a year. Considering the technological, geographical, and legal

constraints to development in the region (see Introduction), we investigated the Central California Coast study domain feasible for development defined by spatial points north of Point Conception (north of 34.5°N), outside National Marine Sanctuaries, 3 nm off the coast, and a maximum depth of 1200 m, with a focus on the BOEM Call Areas in this region. We then characterized the temporal variation in spatial-mean power over each Call Area daily and seasonally.

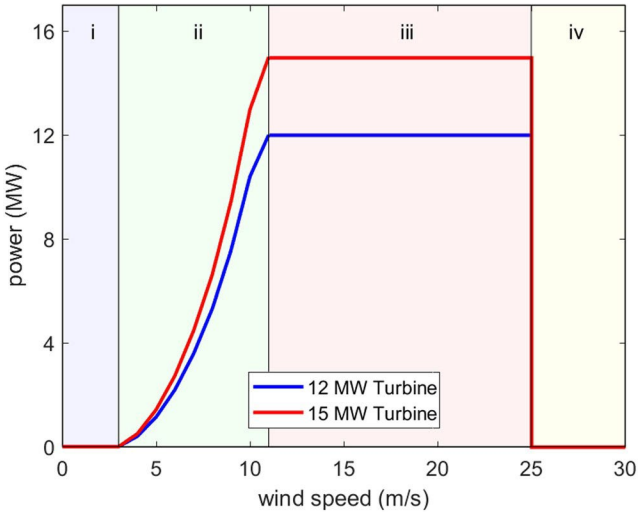

Figure 4.2. Power curves of 12- and 15-MW wind turbines, estimated by NREL.
Note: Background colors represent the following categories: (i) the wind speed range below cut-in wind speed (3 m/s), (ii) between cut-in and rated wind speed (11 m/s), (iii) between rated and cut-out wind speed (25 m/s), and (iv) beyond cut-out wind speed, respectively (Musial et al. 2019).

Since a Call Area could be subdivided into multiple leasing sites, we examined the power produced and area covered (i.e., footprint) for turbine types, wind farms of different production levels, and different spacing scenarios. To date, there is still no consensus on the ideal spacing of turbines, but most configurations range from 7 D between turbines to up to 10 or more D (Musial et al. 2013). Therefore, the spacing will impact the total area needed for a wind facility of a given production level, and influence the power produced per unit area. We considered 7D x 7D and 8D x 10D spacing scenarios (e.g., Beiter et al. 2020, Glenn et al. 2015, Musial et al. 2019), which represent the likely highest and lowest density configurations, and evaluated 60 MW, 240 MW, and 960 MW power production levels, to represent the installed capacity of a hypothetical pilot-scale, medium-scale, and commercial-scale wind farm, respectively. For each wind farm production level and spacing scenario considered, we captured the full range of its footprint by evaluating two extreme patterns of development within a Call Area: one that assumes turbines are placed at locations with the highest power production (creating the smallest possible footprint for that wind farm production level and spacing scenario), and one that assumes turbines are placed at locations with the lowest power production (creating the largest footprint). Finally, to provide realistic results with practical utility, we focused our analysis on estimates of realized power production, calculated as the mean annual power produced using WIND Toolkit hub-height wind speeds for the years for which data are available (i.e., 2007–2013) and the projected power curves for 12 and 15 MW turbines. We calculated the capacity factor by dividing the mean annual power produced by the rated power. To provide context, we compared our results to the realized power production from the Diablo Canyon Nuclear Power Plant (DCNPP) of 1980 MW (2200 MW rated power with an estimated capacity factor of 0.9) (EIA 2012). The DCNPP can supply nearly 10% of California's energy portfolio and is scheduled to be decommissioned in 2024–2025 (PG&E 2020).

4.3 Results

4.3.1 Relative frequency of hub-height wind speed

To examine the distribution of wind speeds in the study domain, we plotted the relative frequency of hourly hub-height wind speed at every grid cell within each Call Area over 2007–2013 for a hypothetical 12 MW turbine (Figure 4.3). We color-coded data into four wind speed categories: i) below cut-in, ii) cut-in to rated, iii) rated to cut-out, and iv) above cut-out. The relative frequencies in these wind speed categories reveal the percentage of time a turbine has no power production (Category i and iv), increasing power production (Category ii), and rated power production (Category iii).

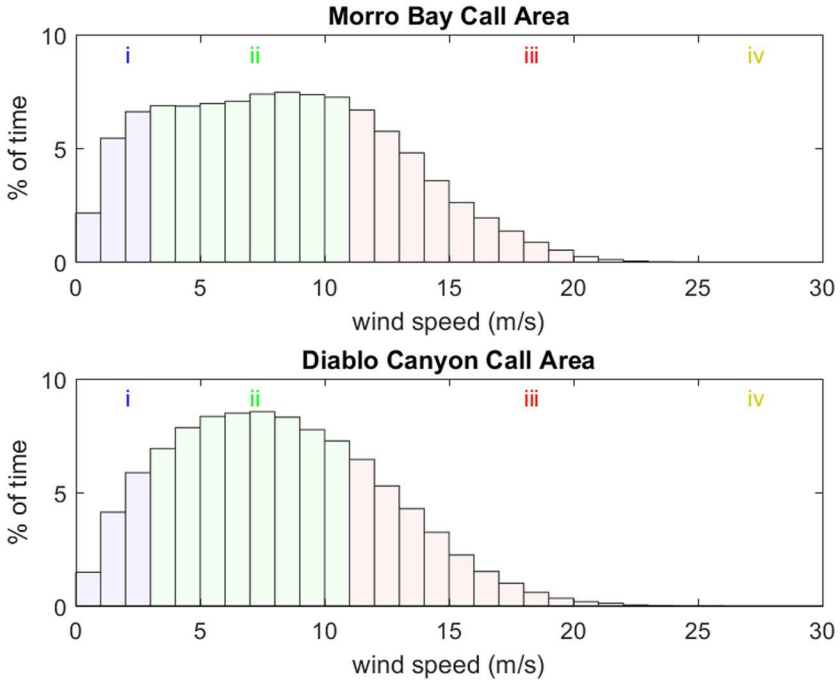

Figure 4.3. Frequency distribution of hourly hub-height wind speed (modeled for a 12-MW turbine) in each 2-km x 2-km grid cell within the Morro Bay Call Area (top) and the Diablo Canyon Call Area (bottom) over 2007–2013.

Note: Roman numerals and bar color corresponds with wind speed categories shown in Figure 2: (i) below cut-in wind speed (≤ 3 m/s), (ii) between cut-in and rated wind speed (> 3 m/s and < 11 m/s), (iii) and between rated and cut-out wind speed (≥ 11 and ≤ 25 m/s). Because less than 1% of wind speed data is in category (iv) above cut-out wind speed (> 25 m/s) regardless of call areas and wind turbines, its frequency is not discernible. Note that frequencies of each wind speed group with 15-MW turbines are almost identical to that with 12-MW turbines. The trivial differences between two types of turbines are due to slightly stronger offshore wind speed at higher hub height. Also note that the frequency of the cut-in wind speed category is equivalent to the frequency of zero power production and the frequency of the between rated and cut-out wind speed category is equivalent to the frequency of rated power production

The two Call Areas shared a similar pattern of relative frequencies in different wind speed ranges. Hub-height wind speed was between the cut-in and rated wind speed (e.g., producing some power, but less than rated power) 57-63% of the time, between rated and cut-out wind speed (e.g., producing rated power) 25-29% of the time, and below cut-in wind speed (e.g., producing no power because of insufficient winds) 11-14% of the time. Extremely strong wind events greater than cut-out wind speed (in which turbines would shut down and produce no power) were very rare in this region: about 0.3% of the time in the Morro Bay Call Area and 0.6% of the time in the Diablo Canyon Call Area.

Although small, there was some spatial variation in the relative frequency of wind speeds between the Call Areas. The Morro Bay Call Area experienced slightly more hours of wind speed below the cut-in (Category i), and the rated and cut-out category (Category iii), and fewer hours of wind speed in the cut-in and rated category (Category ii) compared to the Diablo Canyon Call Area. Although the 15 MW turbine captured slightly stronger wind speed at its higher hub height than the 12 MW turbine, the frequency distribution of wind speeds was nearly identical between the two hub heights (Figure B2).

4.3.2 Spatial and temporal variation in power generation

There was substantial spatial variation in potential power generation across the feasible area for development in the Central California Coast study domain (Figure 4.4). Potential power production increased with distance from shore due to stronger wind speed offshore (Figure 4.4). Although per-turbine power production was greater for 15 MW turbines, the spatial pattern of power production across the domain was very similar for both the 12 MW and 15 MW turbines (Figure 4.4).

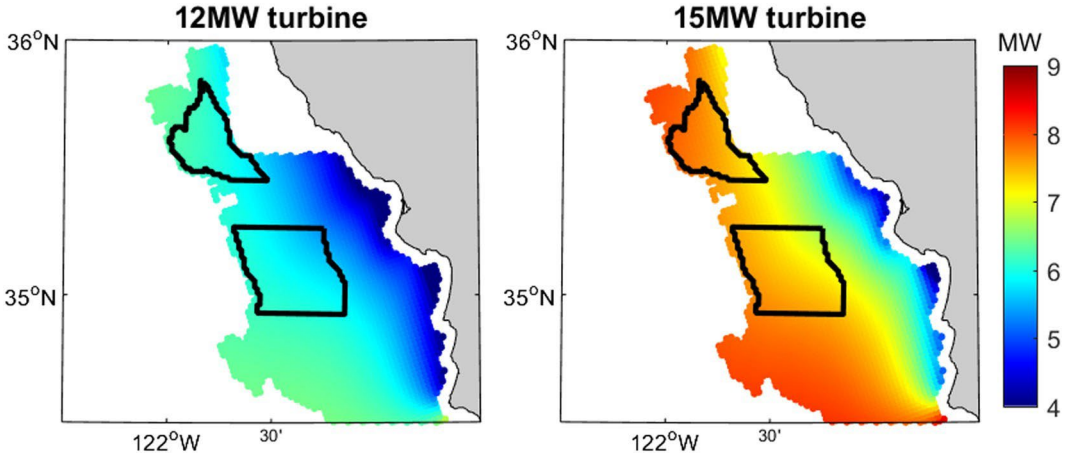

Figure 4.4. Mean power production over 2007–2013 across the areas feasible for development, given one 12-MW turbine (left) and 15-MW turbine (right) per grid cell.
Note: Call Areas are marked by black polygons. Developable areas are established by spatial grid points north of 34.5°N, outside National Marine Sanctuaries, three nautical miles off the coast, and a maximum depth of the 1200-m isobath

Capacity factor also varied across the domain in a pattern similar to power production: it was higher with increased distance from shore, and it was nearly identical for 12 and 15 MW turbines (Figure 4.5 and Figure B3). Within each Call Area, the spatial mean capacity factor in the Morro Bay Call Area was 0.51, while that in the Diablo Canyon Call Area was 0.49 (Table 4.2).

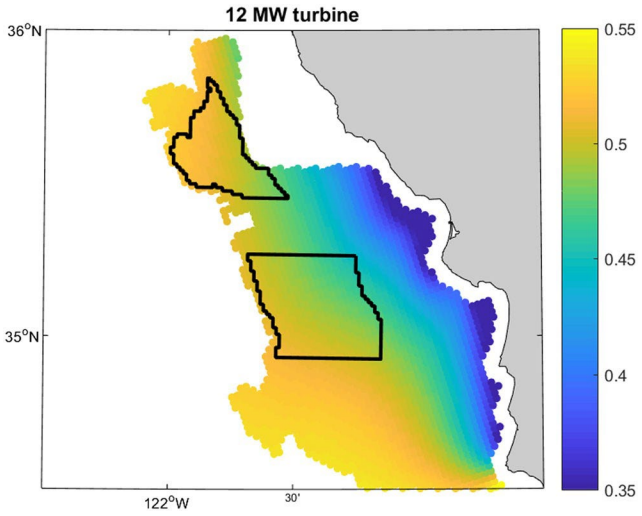

Figure 4.5. Capacity factor over 2007–2013 across the developable areas with one 12-MW turbine per grid cell.
Note: Call Areas are marked by black polygons

Table 4.2: Summary of capacity factor if each Call Area is fully built out with one turbine for each 2 km x 2 km grid cell.

Scenario	Morro Bay	Diablo Canyon
No. of turbines at 1 per 2 km^2 grid cell	192 turbines	346 turbines
Capacity Factor based on 12-MW turbines	0.51	0.49
Capacity Factor based on 15-MW turbines	0.51	0.49

Note: Capacity factor = Mean of hourly actual power/Rated power.

The two Call Areas showed similar daily and seasonal variation in spatially-averaged power production. Offshore wind power production was generally lower in the morning and higher in the evening (Figure 4.6). Seasonally, power production was greatest in spring, followed by summer, fall, and winter. The daily and seasonal patterns were consistent between the 12 MW and 15 MW turbines and matched patterns from previous research that considered 10 MW turbines (Wang et al. 2019b), suggesting that the temporal variation in power production in the Call Areas is likely independent of the specific size or specifications of the turbine(s) used.

The two Call Areas exhibited small but noticeable differences in daily and seasonal variation in terms of magnitude and timing of maximum and minimum power production levels (Figure 4.6). For example, average per-turbine power production in the Morro Bay Call Area was generally higher than that in the Diablo Canyon Call Area, with a few exceptions between hours 12-18 (i.e., 12-6 pm local time) in the spring and 14-22 (i.e., 2-10 pm local time) in the winter. Power production in the Morro Bay Call Area was about 0.5 MW higher than that in the Diablo Canyon Call Area in summer evenings (Figure 4.6), Also, the Morro Bay Call Area typically reached its daily minimum and maximum power production levels one or two hours after that of the Diablo Canyon Call Area.

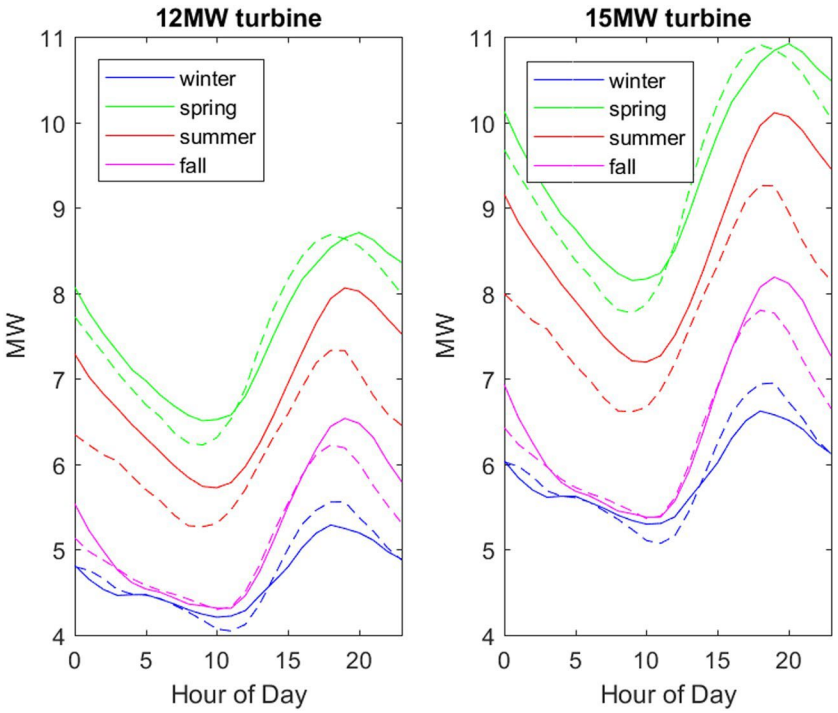

Figure 4.6. Seasonal means of hourly spatial-mean power generation.
Note: blue: winter (Dec-Jan-Feb), green: spring (Mar-Apr-May), red: summer (Jun-Jul-Aug), magenta: fall (Sep-Oct-Nov) over the Morro Bay Call Area (solid line) and the Diablo Canyon Call Area (dashed line) for a 12-MW wind turbine (left) and a 15-MW wind turbine (right)

4.3.3 Different spacing scenarios

Turbine spacing influences potential power production per unit area. The 7D x 7D spacing supported greater total potential power production than 8D x 10D spacing, because turbine density was higher (Table 4.3). A full build out of the Morro Bay Call Area with 12 MW turbines and the 7D x 7D spacing would produce about almost 100% of the realized power of the DCNPP (1980 MW). In comparison, the total power production under the 8D x 10D scenario was only about 1.2 GW, or 60% of its 7D x 7D counterpart. With 12 MW turbines, the average combined annual power production from both Call Areas was 5.32 GW under the 7D x 7D scenario and 3.26 GW under the 8D x 10D scenario. Although 15 MW turbines have higher rated power than 12 MW turbines, its larger rotor diameter requires greater spacing, resulting in fewer turbines per unit area. Interestingly, as a consequence of this adjustment in spacing, the per unit area power production was nearly identical between 12 and 15 MW turbines for a given spacing scenario (7D x 7D, or 8D x 10D, Table 4.3).

Table 4.3. Summary of realized power production for different turbine spacing scenarios: a. 7D X 7D and b. 8D X 10D

a.

7D X 7D Turbines	12 MW	15 MW
Spacing (km^2/turbine)	2.42	3.01
Turbines per 4-km^2 grid cell	1.66	1.33
Realized power in Morro Bay Call Area if it is fully built out (MW)	1946.30	1949.50
Realized power from a fully built out MB Call Area, relative to realized power produced by DCNPP (1980 MW)	98.30%	98.46%
Realized power in DC Call Area if it is fully built out (MW)	3369.86	3375.39
Realized power from a fully built out DC Call Area relative to realized power produced by DCNPP (1980 MW)	170.19%	170.43%

b.

8D X 10D Turbines	12 MW	15 MW
Spacing (km^2/turbine)	3.94	4.92
Turbines per grid cell	1.01	0.81
Realized power in MB Call Area if it is fully built out (MW)	1192.11	1194.07
Realized power from a fully built out MB Call Area, relative to realized power produced by DCNPP (1980 MW)	60.21%	60.31%
Realized power in DC Call Area if it is fully built out (MW)	2064.04	2067.43
Realized power from a fully built out DC Call Area relative to realized power produced by DCNPP (1980 MW)	104.24%	104.42%

4.3.4 Different potential development scenarios

The hypothetical pilot-scale, medium-scale, and commercial-scale wind farms required approximately 10, 40, and 160 turbines to meet their corresponding realized production levels (Tables 4.4-4.5). Not surprisingly, footprint also increased with farm production level, approximately 23 km^2 (60 MW farm, 12 or 15 MW turbines with 7D x 7D spacing) to approximately 666 km^2 (960 MW farm, 12 MW turbines with 8D x 10D spacing) (Tables 4.4-4.5). Farms with 15 MW turbines required approximately 20% fewer turbines, but only a slightly smaller footprint, than farms generating the same production levels using 12 MW turbines. Regardless of turbine type, these hypothetical pilot-, medium-, and commercial-scale farms produced realized power levels that were approximately 3%, 12%, and 48% of the realized power production of the DCNPP, respectively (Tables 4.4-4.5). Whatever the farm, fewer wind turbines and thus a smaller footprint was required in the Morro Bay Call Area than the Diablo Canyon Call Area, because it experienced stronger wind speed on average and has a higher capacity factor. The difference between the two Call Areas in turbine number per farm ranged from less than one (pilot-scale wind farm) to about ten (commercial-scale wind farm). Compared to realized power production, the number of turbines and footprint based on rated power production were smaller and did not depend on which Call Area the farm was placed (Table B1).

Table 4.4. Summary of realized power production for different wind farm size scenarios in Morro Bay Call Area: a. 12MW, b. 15 MW

a. 12MW Scenario

Farm size (realized MW)	60	240	960
No. of turbines under 7D x 7D	9.56-10.42	38.39-41.14	155.12-160.71
7D x 7D footprint (km^2)	23.04-25.11	92.52-99.15	373.84-387.31
No. of turbines under 8D x 10D	9.57-10.39	38.48-40.83	156.63-158.84
8D x 10D footprint (km^2)	37.71-40.94	151.61-160.87	617.12-625-83
Realized power relative to realized power produced by DCNPP (1980 MW)	3.03	12.12	48.48

b. 15MW Scenario

Farm size (realized MW)	60	240	960
No. of turbines under 7D x 7D	7.60-8.33	30.53-32.87	123.52-128.31
7D x 7D footprint (km^2)	22.88-25.07	91.90-98.84	371.80-386.21
No. of turbines under 8D x 10D	7.61-8.31	30.61-32.62	124.81-126.73
8D x 10D footprint (km^2)	37.44-40.89	150.60-160.49	614.07-623.51
Realized power relative to realized power produced by DCNPP (1980 MW)	3.03	12.12	48.48

Table 4.5. Summary of realized power production for different wind farm size scenarios in Diablo Canyon Call Area: a. 12MW, b. 15 MW

a. 12MW Scenario

Farm size (realized MW)	60	240	960
No. of turbines under 7D x 7D	9.75-11.04	39.23-43.42	158.46-169.23
7D x 7D footprint (km^2)	23.50-26.61	94.54-104.64	381.89-407.84
No. of turbines under 8D x 10D	9.77-10.98	39.35-43.06	159.39-167.13
8D x 10D footprint (km^2)	38.49-43.26	155.04-169.66	628-666.37
Realized power relative to realized power produced by DCNPP (1980 MW)	3.03	12.12	48.48

b. 15MW Scenario

Farm size (realized MW)	60	240	960
No. of turbines under 7D x 7D	7.76-8.82	31.24-34.70	126.25-135.15
7D x 7D footprint (km^2)	23.36-26.55	94.03-104.45	380.01-406.80
No. of turbines under 8D x 10D	7.78-8.78	31.34-34.41	127.02-133.43
8D x 10D footprint (km^2)	38.28-43.20	154.19-169.30	624.92-656.48
Realized power relative to realized power produced by DCNPP (1980 MW)	3.03	12.12	48.48

4.4 Discussion and Conclusions

Analysis of potential power production by floating offshore wind energy turbines along the Central California Coast revealed similar frequency distributions of hub-height wind speeds between the Morro Bay and Diablo Canyon Call Areas. The Call Areas also exhibited a similar diurnal pattern of wind speed (lower in the morning, higher in the evening), which is coincidentally complementary to the diurnal pattern of solar energy (peak at mid-day) and demand (peak in evening) (Wang et al. 2019b). These findings suggest that power produced by offshore winds in the Call Areas may be able to meet evening demand for electricity as solar power wanes. In the Call Areas, as well as throughout the study domain representing all feasibly developable areas off Central California, potential power production and capacity factor increased with distance from shore, due to stronger winds further offshore. The frequency distributions of wind speeds, and the diurnal and spatial patterns of wind speed, were all relatively insensitive to turbine type (12 MW versus 15 MW), despite their different hub heights.

Total potential power production from a fully-built out Call Area was estimated to be greater using smaller inter-turbine spacing (7D x 7D) scenario because turbine density was higher. Similarly, total power production was estimated to be greater in the Diablo Canyon Call Area compared with in the Morro Bay Call Area due to its larger size. Interestingly, we found that deployment of 15 MW over 12 MW turbines would not appreciably increase total power production. While a larger turbine generates more power per-turbine, inter-turbine spacing is relative to rotor diameter. The larger rotor of the 15 MW turbine required commensurately larger spacing, such that overall power production was similar to that of a more tightly-packed array of 12 MW turbines.

A commercial-scale wind farm with a realized power output of 960 MW would occupy at least half of the Morro Bay Call Area or at least a quarter of the Diablo Canyon Call Area. In other words, the two Call Areas can collectively contain a maximum of around six commercial-scale wind farms of this size. If fully built out using the higher density 7D x 7D spacing and 12 MW turbines, the Morro Bay and Diablo Canyon Call Areas would produce a combined annually-averaged energy production of 46,596 GWh, which is about 23% of the State's electric energy generation of 200,475 GWh (CEC 2019). The combined energy production from both Call Areas would equate to 17% of the State's total electric energy mix of 277,704 GWh, which includes both in-state generation and imports (CEC 2019).

The framework demonstrated here could be applied to other wind datasets such as NREL's new wind resource dataset (CA 20) developed to replace the WIND Toolkit (Optis et al. 2020). If NREL's new dataset is used, which shows stronger hub-height winds and thus higher gross capacity factor up to 58% for the Call Areas in the Central California Coast (assuming15-MW turbines and the 7D x 7D spacing, cf. Beiter et al. 2020), the fully built out and realized power production could reach 2773 MW and 4997 MW for the Morro Bay and Diablo Canyon Call Areas, respectively, which is 42% and 48% higher than the estimate using the WIND Toolkit. However, we note that the WIND Toolkit dataset has been extensively validated against surface buoys along the Central Coast using a variety of statistical metrics across seasonal and daily time scales (Wang et al. 2019) and neither dataset (WIND Toolkit or CA 20) has been validated at hub height. The framework could also be used to assess potential power production in other regions. More generally, analyses of domains being pursued for offshore wind energy development in the U.S. (e.g., Oregon, Hawaii) and internationally (e.g., U.K.) could provide guidance to the industry, permitting agencies and regulators, project developers, the public, and other stakeholders about the suitability and value of these locations for wind farms.

In this study we focused on "gross" power production, which is the power a wind farm would produce without any losses, as opposed to "net" power production, which accounts for losses from several sources. For example, we did not quantify wake loss, which reduces wind speeds and potential power production downstream of a turbine. Wake loss is likely to be greater under the narrower spacing scenario (e.g., 7D x 7D vs 8D x 10D; Musial et al. 2013). We also did not consider energy loss during transmission from a wind farm to shore, which scales with distance to the shore-based grid connection. Transmission loss is likely to be greater for a wind farm in the Morro Bay Call Area than one in the Diablo Canyon Call Area, because the former is farther from the nearest grid connection facility on shore. Energy loss due to wake effects, transmission loss, and other factors can be as high as 20% of gross power production, though this estimate varies with site characteristics and is declining with technological advancements (Musial et al. 2016). According to Beiter et al. 2020, the total losses in the Central California Coast Call Areas were around 15% of gross power production. Valuation of the energy from offshore wind farms will further require estimates of the cost of these losses (Beiter et al. 2020; Beiter et al. 2016), and socio-economic analysis of the interactions among energy development, production, and demand across energy sectors (offshore wind, terrestrial and marine renewables, non-renewables, and non-electricity energy generators such as gas), across the State of California, and over time in relation to policy changes (e.g., regulating greenhouse gas emissions and broader renewable energy portfolios, as in SB-100 in California).

This study addresses important information gaps related to temporal and spatial characteristics of offshore wind power within the Central Coast Call Areas in California. We evaluated wind resources and areas covered by development by considering alternative scenarios in turbine type, spacing, and wind farm sizes, which were not explored or only partly explored by earlier studies (e.g., Beiter et al. 2020 and Musial et al. 2013). Importantly, this study was not intended to mimic how a real wind farm would be deployed or where turbines should be placed within a Call Area. Rather, we provide an approximation of power production and the footprint such power production would occupy across a variety of scenarios to inform the conversation for stakeholders and policymakers with an interest in offshore wind energy development along the Central Coast of California.

We emphasize that the BOEM Call Areas we analyzed in this study had been already identified in partnership with the State of California. However, our approach to estimate energy production and its value (e.g., Wang et al. 2019a) could be integrated with analyses of relevant economic, cultural, and environmental factors to inform future offshore wind farm siting—and the development of future Call Areas—in relation to industry, regulatory, and societal objectives. For example, many areas with developable wind energy resources are important for commercial fisheries and marine wildlife (e.g., marine mammals and seabirds), all of which may be impacted by offshore wind energy development (Miller et al. 2014). Previous spatial planning research indicates that accounting for these potential economic and conservation impacts (loss of fisheries revenue, displacement of marine mammals, seabird collisions, loss of ecosystem services, etc.) alongside the potential available gains in energy production and value could help identify profitable, productive, and acceptable locations for wind farm development that are both high value and low impact (White et al. 2012). Combining analyses similar to those we presented here with analyses of impacts of wind energy development in a marine spatial planning framework will allow stakeholders to better understand the benefits and costs of offshore wind energy development in locations where planning has not yet begun. Such information will help other regions that may be suitable for offshore wind energy determine whether, how, and where to implement offshore wind energy to achieve sustainable and productive use of marine resources for meeting its renewable energy targets.

5 Potential environmental effects of deepwater floating offshore wind energy facilities

5.1 Introduction

Increased demand for electrical energy and concerns about the impacts of climate change have prompted many governments at all levels to set aggressive goals to reduce greenhouse gas emissions and increase the proportion of their energy portfolios produced from renewable energy sources such as solar and wind (Graabak and Korpås 2016). One response to these changes is the recent, dramatic increase in the design, development, and deployment of commercial-scale offshore wind energy facilities (OWFs; IRENA 2016). The total installed offshore wind capacity globally rose over 4 GW in 2017 alone to nearly 19 GW, and in 2018, was forecasted to reach 120 GW by 2030 (GWEC 2018).

Over the last few decades, the offshore wind energy industry has expanded its scope from turbines mounted on foundations driven into the seafloor and standing in less than 60 m of water (e.g., Vindeby, Denmark; 4C Offshore 2017), to floating turbines moored in 120 m of water (e.g., Hywind Scotland, Scotland; 4C Offshore 2018), to prospecting the development of floating turbines moored in ~1,000 m of water (e.g., BOEM Call Areas and the Castle Winds proposal in California, USA; BOEM 2018, Trident Winds 2016). Major incentives to develop deepwater, floating OWFs include reduced impacts on human activities and marine ecosystems, the ability to leverage existing infrastructure and technological advancements from the offshore oil and gas industry, and access to larger and more consistent wind speeds offshore (Musial and Ram 2010, James and Costa Ros 2015, Wang et al. 2019a, Wang et al. 2019b). However, technology supporting deepwater, floating OWFs is still in its infancy, with few prototype turbines and mooring systems currently deployed. Thus, the potential effects of these technologies on the marine environment are speculative.

To our knowledge, there is no scientific synthesis to date on the potential environmental effects of deepwater, floating OWFs. We aim to fill this gap by providing a synthesis of the available scientific literature and an assessment of how the operation of such facilities may affect the physical and biological marine environment. Such information will be useful for informing the evaluation and permitting processes of sites for the development of deepwater, floating OWFs, as well as for guiding mitigation strategies of operational facilities. While a robust empirical study and test of such effects is not yet possible due to the lack of deepwater, floating OWFs currently in operation, the plausible types of effects and their potential magnitudes can be estimated and reviewed through a synthesis of the scientific literature on appropriate analogs (e.g., fixed-bottom OWFs, land-based wind energy facilities, marine renewable energy [MRE] devices, oil and gas platforms).

For this review we identified, evaluated, and categorized potential environmental effects of deepwater, floating OWFs. We also identified and discuss potential mitigation strategies that might reduce the magnitude of these effects, thereby providing guidance on which effects may be most problematic, which could be resolved, and which need further study. This synthesis can serve as a reference document on the potential environmental effects of deepwater, floating OWFs—a nascent technology expected to become increasingly employed worldwide. This synthesis is aimed toward marine scientists and engineers, the energy industry, permitting agencies and regulators of the energy industry, project developers, and other stakeholders such as coastal residents, conservationists, and fisheries that could be affected by the development of deepwater, floating OWFs.

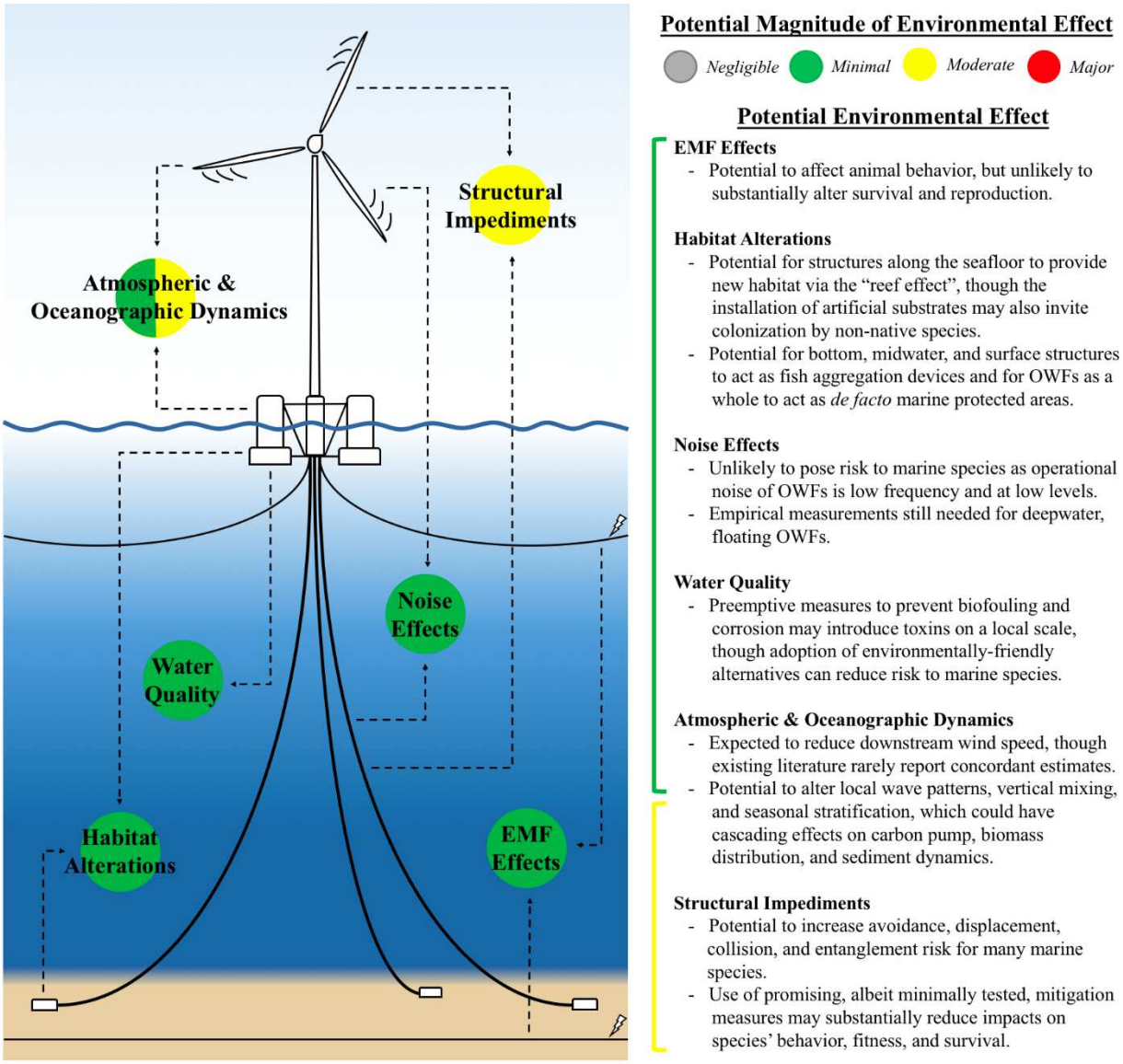

Figure 5.1. Type and magnitude of potential environmental effects of deepwater, floating offshore wind energy facilities.
Note: Effect magnitudes were determined using the four-level classification scheme (negligible, minor, moderate, and major) used to characterize impact levels for biological and physical resources defined in MMS (2007).

5.2 Methods

We conducted a qualitative systematic review of potential environmental effects of deepwater, floating OWFs. Systematic reviews involve a comprehensive plan and search strategy defined by the research question(s), the search engine(s) used, and *a priori* inclusion/exclusion criteria to identify relevant studies based on keywords, topical relevance, study date and location, and quality and type of study (Uman 2011, Paré et al. 2015). Using standard literature search engines (e.g., Google Scholar, Web of Science), and an online database specifically focused on environmental effects of wind and marine renewable energy (Tethys), we conducted a comprehensive literature search using keyword searches and citation chaining to identify scientific information relevant to the potential environmental effects of deepwater, floating

OWFs. Overall, we searched for literature covering, or relevant to, the general topic defined by the keywords "environmental impact/effect" and "offshore renewable energy".

A synthesis on environmental and ecological effects of ocean renewable energy development by Boehlert and Gill (2010) identified six environmental stressors: energy removal effects, electromagnetic field (EMF) effects, physical presence of devices, dynamic effects of devices, acoustic effects, and chemical effects. A large report on environmental effects of MRE by Copping et al. (2016) discussed these stressors in relation to risks and impacts defined by changes in physical systems due to energy removal and changes in flow, EMF effects on marine animals from cables, changes in benthic habitat and reef fish communities by the energy devices, risks to animals from underwater sound, and collision risk around turbines. We organized the stressors and risks/impacts identified by Boehlert and Gill (2010) and Copping et al. (2016) into six categories of potential environmental effects of deepwater, floating OWFs that are the focus of our synthesis: (1) changes to atmospheric and oceanic dynamics due to energy removal and modifications, (2) EMF effects on marine species from cables, (3) habitat alterations to benthic and pelagic fish and invertebrate communities, (4) underwater noise (acoustic) effects on marine species, (5) structural impediments to wildlife, and (6) changes to water quality (Figure 5.1).

To perform an extensive search of the literature on each relevant subtopic, we refined our search with multiple keywords representing each of the six environmental effect categories (e.g., "electromagnetic field", "electric field"; "noise", "auditory"), and with keywords describing specific potential effects discussed in the literature and identified from citation chaining, such as "avian collision", "displacement", "marine mammal entanglement", "reef effect", "wake effect", and "biofouling". We also included in our search "mitigation strategies" to identify potential strategies for reducing or regulating effects. We conducted our literature search from 2016 to 2019, and included in our search only peer-reviewed articles and reports published by researchers, project developers, and government agencies, with no restrictions placed on country of origin.

Due to the lack of deepwater, floating OWFs currently in operation, and thus the limited availability of empirical studies and monitoring efforts directly investigating their environmental effects, we expanded our literature review to include other technologies that could, at least in some contexts, serve as analogs for highlighting potential environmental effects of deepwater, floating OWFs. We considered several analogs where appropriate, including fixed-bottom OWFs, land-based wind energy facilities, MRE technologies (such as wave and tidal), offshore oil and gas platforms, ocean vessels, fisheries, subsea cables, and other coastal infrastructure. Thus, phrases describing these analogs (e.g., "wind turbine", "wave energy converter") were included with the keywords listed above to identify relevant literature. The literature on environmental effects of these analogs is extensive (e.g., > 50,000 articles related to environmental effects of offshore oil and gas platforms), and, in many cases, with a long history (e.g., 100s of articles published prior to 1900 that relate to environmental effects of ocean vessels). Therefore, we used a combination of original research articles and review articles to keep the length (and reference list) of this review manageable. To focus on the most current knowledge and information, we excluded studies whose results were later advanced or superseded by subsequent research. We also excluded review articles published prior to 2000 as well as any studies that were not related to our specific research questions on the environmental effects of deepwater, floating OWFs (Xiao and Watson 2017).

In addition to synthesizing the data and information we obtained from our systematic review, we used our results to generate qualitative inferences on the potential magnitude of the environmental effects of deepwater, floating OWFs. That is, we conducted a qualitative systematic review, as opposed to a quantitative systematic review, such as a meta-analysis, that uses statistical techniques to collectively analyze data from the studies (Paré et al. 2015). We employed the four-level classification scheme—negligible, minor, moderate, and major—used by BOEM to characterize impact levels for biological and physical resources (MMS 2007). The levels are defined by the characteristics of the environmental effect (MMS 2007): (1) no measurable effects (negligible); (2) effects that could be avoided with proper

mitigation, or that would eventually cause no change on the system without any mitigation once the impacting agent is eliminated (minor); (3) effects that are unavoidable and possibly with irreversible outcomes, but that do not threaten the viability of the system, which would fully recover if proper mitigation is applied during the life of the project or proper remedial action is taken once the impacting agent is eliminated (moderate); and (4) effects that are unavoidable and that may threaten the viability of the system, which would not fully recover even if proper mitigation is applied during the life of the project or proper remedial action is taken once the impacting agent is eliminated (major). Following convention for conducting a qualitative review, we attempted to make our conclusions as transparent as possible, and to explain conflicting results (Templier and Paré 2015).

5.3 Results

A total of 89 articles were ultimately included in this review: 16 for describing changes to atmospheric and oceanic dynamics (Table 5.1), 8 for describing electromagnetic field (EMF) effects (Table 5.2), 14 for describing habitat alterations (Table 5.3), 11 for describing noise effects (Table 5.4), 28 for describing structural impediments (Table 5.5), and 14 for describing changes to water quality (Table 5.6). None of the articles focused on environmental effects of deepwater, floating OWFs specifically, which is not surprising given that the technology is still in its infancy, with few prototype turbines and floating systems currently deployed in relatively shallow waters (e.g., Hywind, Scotland in 120 m depth; 4C Offshore 2018). Fifty-eight (65.2%) of the 89 articles contained original research; the remainder were literature review and synthesis articles and reports. While the articles cover the full range of analogs considered, much of the referenced literature focuses on particular regions, species, and/or technologies. For example, 12 (43%) of the articles on structural impediments focus specifically on Europe (Table 5.5), as that region has far outpaced North America and other regions of the world in the development of fixed-bottom OWFs. Likely for similar reasons, many studies examine potential effects on harbor porpoises (*Phocoena phocoena*), since they are a protected species in much of Europe and there is concern about how they may interact with European fixed-bottom OWFs. The limited availability of research and data on OWF's effects on different species and different regions is discussed further in Section 5.4.

Numerous potential effects of deepwater, floating OWFs were identified across all six categories of environmental effects (Figure 5.1, Tables 5.1-6). For each category, the magnitudes of the environmental effects therein were inferred to be either minor or moderate (Figure 5.1). In the below sections, and in Tables 5.1-6, we describe in detail the potential environmental effects, their magnitude, and possible strategies for mitigating the effects.

Table 5.1. Changes to Atmospheric and Oceanic Dynamics literature summary table

Reference	Study Area	Object(s)	Methodology	Relevant Significant Findings
Carpenter et al. (2016)	German Bight, North Sea	Oceanic dynamics	Idealized models and field measurements were used to assess OWFs effects on large-scale stratification.	The mixing induced by an OWFs' foundations generate significant impact on large-scale stratification.
Cazenave et al. (2016)	South-western UK shelf	Oceanic dynamics	A 3D unstructured hydrodynamic model was used to model the impact of wind farm turbine monopiles in a seasonally stratified shelf sea.	Model simulations indicated that the introduction of turbine monopiles induced changes in velocity fields, tidal harmonics, vertical mixing, and seasonal stratification.
Christensen et al. (2013)	Horns Rev OWF, North Sea	Atmospheric and oceanic dynamics	A parametric study was conducted to examine the influence of three processes (energy dissipation due to drag resistance, wave reflection/diffraction, and a modified wind field) on the wave field in and around an OWF.	Results indicated that OWFs in shallow waters may result in the modification of wave propagation shoreward due in part to the reflection and/or diffraction of wave energy by the turbines' substructures and in part to the extraction of wind energy and reduced wind velocity shear.
Christiansen and Hasager (2005)	Horns Rev OWF, North Sea and Nysted OWF, Baltic Sea	Atmospheric dynamics	Satellite synthetic aperture radar-derived wind speed images were used to quantify wake velocity deficits downstream from two OWFs.	An average deficit of 8-9% in mean wind speed immediately downstream of the OWFs, and recovery to within 2% of the free stream velocity within 5-20 km downstream, were observed.
Clark et al. (2014)	Global	Atmospheric and oceanic dynamics	Literature review and synthesis.	Potential impacts of OWFs on turbulence and mixing, surface wave energy, sediment dynamics, biogeochemistry, mesoscale flows, upwelling and downwelling, and meteorology are highlighted.
Copping et al. (2013)	Global	Atmospheric and oceanic dynamics	Literature review and synthesis.	Several possible environmental concerns associated with the presence of, and removal of energy by, MRE devices, including changes in water movement, vertical mixing, and water column stratification, are highlighted.
Fiedler and Bukovsky (2011)	Central US	Atmospheric dynamics	A regional climate model and 62 years of reanalysis data were used to investigate the effect of a wind farm on precipitation.	A statistically significant increase in average precipitation was observed.
Floeter et al. (2017)	Global Tech I OWF and BARD Offshore 1 OWF, North Sea	Oceanic dynamics; plankton and fish communities	Satellite measurements and field measurements taken by a remotely operated towed vehicle were used to assess the effects of non-operating OWFs' foundations on ambient hydrography, local nutrient concentrations, plankton densities, and fish distribution.	Data indicated that the presence of OWF foundations increased vertical mixing and enhanced local upwelling; however, the changes may still fall under natural variability.

Reference	Study Area	Object(s)	Methodology	Relevant Significant Findings
Keith et al. (2004)	Global	Atmospheric dynamics	Two circulation models were used to assess the influence of large-scale wind power on climate at both regional and global scales.	Model simulations indicated that while large-scale use of wind energy can alter turbulent transport in the atmospheric boundary layer, its climatic impact relative to other anthropogenic climate forcing, such as greenhouse gas emissions, is likely to be negligible.
Li et al. (2018)	Sahara and Sahel regions, Africa	Atmospheric dynamics; vegetation	Climate models were used to investigate the effect of large-scale wind farms on regional climate and vegetation.	Model simulations showed that large-scale wind farms led to local temperature and precipitation increases in the two desert regions.
Ludewig (2015)	German Bight, North Sea	Atmospheric and oceanic dynamics	Model simulations and climatological and reanalysis data were used to analyze the impact of an OWF's wind wake on the ocean.	Wind speeds were reduced up to 70% downstream from the OWF for an area 100 times larger than the OWF. The OWF induced numerous changes in ocean dynamics and hydrographic conditions, including changes in vertical mixing and an excursion of the thermocline.
Maria and Jacobson (2009)	Global	Atmospheric dynamics	A Blade Element Momentum model was used to examine the effect of large wind farms on energy in the atmosphere.	When averaged over large geographic regions, energy loss in the lowest 1 km of the atmosphere was estimated to be only 0.007%, even if wind energy was scaled to supply the energy needs of the entire world.
Nagel et al. (2018)	N/A	Atmospheric and oceanic dynamics	An idealized numerical model of the ocean and sediment layers was used to investigate the effect of an offshore wind turbine wake on the coupled atmosphere-ocean-sediment system.	The turbine wake impacted both the ocean and sediment bed layers, and in some cases, generated large-scale eddies.
Porté-Agel et al. (2013)	Horns Rev OWF, North Sea	Atmospheric and oceanic dynamics	Large-eddy simulations were performed to investigate the effect of wind direction on turbine wakes and power losses.	Numerous simulations showed that wind direction can strongly affect the velocity deficit and turbulence intensity of turbine wakes, as well as total power output.
Possner and Caldeira (2017)	Global	Atmospheric dynamics	Model simulations were used to identify areas of open ocean where the large-scale downward transport of kinetic energy may sustain greater wind energy extraction rates than on land.	Results suggested that over some open ocean areas, the downward transport of kinetic energy from the free troposphere is enough to replenish the energy removed by large OWFs.
Vautard et al. (2014)	Europe	Atmospheric dynamics	A regional climate model was used to investigate the effects of current and future European wind farms on regional climate.	Results indicated a limited impact of wind farms on regional climate, with the only statistically significant change in temperature and precipitation found in winter.

Table 5.2. Electromagnetic Field (EMF) Effects literature summary table

Reference	Study Area	Object(s)	Methodology	Relevant Significant Findings
Copping et al. (2016)	Global	EMF-sensitive marine animals	Literature review and synthesis.	Several taxonomic groups of species can detect and respond to the electric and magnetic fields from MRE devices, but there was no evidence that such species are negatively affected.
Dunlop et al. (2016)	Wolfe Island Submarine Cable, Lake Ontario, Canada	Laurentian Great Lakes fish community	Nearshore electrofishing and offshore fisheries acoustic surveys were conducted to investigate whether the presence of a HVAC cable affected the spatial pattern and composition of fish communities.	No detectable effects of the cable on the fish community were found.
Gill et al. (2014)	Global	EMF-sensitive marine animals	Literature review and synthesis.	The properties, sources, and detection of anthropogenic EMFs, as well as the evidence base regarding marine animals' interactions with EMFs, are highlighted.
Hutchison et al. (2018)	Cross Sound Cable, Connecticut, US	American lobster (*Homarus americanus*) and Little skate (*Leucoraja erinacea*)	Field-deployed enclosures and acoustic telemetry were used to assess the effect of exposure to EMF from a buried HVDC cable on lobster and skate behavior.	The Little skate exhibited a strong behavioral response to the EMFs from the energized subsea cable, while the American lobster exhibited only a subtle change in behavioral activity. For either species, the cable did not constitute a barrier to movement.
Love et al. (2015)	Las Flores Canyon, California, US	Rock crabs (*Metacarcinus anthonyi* and *Cancer productus*)	Individual rock crabs were placed in boxes along either an energized or unenergized cable to investigate potential behavioral responses.	No significant difference was detected between response of crabs placed along energized and unenergized cables.
Thomsen et al. (2015)	Thorntonbank OWF and Northwind OWF, Belgium	EMF emissions	Electric and magnetic fields from industry standard inter-array and export cables (AC) were measured during operation using The Swedish Electromagnetic Low-Noise Apparatus.	EMFs emitted from the turbines were considerably weaker than those from the export and inter-array cables. EMFs emitted from the turbines were considerably weaker than those from the export and inter-array cables. E-fields measured were within the range of known detection by sensitive receptor species, while the B-fields were at the lower range of detection.
Westerberg and Lagenfelt (2008)	Kalmar Strait, Baltic Sea	European eel (*Anguilla anguilla*)	Sixty tagged eels' migration speeds were recorded during transit through a strait with a 130 kV AC power cable to investigate potential changes to movement or migration.	Eel swimming speed was significantly lower around the cable, though there was no evidence that the cable acted as an obstruction to migration.

Table 5.3. Habitat Alterations literature summary table

Reference	Study Area	Object(s)	Methodology	Relevant Significant Findings
Bulleri and Airoldi (2005)	North-east coast of the Adriatic Sea	Green alga (*Codium fragile* ssp. *tomentosoides*)	A field survey was used to investigate the distribution and dynamics of an introduced green alga on breakwaters.	Results indicated that artificial structures can facilitate the spread of non-indigenous species.
Castro et al. (2002)	Global	Fish	Literature review and synthesis.	More than 300 fish species from 96 families were found to be associated at least occasionally with floating objects.
Claisse et al. (2014)	Southern California, US	Fish communities	Data from annual visual surveys were used to calculate and compare secondary fish production, total fish density, and total fish biomass on oil and gas platforms to those on natural reefs and other marine habitats.	Results showed that oil and gas platforms off the southern California coast have the highest secondary fish production per unit area of seafloor of any marine habitat studied due to the amount of hard habitat created and resulting recruitment.
Copping et al. (2016)	Global	Benthic habitats and reefing patterns	Literature review and synthesis.	No studies to date have demonstrated significant deleterious effects of changes in habitat due to OWF development on reef fish or benthic communities.
Hammar et al. (2016)	Global	Seabed habitats and benthos, epifouling benthos, fish, marine mammals, and seabirds	Literature review and synthesis.	With the exception of several seabird species, OWFs may be at least as effective as marine protected areas by creating refuges for and increasing the biodiversity and abundance of benthic organisms, fish, and marine mammals.
Kramer et al. (2015)	US West Coast and Hawaii	Fish	Literature review and synthesis.	MRE devices placed on or near the seabed may act as artificial reefs, while midwater and floating devices in tropical waters may act as a *de facto* fish aggregating device.
Krone et al. (2013)	Southern German Bight, North Sea	Mobile demersal megafauna communities	Diving censuses were used to assess the mobile demersal megafauna communities associated with soft bottom habitats, several shipwrecks, and an offshore research platform.	The megafaunal communities found at the research platform foundations were similar to those found at wrecks, though its upper regions were more scarcely colonized.
Langhamer (2012)	Global	Fish and invertebrates	Literature review and synthesis.	Offshore renewable energy structures on the seafloor may function as artificial reefs by introducing hard substrate that can become colonized by invertebrates and reef-associated fishes.

Reference	Study Area	Object(s)	Methodology	Relevant Significant Findings
Love and York (2005)	Santa Barbara Channel, California, US	Fish communities	A manned research submersible was used to survey for fishes along part of an oil pipeline and the surrounding seafloor in shallow and deep waters.	Fish densities along the pipeline were six to seven times greater than those on the adjacent seafloor habitats.
Molnar et al. (2008)	Global	Invasive (non-native) marine species	A quantitative global assessment of invasive species' distributions, their impacts on biodiversity, and invasive species introduction pathways was conducted.	Invasive species' threat to marine biodiversity can have far-reaching ecological and economic consequences, and only 16% of marine ecoregions have no reported marine invasions.
Reubens et al. (2014)	C-Power OWF, North Sea	Atlantic cod (*Gadus morhua*)	Catch statistics, telemetry, stomach content analysis, and visual observations were used to assess the impact of OWFs on the ecology of benthopelagic fish.	Specific age groups of Atlantic cod were seasonally attracted to the OWF, but no evidence of an ecological trap was observed.
White et al. (2012)	Massachusetts Bay, Massachusetts, US	American lobster (*Homarus americanus*) and flounder fisheries, and whale-watching tourism	A spatially explicit, tradeoff analysis, involving a coupled biological–economic model, was used to evaluate the potential impacts of OWF installations on commercial fisheries and whale-watching tourism and conservation.	Marine spatial planning provided added value over single sector management, and has the potential to prevent losses in value by fisheries and whale-watching sectors at no cost to the OWF sector.
Wilhelmsson and Langhamer (2014)	Global	Fish and crustaceans	Literature review and synthesis.	OWFs may act as *de facto* marine protected areas, creating refuges for some marine species, increasing local species abundances, and generating spillover effects to adjacent areas.

Table 5.4. Noise Effects literature summary table

Reference	Study Area	Object(s)	Methodology	Relevant Significant Findings
Brandt et al. (2011)	Horns Rev II OWF, North Sea	Harbor porpoises (*Phocoena phocoena*)	Passive acoustic monitoring was used to investigate the behavioral responses of harbor porpoises to OWF construction and pile driving.	Harbor porpoise acoustic activity significantly decreased during construction (by 100% during the first hour and stayed below normal levels for 24 to 72 h at a distance of 2.6 km). The duration of the effect declined with increasing distance, and no negative effect was found at a mean distance of 22 km.
Götz et al. (2009)	Global	Marine animals	Literature review and synthesis.	Anthropogenic noise sources have the potential to displace, physically injure, and/or affect many marine organisms' ability to communicate, forage, and otherwise interact with their environment.
Madsen et al. (2006)	Global	Noise emissions and marine mammals	Literature review and synthesis.	Operational noise from existing, fixed-bottom OWFs is low, does not exceed ambient noise levels, and is unlikely to impair hearing in marine mammals.
Marmo et al. (2013)	N/A	Several marine mammal and fish species	Acoustic modelling was used to assess the acoustic output of an operational wind turbine on three different foundation types and marine species' responses.	Foundation type influenced sound pressure level and sound field. Results indicated that the modeled noise levels may be audible to some marine mammals and fishes. Modeled scenarios predicted that only a small proportion (< 10%) of minke whales (*Balaenoptera acutorostrata*; low-frequency specialists) and harbor porpoises (*Phocoena phocoena*) would exhibit behavioral responses up to ~18 km away from an OWF, while the majority of animals studied would not show a behavioral response, indicating low potential for displacement.
NYSERDA (2017)	Global	Marine mammals and sea turtles	Literature review and synthesis.	Noise from operational OWFs is likely to pose low risk to marine mammals and sea turtles.

Reference	Study Area	Object(s)	Methodology	Relevant Significant Findings
Russel et al. (2016)	Inner Dowsing OWF, Lynn OWF, Sheringham Shoal OWF, and Lincs OWF, The Wash, North Sea	Harbor seals (*Phoca vitulina*)	Telemetry data from animal-borne tags were used to compare the abundance of harbor seals during the pile driving, construction, and operation of several OWFs.	Seal abundance was significantly reduced during pile driving, but no significant displacement was observed during OWF construction or operation.
Thomsen et al. (2015)	Global	Marine animals	Literature review and synthesis.	Operation noise of OWFs occurs within regulatory thresholds, making these noise sources less of a concern than those by OWF construction, which have the greatest potential for conflict with marine organisms. Some fish and marine mammals may be capable of detecting operational noise from OWFs at distances of several kilometers.
Thomsen et al. (2015)	Thorntonbank OWF and Northwind OWF, Belgium	Noise emissions	Underwater sound pressure measurements were recorded using a drifting platform and an acoustic hydrophone suspended below a vessel.	Monopiles emitted higher sound levels than jacket foundation turbines.
Tougaard et al. (2006)	Horns Rev OWF, North Sea	Harbor porpoises (*Phocoena phocoena*)	A long-term monitoring program involving seven years of field surveys and five years of acoustic recordings was conducted.	The harbor porpoises exhibited a weak negative reaction during construction and semi-operation, and no effects were observed during operation.
Tougaard et al. (2009)	Middelgrunden OWF and Vindeby OWF, North Sea and Bockstigen-Valar OWF, Baltic Sea	Harbor porpoises (*Phocoena phocoena*) and harbor seals (*Phoca vitulina*)	Underwater noise measurements were recorded at three OWFs during normal operation to assess potential effects on hearing.	Analysis of noise measurements concluded that noise from the OWFs was unlikely to harm or mask acoustic communication in harbor seals and harbor porpoises.
Wahlberg and Westerberg (2005)	Global	Fish	Literature review and synthesis.	Noise from operational OWFs may mask communication and orientation signals in fish, but is unlikely to cause physiological damage or consistent avoidance.

Table 5.5. Structural Impediments literature summary table

Reference	Study Area	Object(s)	Methodology	Relevant Significant Findings
Adams et al. (2016)	California Current System, California and Oregon, US [and Baja California, Mexico]	81 marine bird species	A vulnerability assessment was used to examine avian species' risk of collision and displacement at the population level.	Results showed that pelicans, terns, gulls, and cormorants are at the greatest risk of collision, and alcids, terns, and loons are at the greatest risk of displacement.
Arnett et al. (2008)	US and Canada	Bats	Literature review and synthesis.	Patterns of bat collision mortality at land-based wind energy facilities reveal that weather, season, and habitat type are key factors influencing collision risk. Results show a predominance of migratory, foliage-, and tree-roosting lasiurine species colliding with turbines.
Barlow and Cameron (2003)	California and Oregon coasts, US	Marine mammals	A field experiment was carried out to investigate the effectiveness of pingers to reduce marine mammal mortality in a drift gill net fishery.	The use of acoustic deterrent devices reduced cetacean and pinniped entanglement rates in the gill net fishery by two-thirds.
Barrios and Rodríguez (2004)	E3 and PESUR wind farms, Tarifa, Spain	Birds	Carcass surveys, behavioral observations, and generalized linear modeling were used to assess the influence of various factors on bird mortality.	Results indicated that avian collision mortality at wind energy facilities were a function of spatial, temporal, and species-specific factors.
Benjamins et al. (2014)	N/A	Marine megafauna	In addition to literature review and synthesis, a qualitative assessment of relative entanglement risk was conducted based on both biological risk parameters and physical risk parameters of mooring elements.	Results suggested that while MRE device moorings are unlikely to pose a major threat to most marine megafauna groups, baleen whales incurred the greatest risk of entanglement among cetaceans and small, toothed whales incurred the least risk. Results indicated that catenary moorings presented the greatest risk of entanglement while taut systems presented the lowest relative risk due to their lower swept volume ratios, reduced curvatures, and stiffer behavior.

Reference	Study Area	Object(s)	Methodology	Relevant Significant Findings
Carlström et al. (2009)	Bloody Bay and Lagabay, Scotland, UK	Harbor porpoises (*Phocoena phocoena*)	Shore-based observations and porpoise click train detectors were used to investigate the spatial and temporal responses of harbor porpoises to pingers on a bottom-set gill net.	Results showed that pingers could reduce harbor porpoise abundance at greater distances than previously observed, potentially resulting in local habitat exclusion.
Cassoff et al. (2011)	Atlantic waters of US and Canada	Minke whale (*Balaenoptera acutorostrata*), Bryde's whale (*B. brydei*), North Atlantic right whale (*Eubalaena glacialis*), and humpback whale (*Megaptera novaeanglia)*	The available sighting history, necropsy observations, and subsequent data analyses for 21 cases of baleen whale entanglement were reviewed and analyzed.	Acute drowning, impaired foraging and starvation, infection, and/or severe tissue damage were identified as major causes of mortality in entangled baleen whales.
Cox et al. (2001)	Bay of Fundy	Harbor porpoises (*Phocoena phocoena*)	A field experiment involving a moored pinger was conducted to determine whether harbor porpoises habituate to pingers.	Results showed that initial displacement decreased over time and that the harbor porpoises habituated to the presence of the pinger.
Desholm and Kahlert (2005)	Nysted OWF, Baltic Sea	Ducks, mainly common eider (*Somateria mollissima*), and geese	Flight trajectories were collected using surveillance radar during pre-construction and initial operation to investigate avoidance response and collision risk.	The percentage of flocks of ducks and geese entering the OWF area decreased by a factor of 4.5 between pre-construction and initial operation periods. Less than 1% of the migrants that entered the facility flew close enough to turbines to risk collision.
Erickson et al. (2005)	US	Birds	Literature review and synthesis.	Buildings, powerlines, and cats comprise approximately 82% of annual avian mortality from anthropogenic sources, while land-based wind turbines comprise only 0.003%.
Garthe and Hüppop (2004)	Exclusive Economic Zone and national waters of Germany, North Sea	Seabirds	A wind farm sensitivity index for seabirds was developed and applied to estimate vulnerability to collision with OWFs.	Results indicated that seabird vulnerability decreases with distance from shore and was species-specific, with black- and red-throated divers at the greatest risk.
Harcourt et al. (2014)	Cape Solander, Sydney, Australia	Humpback whales (*Megaptera novaeangliae*)	Observations of 137 migrating humpback whale pods were made as they passed a moored acoustic alarm.	There was no evidence that the acoustic alarm served as an effective deterrence.

Reference	Study Area	Object(s)	Methodology	Relevant Significant Findings
Hüppop et al. (2006)	German Bight, North Sea	Migrating birds	Measurements from radar, thermal imaging, and visual and acoustic observations were compiled to investigate bird migration and potential collision risk.	Results indicated that large numbers of diurnal and nocturnal birds migrate through the German Bight year-round, and nearly half fly at altitudes considered to increase collision risk.
Hüppop et al. (2006)	German Bight, North Sea	Migrating birds	Between October 2003 and December 2004, bird carcasses found at the FINO I offshore research platform were documented, measured, and examined.	A total of 442 birds of 21 species (predominantly passerines) were found dead, 76.1% of which had outwardly apparent injuries likely due to collision with FINO 1. However, over 50% of the strikes occurred in just two nights, both characterized by poor visibility.
Johnson et al. (2016)	US	Birds	Three publications estimating avian mortality at wind energy facilities were compared and contrasted.	Estimates indicated that roughly 250,000-500,000 birds are killed annually by colliding with wind turbines.
Kot et al. (2012)	Mingan Archipelago, Gulf of St. Lawrence, Canada	Minke whales (*Balaenoptera acutorostrata*)	A series of field experiments were conducted involving both visual and acoustic monitoring of whale behaviors near experimental ropes and buoys of different colors.	Results showed that minke whales were able to detect and avoid some fishing ropes and that use of high contrast, black and white ropes in particular may reduce entanglement risk.
Kraus et al. (2014)	Cape Cod Bay, US	North Atlantic right whale (*Eubalaena glacialis*)	Field trials involving colored rope-mimics were conducted to document changes in behavior and the distance at which a change occurred.	Results indicated that North Atlantic right whales can detect red and orange colored rope mimics at significantly greater distances than green ones.
Marques et al. (2014)	Global	Birds	Literature review and synthesis.	A wide range of factors influencing avian collisions at wind energy facilities, including species-, site-, and facility-specific factors are highlighted. The relationship between turbine size and avian collision rate may be site- or species-dependent.
Masden et al. (2009)	Nysted OWF, Baltic Sea	Common eiders (*Somateria mollissima*) and other migrating waterbirds	Flight trajectories were collected using surveillance radar during pre- and post-construction to assess the OWF's effect on migration distance.	Birds adjusted their flight trajectories to avoid the OWF post-construction, but the energetic cost of the additional distance travelled to circumvent the OWF was insignificant.

Reference	Study Area	Object(s)	Methodology	Relevant Significant Findings
Masden et al. (2012)	Nysted OWF, Baltic Sea	Common eiders (*Somateria mollissima*)	Flight trajectory data collected during operation were used to parameterize models of the movements of birds in response to wind turbines and to assess the effects of facility-specific factors on avoidance response.	For species vulnerable to collision, facility configuration, turbine row spacing, and column number were shown to influence the number of birds entering the OWF.
Montevecchi (2006)	Global	Marine species	Literature review and synthesis.	Vessels, lighthouses, light-induced fisheries, and oil and gas platforms are all major sources of artificial light in marine environments, each with significant influences on the reproductive physiology, migration, and foraging habits of many marine species, as well as avian collision risk.
Poot et al. (2008)	Nederlandse Aardolie Maatschappij natural gas production site, Ameland, Netherlands	Birds	An experiment using lamps with red, green, blue, and white filters was conducted to observe the reactions of nocturnally migrating birds to different light conditions.	Results indicated that the use of blue and green lighting disorient nocturnally migrating birds less than red and white lighting.
Russell et al. (2014)	Alpha Ventus OWF, Germany and Sheringham Shoal OWF, UK	Harbor seals (*Phoca vitulina*) and grey seals (*Halichoerus grypus*)	High resolution GPS data and state-space models were used to assess potential associations with anthropogenic structures.	The data suggest that the seals maneuvered between OWF components unharmed and used anthropogenic structures within the OWF for foraging.
Russell et al. (2016)	Inner Dowsing OWF, Lynn OWF, Sheringham Shoal OWF, and Lincs OWF, The Wash, North Sea	Harbor seals (*Phoca vitulina*)	Telemetry data from animal-borne tags were used to compare the abundance of harbor seals during the pile driving, construction as a whole, and operation of several OWFs.	Seal usage was significantly reduced during pile driving, but no significant displacement was observed during OWF construction as a whole or operation.
Scheidat et al. (2011)	Egmond aan Zee OWF, North Sea	Harbor porpoises (*Phocoena phocoena*)	Stationary passive acoustic monitoring was used prior to construction and during operation of an OWF to examine potential effects on harbor porpoise occurrence.	Acoustic activity of harbor porpoises substantially increased from baseline to operation of the OWF, indicating a general increase in occurrence.

Reference	Study Area	Object(s)	Methodology	Relevant Significant Findings
Skov et al. (2018)	Thanet OWF, Kent, UK	Northern gannet (*Morus bassanus*), black-legged kittiwake (*Rissa tridactyla*), herring gull (*Larus argentatus*), great black-backed gull (L. *marinus*), and lesser black-backed gull (*L. fuscus*)	A multi-sensor monitoring system was used to collect avoidance behavior and the Empirical Avoidance Rates (EARs) methodology was developed and used to quantify avoidance rates.	96.8% of recorded seabirds avoided turbines by flying between turbine rows while the remaining 3.2% adjusted their flight height to fly below the rotor-swept zone.
Thompson et al. (2017)	US and Canada	Bats	Literature review and synthesis.	Avian collision mortality at wind energy facilities is greatest for migratory tree-roosting species between July and October.
Wood and Carter (2008)	Global	Whales	Information derived from global cable fault databases were used to identify instances of whale entanglement.	As a result of advances in cable design, marine surveying, and cable laying techniques, no entanglements with telecommunication cables have been reported since 1959.

Table 5.6. Water Quality literature summary table

Reference	Study Area	Object(s)	Methodology	Relevant Significant Findings
Bejarano et al. (2013)	Atlantic Outer Continental Shelf	Chemical releases	In addition to a literature review and synthesis, a consequence analysis was conducted to assess the potential environmental effects of chemical releases from OWFs.	Oil and chemical releases associated with the routine maintenance of OWFs, or in the unlikely event of catastrophic facility failure (e.g., toppling of a turbine or electrical service platform), may result in low to moderate adverse impacts to marine resources. Depending on the volume of the release, highly viscous oils (e.g., biodiesel and dielectric insulating fluids) may pose moderate fouling risks to marine mammals and birds.
Borg and Trombetta (2010)	Laboratory study	Brook trout (*Salvelinus fontinalis*)	Electron microscopy and histological analysis were used to investigate the acute effects of copper pyrithione on juvenile brook trout.	Results indicated that copper pyrithione is potentially harmful to nontarget marine organisms at environmentally relevant doses.

Reference	Study Area	Object(s)	Methodology	Relevant Significant Findings
Bryan et al. (1986)	South-west England	Common dogwhelk (*Nucella lapillus*)	A survey of dogwhelks at several sites and an experimental tank test were used to assess the effect of tributyltin on penis development in females.	Concentrations as low as 20 ng/L caused imposex in female dogwhelk.
Chambers et al. (2006)	Global	Marine antifouling coatings	Literature review and synthesis.	Modern approaches to environmentally effective antifouling systems, such as those using tin-free self-polishing copolymers and foul release technologies, and their performance are highlighted.
Ciriminna et al. (2015)	Global	Marine antifouling coatings	Literature review and synthesis.	Biofouling protection throughout marine industries is largely achieved through the use of zinc and/or copper based conventional or self-polishing copolymer antifouling paints. Recent advances in nanochemistry have led to the development of several non-toxic alternatives to biocidal antifouling paints, including silicon-based and sol-gel coatings.
Gomiero et al. (2015)	Central Adriatic Sea	Mediterranean mussel (*Mytilus galloprovincialis*)	Biological and chemical data were used to investigate the biological effects of offshore gas platforms on mussels.	Higher levels of zinc and cadmium in the tissues of mussels sampled near offshore gas platforms suggested that galvanic anode corrosion might be the source of metal accumulation.
Kirchgeorg et al. (2018)	Global	Corrosion protection systems	Literature review and synthesis.	Cathodic protection systems using galvanic anodes or impressed current cathodic protection systems, corrosion allowances, and coatings and their potential for chemical emission from OWFs are presented. Corrosion protection measures are a direct source of chemical emissions, but the available data from OWFs is scarce and there is currently no clear evidence of a negative impact on the marine environment.
Konstantinou and Albanis (2004)	Global	Booster biocides	Literature review and synthesis.	The occurrence and effects of the most commonly used booster biocides in marine antifouling coatings are highlighted.
Legg et al. (2015)	Global	Acoustic methods for biofouling control	Literature review and synthesis.	Acoustic techniques for biofouling control and their potential impacts on marine life are highlighted.
Nurioglu et al. (2015)	Global	Marine antifouling coatings	Literature review and synthesis.	Non-toxic, non-biocide-release antifouling coating strategies are highlighted, with an emphasis on the chemical and physical aspects of their antifouling mechanisms.

Reference	Study Area	Object(s)	Methodology	Relevant Significant Findings
Price and Figueira (2017)	Global	Corrosion protection systems	Literature review and synthesis.	Corrosion protection measures for OWFs typically involve numerous epoxy-based coatings, a polyurethane topcoat, and cathodic protection.
Takahashi et al. (2009)	Global	Antifouling coating biocides	Literature review and synthesis.	Recent advances in the understanding of antifouling biocides in the marine environment, including their behavior, toxicity, biological impacts, and regulation are presented .
Thomas and Brooks (2010)	Global	Antifouling coating biocides	Literature review and synthesis.	The environmental fate and occurrence of antifouling paint biocides, including their effects on non-target species, are highlighted.
Vermeirssen et al. (2017)	Laboratory study	Corrosion protection coatings	Two experiments were conducted using a series of bioassays to investigate the release of toxicity from four epoxy based anti-corrosion coatings.	Bioassay results indicated that one of four tested products released large amounts of bisphenol A.

5.3.1 Changes to atmospheric and oceanic dynamics

Researchers have examined several potential consequences of wind energy extraction on local and regional climate (Table 5.1). The most widely documented consequence is the wake effect, or the reduction in wind speed and kinetic energy downstream of a wind energy facility (Ludewig 2015). Predominantly modulated by wind speed and direction, wind wakes may also impact local weather, ocean, and sediment dynamics (e.g., Porté-Agel et al. 2013, Clark et al. 2014, Ludewig 2015, Nagel et al. 2018). For example, several studies using climate models suggest that the installation of large-scale wind facilities can drive increases in local precipitation (e.g., Fiedler and Bukovsky 2011, Li et al. 2018). When modeling the interactions between wind facilities and the atmosphere, Vautard et al. (2014) found changes within ± 0.3°C and 0-5% for precipitation during winter months, making it difficult to discern such effects from those of natural variability. Using wind models, Ludewig (2015) and Christensen et al. (2013) estimated wind speed reductions downstream of fixed-bottom OWFs of up to 70-90%. However, the actual wake effect may be less severe; satellite synthetic aperture radar (SAR) data used to quantify wind velocity deficits near Horns Rev in the North Sea and Nysted in the Baltic Sea revealed an average deficit of only 8-9% immediately downstream of the OWFs, and recovery to within 2% of the free stream velocity within 5-20 km downstream (Christiansen and Hasager 2005). The substantial differences between these modeled and remotely sensed effects underscore the uncertainty in the current understanding of the impact of OWFs on atmospheric dynamics.

Nonetheless, the overall effect of deepwater, floating OWFs on regional climate is likely to be minor to moderate. When averaged over large geographic regions, energy loss in the lowest 1 km of the atmosphere is estimated to be only 0.007%, even if wind energy is scaled to supply the energy needs of the entire world (Maria and Jacobson 2009). Moreover, while large-scale use of wind energy can alter turbulent transport in the atmospheric boundary layer; its climatic impact relative to other anthropogenic climate forcing, such as greenhouse gas emissions, is likely to be negligible (Keith et al. 2004). Recent research even suggests that over some open ocean areas, the downward transport of kinetic energy from the free troposphere is enough to replenish the energy removed by large OWFs (Possner and Caldeira 2017).

Our current understanding of the effects of deepwater, floating OWFs on oceanic dynamics is similarly limited and uncertain. However, Copping et al. (2013) highlighted several possible environmental concerns associated with the presence of, and removal of energy by, MRE devices, including changes in water movement, vertical mixing, and water column stratification. Similarly, several modeling analyses and empirical research of fixed-bottom OWFs indicate that the mere presence of turbines' fixed substructures can enhance localized vertical mixing across isopycnals and alter seasonal stratification and nutrient transport (e.g., Carpenter et al. 2016, Cazenave et al. 2016, Floeter et al. 2017). Deployment of fixed-bottom OWFs in shallow waters may result in the modification of wave propagation shoreward due in part to the reflection and/or diffraction of wave energy by the turbines' substructures and in part to the extraction of wind energy and reduced wind shear (Christensen et al. 2013). If the operation of deepwater, floating OWFs similarly induces localized changes to surface waves, vertical mixing, or water column stratification, cascading effects to the biological (carbon) pump (process by which inorganic carbon is fixed into organic matter via photosynthesis at the surface and the subsequent sinking and sequestration at depth; Geider 2001), biomass distribution, sediment dynamics, and other processes that scale with the OWF's footprint may result. Though deepwater, floating OWFs' substructures and mooring systems are expected to be less disruptive to ocean currents and waves (and hence sediment dynamics) than those with fixed foundations in shallow waters, such effects may still result from potential changes to local weather and wind forcing, and should be explored in future work.

5.3.2 Electromagnetic field (EMF) effects

As deepwater, floating OWFs expand in size and increase in distance from shore, additional, longer, and higher capacity subsea cables will be required to interconnect facility components to each other, to the seafloor, and to shore. For example, floating OWFs' use of inter-array cables suspended within the water column, rather than solely along the seafloor as is often the case with fixed-bottom OWFs, may increase the scope of anthropogenic EMFs in the water column and potentially interact with a greater diversity and abundance of marine organisms. However, EMFs from inter-array cables may be less than those from export cables because of the lower amount of power being transmitted (Thomsen et al. 2015). Additional factors that may influence the strength of EMFs generated from subsea cables include the distance between conductors, balance of the load, and the type of cable (Copping et al. 2016). Three-phase alternating current (AC) cables, which produce both electric and magnetic fields, are the most commonly employed cables in MRE arrays and OWFs (Gill et al. 2014, Copping et al. 2016). Though magnetic fields emitted from AC cables are typically low (i.e., in the μT to pT range within several meters from the cables), deepwater, floating OWFs' longer transport distances may necessitate the use of high voltage direct current (HVDC) cables, which typically emit higher intensity magnetic fields over a greater spatial scale (Gill et al. 2014).

Several taxonomic groups of species, including elasmobranchs, crustacea, cetacea, bony fish, and marine turtles, are sensitive to electric and/or magnetic fields (Gill et al. 2014, Copping et al. 2016). The most likely effects of anthropogenic electric and magnetic field emissions include physiological impacts, such as altered development, and behavioral effects, such as attraction, avoidance, and impaired navigation and/or orientation (Gill et al. 2014, Thomsen et al. 2015, Copping et al. 2016) (Table 5.2). However, the research to date is limited and observed responses are often species-specific or even individual-dependent (Gill et al. 2014, Copping et al. 2016). For example, Hutchison et al. (2018) found the Little skate (*Leucoraja erinacea*) exhibited a strong behavioral response to the EMFs while the American lobster (*Homarus americanus*) exhibited only a subtle change in behavioral activity. A study in California, United States (U.S.) found no significant difference between the response of caged rock crabs (*Metacarcinus anthonyi* and *Cancer productus*) placed along unenergized and energized subsea cables (Love et al. 2015). While the swimming speed of European eels (*Anguilla anguilla*) in the Baltic Sea was significantly lower near a subsea transmission cable, Westerberg and Lagenfelt (2008) noted that the delay would likely have negligible effects on the eels' fitness and that there was no evidence that the

cable acted as an obstruction to migration. Moreover, a study of nearshore and offshore fishes in the North American Great Lakes found no detectable effects of high voltage transmission cables on species' spatial patterns and composition (Dunlop et al. 2016). In the San Francisco Estuary, Kimley et al. (2017) found that distortions in the Earth's main geomagnetic field produced by bridges were an order of magnitude greater than those from a transmission cable on the estuary seafloor. Using an array of acoustic tag-detecting monitors, they found significant numbers of Chinook salmon (*Oncorhynchus tshawytscha*) migrating past the bridges, as well as adult green sturgeon (*Acipenser medirostris*) successfully swimming through the estuary on their way to and from their spawning grounds, indicating that magnetic anomalies produced by bridges and subsea transmission cables do not present a strong barrier to the natural seasonal movement patterns of these fishes (Kimley et al. 2017). Overall, the research to date has demonstrated that the effect of anthropogenic EMFs on receptor species appears to be minor, but there are still large gaps in our understanding, particularly on the interaction of pelagic, demersal, and benthic species with subsea cables (Copping et al. 2016).

5.3.3 Habitat alterations

The deployment of any novel, offshore structure (e.g., OWFs, MRE devices, oil and gas platforms) may induce physical changes in habitats that have the potential to alter species composition and abundance at localized scales or provide opportunities for colonization by new species (Table 5.3). At the seafloor, the mooring anchors and subsea cables associated with deepwater, floating OWFs, if not entirely buried, may function as artificial reefs by introducing hard substrate that can become colonized by invertebrates and reef-associated fishes (Langhamer 2012). Often regarded as a valuable conservation tool, this "reef effect" of anthropogenic structures on the benthos serving as artificial reefs is well-documented at OWFs, oil and gas platforms, and subsea pipelines (e.g., Love and York 2005, Krone et al. 2013, Claisse et al. 2014, Reubens et al. 2014). Off the coast of Sweden, Wilhelmsson et al. (2006) found evidence to suggest that OWFs can function as both artificial reefs and fish aggregation devices for demersal fish. However, the installation of artificial hard substrates may also invite colonization by non-native (invasive) species, whose threat to marine biodiversity can have far-reaching ecological and economic consequences (Molnar et al. 2008). For example, Bulleri and Airoldi (2005) found that the proliferation of artificial marine structures in nearshore areas facilitated the spread of a non-indigenous green algae (*Codium fragile* ssp. *tomentosoides*) along the coasts of the north Adriatic Sea. However, no OWF studies to date have demonstrated significant deleterious effects on reef fish or benthic communities (Copping et al. 2016) and the offshore locations of deepwater, floating OWFs make these pathways less likely than those nearshore.

Midwater and surface structures, namely mooring lines and floating substructures, may similarly act as fish aggregation devices (Kramer et al. 2015), as well as settlement surfaces for invertebrates and algae. Hundreds of different fish species from dozens of taxonomic families aggregate around floating structures (Castro et al. 2002), suggesting that floating OWFs may attract a variety of species and potentially alter species composition in midwater and surface ecological communities. In instances where fishing activity is restricted within and around OWFs, they may act as *de facto* marine protected areas, creating refuges for some marine species, increasing local species abundances, and generating spillover effects to adjacent areas (White et al. 2012, Wilhelmsson and Langhamer 2014, Hammar et al. 2016). Overall, any habitat alterations that may result from the operation of deepwater, floating OWFs are likely to have minor impacts on local marine organisms and are unlikely to present many novel challenges that have yet to be observed and addressed with the deployment of other marine structures.

5.3.4 Noise effects

Anthropogenic noise sources have the potential to displace, physically injure, and/or affect many marine organisms' ability to communicate, forage, and otherwise interact with their environment (Götz et al. 2009) (Table 5.4). However, operational noise from existing, fixed-bottom OWFs typically occurs within

regulatory thresholds, is low in frequency and level, and is likely to pose low risk (Madsen et al. 2006, Thomsen et al. 2015, NYSERDA 2017). Research indicates that while OWF operational noise, which would be continuous, may be detectable to some marine mammals and fishes, it is unlikely that these noise levels would result in physiological damage (Wahlberg and Westerberg 2005, Madsen et al. 2006, Tougaard et al. 2009, Marmo et al. 2013). However, sounds from turbines also generate particle motion (back-and-forth motion of the medium), which is the primary acoustic stimulus for all fishes; the impact of increased particle motion on the hearing of marine species has received little research attention and remains uncertain (Popper and Hawkins 2019). Furthermore, differential effects of operational noise on fish with and without a swim bladder, which is used in sound frequency detection (Blaxter 1981), is unknown. Nonetheless, behavioral responses by marine species to operational wind turbine noise appears to be minimal; modeled scenarios presented in Marmo et al. (2013) predicted that only a small proportion (< 10%) of minke whales (*Balaenoptera acutorostrata*) and harbor porpoises (*Phocoena phocoena*) would exhibit behavioral responses up to ~18 km away from an OWF, while the majority of animals studied would not show a behavioral response, indicating low potential for displacement. Monitoring at Horns Rev in the North Sea revealed that the OWF's operational noise had no detectable effect on harbor porpoise abundance (Tougaard et al. 2006). Further, analysis of noise measurements from two Danish (Middelgrunden and Vindeby) and one Swedish (Bockstigen-Valar) fixed-bottom OWFs concluded that operational noise levels are unlikely to harm or mask acoustic communication in harbor seals (*Phoca vitulina*) and harbor porpoises (Tougaard et al. 2009).

However, field measurements and modelling efforts to estimate operational noise levels have predominantly focused on fixed-bottom OWFs in shallow, nearshore environments (< 100 m depth; e.g., Tougaard et al. 2009, Marmo et al. 2013, Thomsen et al. 2015). Though measurements of and research on OWFs' operational noise remain a low priority in comparison to that of construction noise (Popper and Hawkins 2019, Thomsen et al. 2015), an in-depth examination of the acoustic propagation characteristics of floating substructures and their associated moorings, as well as the overall noise levels of operational floating, deepwater OWFs would enhance the current understanding of the interactions of these facilities and marine organisms. Because sensitivity to acoustic frequencies differs among species (Popper and Hawkins 2019, Southall et al. 2019), a thorough investigation of the topic will need to cover a broad range of taxonomic diversity of marine organisms. Additionally, as larger turbines are deployed, evaluation of the noise levels from these turbines will be needed to assess their potential effects. Nevertheless, the ocean soundscape is complex and discerning effects from natural variability in ambient noise levels, including those from commercial vessel traffic, may prove difficult without further long-term studies.

5.3.5 Structural impediments

The physical presence of offshore structures, whether dynamic or static, may present both novel obstacles and benefits to marine organisms, and deepwater, floating OWFs are likely no exception (Table 5.5). The deployment of such facilities, for example, may result in displacement of individuals from key habitats such as foraging and breeding grounds. Russell et al. (2016), however, found no evidence of harbor seal (*Phoca vitulina*) displacement during the operation of several OWFs in the U.K., Russel et al. (2014) even demonstrated two seal species' (*Phoca vitulina* and *Halichoerus grypus*) ability to maneuver between OWF components unharmed and inferred that these animals were using the structures to forage. Similarly, Scheidat et al. (2011) presented evidence of a substantial increase in acoustic activity of harbor porpoises within the Dutch OWF Egmond aan Zee, and posited that an increase in food availability and/or an absence of vessels may explain the apparent preference.

Deepwater, floating OWFs may, however, exhibit barrier effects on migrating birds, bats, marine mammals, and fishes. Avoidance of OWFs may cause migrating bird species to use more circuitous routes and expend more energy (Fox et al. 2006). Though the consequences of such barrier effects on flight energetics remain largely unknown (Hüppop et al. 2006), comparison of pre- and post-construction

data from Nysted in the North Sea suggests that, while birds exhibit avoidance responses, the energetic cost of the additional distance travelled to circumvent the OWF is insignificant (Masden et al. 2009). Monitoring of bird behavior at the Thanet OWF in Kent, U.K., found that 96.8% of recorded seabirds avoided turbines by flying between turbine rows while the remaining 3.2% adjusted their flight height to fly below the rotor-swept zone (Skov et al. 2018), again suggesting that avoidance responses may not require more circuitous routes and increased energy expenditure. Conversely, the percentage of flocks of ducks and geese entering the Nysted area decreased by a factor of 4.5 between pre-construction and initial operation periods, signifying a substantial, and possibly a species-specific, avoidance response (Desholm and Kahlert 2005). Even so, less than 1% of the migrants that entered the facility flew close enough to turbines to risk collision (Desholm and Kahlert 2005).

Avian collision risk remains among the most publicized concerns regarding wind energy facilities, despite the estimate that mortality from these facilities is substantially lower than from other anthropogenic sources. Buildings, powerlines, and cats comprise approximately 82% of annual avian mortality from anthropogenic sources, while land-based wind turbines comprise only 0.003% (Erickson et al. 2005). Avian collision mortality at land-based wind energy facilities, estimated at 250,000-500,000 birds annually in the U.S. (Johnson et al. 2016), is a function of spatial, temporal, and species-specific factors (Barrios and Rodríguez 2004). Similarly, patterns of bat collision mortality at land-based facilities in North America reveal that weather, season, and habitat type are key factors influencing collision risk, as well as a predominance of migratory, foliage-, and tree-roosting lasiurine species colliding with turbines (Arnett et al. 2008, Thompson et al. 2017). For offshore locations, a vulnerability assessment examining avian species in the California Current System found that pelicans, terns, gulls, and cormorants are at the greatest risk of collision, and alcids, terns, and loons are at the greatest risk of displacement (Adams et al. 2016). In the North Sea, seabird vulnerability is similarly species-specific and decreases with distance from shore (Garthe and Hüppop 2004). Wind speed and direction also have an important effect on seabird flight height, behavior, and relative vulnerability to collision with OWFs; Ainley et al. (2015) found that species that exhibit a prevalence of gliding versus flapping behavior are more vulnerable to OWFs because they often increase their flight height to within the blade-swept zone when winds are strong and are generally less maneuverable.

Wind facility-specific factors, including turbine features, blade height and visibility, and lighting, also influence avian collision risk (Marques et al. 2014). For example, facility configuration, turbine row spacing, and column number influence the number of birds entering wind farms and thus being at risk of collision (Masden et al. 2012). OWFs' artificial lighting may also attract bird and bat species, thus increasing the potential for collision. Vessels, lighthouses, light-induced fisheries (e.g., harvesting squid), and oil and gas platforms are all sources of artificial light in marine environments that may have significant influences on the reproductive physiology, migration, and foraging habits of many marine species, as well as avian collision risk (Montevecchi 2006). Although OWFs will undoubtedly contribute to the presence of artificial light in the marine environment, the use of blue and green lighting may reduce disorientation in nocturnally migrating birds more than red and white lighting (an industry standard), thus reducing avian collision risk at offshore facilities (Poot et al. 2008). Other viable collision mitigation strategies may include the use of auditory deterrents and restricting turbine operation at certain times, seasons, or during specific weather conditions (Marques et al. 2014). However, preventative initiatives, such as careful siting of OWFs to ensure minimal overlap with important habitats, migration corridors, and large populations of high risk species, may be the most effective method to minimize risk to marine species (White et al. 2012).

Additional concerns regarding deepwater, floating OWFs are the potential for marine mammal collision and entanglement, or the inadvertent restraint of marine animals by anthropogenic materials, such as fishing nets and lines (Benjamins et al. 2014). Since floating OWFs require mooring systems to keep their substructures stationary, marine mammal entanglement risk will likely be influenced by the type of

mooring system employed (slack or taut-moored systems), mooring characteristics, and turbine array configuration. Benjamins et al. (2014) provided an in-depth qualitative assessment of relative entanglement risk, taking into consideration both biological risk parameters (e.g., body size, flexibility, and ability to detect moorings) and physical risk parameters of mooring elements (e.g., tension characteristics, swept volume, and mooring curvature). They found that due to their large size and foraging habits (i.e., rapidly engulfing dense prey aggregations), baleen whales incur the greatest risk of entanglement among cetaceans while small, toothed whales incur the least risk (Benjamins et al. 2014). Additionally, catenary moorings present the greatest risk while taut systems present the lowest relative risk due to their lower swept volume ratios, reduced curvatures, and stiffer behavior (Benjamins et al. 2014). Still, given the size and physical characteristics of the mooring systems required for deepwater, floating OWFs, it is unlikely that upon encountering such facilities, a marine mammal of any size would become directly entangled in the moorings themselves. Mooring systems in the offshore renewables industry typically employ high modulus polyethylene ropes and chains averaging between ~100 to 240 mm in diameter (Benjamins et al. 2014), while fishing gear, which has been identified as a major entanglement risk for whales (NOAA 2018), is typically ~1 to 7 mm in diameter (Wilcox et al. 2014). Thus, marine mammals are more likely to be at risk from secondary entanglement, in which an organism becomes entangled in derelict fishing gear that has accumulated on a facility component, and tertiary entanglement, in which an organism already entangled in gear swims through a floating OWF, and the gear becomes entangled with a facility component. Whether direct, secondary, or tertiary, entanglement may result in severe injury or mortality via tissue damage, starvation, or drowning (Cassoff et al. 2011); however, the actual risks posed by floating OWFs' mooring lines are not yet known.

Similar risks may be associated with OWFs' subsea transmission cables, which interconnect components of OWFs and export energy to onshore electricity grids. However, as a result of advances in cable deployment techniques, such as cable burial procedures, no entanglements with telecommunication cables have been reported since 1959 (Wood and Carter 2008), suggesting that entanglement with subsea cables poses less of a risk to marine mammals than secondary or tertiary entanglement with mooring systems. Though cable burial in depths of up to 1,500 m are common (Carter et al. 2009), developers may deem routing the cables that interconnect facility components to the seafloor impractical and may instead seek to employ subsurface buoys to submerge cables to depths within the water column (e.g., Trident Winds 2016), thus creating additional obstacles for marine mammals and, depending on the characteristics of these cables, providing additional avenues for secondary or tertiary entanglement.

Recent work has demonstrated the value of specific collision and entanglement mitigation strategies. Kot et al. (2012) demonstrated that minke whales are able to detect and avoid some fishing ropes and that use of high contrast, black and white ropes in particular may reduce entanglement risk. Similarly, Kraus et al. (2014) found that North Atlantic right whales (*Eubalaena glacialis*) could detect red and orange colored rope mimics at significantly greater distances than green ones. Barlow and Cameron (2003) found that the use of acoustic deterrent devices reduced cetacean and pinniped entanglement rates in a gill net fishery by two-thirds. Conversely, Harcourt et al. (2014) found no discernible response of migrating humpback whales (*Megaptera novaeangliae*) to acoustic alarms, suggesting that responses may be species-specific. Additional challenges regarding the use of acoustic alarms as a means to reduce collision and entanglement include habituation risk (Cox et al. 2001), local habitat exclusion (Carlström et al. 2009), and device durability and regulatory compliance (Dawson et al. 2013). Thus, the most effective way to reduce marine mammal collision and entanglement may be through siting OWFs in areas that reduce overlap with biologically important areas, such as feeding grounds and migration corridors.

5.3.6 Changes to water quality

Developers of OWFs will almost certainly include preemptive measures to prevent corrosion and biofouling, since seawater is highly corrosive and maintenance of offshore structures, especially those far from shore, is difficult and expensive (Table 5.6). Corrosion protection measures for OWFs typically

involve numerous epoxy-based coatings, a polyurethane topcoat, and cathodic protection (Price and Figueira 2017). These corrosion protection measures are a direct source of chemical emissions, including organic compounds such as bisphenol A, and metals such as aluminum, zinc, and indium (Kirchgeorg et al. 2018). For example, Vermeirssen et al. (2017) demonstrated the release of large amounts of bisphenol A from epoxy resin-based anti-corrosion coatings on onshore infrastructure. Gomiero et al. (2015) analyzed mussels (*Mytilus galloprovincialis*) from offshore gas platforms in the Adriatic Sea and hypothesized that galvanic anodes (a form of cathodic protection) were the potential source of zinc and cadmium accumulation in the mussels. Although the available data from OWFs is scarce, there is currently no clear evidence of a negative impact on the marine environment from these sources (Kirchgeorg et al. 2018).

Prior to the global ban of organotin-based antifouling paints in 2008, biofouling protection measures predominantly involved tributyltin, a highly toxic, broad-spectrum biocide whose prolonged use in the shipping industry has had detrimental effects on non-target species (Bryan et al. 1986, Takahashi et al. 2009, Nurioglu et al. 2015). In response to the ban, biofouling protection throughout many marine industries is now largely achieved through the use of zinc and/or copper based conventional or self-polishing copolymer antifouling paints (Takahashi et al. 2009, Ciriminna et al. 2015). To increase the length and functionality of these coating systems, booster biocides such as zinc pyrithione and copper pyrithione are typically incorporated despite the need for further research into their long-term fate in, and effects on, the marine environment (Konstantinou and Albanis 2004, Chambers et al. 2006). Copper pyrithione, for example, can induce morphological changes and oxidative stress in juvenile brook trout (*Salvelinus fontinalis*) at environmentally relevant doses (Borg and Trombetta 2010). Moreover, dissolved copper concentrations exceeding U.S. federal standards of 3.1 μg/L can affect the development and survival of several fish, mollusk, and echinoderm species (Thomas and Brooks 2010); however, such impacts are typically limited to marinas, harbors, and ports, which can contain elevated copper concentrations due to high boating activity and increased residence times (Takahashi et al. 2009). Thus, continued use of conventional antifouling agents will certainly introduce additional chemicals into the marine environment via passive leaching, but the extent to which the chemicals released from deepwater, floating OWFs may harm sensitive marine species remains unclear.

However, following increased health and environmental concerns regarding heavy metal and booster biocide use in antifouling coatings, stricter regulations have initiated the research and development of alternative approaches to biofouling protection, such as fouling release, biomimetics, acoustic approaches, and more commonly, the use of various non-toxic, non-biocide-release antifouling coatings (Chambers et al. 2006, Ciriminna et al. 2015, Legg et al. 2015, Nurioglu et al. 2015). Ultimately, the magnitude of the water quality effects from deepwater, floating OWFs may depend on whether the offshore wind energy industry adopts (by choice or regulation) such environmentally-friendly alternatives to biofouling protection, but will likely be minor nonetheless. Once again, these challenges are not unique to deepwater, floating OWFs and have been addressed in other marine industries.

5.4 Discussion

This study provides the first synthesis of the potential environmental effects of deepwater, floating OWFs during operation, as well as potential mitigation strategies to some of the effects. Using the available scientific literature concerning appropriate analogs (e.g., fixed-bottom OWFs, land-based wind energy facilities, MRE devices), we evaluated six major categories of potential effects (cf. Boehlert and Gill 2010, Copping et al. 2016). If mitigation strategies and best-practice protocols are properly adopted, our research suggests that the effects associated with EMFs, noise, habitat alterations, and changes to water quality are likely to have minor impacts on marine organisms. Similarly, preventative initiatives such as the careful siting of deepwater, floating OWFs outside of important habitats, may reduce otherwise moderate impacts of displacement, avian collision, and marine mammal collision and entanglement (e.g.,

White et al. 2012). Lastly, deepwater, floating OWFs' overall effect on atmospheric and oceanic dynamics is likely minor to moderate, but given the potential for such technologies to have cascading effects on large-scale atmospheric and oceanic processes, future work on the underlying uncertainties of this impact is needed. Additionally, it is important to note that the magnitude of each potential effect will likely scale, either linearly or nonlinearly, with the size and configuration of an OWF. Monitoring of pilot and future deepwater, floating OWFs will help to calibrate these findings.

Although the scope of this work does not encompass potential environmental effects of deepwater, floating OWFs outside of the operational stage, there are likely effects associated with other stages of an OWF's life cycle that warrant mention. For example, oil and chemical releases (e.g., fuel spills) associated with the routine maintenance of OWFs, or in the unlikely event of catastrophic facility failure (e.g., toppling of a turbine or electrical service platform), may result in minor to moderate adverse impacts to marine resources (Bejarano et al. 2013). Depending on the volume of the release, highly viscous oils (e.g., biodiesel and dielectric insulating fluids) may, for example, pose moderate fouling risks to marine mammals and birds (Bejarano et al. 2013). Implementation of oil/chemical transfer spill prevention measures and best-practice protocols, however, may reduce the likelihood and extent of both accidental and intentional releases from OWFs' components and support vessels. Additionally, the majority of greenhouse gas emissions from renewable energy technologies likely occur prior to and after facility operation. Raw material extraction, component manufacturing, transportation to the offshore site, installation, and decommissioning will all have air quality effects. A recent life cycle analysis of floating offshore wind projected greenhouse gas emissions of ~15.35 kg CO_2-eq/MWh, with manufacturing as the major contributor. However, even with an uncertainty range of 8.58-30.17 kg CO_2-eq/MWh, the maximum emissions estimate for floating offshore wind was still less than $1/10^{th}$ and $1/20^{th}$ the minimum emission estimates for natural gas and coal, respectively (Bang et al. 2019). Furthermore, since deepwater, floating OWFs lack fixed foundations, they do not require pile driving. Pile driving is among the most environmentally impactful practices associated with the construction of fixed-bottom OWFs, since it typically emits relatively high noise levels that cause displacement and injury of marine mammals and changes to fish behavior (Brandt et al. 2011, Thomsen et al. 2015, Russell et al. 2016). Also, deepwater, floating OWFs can be constructed onshore prior to transportation to the offshore site, which further reduces both the amount and duration of anthropogenic noise emissions (e.g., vessel noise) and other construction-related impacts in marine habitats. These factors suggest that a deepwater, floating OWF will have relatively minor effects during non-operational stages of its life cycle; nonetheless, research on OWFs during their construction and decommission stages is required to generate more accurate estimate of their effects.

Much of the referenced literature in this review is based on research focused on specific regions, species, and/or technologies, and the conclusions drawn therein may be as well. Given the limited availability of information specifically on deepwater, floating OWFs, we have extrapolated, when appropriate, from research on fixed-bottom OWFs, MRE, and other appropriate analogs. Development of fixed-bottom OWFs in northern Europe has far outpaced that in North America, Asia, and other regions of the world. Therefore, much of the available literature is geographically-biased toward northern Europe, which has had such technologies in operation for some time. Further, the species within these regions, as well as those afforded various protections or that are considered commercially valuable, tend to be the focus of many studies, such as harbor porpoises in northern Europe. However, the findings of such studies are not necessarily specific to harbor porpoises, and may be applicable to other marine mammals as well as seabirds. Likewise, much can be learned from research on OWFs in northern Europe, and from research on analogous industries, and applied to inform our understanding of the nature and magnitude of the potential effects deepwater, floating OFWs may have around the world. There also may be environmental effects, not identified by this review, that are outside the six categories of effects that we considered based on the stressors and risks/impacts identified by Boehlert and Gill (2010) and Copping et al. (2016). Finally, this synthesis is based on a literature review up through 2019, and since then more information

has been learned about potential environmental effects of deepwater floating OWFs (e.g., ICF 2020). Thus, this synthesis should be considered as a benchmark for the state of knowledge that can be improved upon through an updated synthesis covering the most recent scientific literature. Ultimately, the conclusions drawn in this study are not meant to preclude future empirical studies and monitoring of the environmental impacts of deepwater, floating OWFs in specific regions and on specific species. Rather, the aim of this literature review is to synthesize the available literature to better estimate how the operation of deepwater, floating OWFs may affect the physical and biological marine environment.

Knowledge of deepwater, floating OWFs' potential effects on the marine environment remains limited due to the lack of these facilities in operation at this time. Thus, this synthesis takes the necessary first steps in summarizing the available information on the potential environmental effects of deepwater, floating OWFs and some associated mitigation strategies, and can serve as a reference document for marine scientists and engineers, the energy industry, permitting agencies and regulators of the energy industry, project developers, and concerned stakeholders such as coastal residents, conservationists, and fisheries. Given the likely integration of deepwater, floating OWFs into an increasingly crowded seascape, it is vital that the drive to reduce greenhouse gas emissions, diversify energy portfolios, and combat climate change account for the proper assessment and mitigation of these facilities' potential environmental effects.

6 Spatial and temporal characteristics of California commercial fisheries from 2005 to 2019 and potential overlap with offshore wind energy development

6.1 Introduction

Fisheries in California are diverse and highly productive, fueled in part by strong seasonal upwelling in the California Current Large Marine Ecosystem (CCLME) (Checkley and Barth 2009, McClatchie 2014). These fisheries have been an important part of the State's economy, supporting local and regional economies and working waterfronts across California for decades (Miller et al. 2017). The National Marine Fisheries Service estimated that commercial fishing in California generated nearly $200 million in ex-vessel value in 2018 (NMFS 2021), and that commercial and recreational fishing activity was responsible for nearly $25 billion in economic activity and the creation of 142,000 jobs in 2016 (NMFS 2018).

Because of its economic importance, state and federal fishery regulators invest significant resources into managing these fisheries to ensure both economic productivity and ecological sustainability (Richmond et al. 2019, Mamula and Kosaka 2019). However, the diverse nature of these fisheries can complicate their management, since a great deal of information is needed to support regular stock assessments for a wide range of species, each of which has its own particular biology, ecology, and fishery dynamics that vary both temporally and spatially (Allen et al. 2006). To drive these important assessments, as well as manage trade-offs associated with competing interests in marine environments, managers rely on numerous data sources, most notably state fishery landings, which can provide temporally- and spatially-resolved catch information for a range of different species. In addition to assessing stocks and setting catch regulations, fisheries landings data are used to explore potential conflicts with other ocean sectors such as aquaculture and wind energy, examine the impacts of climatic variation and marine heatwave events, and identify spatial trophic 'hotspots' (White et al. 2012, Santora et al 2014, Lester et al. 2018, Barbeaux et al. 2020, Suryan et al. 2021).

Fisheries landings data also are used to examine changes in California fisheries through time, revealing substantial shifts in the relative importance of different species and locations (e.g., Thomson 2015, Miller et al. 2017). In the first half of the 20th Century, California's commercial fisheries were dominated by a few lower trophic level coastal pelagic species, mainly sardines. Fisheries became more diversified in the latter part of the last century, with an increased proportion of the landings represented by groundfish, such as rockfish and flatfish, and invertebrate species, such as urchins, lobster, and Dungeness crab (Miller et al. 2017). Along with this diversification was a shift away from higher biomass-lower value species and toward lower biomass-higher value species (Miller et al. 2017). Additionally, landings data have revealed clear shifts in fisheries linked to large-scale climate oscillations. For example, the large ENSO events in 1982-83 and 1997-98, which substantially decreased oceanic and nearshore primary production, precipitated substantial declines in landings of shorter-lived species at lower trophic levels, such as coastal pelagic fishes and squid (Zeidberg et al. 2006). Additionally, multidecadal shifts in oceanic and atmospheric forcing in the Pacific Ocean (e.g., Pacific Decadal Oscillation) impacted the proportional abundance of sardines versus anchovies, as well as other important species like salmon, throughout the CCLME (Mantua et al. 1997, Chavez et al 2003).

Over the past few decades, fisheries in California and their management have continued to change and evolve, as has the marine ecosystem. It is now clear that anthropogenic activities and climate change are impacting the CCLME. Multiple stressors, including habitat loss and climatic stress (e.g., increased temperatures, deoxygenation, ocean acidification, marine heatwaves (MHW)), have increased (Marshall et al. 2017, Hart et al. 2020), and species ranges have begun to shift with these oceanographic changes

(Zacherl et al. 2003, Lonhart et al. 2019, Sanford et al. 2019). Climate models predict that MHW, such as the record 2014–2016 North Pacific Marine Heatwave (2014 warm "blob" followed by the record 2015–2016 ENSO event) and ENSO events, will increase in frequency and intensity (Power et al. 2013, Cai et al. 2015, Frolicher et al. 2018, Holbrook et al. 2019, Wang et al. 2019), which has the potential to disrupt local marine ecosystems and fisheries (Smale et al. 2019, Rogers-Bennet and Catton 2019). Additionally, this century has seen an increased emphasis on sustainable fisheries management, including legislation that mandates sustainability in federal fisheries (e.g., reauthorization of the Magnuson-Stevens Act), as well as new technical approaches to fishing and fisheries monitoring. For example, stock assessments and population modeling have become more sophisticated (Methot and Wetzel 2013, Punt et al. 2014), and there is an increased recognition of the importance of habitat and spatial planning in the management of fisheries (White et al. 2012, Hazen et al. 2013, Maxwell et al. 2015, Kroodsma et al. 2018, Murray and Hee 2019). There continues to be a culturally and legally-mandated emphasis on fishery sustainability, including efforts to move to true ecosystem-based management plans that incorporate risk assessment (Field and Francis 2006, Samhouri et al. 2019). Finally, fishery managers are increasingly planning for the impacts of climate change and ocean acidification (Chavez et al. 2017, Marshall et al. 2017), new uses of ocean space (Yates et al. 2015, Lester et al. 2018), and protection of endangered species (e.g., Santora et al. 2020).

As a result of these changes, the dynamics of California fisheries are likely much different now than they were just a few decades ago (e.g., as described from 1931–2005 by Miller et al. 2017). Thus, updated information on the status and trends of the State's fisheries is critical for supporting current fisheries management. This study aims to help address this need by describing the recent spatiotemporal dynamics of California fisheries in terms of commercial landings and ex-vessel value (revenue) across different fisheries groups over 15 years (2005 to 2019). The results presented here are statewide and could be used to support stock assessments, spatial planning, economic impact analyses, climate change mitigation efforts, and other marine management and research efforts requiring current, spatial and temporal characteristics of California's commercial fisheries. This work aims to help managers, policymakers, and other stakeholders design and plan for the sustainability and economic vitality of fisheries in California and the industries that depend on them over the coming decades.

6.2 Data and Methods

This study used commercial fisheries landings receipts ('fish ticket data') for California commercial marine fisheries, provided by the California Department of Fish and Wildlife through a data sharing agreement, from 2005 to 2019 (CDFW, unpub. data). Fish tickets were submitted to CDFW by commercial fish businesses at port when vessels return from a fishing trip with harvested fish. Each fish ticket recorded the landing weight (hereafter, landing) and unit price (i.e., price per pound) and of the fish species caught, the landing date and port, and a fishing block catch location, as well as unique identification numbers for vessels, fishers, and businesses. Most of the fishing blocks within the Exclusive Economic Zone (EEZ, 200 nm) are defined by a 10' by 10' (~10 nm on a side) grid, with a few blocks that range up to 30' or 40'; these blocks are assigned a three-digit identification (ID) number. Additionally, there are ten larger fishing blocks that are assigned a four-digit ID number (Figure C1). These larger blocks are effectively latitudinal bins that extend from the coast to the edge of the U.S. EEZ. They are generally used for trawling surveys where vessels do not specify a three-digit block fishing block, but are occasionally used by other fisheries as well (Todd Nearhr, pers. comm.).

Following Miller et al. (2017), we categorized landed species into nine broad taxonomic/functional groups (Table C1). We excluded the 'Abalone' group since the commercial fishery for abalone in California has been closed since 1997 (Rogers-Bennett et al. 2002). The nine taxonomic groups in Table C1 are representative of California's commercial fisheries, accounting for more than 95% of the total landings in the data.

The ex-vessel value or revenue of the catch landed (hereafter, value) was calculated by multiplying the landing in pounds by the unit price in U.S. dollars reported on each fish ticket. Prior to calculating value, we corrected unit prices for inflation by multiplying the original unit price by the consumer price index in 2019 December divided by the consumer price index in the month and year the fish ticket data were submitted (data.bls.gov/timeseries/CUUR0000SA0).

A small fraction of fish ticket records reported implausible unit prices, which led to erroneous value estimates. We adjusted these outliers as follows. We replaced reports of $0/lb unit price (~ 0.35% of total landings) by the median of all non-$0 unit prices within that fishery's taxonomic group. This adjustment accounts for the presumed economic value of landings with no reported value. We also adjusted price outliers greater than a set upper threshold by replacing these with the median price for the group. We chose an upper threshold of $27/lb, since this number exceeds the reasonable ex-vessel price of any of the landed seafood. It also accounts for less than 0.0005% of total landings; a sensitivity analysis found that the results were largely unaffected by any upper threshold ≥ $25/lb.

In addition to characterizing statewide statistics averaged over the 15-year time series, we explored temporal and spatial variation. We computed annual landings and values for individual fishery groups and their proportional contribution to total landings and values. The four-digit blocks are too large to reveal detailed spatial information, and it is unknown how these data would have been distributed in the three-digit blocks had three-digit blocks been used. Thus, we mapped the annual average of landings and values using catch in three-digit blocks only. Given that not all three-digit blocks are the same size, we calculated the area of each block and divided the annual average by the area of that block for visualization. In the maps, fishing blocks with less than three unique vessel, fisher, and business IDs are not displayed to protect the privacy of vessel operators (e.g., the so-called "rule of three", cf. CDFW). The fish ticket data in these blocks are still included in the calculations in the tables and other figures that are not spatially explicit. We computed Moran's I to objectively quantify spatial clustering of landings across three-digit blocks for each fish group. Moran's I ranges from -1 to 1, with a value of 1 indicating perfect clustering, a value of 0 corresponding to randomness, and a value of -1 signifying perfect dispersion (Cliff and Ord 1981). We also mapped the depth limit of each taxonomic group (see Miller et al. 2017; Table C1); to explore the spatial accuracy of block information, we compared catch reported in three-digit blocks inside of the prescribed depth limit with catch reported outside of the depth limits in three-digit blocks, and compared these values to catch reported in the four-digit blocks. Finally, we investigated annual spatial patterns—effectively latitudinal trends—in four-digit blocks for Dungeness crab and groundfish, the two taxonomic groups with the highest-value reported in four-digit blocks.

To better understand regional trends, we divided ports along the California coast into five regions following Thomson (2015). We calculated the relative importance of landings and value for key fishery groups in each region based on the port of landing reported in fish tickets. The five regions are: Northern California (Eureka Area), North Central California (Fort Bragg, Bodega Bay, and San Francisco Area), Central California (Monterey and Morro Bay Area), South Central California (Santa Barbara/Ventura Area), and Southern California (Los Angeles and San Diego Area) (Figure C2).

To assess potential overlap between offshore wind development and commercial fisheries in California, we used fish ticket data to estimate fishing activity in relation to the Humboldt and Morro Bay Wind Energy Areas (WEAs, Figure S3; BOEM 2022). We calculated the relative importance of landings and value for each fishery group in the Humboldt and Morro Bay regions and WEAs by summing data in the following way: a) all local ports in the respective regions, b) all blocks that overlapped with the WEAs in the respective regions, and c) all blocks that overlapped with the WEAs in the respective regions and were also within the biological depth limits of a given fishery group. For the Humboldt Wind Energy Area, the

local port complex included Crescent City, Klamath, Arcata Bay, Eureka, Fields Landing, Humboldt Bay, King Salmon, Orick, Shelter Cove, Trinidad. For the Morro Bay Wind Energy Area, adjacent ports included Avila/Pt. San Luis, Morro Bay, and San Simeon. Note that this analysis only considers data from the three-digit blocks, since data from four-digit blocks have little to no useful spatial information.

6.3 Results

6.3.1 Long-term, statewide comparison among taxonomic groups

California statewide landings over the 15-year evaluation period (2005-19) were dominated by 'Market Squid' and 'Coastal Pelagic Species (CPS)' (Figure 6.1). However, these two groups were not as valuable as several low-volume, high-value species groups, such as 'Dungeness Crab' and 'Groundfish', which had significant economic value despite their smaller landings (Figure 6.2). The top three species in revenue value for each broad taxonomic group are listed in Table C1. For example, in the groundfish group, the top three species were sablefish (~39%), rockfish (~14%), and thornyheads (~14%).

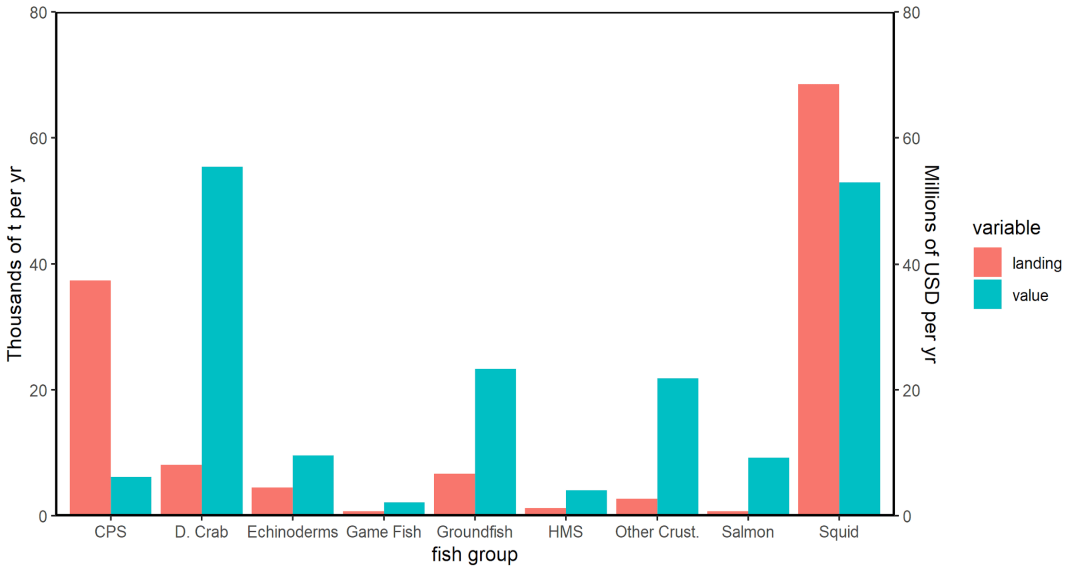

Figure 6.1. Statewide landings (left y-axis) and value (right y-value) averaged over the entire time series for individual taxonomic groups recorded in all blocks.

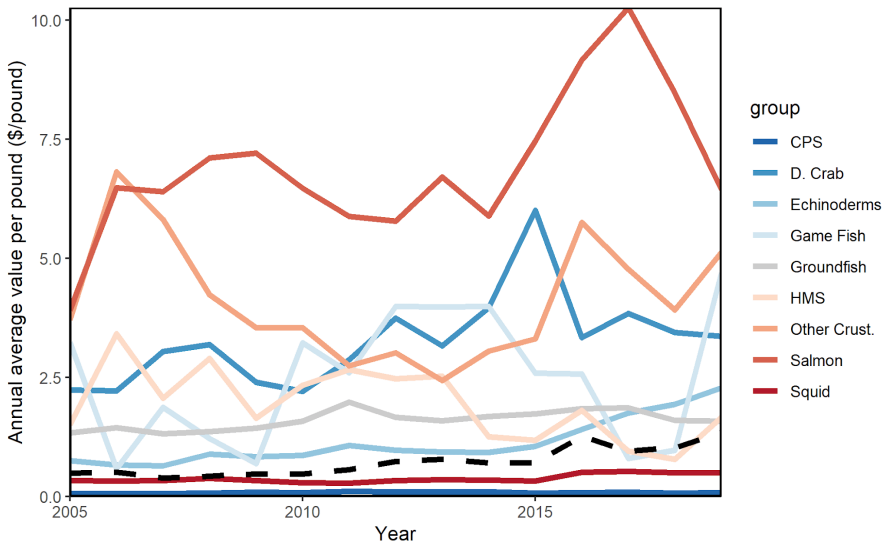

Figure 6.2. Statewide annual average value per pound ($/pound) for each taxonomic group.
Note: Dashed line represents the annual average value per pound using all nine taxonomic groups.

For some taxonomic groups, a large proportion of landings was reported in four-digit blocks, which effectively only provides information on the latitudinal range for landings data in those blocks (Figure 6.3). For example, approximately 70% of the landings of 'Other Crustacean' was reported in four-digit blocks (however, only about 10% of this group's value was from landings reported in four-digit blocks, due to a lower price reported for landings in those blocks versus in three-digit blocks). For Dungeness crab and groundfish, approximately 43% and 53% of their landings were reported in four-digit blocks, representing about 41% and 34% of their respective value.

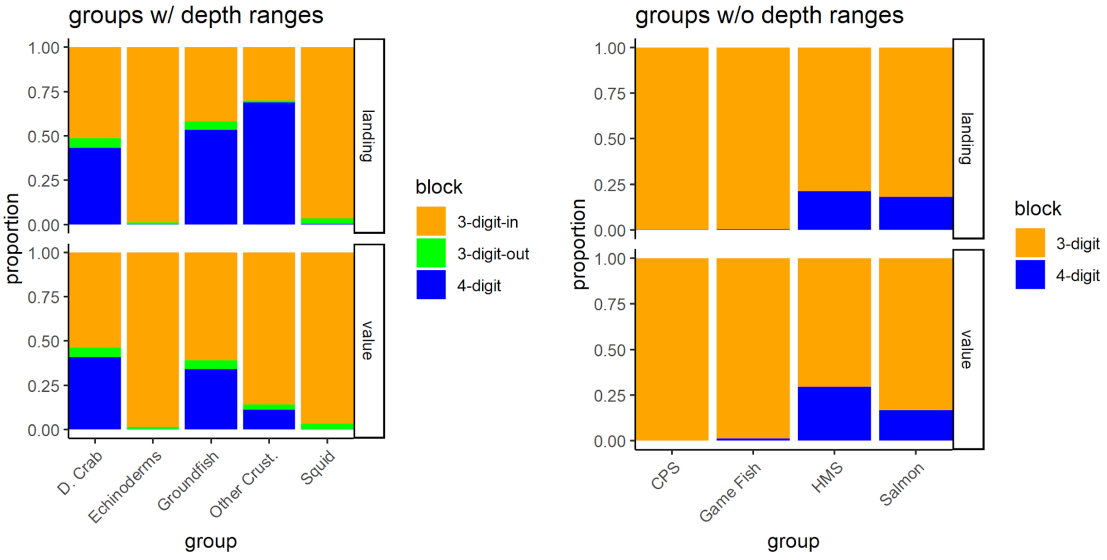

Figure 6.3. Proportion of landings (top) and value (bottom) under different block-depth criteria for each taxonomic group.
Note: Left: Groups with depth limits (see Table C1). Right: Groups without depth limits (i.e., CPS, game fish, HMS, and salmon).

For the groups with a prescribed depth limit (see Methods), the landings reported in three-digit blocks outside the depth limit was relatively small (Figure 6.3). While Dungeness crab had the highest number of landing receipts reported from blocks outside their prescribed depth limit, these apparent misreports comprised less than 6% of the total landings and value for this species.

6.3.2 Temporal variation in landings and value

Statewide landings showed a general decline over the 15-year time series; 2019 landings were approximately one-third of those in 2005 (Figure 6.4; Figure C4). In contrast, overall value remained relatively constant, due to the shifting focus toward higher value species. Average price per pound across all fisheries increased over 170% between 2005 and 2019, even when accounting for inflation (Figure 6.2).

Statewide landings and value also varied considerably among years, though not necessarily in concert with one another (Figure 6.4). Landings peaked in 2010 and were dominated by squid, while value peaked in 2013, largely driven by Dungeness crab and squid. Both total statewide landings and value dropped precipitously in 2015 to around half of what they were in 2014, largely due to lower landings of both Dungeness crab and squid.

The relative importance of each fisheries group varied substantially over time (Figure 6.5). CPS was the top contributor to overall landings until 2008, but was replaced by squid thereafter. At its peak in 2017, squid accounted for nearly 70% of overall statewide landings. While squid fisheries declined in recent years, high-value fisheries such as Dungeness crab remained relatively stable.

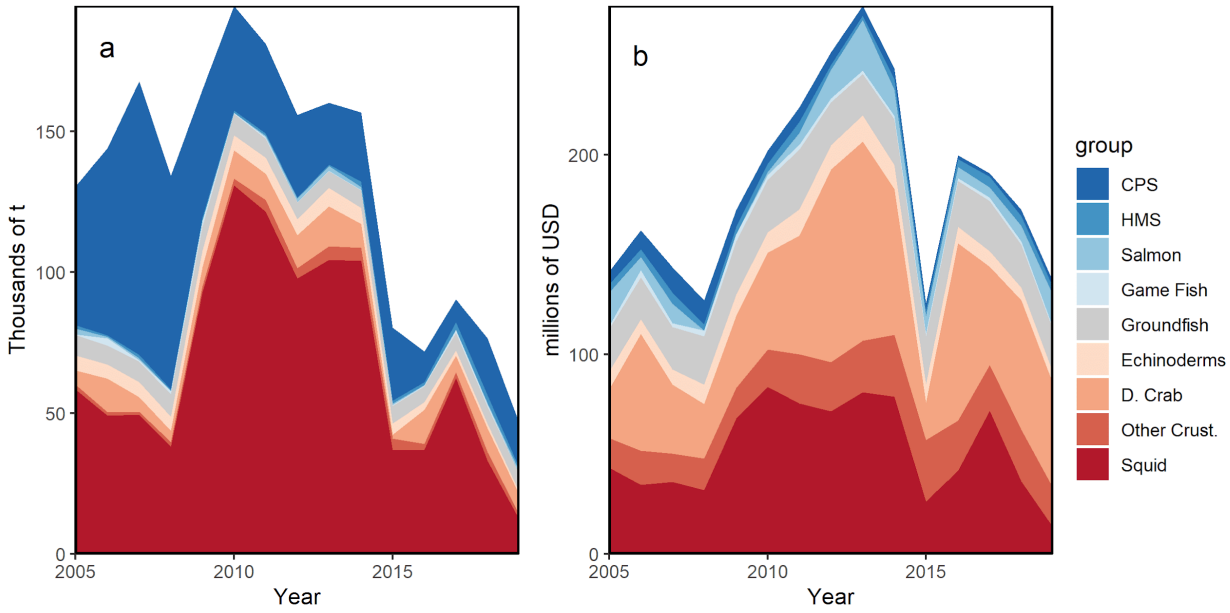

Figure 6.4. Statewide annual time series of (a) landings and (b) value recorded in all blocks.

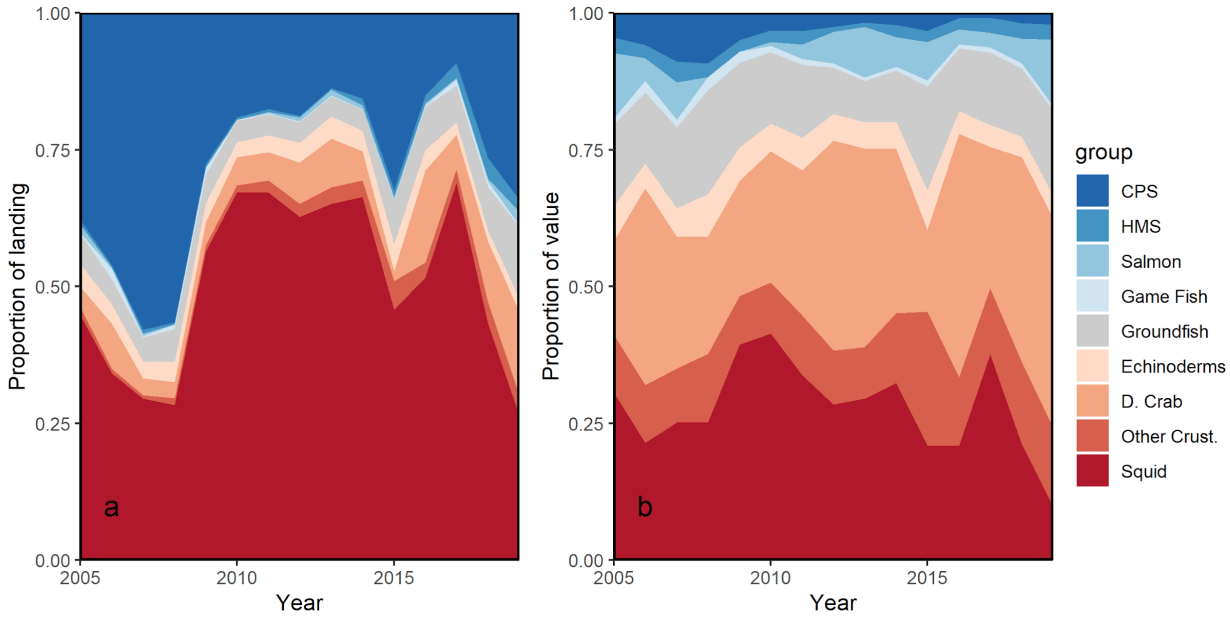

Figure 6.5. Statewide annual times series of proportion of each taxonomic group (a) for landings and (b) value recorded in all blocks.

6.3.3 Spatial distribution across regions

Fisheries landings and values varied substantially from region to region (Figure 6.6). For much of the time series, Southern California was the dominant region, constituting nearly 50% of the statewide landings until 2013, after which it declined to less than 25%. Northern and North Central California contributed the least to statewide landings; however, their combined landings and values gradually increased over the time series. Despite having moderate landings, Central California consistently had the lowest total value among the regions.

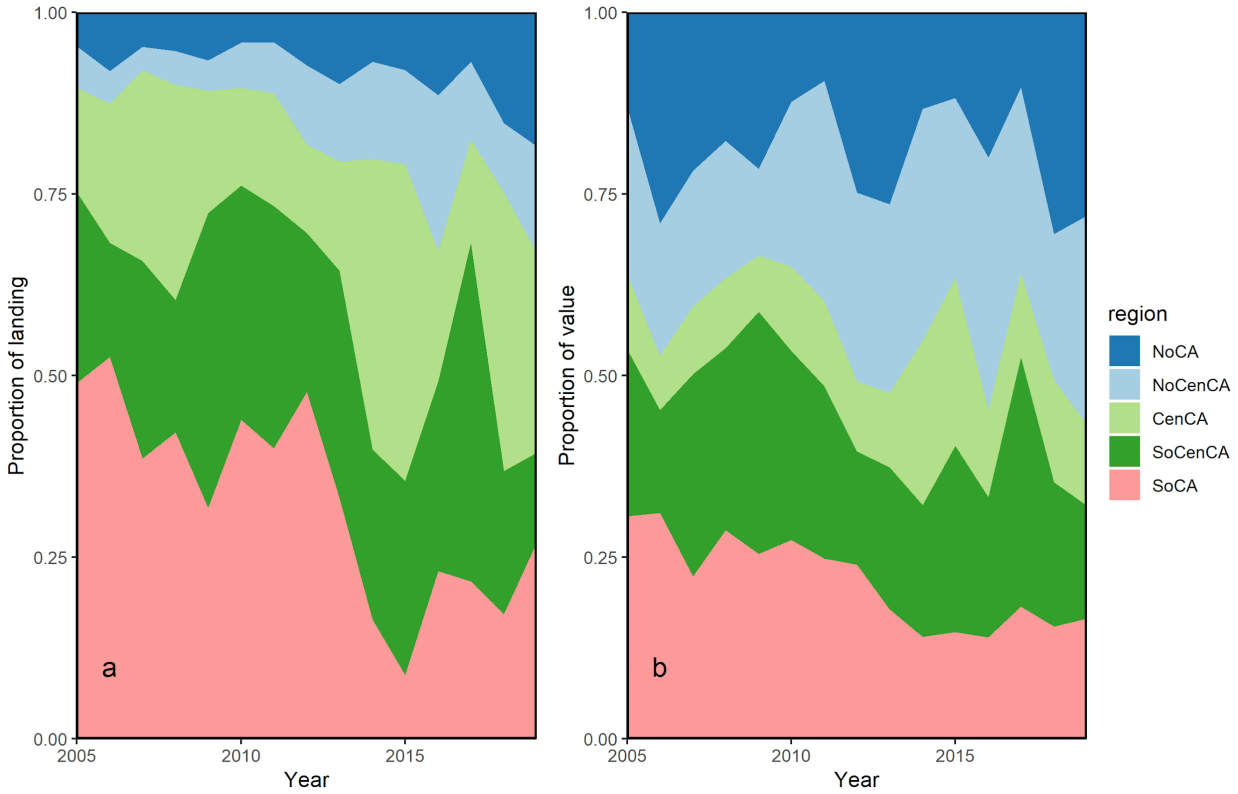

Figure 6.6. Annual proportion of fisheries in each region (a) for landings and (b) value recorded in all blocks.

Regional fisheries also showed significant variation in landings among the broad taxonomic groups (Figure 6.7). Fisheries in Northern California were dominated by Dungeness crab and groundfish, though the landings of other crustacean were substantial in some years (e.g., 2015). Compared to Northern California, North Central California fisheries were more diverse, with significant contributions from Dungeness crab, groundfish, salmon, echinoderms, and even squid and CPS in some years. Central California was dominated by CPS and squid; the low price per pound for these species contributed to the low total value for this region. Like Central California, Southern California supported mainly CPS and squid fisheries. Southern California had higher value than Central California because of the contribution of high-value other crustacean fisheries, mostly spiny lobster. In South Central California, squid was the most important species, accounting for more than 75% of landings almost every year.

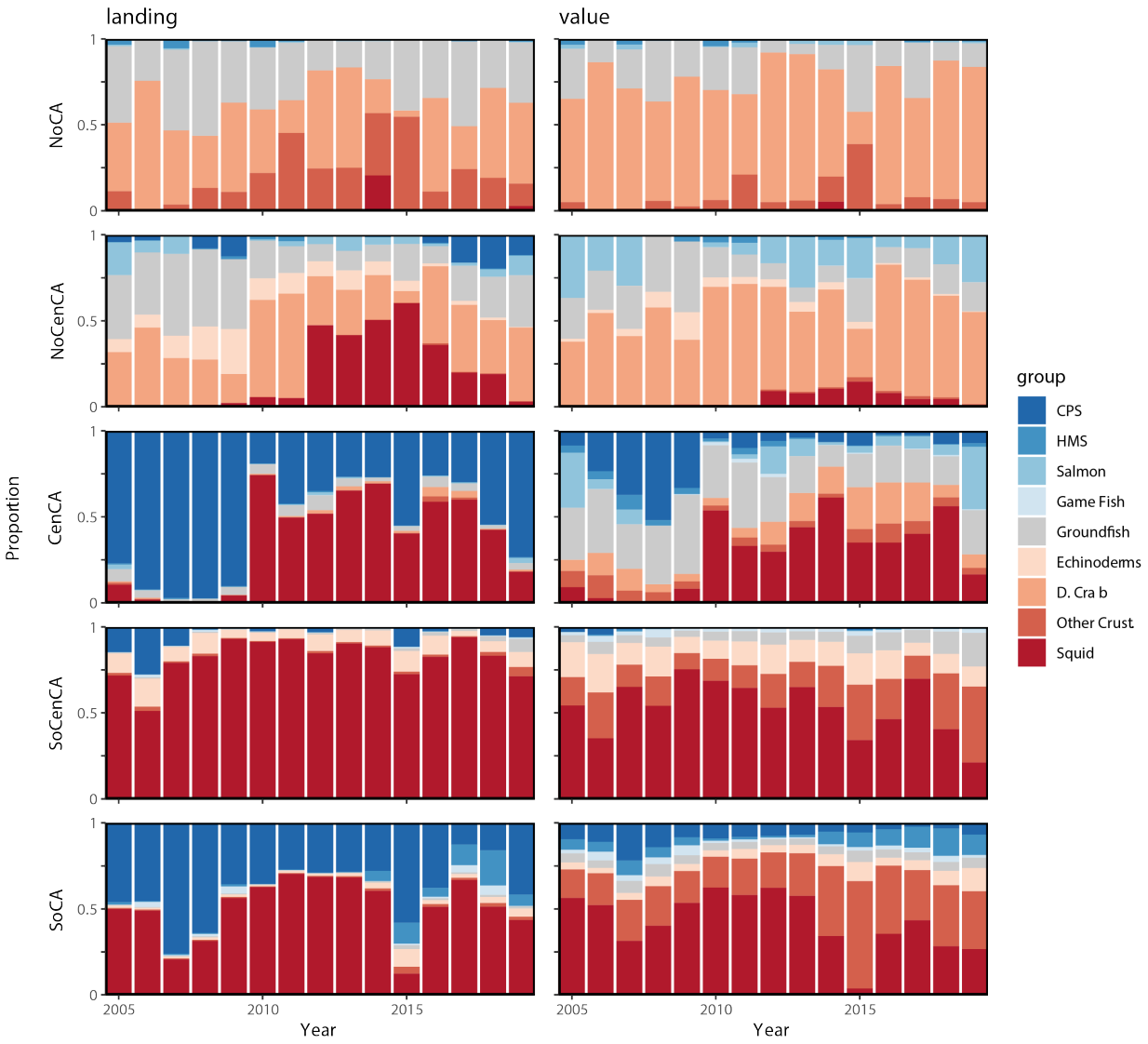

Figure 6.7. Annual proportion of landings (left) and value (right) for each taxonomic group in different regions.
Note: The rows from top to bottom represent regions: Northern California (NoCA), North Central California (NoCenCA), Central California (CenCA), South Central California (SoCenCA), and Southern California (SoCA).

6.3.4 Spatial distribution across blocks

Detailed three-digit block landings and values after applying the "rule of three" are shown across the individual taxonomic groups in Figures 6.8 and 6.9, respectively. For display purposes, taxonomic groups are divided into finfish groups (groundfish, CPS, salmon, HMS, and game fish) and invertebrate groups (echinoderm, squid, Dungeness crab, and other crustacean). In general, the spatial patterns of landings and value were similar for most groups.

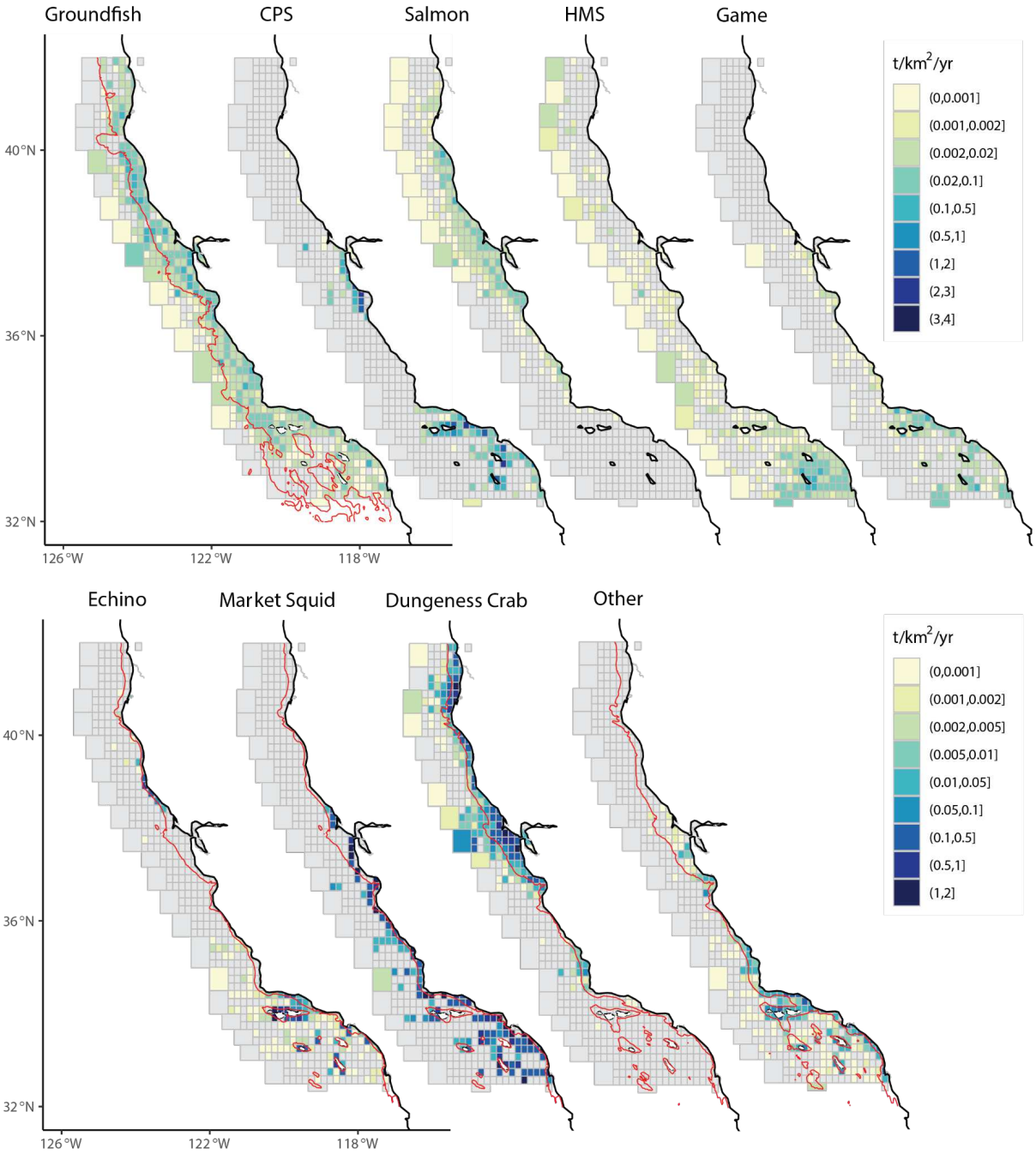

Figure 6.8. Annual average landings per unit area for (top) finfish groups (groundfish, CPS, salmon, HMS, and game fish) and (bottom) invertebrate groups (echinoderm, squid, Dungeness crab, and other crustacean) from 2005–2019 after applying "rule of 3".
Note: "Other crustacean" is labeled as "Other". If applicable, the prescribed depth limit is contoured in red (Miller et al. 2017; Table C1).

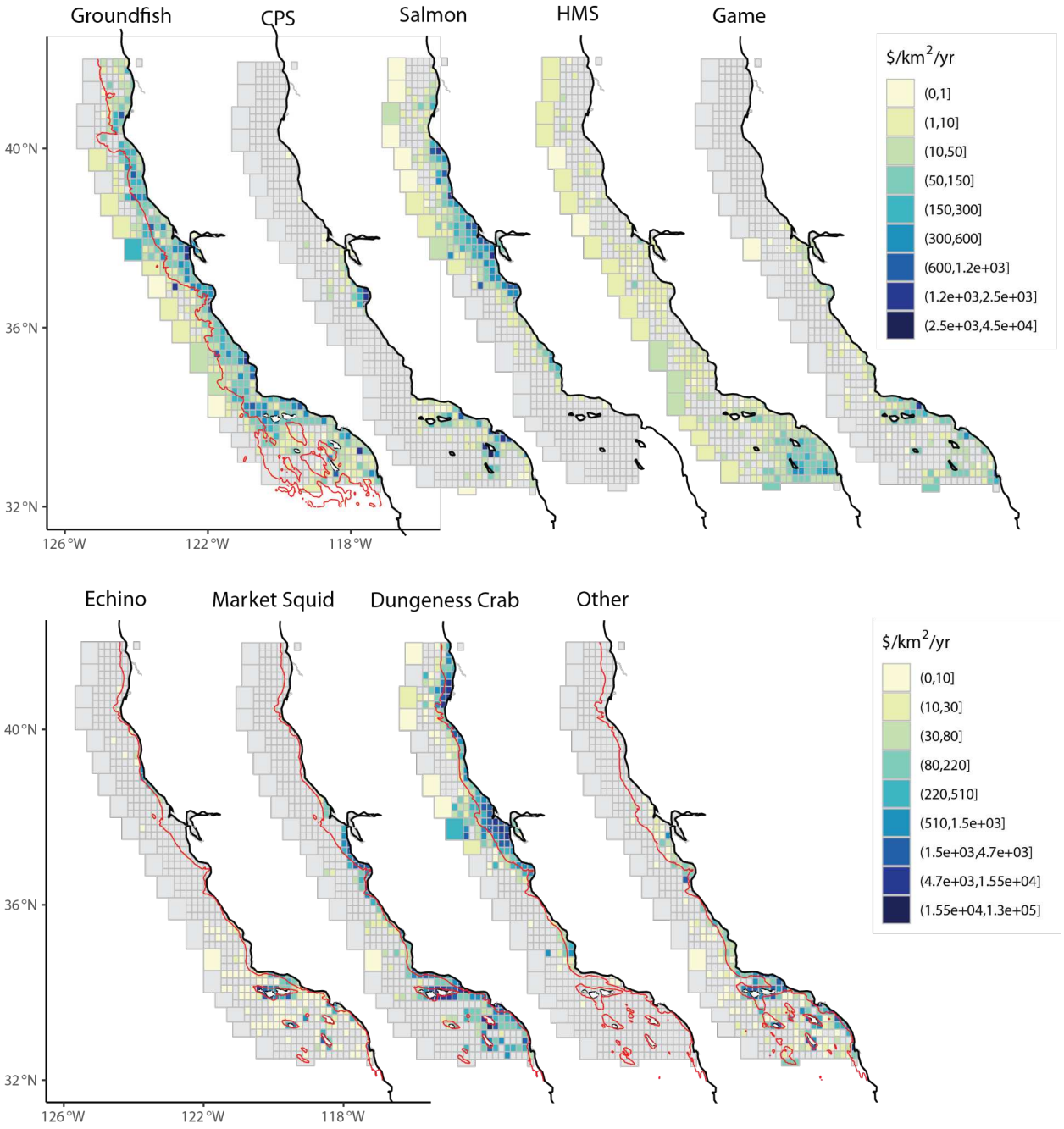

Figure 6.9. Annual average value per unit area for (top) finfish groups (groundfish, CPS, salmon, HMS, and game fish) and (bottom) invertebrate groups (echinoderm, squid, Dungeness crab, and other crustacean) from 2005–2019 after applying "rule of 3".
Note: "Other crustacean" is labeled as "Other".

For finfish groups, groundfish was caught across the entire EEZ. Most groundfish catch was reported within the maximum depth limit (i.e., 1200-m isobath), though some were reported farther offshore. In comparison, CPS fisheries were concentrated in the Southern California Bight and near Monterey Bay, whereas salmon fisheries were scattered north of 36ºN. Game fish were mainly caught in the Southern California Bight. HMS fisheries were concentrated further south near the U.S.-Mexico border. Invertebrate groups were primarily distributed close to the shore within their respective depth ranges. Both echinoderm and other crustacean fisheries were clustered near the Channel Islands in southern California, squid fisheries were mainly located south of 38ºN, and most Dungeness crab were caught north of 36ºN. These findings are consistent with those presented by region (Figure 6.7). Among all taxonomic groups, Dungeness crab had the highest Moran's I, indicating high spatial clustering, whereas groundfish had the smallest Moran' I, suggesting that fishing activity for groundfish is more evenly distributed across the state (Table 6.1).

Table 6.1. Moran's I and its p-value for each taxonomic group based on fishing blocks with neighbors that share at least one vertex

Taxonomic group	Moran's I	p-value
Groundfish	0.09	< 0.005
CPS	0.22	< 0.001
Salmon	0.32	< 0.001
HMS	0.48	< 0.001
Game Fish	0.19	< 0.001
Echinoderm	0.26	< 0.001
Market Squid	0.12	< 0.001
Dungeness Crab	0.52	< 0.001
Other Crustacean	0.15	< 0.001

Given the significant proportion of values reported in four-digit blocks for Dungeness crab and groundfish, we further characterized Dungeness crab and groundfish fisheries in four-digit blocks, which displayed spatial inconsistency over time (Figure C5). Dungeness crab fisheries in the northmost four-digit block accounted for over 40% of landings in 2006, 2009, and 2018. In comparison, groundfish fisheries in the second northmost four-digit block were more important than others, which contributed to over 40% of annual landings in the past five years.

6.3.5 Wind Energy Area case study

Using the fish ticket data, we identified fisheries that could be affected by offshore wind development (Figure 6.11). For the ports adjacent to a WEA, the most valuable fisheries were Dungeness crab in the Humboldt Bay port complex and groundfish in the Morro Bay/Port San Luis port complex. Landings in the self-reported fishing blocks that overlapped with the respective WEAs revealed the same general results. However, when imposing the prescribed depth limits for each fishery (e.g., Table C1; Miller et al. 2017), the relative importance of fisheries shifted substantially. The Humboldt WEA is outside the depth range of Dungeness crab, so removing that species—which is likely not caught in that WEA (Miller et al. 2017)—made groundfish and salmon the most important fisheries in the region. In the Morro Bay WEA, groundfish remained the highest value fishery, and even increased in relative value due to the number of squid reported in the Morro Bay WEA that is outside the prescribed depth limit for that fishery.

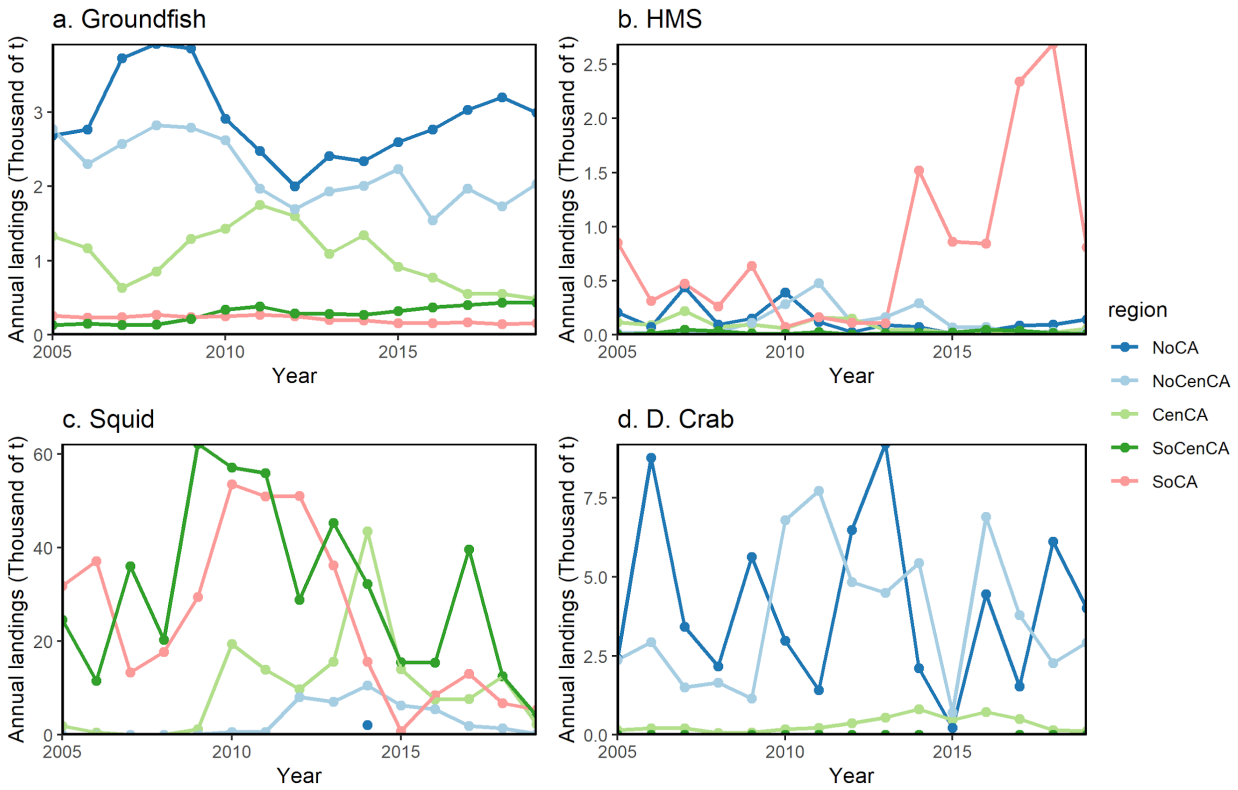

Figure 6.10. Regional annual landings (Thousand of t) for (a) groundfish, (b) HMS, (c) squid, and (d) Dungeness crab.

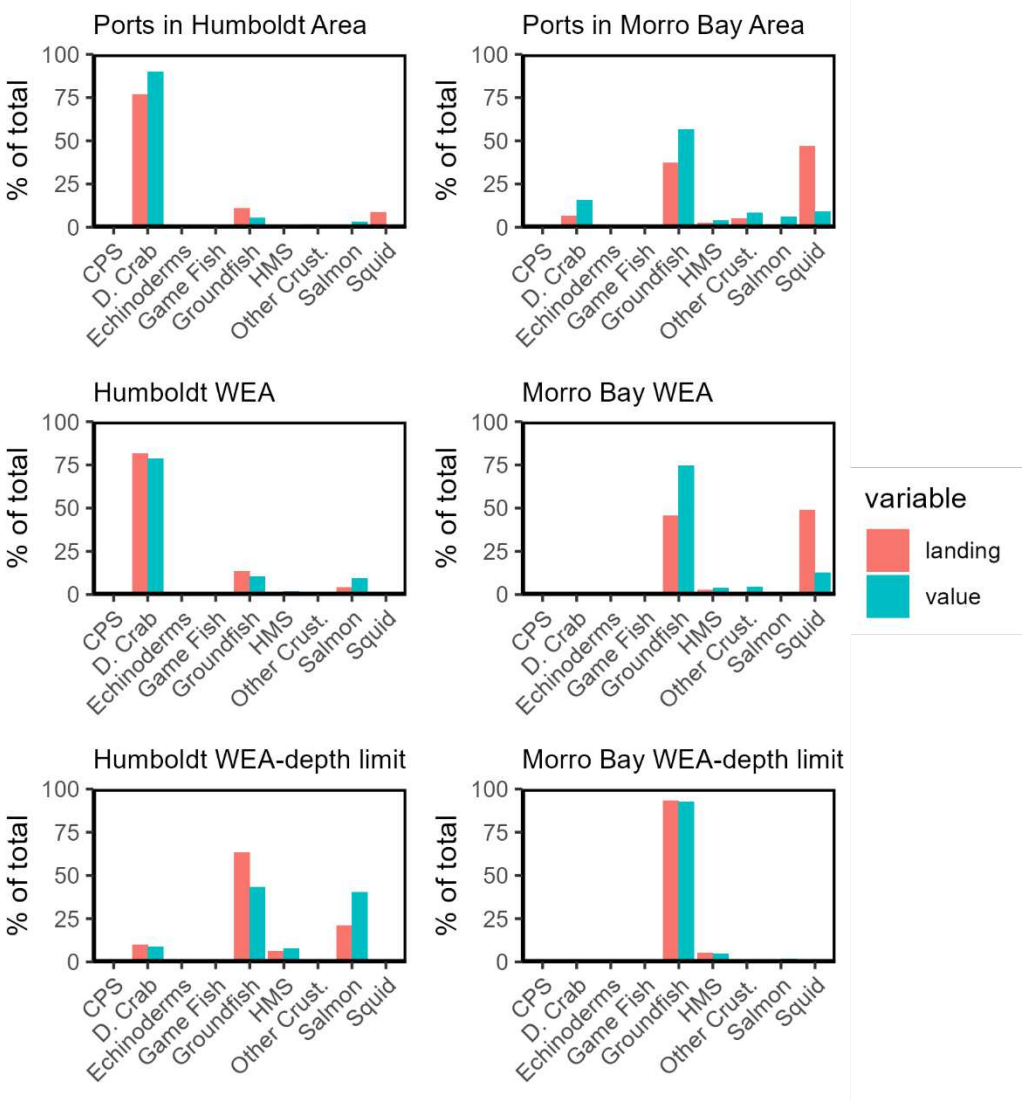

Figure 6.11. Percent of total landings and values based on fishery recorded in three-digit blocks under different conditions.

Note: (top left) Fisheries landed in ports in the Humboldt area (i.e., Eureka, Trinidad, Shelter Cove, Crescent City, Fields Landing, King Salmon, Klamath, Humboldt Bay); (top right) fisheries landed in ports in the Morro Bay area (i.e., Avila/Pt. San Luis, Morro Bay, San Simeon); (middle left) fisheries recorded in the blocks overlapping Humboldt Wind Energy Area (WEA); (middle right) fisheries recorded in the blocks overlapping Morro Bay WEA; (bottom left) fisheries in Humboldt WEA and within prescribed depth limit in Table C1; (bottom right) similar to bottom left but for Morro Bay WEA.

6.4 Discussion

This study characterizes temporal and spatial variation in California commercial fisheries landings and value of key fishery groups from 2005 to 2019. Individual fish groups exhibited substantial interannual variability in landings and values, though they did not always synchronize. Over the 15-year dataset, total landings showed a downward trend, with the 2019 landings being about one-third of the 2005 landings. Despite this decline in landings, the total value of these commercial fisheries remained relatively stable. This trend was due to a steady shift toward lower biomass-higher value species, as well as rising prices, even after accounting for inflation. Spatially, landings and values varied among different regions in both magnitude and species composition. Southern California fisheries decreased in relative importance over the past fifteen years, while the Northern and North Central regions gradually expanded their contribution to statewide landings and values. Many fisheries were also more spatially constrained (e.g., Dungeness crab, game fish, squid), while a few were more widespread (e.g., groundfish) throughout the State.

Variation in fisheries often reflect the dynamics of socio-ecological systems, which are influenced by several factors, including economic conditions, regulatory frameworks, and environmental variation and stressors. For example, increasing fuel prices have been shown to correspond with a decrease in fishing effort (Kroodsma et al. 2018), and changes in regulations can have profound effects on fishery dynamics (Mamula and Kosaka 2019). Decreases in population sizes of target species can lead to fisheries collapse and closure, as happened for salmon fisheries in 2008–2009 (Figure 6.4; Figure C4) (Richerson and Holland 2017). In addition, the impact of climate-driven environmental changes—such as MHW—on commercial fisheries and marine ecosystems can be profound and long-lasting (e.g., Suryan et al 2021). The downward trend of the statewide landings (Figure 6.4a) may be evidence of long-term fisheries impacts from climate change that is projected to reduce catch potential in many temperate and subtropical regions, including waters off California (Cheung et al. 2010).

The variation in California commercial fisheries is complex, since individual fish species have unique biological responses at different life stages that respond differently to changes in environmental or ecological conditions. As a result, different fishery groups are likely to display varying levels of resilience to climate change induced effects. For example, the groundfish fishery is the most geographically widespread across California (e.g., smallest Moran's I; Table 6.1) and includes a range of different species with differing life histories, habitat requirements, and population dynamics. As such, this broad fishery group exhibits relatively stable annual landings in each region over the past fifteen years (Figure 6.10a). The HMS group may also be more resilient than other groups to ongoing and future climate change stressors. Even though the fishery is fairly spatially clumped (2nd highest Moran's I; Table 6.1), with most activity occurring in Southern California (Figure 6.8), the target species are pelagic and are thus able to migrate in response to changes in oceanographic conditions. The migratory feature of the HMS group is evidenced by the significant increase in landings from 2014 onward (Figure 6.10b), which coincided with warm waters associated with the North Pacific MHW and a major phase shift of both the North Pacific Gyre Oscillation (http://www.o3d.org/npgo/index.html) and Pacific Decadal Oscillation (https://oceanview.pfeg.noaa.gov/erddap/tabledap/cciea_OC_PDO.html). As with HMS, adult squid are pelagic; the decrease in landings in the Southern and South Central regions corresponded with an increase in landings in the Central region in 2014, suggesting that squid moved poleward in response to warmer ocean waters during the North Pacific MHW (Figure 6.10c; Cavole et al. 2016). At the same time, adult squid lay their eggs benthically in shallow waters, potentially putting them at risk of warming and/or low dissolved oxygen/pH events, all of which that are increasing in frequency in shallow nearshore waters (Long et al. 2016).

On the other hand, a fishery like Dungeness crab—one of the most valuable in the State—may be much more susceptible to changes induced by climate change. The Dungeness crab fishery is the most spatially clumped (the highest Moran's I; Table 6.1), with the vast majority of fishing activity occurring in the

Northern and North Central regions (Figure 6.7). Dungeness crabs are mostly found in shallower waters closer to shore, where ocean acidification and hypoxia effects are more pronounced due to the upwelling of low DO and pH sub-thermocline waters, large algal blooms, and eutrophication (Grantham et al. 2004). For example, the Dungeness fishery along the Oregon coast has experienced mass die-offs from upwelling-driven hypoxic events (Grantham et al. 2004). Likewise, in California, the drop in 2015 (Figure 4 and Figure 6.10d) resulted at least in part from the delayed fishery opening in response to domoic acid created by widespread harmful algal blooms (Santora et al. 2020), which also may be increasing as climate changes (Gobler, 2020).

Whatever the drivers are of the patterns observed here, a changing climate will continue to impact California fisheries; the variation in California fisheries documented by this study can provide insight and a reference for evaluating the response of fisheries to future climate change. As the climate continues to change, anomalous events such as MHWs are predicted to increase in frequency and intensity (Frolicher et al. 2018), and California fisheries landings may further decline and/or redistribute as some species continue to expand poleward (Cheung and Frolicher 2020; Chaudhary et al. 2021). However, predicting future dynamics of California fisheries can be difficult, given that upwelling and productivity in the California Current may vary more in both time and space under future climate change, which can further complicate biological responses and food web dynamics in higher trophic-level species that are often the primary targets of fisheries (Brady et al. 2017; Xiu et al. 2018), potentially resulting in moving targets for management.

The findings of this study can be used to support and improve current fisheries management. The temporal and spatial variation in key fishery groups can not only help fisheries managers evaluate the effectiveness of regulations on a certain fishery, but also shed some light onto the resilience of a fishery group and the response of fishers to climate-driven oceanographic conditions (Fisher et al. 2021). Combining a better understanding of fisheries variation with near real-time environmental monitoring can further benefit the development of dynamic fisheries management approaches. Our findings can also imply the interactions between different fishery groups and across trophic levels, given interlinked food web dynamics. For example, some fish species such as squid and coastal pelagics are important prey for other top consumers such as seabirds and marine mammals; declining catch of these species may reflect low prey availability, with potentially cascading effects across marine ecosystems (e.g., Bertrand et al. 2012). Therefore, the characteristics of multiple fishery groups documented by this study can provide useful information toward a more comprehensive stock assessment of marine ecosystems and a more advanced ecosystem-based fisheries management.

In addition to commercial fisheries, there are other ocean uses that support the Blue Economy, including aquaculture, tourism, offshore renewable energy, and infrastructure (Dundas et al. 2020). These analyses allowed us to identify the dominant fisheries in the two WEAs for potential offshore wind development off the coast of California, both of which are dominated by groundfish; however, the latter result only holds if the prescribed depths for Dungeness (Humboldt) and squid (Morro Bay) are correct.

While reported catches in the CDFW fish ticket data enable us to explore the temporal and spatial dynamics of California fisheries, there are some potential limitations. First, while the reported block information allows for the identification of spatial hotspots for different fisheries, the landings reported in the much coarser four-digit blocks (compared to the three-digit blocks seen in Figures 6.8 and 6.9) are significant. Because the four-digit blocks are essentially latitudinal bins, we are unable to calculate landings and value per unit area for them. Consequently, the landings and value per unit area may be underestimated considerably for the fishery groups that had a substantial proportion of catch reported in the much larger four-digit blocks. This includes several high-value fisheries like Dungeness crab and groundfish. Second, there was a noticeable fraction of catch reported outside of species' prescribed depth limits, including in regions that are being pursued for offshore wind energy. This mismatch could be due to changing environmental conditions not yet considered by species' depth estimates, misreporting by

fishers, and other factors. While improving the precision and accuracy of fishing locations is beyond the scope of this study, it highlights the need for accurate, higher resolution spatial information to support fisheries management and science that is needed for future work. One approach for calibrating and increasing resolution in spatial information in landings data would be to combine it with other independently-collected high-resolution spatial fisheries data, such as Vessel Monitoring Systems data (e.g., Watson et al. 2018).

6.5 Conclusions

This study significantly advances our understanding of the spatiotemporal dynamics of marine commercial fisheries landings and value across the entire State of California over the last two decades, updating the research by Miller et al. (2017). These updated results confirm the shift from higher biomass, lower value species to lower biomass, higher value species that began several decades ago (Miller et al. 2017). In addition, we document clear spatial patterns and trends in fisheries activity across the State, and the data illustrate how the intensity of specific fisheries have changed statewide, possibly in response to changes in ocean climate or species range shifts. While we also demonstrate some limitations of the spatial accuracy of the fishing ticket block data, these data can help advance a number of current management challenges that intersect with fisheries across the State, including planning for a changing climate, marine spatial planning for additional users of ocean space such as offshore wind, and sustainability of fishery activity into the 21st Century.

7 High resolution assessment of commercial fisheries activity along the U.S. West Coast using Vessel Monitoring System data with a case study using California groundfish fisheries

7.1 Introduction

Commercial fisheries along the U.S. West Coast are diverse and productive (NMFS 2021), generating economic benefits for local and regional economies and working waterfront communities (Norman et al. 2007). On the U.S. West Coast, commercial fisheries employ over 2,800 vessel owners and a much larger number of crew (Holland et al. 2020), and in California generate hundreds of millions of dollars of ex-vessel revenues annually (Hackett et al. 2009). The potential socio-economic impacts of fishery management decisions have led to a considerable research focus on assessing the spatial and temporal patterns in fishing effort, fish stocks, and fisheries landings and ex-vessel value.

Understanding the spatial distribution of activity across U.S. West Coast fisheries is becoming more important to ensure fisheries sustainability as other ocean uses increase and regulatory and management approaches increase in complexity. Vessel traffic for shipping has been increasing in recent years, and planning for offshore wind energy and marine aquaculture is moving forward on the West Coast (BOEM 2023a; BOEM 2023b; NOAA 2023). Networks of marine protected areas have been established in California, Oregon, and Washington over the last 12 years (CDFW 2023; Oregon Ocean Information 2023; Washington Department of Fish and Wildlife 2023), and the size and shape of Rockfish Conservation Areas that span the U.S. West Coast have changed multiple times in the last decade and are likely to change again as stocks recover (NOAA Fisheries 2023). Furthermore, commercial fisheries are responding dynamically to changes in the marine environment driven by climate change (Gruber 2021; Pozo et al. 2021; Selden et al. 2020). To support improved fisheries management and support decision making for multiple uses of ocean space along the U.S. West Coast in a changing marine environment, more accurate and precise data are needed on current spatiotemporal fisheries dynamics across the region.

Recent analyses of California commercial fisheries landings receipts ("fish tickets") at relatively coarse grid-block spatial resolution (the highest spatial resolution of 10' x 10' blocks, approximately 15 km zonally and 18.5 km meridionally depending on latitude) has revealed some important patterns and trends. There has been a shift from high-volume, low-value species toward low-volume, high-value species (Miller et al. 2017; Wang et al. 2022), along with changes in regional spatial patterns of fishing activity over the last decade (Wang et al. 2022). While useful for broad-scale analyses, fish ticket data are limited in their application. First, the spatial resolution of fish ticket data is coarse, resulting in highly imprecise landings data in many fisheries (Wang et al. 2022). Second, self-reported block information that accompanies commercial fish tickets may be inaccurate—for example, reporting blocks that are unrealistic because they are outside the biological depth limit of the target species (Wang et al. 2022; Love et al. 2021). Finally, fish ticket data report landings and ex-vessel value (i.e., revenue), but lack reliable spatially-explicit estimates of fishing effort, reducing their utility in assessing fishing activity. As a result, fish ticket data are limited on their own in fishery management and marine spatial planning applications that require more precise information about fishing activity.

Analyses of vessel monitoring system (VMS) data have been increasingly used to explore spatial fishing activity and inform fisheries management (e.g., Campbell et al. 2014; Cronin et al. 2016; Feist et al. 2021; Gerritsen and Lordan 2011; Russo et al. 2018). VMS provides near real-time transmission of the spatial position of a specific vessel at discrete time intervals (typically every hour in the U.S.), allowing for highly-accurate monitoring of fishing vessel movements. While VMS does not explicitly differentiate between fishing activity and non-fishing activities (e.g., transit), these activities can be distinguished in relation to vessel speed calculated from consecutive VMS points (see e.g., Gerritsen and Lordan 2011;

Deng et al. 2005; Joo et al. 2015). Moreover, VMS provides high spatial accuracy of vessel location (~100 m spatial resolution), greatly reduces misreporting of fishing location, and enables quantification of fishing effort (NOAA 2017).

While there is a growing use of VMS data in fisheries science and management (Campbell et al. 2014; Gerritsen and Lordan 2011; Somers et al. 2020; Watson et al. 2018), these data present challenges of their own. Most importantly, VMS data do not provide fisheries landings or ex-vessel value estimates, nor is VMS required for all vessels and fisheries. However, for fisheries and fleets where VMS is widely adopted and/or required by law, VMS data can provide reliable and representative spatial estimates of fishing effort. Further, VMS data contain a unique vessel identification number for a specific vessel, which can be matched with vessel identification number and date-stamp data in fish tickets, thereby allowing the two datasets to be linked (Feist et al. 2021; Samhouri et al. 2021; Liu et al. 2023). Fish ticket landings and ex-vessel value reports can then be mapped onto VMS vessel tracks to generate accurate and spatially resolved estimates of landings and ex-vessel value that cannot be provided by fish ticket or VMS data alone.

In this study, we focused on VMS data rather than Logbook and Observer data since VMS data are relatively underexplored. We processed the data, and produced spatial maps of relative fishing effort across the entire U.S. West Coast, encompassing, a variety of commercial fisheries that collected VMS data (see Data and Methods). We then compared VMS data with independent Observer data and Logbook data and found similar spatial patterns that suggest that our analysis on VMS data can reasonably capture fishing activity patterns. Because VMS is required for all vessels fishing in U.S. federal waters for groundfish (NMFS 2020), as a test case we conducted a more comprehensive analysis of the spatiotemporal dynamics of groundfish in particular by matching VMS polls in California with concurrent California fish ticket landings and ex-vessel value data for groundfish. The resulting VMS-fish ticket dataset enabled us to assess patterns of effort, landings and ex-vessel value at high resolution along the entire California coast. The data synthesis framework demonstrated here for the groundfish fishery using independent tracking (VMS) and reporting (fish ticket) data can be used for a variety of marine spatial planning and fishery management applications for groundfish, and our framework, which builds upon previous research using VMS data to quantify fisheries activities (Campbell et al. 2014; Gerritsen and Lordan 2011; Somers et al. 2020; Watson et al. 2018 and others) can be applied to other fisheries to generate similar information on spatial fisheries dynamics.

7.2 Data and Methods

7.2.1 Data

7.2.1.1 Vessel Monitoring System

We obtained VMS data from National Oceanic and Atmospheric Administration's (NOAA) National Marine Fisheries Service (NMFS) Office of Law Enforcement (OLE) (NOAA 2017) from 2010 to 2017 to estimate fishing effort across the entire U.S. West Coast within the U.S. Exclusive Economic Zone (EEZ, 200 nautical miles [nm] from the coast). VMS is a spatial monitoring system required on certain fishing vessels that uses satellite and cellular-based communications from onboard transceiver units to track the geographic location of U.S. commercial fishing vessels. The transceiver units send 'polls' (also referred to as 'pings' and 'records'), which are transmissions of data that include vessel identification, time, date, location, and average speed (NOAA 2021). VMS data tracks vessel locations at high temporal frequency (NOAA Fisheries 2023); of the VMS data used in this study, over 87% of the polls had transmission intervals less than or equal to one hour.

On the U.S. West Coast, VMS transceivers are required for commercial fishing vessels registered with a Pacific Coast groundfish limited entry permit, a fishing permit issued by NOAA NMFS. This includes vessels that take, retain, or possess groundfish within federal waters in the EEZ, or land groundfish taken in the EEZ (NOAA Fisheries 2023). 'Groundfish' includes all benthically associated fishery species on the west coast, such as sablefish, flatfish (e.g., Dover sole), and rockfishes (Miller et al. 2017; Wang et al. 2022). In addition, VMS is required on drift gillnet vessels participating in Highly Migratory Species (HMS) fisheries, and any vessel that uses non-groundfish trawl gear in the EEZ (NOAA Fisheries 2023). Although the VMS system is associated with permitted fishing in federal waters, vessels regulated to have VMS are required to operate the transceiver during all fishing trips, whether in federal or state waters. Note that vessels that fish for groundfish only in state waters (out to 3 nautical miles from shore) are not required to have VMS. In addition, vessels that operate under a permit associated with VMS (e.g., Pacific Coast groundfish limited entry permit) are also required to operate a VMS transceiver during all fishing trips, even when fishing with gear or targeting fish species outside the jurisdiction of the VMS requirement (e.g., Dungeness crab fishery, salmon fishery). In addition to tracking information, the VMS polls include a declaration code characterizing the fishing activity, including gear and target species, which are generally associated with a specific fishing permit (Table 7.1). Thus, VMS not only has nearly complete coverage of commercial groundfish fisheries operating in federal waters, but also covers many other commercial fisheries in the region (albeit with varying, potentially low, levels of representation). Because the groundfish fisheries have high coverage, we matched its VMS data with the fish ticket data for groundfish landings to create high-resolution maps of landings and ex-vessel value.

Table 7.1. Information Summary for VMS declaration codes (NDL represents declarations whose fisheries have no depth limits)

Decl.	Description (dominant gear types)	Number of VMS records	Number of vessels	Cutoff fishing speed (knots): local min	Cutoff fishing speed (knots): slope min	% of fishing effort inside biological depth limit
210*	Limited entry fixed gear not including shore-based IFQ (pots/traps, bottom longline, longline, hook and line)	547,116	266	4.51	2.39	97.4%
211*	Limited entry groundfish non-trawl shore-based IFQ (pots/traps, bottom longline, longline, hook and line)	111,976	47	4.97	2.01	99.2%
220*	Limited entry midwater trawl gear non-whiting shore-based IFQ (midwater trawl for species other than whiting)	85,600	54	4.94	3.63	NDL
221*	Limited entry midwater trawl Pacific whiting shore-based IFQ (midwater trawl for whiting)	316,994	35	4.31	3.27	NDL
222*	Limited entry midwater trawl Pacific whiting catcher-processor sector (midwater trawl for whiting)	174,298	16	5.48	4.13	NDL
223*	Limited entry midwater trawl Pacific whiting mothership sector; catcher vessel or mothership (midwater trawl for whiting)	234,673	32	6.00	3.40	NDL

Decl.	Description (dominant gear types)	Number of VMS records	Number of vessels	Cutoff fishing speed (knots): local min	Cutoff fishing speed (knots): slope min	% of fishing effort inside biological depth limit
230*	Limited entry bottom trawl shore-based IFQ not including demersal trawl	635,890	129	4.41	2.46	~100%
231*	Limited entry demersal trawl shore-based IFQ	7,745	2	4.34	2.01	100%
233*	Open access longline gear for groundfish	186,528	414	4.03	2.01	97.3%
234*	Open access groundfish trap or pot gear	136,693	289	4.00	2.01	98.9%
235*	Open access line gear for groundfish	260,969	307	4.24	2.00	94.0%
240	Non-groundfish trawl gear for ridgeback prawn	21,527	4	4.63	3.00	99.6%
241	Non-groundfish trawl gear for pink shrimp	864,053	141	4.61	2.01	98.3%
242*	Non-groundfish trawl gear for California halibut	44,187	22	4.95	2.92	99.6%
243	Non-groundfish trawl gear for sea cucumber	51,849	11	5.23	2.10	89.7%
250*	Tribal trawl gear	3,156	4	6.00	3.90	100%
260	Open access prawn trap or pot gear	37,153	21	4.92	2.70	96.8%
261	Open access Dungeness crab trap or pot gear	1,211,912	579	4.93	3.11	95.3%
262*	Open access Pacific Halibut longline gear	24,836	124	3.64	2.02	96.1%
263	Open access salmon troll gear	571,713	384	4.40	3.01	NDL
264*	Open access California halibut line gear	37,738	47	4.47	2.53	93.7%
265*	Open access sheephead trap or pot gear	9,802	8	6.00	2.14	73.8%
266	Open access Highly Migratory Species line gear	473,212	344	3.74	6.00	NDL
267	Open access Coastal Pelagic Species net gear	2,277	8	5.17	2.84	NDL
268	Open access California gillnet complex gear	32,966	15	6.00	2.19	NDL
269	A gear that is not listed above	408,909	495	4.55	3.81	NDL

For each VMS declaration code, this table includes the description, number of VMS polls after data processing used in this study, number of vessels represented, fishing-transit cutoff speed determined from the local minimum method, fishing-transit cutoff speed determined from the slope minimum method, and the percentage of fishing effort inside the maximum depth limit relative to the total fishing effort over lease blocks based on the local minimum method (NDL represents declarations whose fisheries have no depth limits).

An asterisk (*) indicates a declaration for the groundfish fisheries that have VMS requirements.

Additional information on VMS data and the declaration codes is provided by NOAA at <https://www.fisheries.noaa.gov/west-coast/resources-fishing/vessel-monitoring-system-west-coast>

7.2.1.2 Fish ticket

We used commercial fisheries landings receipts, known as 'fish tickets,' which offer information about landings and ex-vessel values not provided by VMS data. The fish ticket data in this study focuses on California, as it was provided by California Department of Fish and Wildlife (CDFW) through a data agreement over the same time period as the VMS data. Fish tickets are submitted to CDFW at port following a vessel fishing trip. Along with a unique vessel identification number, each ticket records the landing weight and unit price (i.e., price per pound), species caught, landing port and date, and fishing block catch location (see Wang et al. 2022).

7.2.2 Data processing

7.2.2.1 Vessel Monitoring System

We used raw VMS data for the years 2010–2017. We applied a series of processing and filtering steps to the raw VMS data (Figure 7.1). We first corrected negative latitudes of VMS polls due to transmission errors to positive latitudes (~0.39% of the raw data). We then removed duplicate VMS polls so that there was only one VMS poll at a given time for a vessel (~9.5% of the raw data). To focus on activities along the U.S. West Coast, we removed VMS polls from outside the domain of 32-50°N and 117-130°W, leaving ~78.4% of the raw data retained. Of all VMS polls outside the West Coast domain, 86.9% were in the vicinity of Alaska (within the domain of 50-70°N and 130-180°W), 2.8% were near Hawaii (within the domain of 18-23°N and 154.5-161°W) and most of the remaining VMS polls were distributed across the Pacific. The bulk of the VMS polls in the remaining dataset were from vessels docked in port. A VMS poll was labelled as out of port if it was not on the land of the West Coast states (i.e., California, Oregon, and Washington) and was outside of a 3-km buffer zone of ports for commercial fisheries (~12.5% of the raw data retained for downstream analysis, which includes the calculation of fishing efforts by declarations and the match with fish ticket data for groundfish fisheries). We filtered VMS polls within 3 km of a port as an educated guess to minimize the chance of misidentifying polls from vessels moving slowly near ports as fishing. The VMS data loss in each processing and filtering step is visualized in Figure D.1.

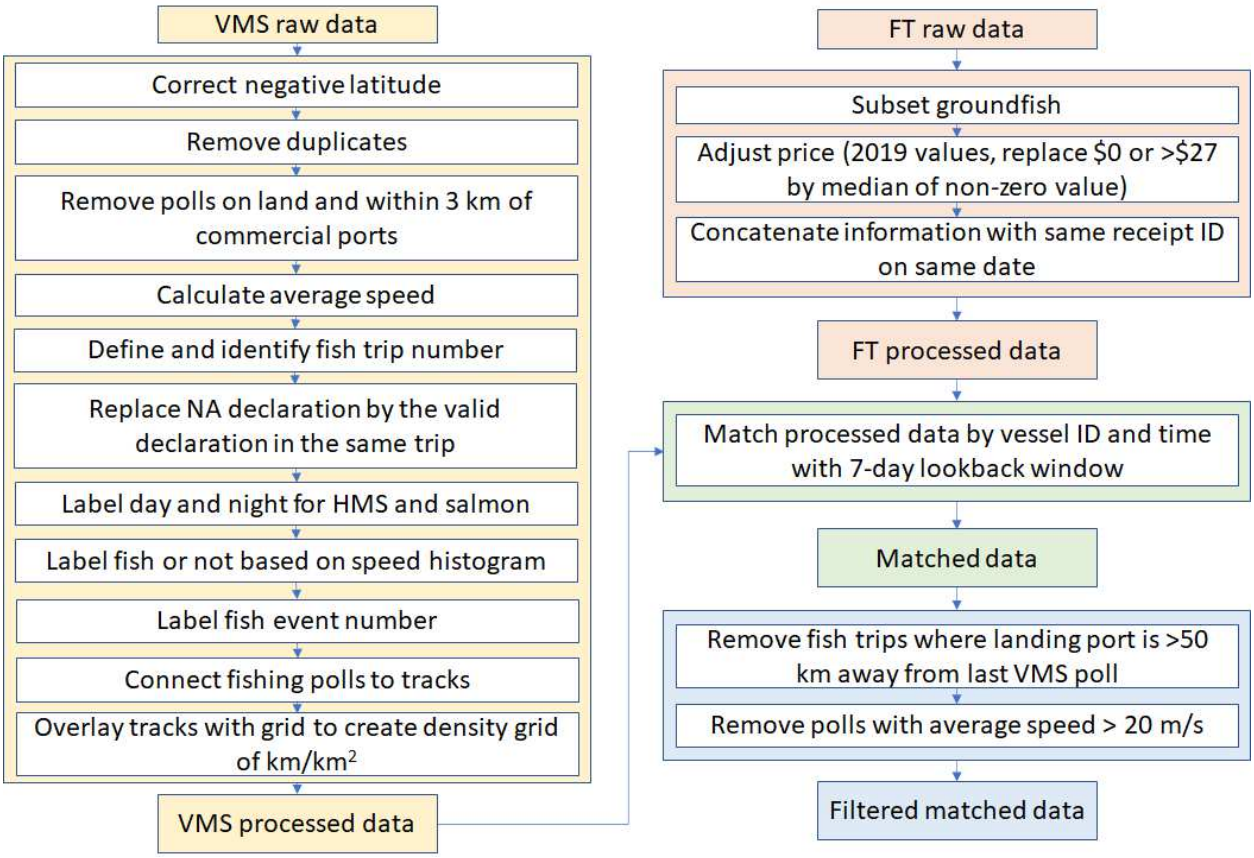

Figure 7.1. Flowchart illustrating the processing of VMS and fish ticket data.

For each vessel, we calculated the average speed at each poll location based on the time and distance between the current poll and previous poll, reflecting the speed a vessel has been traveling over some distance. Our calculated average speed agrees well with the average speed directly provided with the VMS polls and has fewer extremely large outliers than the original average speed. Instantaneous vessel speed is provided by VMS, but we did not use it because reported speed is more susceptible to transient fluctuations in vessel speed and reported speed was missing for many polls. Hereafter, 'speed' refers to the calculated average vessel speed.

Next, we calculated individual trips for a given vessel, with the beginning of a trip defined as when that vessel left a port and the end of the trip when the same vessel returned to a port. Therefore, our analysis included all vessels that returned to the same port or to a different port. All consecutive polls for a given vessel between the start and end of a trip were considered to be part of a single trip, unless two consecutive polls of a vessel were recorded more than five hours apart. In that case, a new trip was defined after the time gap since it is impossible to know where that vessel was during that 5+ hour gap in VMS coverage. With only roughly 0.21% of VMS polls with 5+ hour gaps, the likelihood of these time gaps substantially altering the results is extremely low.

To organize the data by fisheries type, we grouped VMS polls by declaration code (Table 7.1). Approximately 9.83% of the processed polls had invalid or missing declaration codes, which typically arose from entire trips not having any declaration data. These VMS polls were not excluded from matching with fish tickets if other information is available. While a vessel can switch declaration codes on a given trip, less than 1% of the trips recorded more than one valid declaration code.

To estimate fishing versus non-fishing activity, we generated density histograms of vessel speed for all out-of-port VMS polls for each declaration code (Palmer and Wigley 2009; Lee et al. 2010). Many of the declarations had bimodal distributions of speed. We assumed vessels transit to/from fishing grounds at a relatively higher cruising speed than when fishing at the fishing grounds, thus in the histograms the lower mode represented the peak of intensity of speeds while fishing, and the higher mode the peak of intensity of speeds while transiting. Additionally, we estimated the local minimum between the modes in the density histograms as the cutoff speed, with locations with speeds lower than this cutoff classified as fishing and locations with speeds greater than or equal to this cutoff categorized as transiting. We constrained the local minimum between two and six knots (3.7 - 11.1 km/hr), given that previous research found typical fishing speeds for U.S. commercial fisheries vessels to be within or below this range (Palmer and Wigley 2009; Mamula et al. 2020).

To investigate the sensitivity of our results to the method of using the local minimum vessel speed for differentiating between fishing and non-fishing activity, we compared the spatial pattern of fishing effort for each declaration code derived from the local minimum speed method with that derived from an alternative method where we used the minimum slope of the density histogram between two and six knots (i.e., the point of steepest drop, or most negative slope). See Figures D2-D4 for an illustration of the two methods.

For salmon and HMS, we further classified VMS polls as 'daytime' if they occurred between morning and evening nautical twilight and labelled all polls outside this time as 'not fishing' since these two fisheries target visual predators and therefore typically only operate during daytime. Finally, we define a 'fishing event' within each trip as a series of consecutive polls that were classified as 'fishing'. The resulting track of each fishing event was used to quantify fishing effort for each declaration code (Section 7.2.3).

7.2.2.2 Fish tickets

We retained fish tickets for groundfish, since VMS is required for groundfish fisheries in federal waters. The fish tickets pertaining to groundfish species, including leopard shark, sanddabs, founders (starry, unspecified), turbots, soles (bigmouth, rock, fantail, sand, English, butter, tongue), California halibut, cabezon, scorpionfish, staghorn sculpin, yellowfin sculpin, lingcod, petrale sole, Pacific halibut, North Pacific hake, flounder arrowtooth, rockfish, sablefish, spiny dogfish, soles (Dover, rex) and thornyheads, were extracted from the fish ticket raw data (see detailed information in Table C1). Before matching with VMS data, we processed fish ticket data following (Wang et al. 2022). We corrected unit prices for inflation based on the consumer price index for December 2019. We also replaced null values and values of \$0/lb, taking into consideration the presumed economic value of landings where values were not reported, or implausible unit prices (> \$27/lb), with the median price of non-\$0 prices for that species or fishery group. We then calculated the ex-vessel value, or revenue, of the catch landed by multiplying the landing weight in pounds by the unit price reported on each fish ticket. If multiple fish tickets were submitted for a given vessel on the same date, these data were combined.

For visualization of patterns of landings and ex-vessel value by groundfish species, we aggregated the species recorded in fish tickets into either individual species or species functional groups. These seven categories included: halibut (California halibut, *Paralichthys californicus*, and Pacific halibut, *Hippoglossus stenolepis*), flatfish (all other flatfish excluding halibut), roundfish (i.e., cabezon, *Scorpaenichthys marmoratus*, lingcod, *Ophiodon elongatus*, and scorpionfish, *Scorpaena sp.*), rockfish (*Sebastes sp.*), sablefish (*Anoplopoma fimbria*), thornyheads (*Sebastolobus sp.*), and other (i.e., spiny dogfish sharks, *Squalidae acanthias.*). We defined functional groups following PacFIN (https://pacfin.psmfc.org/pacfin_pub/data_rpts_pub/code_lists/sp.txt) with a few modifications. Halibut was evaluated separately from the flatfish category because these species are specifically targeted and

represented by specific declaration codes not associated with the other flatfishes (Table 7.1). Sablefish was separated because of its relatively high commercial ex-vessel value in the study region.

7.2.3 Fishing effort

Using the processed VMS data, we quantified fishing effort for each declaration code across lease blocks designated by BOEM. BOEM lease blocks are 4.8 x 4.8 km polygons covering the EEZ adjacent to California, Oregon, and Washington (BOEM 2023). To calculate fishing effort, for each declaration code we connected the VMS polls within each fishing trip chronologically to create a set of fishing tracks, each corresponding with a fishing event, then we summed the length of the fishing tracks inside each lease block. Following (Somers et al. 2020), we then divided the sum of the fishing track lengths within each lease block by the area of the block, then averaged the solution across the number of years in the dataset (eight) to determine the annual-mean fishing effort in each lease block (km/km^2/year). To assess the spatial reliability of the VMS data, for each declaration code we calculated the percentage of estimated fishing effort across lease blocks within versus beyond the biological depth limit for the target species (delineated by Miller et al. 2017 and FishBase 2023), similar to that conducted by (Wang et al. 2022).

To help validate the spatial accuracy of our results, we compared the estimates of the spatial distribution of fisheries effort generated in this study to estimates of effort generated through the NOAA NMFS Observer Program (Somers et al. 2020), which uses independent scientific observation of fishing activity and catch on commercial groundfish vessels while at sea. Coverage rates for groundfish trawl fisheries (from 2011-present) in the Observer Program are extremely high, generally > 99% (Somers et al. 2022). Therefore, the Observer Program dataset provides a robust 'ground-truth' for estimates of effort derived from VMS data. We focused on groundfish trawl fisheries (primarily represented by Declaration Code 230) in the VMS dataset, since this declaration code is the primary fishery represented in the NOAA groundfish trawl Observer dataset (Somers et al. 2020). We summarized VMS data by years 2011–2015 and 2016–2017 to match similar summary periods in (Somers et al. 2020). We downloaded these Observer datasets from Data Basin (https://databasin.org/datasets/8b0d742d072746cca3bb98be0c9c49d8/) and re-gridded fishing effort at the same BOEM lease block scale used for our analyses to enable direct comparisons between these two datasets. Finally, we performed a spatial correlation analysis on fishing effort over the lease blocks that were available in both the VMS and Observer datasets.

Importantly, the coverage rate of the VMS and Observer data differs between fisheries (Somers et al. 2022). While the VMS covers nearly all trips for groundfish fisheries (because it is required – see e.g., NOAA Fisheries 2023), it likely covers less for other fisheries. We are not aware of any source that explicitly quantifies coverage rate for U.S. West Coast fisheries that utilize VMS.As a result, VMS data may not capture the absolute magnitude of fishing activity for many of the non-groundfish fisheries for which VMS is not required. There are few other datasets with which to ground truth our VMS results, but a map using the Oregon Department of Fish and Wildlife Logbook data made available to the OROWindMap gateway (https://offshorewind.westcoastoceans.org/)https://offshorewind.westcoastoceans.org/) for the Dungeness crab fishery for 2010/2011–2017/18 nearly completely overlaps with our VMS dataset. While we were unable to download the spatial data—and therefore could not statistically compare it to our data—we used this dataset to compare the visual patterns for this fishery.

7.2.4 Matching VMS and fish ticket data for groundfish

To link the processed VMS data (vessel records of fishing vs. non-fishing activity across declaration codes) with the California fish ticket data (port landings and ex-vessel value reported by vessels), we followed methodology developed by NOAA (Feist et al. 2021; Samhouri et al. 2021; Mamula et al. 2020), summarized here. The two datasets were first joined by unique vessel identification numbers and

time. If VMS polls were recorded between two consecutive fish tickets for a given vessel, then those polls were matched to the later fish ticket. If there were more than seven days between two fish tickets, only the VMS polls for the last seven days were included matched to the later fish ticket. We chose a seven-day interval as the cutoff interval between consecutive fish tickets because the frequency distribution of intervals between consecutive fish tickets showed a substantial decline after seven days. If the reported port of landing from the fish ticket was more than 50 km away from the last VMS poll of an associated trip, all VMS polls from that trip were removed from further analysis. Finally, if a VMS poll recorded a speed greater than 20 m/s (~39 knots), it was removed from further analysis. Importantly, we considered only vessel name, location, and date—but not declaration code—when matching vessel trips to fish tickets, so potentially erroneous declaration codes had no influence on the matching process. See Figure1 for a graphical description of the data processing steps for VMS and fish ticket data, including the process to join these datasets.

7.2.5 Fishery landings and ex-vessel value

To estimate the spatial distribution of landings and ex-vessel value, we assigned the landings and value from a given fish ticket to the fishing tracks determined from its matched VMS polls, then distributed landings and value proportionally within each fishing block based on the fraction of the track length that occurred in each block for that fish ticket. In some cases, fish tickets matched multiple VMS trips (22% of fish tickets) so catch for that fish ticket was distributed proportionally over the length of the total fishing tracks for those matching trips (Gerritsen and Lordan 2011). For example, a fish ticket that landed 100 pounds of fish sold at $2/pound that consisted of 10 km of fishing track would have 10 pounds of fish and $20 assigned to each km of fishing track. If that same fish ticket had 6 km of fishing tracks in block A and 4 km in block B, block A would be assigned a value of 60 pounds and $120 over 6 km for that trip, and block B would be assigned a value of 40 pounds and $80 over 4 km. We then summarized the total landings and ex-vessel value by summing the total effort, landings, and ex-vessel value for each block in each year.

We summarized data by species groupings (using the 7 species groupings described in Section 7.2.2) and California ports/port complexes (CDFW 2021). We also evaluated Pearson correlations between the total groundfish fish ticket dataset (i.e., matched plus unmatched), the matched groundfish dataset (i.e., fish tickets that matched to VMS polls), and the unmatched groundfish dataset (i.e., fish tickets that did not match to VMS polls).

7.2.6 Visualization

To visualize our estimated metrics of VMS data and merged VMS-fish ticket (hereafter, VMS-FT) groundfish data fisheries activity (effort, landings and ex-vessel value) across all lease blocks in the region, we created heat maps using cumulative octiles, where each octile (corresponding to one color in the colorbar) represents approximately 12.5% of the sum of the fisheries activity over all the lease blocks (e.g., in a fishing effort map, lease blocks with the first and second color octiles cumulatively represent 25% of the total effort across the mapped domain). Since different fisheries have different magnitudes of a given estimated metric, using cumulative octiles allows us to display detailed spatial patterns of a given fishery in an objective and systematic way. It is important to note that hot spots of some fisheries identified by hot colors can have lower magnitude than low spots of other fisheries identified by cool colors. Lease blocks that include data from less than three unique vessels are not displayed to protect the privacy of vessel operators (e.g., the so-called “rule of three”, cf. NOAA Administrative Order 216-100). Therefore, within the context of the rule of three, cell values in the first color octile do not include zero. The fisheries activity data in blocks that do not meet the rule of three are not included in the calculation of the octiles, but are included in the other, non-map figures describing our results.

7.3 Results

7.3.1 VMS

A total of 247,043 fishing trips were identified within the VMS dataset (2010–2017) across 30 valid vessel declaration codes, including four exemption declarations not shown (Table 7.1). Of these, 37% represented trips targeting groundfish across 16 declaration codes. Analysis of the density histograms of vessel speed for each declaration code using the local minimum method found that the cutoff speed for fishing ranged from 3.64-6 knots (6.74-11.11 km/hr), with a median (mean) across declaration codes of 4.61 (4.74) knots (8.54 km/hr) (Figures D2-D4). Using this cutoff speed generated 685,237 unique fishing events with a total of 6,590,718 VMS polls, which were used for calculating fishing effort.

Comparison of the spatial pattern of fishing effort derived from the local minimum speed method versus the minimum slope method found the latter to generate a lower cutoff fishing speed for all but one valid declaration code (Table 7.1; Figures D2-D4). A lower cutoff always leads to a lower estimate of fishing effort, so the local minimum method yielded higher fishing effort for all but one of the declarations codes. However, the choice of method had a negligible effect on the spatial distribution of relative fishing effort: among all declaration codes, the median (mean) correlation coefficient between spatial effort estimates derived by the two methods was R = 0.99 (0.97). Therefore, all estimates of fishing effort presented and discussed below are derived using the local minimum method for identifying fishing speed.

Comparison of our estimates of groundfish fishing effort using the VMS data to estimates of effort generated independently by the NOAA Observer Program found the spatial pattern of relative fishing effort was similar (R = 0.88 for 2011–2015, R = 0.86 for 2016–2017), although the VMS data using our method had slightly higher levels of effort than those recorded in the Observer data (Figure 7.2). Similarly, visual inspection of Dungeness crab fisheries activity in Oregon between our dataset and data generated by Oregon Department of Fish and Wildlife (OROWindMap, https://offshorewind.westcoastoceans.org/https://offshorewind.westcoastoceans.org/) found the patterns to be congruent (Figure 7.3). For example, there were hotspots of high fisheries activity along the Oregon coast at Astoria and areas north and south of Coos Bay, and lower fisheries activity between Astoria and Newport. The similar spatial patterns across different datasets for the same fisheries suggests that VMS reasonably captures the spatial patterns of relative fishing activity.

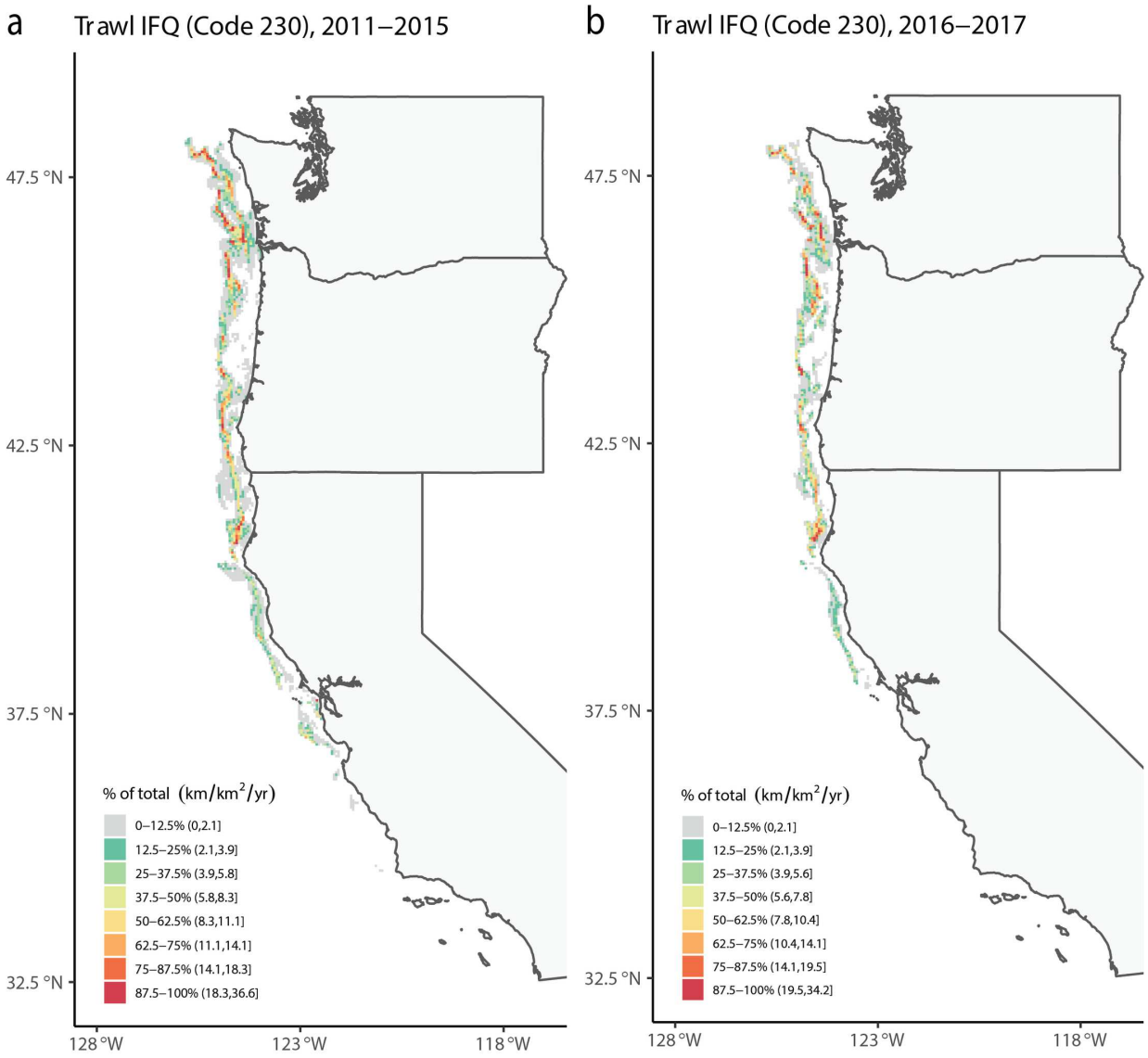

Figure 7.2. Comparison of annual-mean fishing effort between VMS data and Observer data.
Note: Left: Fishing effort from VMS data for limited entry bottom trawl shore-based individual fishing quota (IFQ) not including demersal trawl fisheries (Declaration 230). Right: Fishing effort from Observer data for catch share (CS) bottom trawl. a. 2011–2015 (R = 0.88), and b. 2016–2017 (R = 0.86). The Observer data layer is from (Somers et al. 2020), via Data Basin (https://databasin.org/datasets/8b0d742d072746cca3bb98be0c9c49d8/). For comparisons between datasets with different spatial resolutions, we calculated the zonal mean of fishing efforts based on the Observer data over individual lease blocks using ArcMap 10.8.1. This step ensured a consistent spatial resolution for each dataset. Each color in the legend represents octiles of total fishing effort over the entire domain, such that the lowest octile in gray represents locations that collectively constitute the lowest 0-12.5% of the fishing effort, and the highest octile in red represents locations that collectively constitute the highest 87.5%-100% of the fishing effort. Nearly all of the maps were created using 'rnatureearth' and 'rnaturalearthdata' packages in R, which all use maps in the public domain from Natural Earth Data (https://www.naturalearthdata.com)

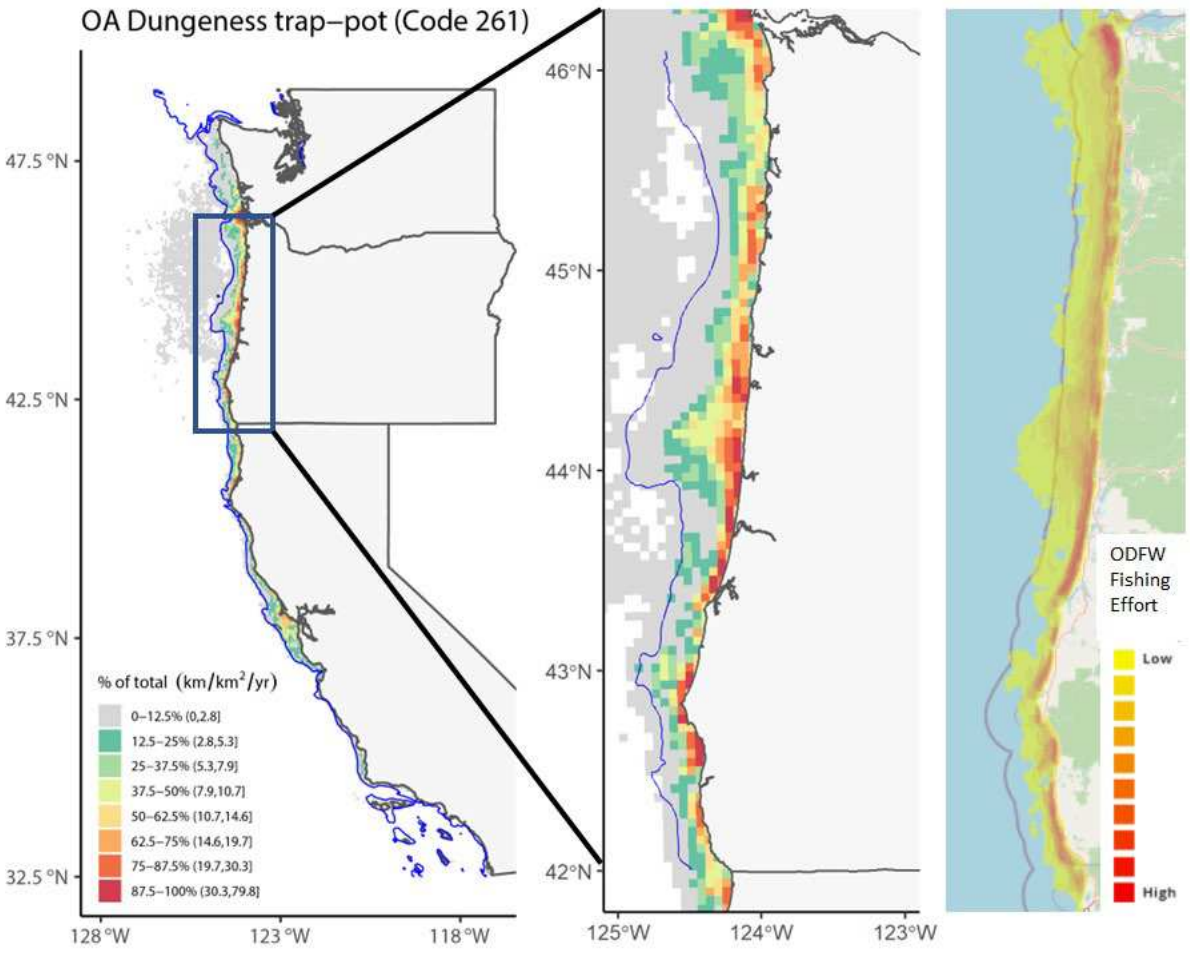

Figure 7.3. Annual-mean fishing effort of Dungeness crab fishery.
Note: Left panel: Annual-mean fishing effort (km/km^2/yr) across lease blocks for open access (OA) Dungeness crab trap and pot fisheries (Declaration Code 261) during 2010–2017. The blue line is the 200 m isobath, representing the maximum biological depth for Dungeness crab. The area outside of the biological depth limit may represent erroneously reported declaration codes, and only represents 4.7% of the total effort for the fishery. Right two panels: Comparison of annual-mean fishing effort of Dungeness crab fisheries in Oregon between VMS data (zoomed-in version of the left panel) and Oregon Department of Fish and Wildlife (ODFW) Logbook data made available on OROWindMap, using an OpenStreetMap (https://www.openstreetmap.org/copyright) (rightmost).

We focused our mapping visualizations on the economically important groundfish fisheries by combining those declarations with similar vessel operations (fixed gear: Figure 7.4; trawl gear: Figure 7.5), along with the economically important Dungeness crab fishery (Figure 7.3) and maps of most of the individual declarations (Figures D5-D25). We excluded declarations 231 and 267 because they had very low overall fishing effort and no grid cells satisfied the rule of three constraint.

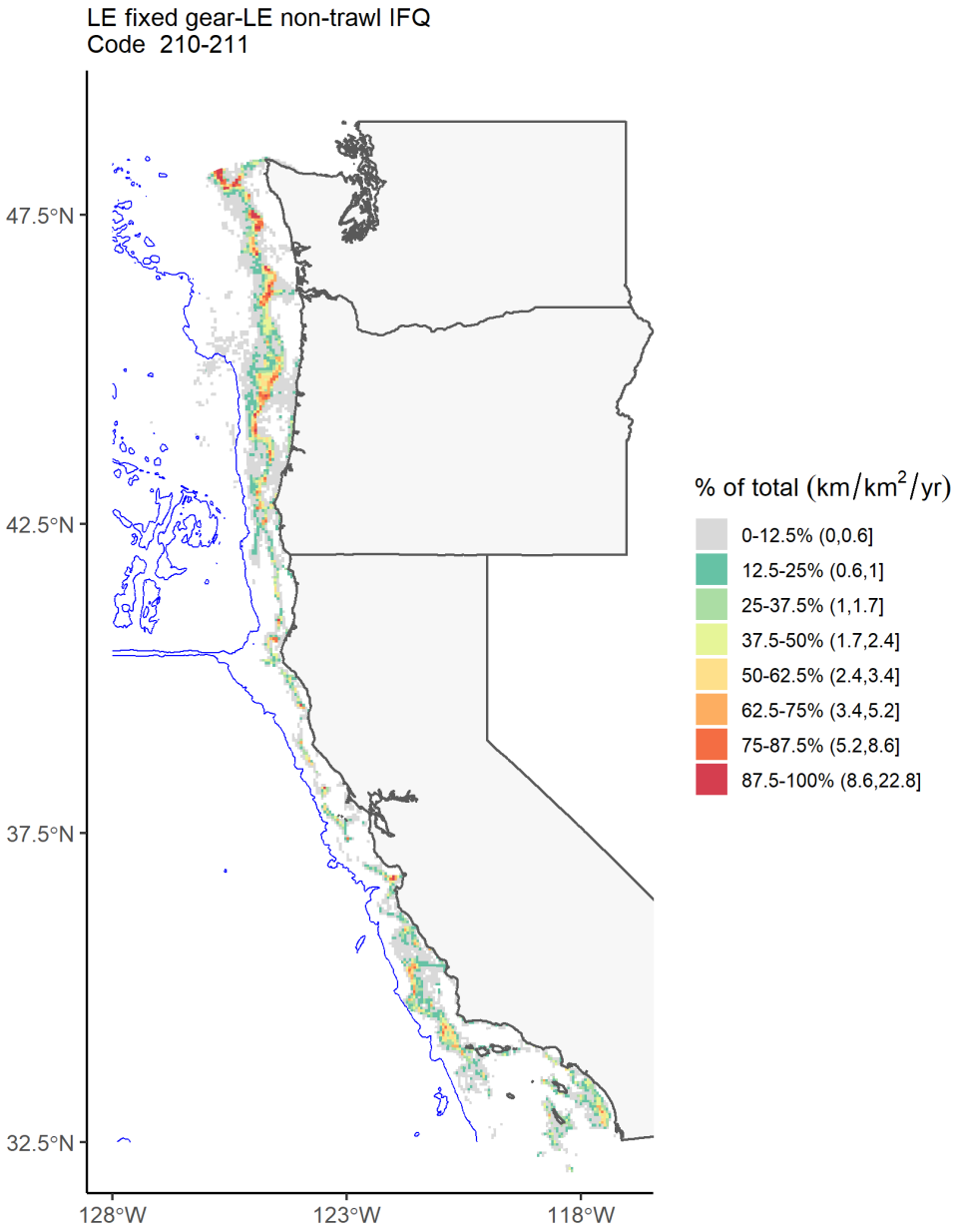

Figure 7.4. Annual-mean fishing effort across lease blocks for fixed-gear limited entry (LE) individual fishing quota (IFQ) fisheries (Declaration Codes 210 and 211).
Note: The unit is km/km^2/yr. The blue line is the 2700 m isobath, representing the maximum depth for all groundfish fisheries except for midwater trawl. The area outside of the biological depth limit may represent erroneous declaration codes, and only represent 2.3% of the total effort for the fishery.

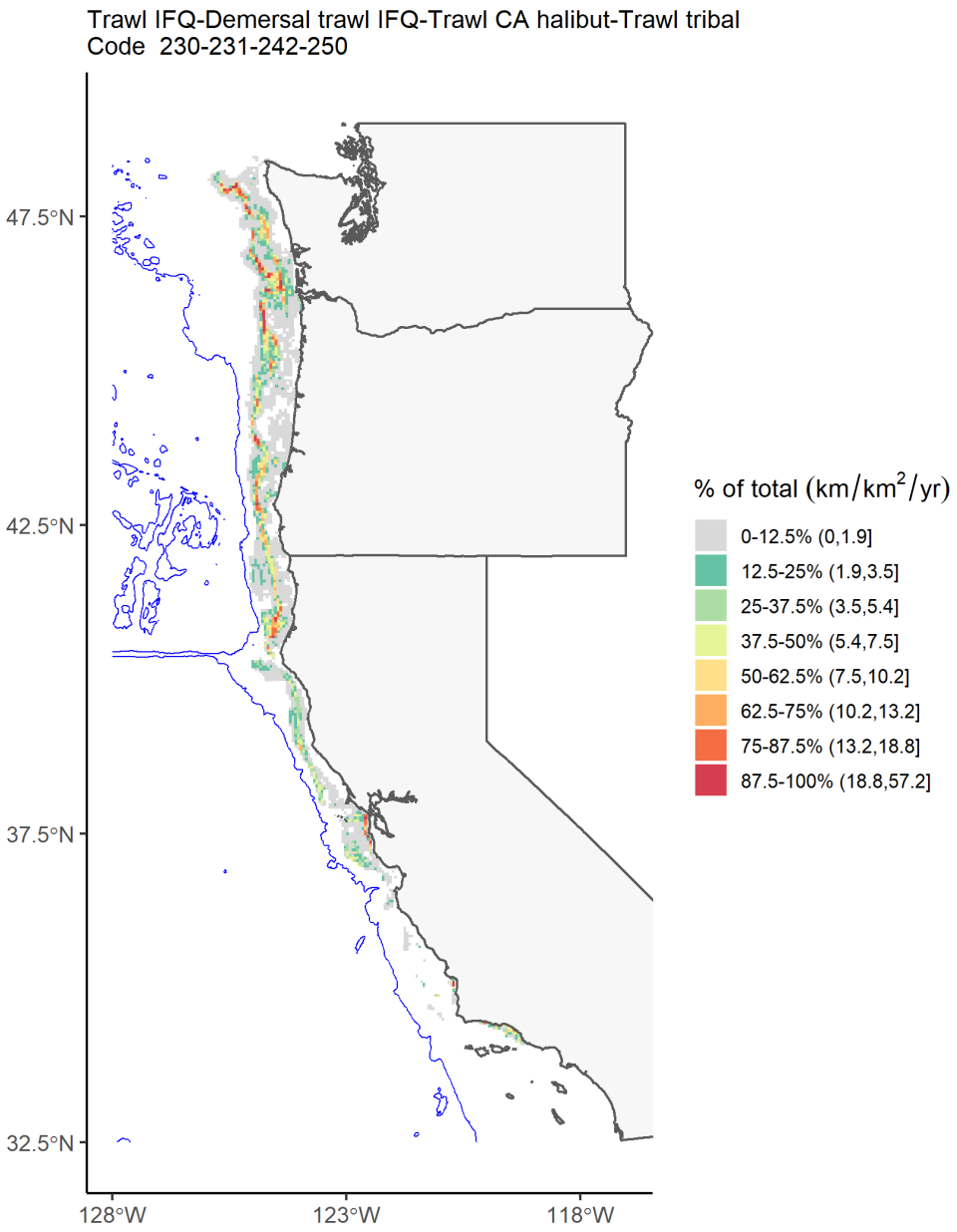

Figure 7.5. Annual-mean fishing effort for groundfish trawl fisheries, including individual fishing quota (IFQ), demersal trawl IFQ, California halibut trawl, and tribal trawl fisheries (Declaration Codes 230, 231, 242, and 250).
Note: Similar to Figure 7.4. Almost all of the data (~100%) are inside the biological depth limit for the species.

Fishing effort for fixed-gear limited entry fisheries (Declaration Codes 210 and 211) was highly variable across the U.S. West Coast, with hot spots mostly in offshore zones and within the depth limit from Central California north through Washington (Figure 7.4). For the groundfish trawl fisheries (Declaration Codes 230, 231, 242, and 250), effort was mostly limited to inside the depth limit north of Monterey Bay (Central California; Figure 7.5), with very little effort in Tribal Trawl Gear (Declaration 250; Figure D17) and limited entry demersal trawl shore-based individual fishing quota (IFQ) (Declaration 231; not mapped because no cells met the "rule of three"). For Dungeness crab (Declaration Code 261), fishing effort was concentrated along the coast and occurred across the entire U.S. West Coast north of Point Conception (northern end of Southern California Bight), with the highest effort in Oregon and

Washington (Figure 7.3). Some effort appeared to occur outside of the species' depth limit, although at low intensities.

Among 17 fisheries declaration codes targeting a species with a known biological depth limit, the vast majority (15) showed that > 90% of the fishing effort occurred within the target species' depth limit (Table 7.1; also see figure maps for depth limit contours). For the remaining three declaration codes, non-groundfish trawl gear for sea cucumber (243), and open access sheephead trap or pot gear (265), which collectively represented only 1.43% of the total calculated fisheries effort, > 73% of the fishing effort occurred within the target species' depth limit.

7.3.2 Fish ticket data

Our dataset for the California groundfish fishery included 98,788 fish tickets from 2010–2017. Landings reported per ticket for a unique vessel ranged considerably, from 1 pound to 55,185 pounds; the median of all landings per ticket per vessel was 735 pounds. Individual vessels that reported a relatively small number of fish tickets over the 8 years of this dataset tended to also catch less fish per trip (Figure D26); the vessels that reported a total of five or fewer fish tickets represented only 0.91% to the total landings, indicating that vessels that fish infrequently catch less per trip and therefore contribute very little to the total landings for the fishery. See Wang et al. 2022 for more detailed analyses of the fish ticket dataset.

7.3.3 Matched VMS-fish ticket (VMS-FT) groundfish data

Our approach successfully matched 38,745 fish tickets with VMS trip data. Although only 39.2% of the available California groundfish fishery fish tickets were matched to VMS data, these matched fish tickets represented 87.4% and 76.3% of the total groundfish landings and ex-vessel value from the fish ticket data. Vessels fishing only in California state waters are not required to use VMS, and therefore fish tickets from those trips cannot be matched with VMS data. Other errors such as incorrect date or vessel name from fish tickets also prevented matching with VMS trips. In the total fish ticket data, 96.6% of the vessels (1,990 out of 2,061) reported relatively small or moderate landings (< 100 metric tons); after matching this percentage dropped to 89% (511 out of 574 vessels). Consequently, the matched data contains relatively more vessels with a large number of fish ticket records and landings than the before-match data. Approximately 15% of VMS polls in the matched data were from non-groundfish fishery declaration codes, with the most (4.7% of VMS polls) attributed to the Dungeness crab fishery (Declaration Code 261), but since declaration codes were not considered in the matching process, these presumably erroneous declaration codes had no impact on the matched dataset.

In addition, data aggregated either at the groundfish species group level or port level showed reasonably high correlations for landings and ex-vessel value when compared among the total groundfish fish ticket dataset, the matched data, and unmatched data (Table 7.2). Note that there are 7 species groups for all comparisons, but the number of ports varied depending on the subset used (n = 85 ports for the total dataset, n = 48 ports for the matched data, and n = 81 ports for the unmatched data). To compare the species and port characteristics, we performed correlation analysis. For a port without any reported landings or ex-vessel value, the landings and ex-vessel value are set to zero for that port. The correlations between the full groundfish dataset and the matched data were very high ($R \geq 0.98$ in all cases; Table 7.2). However, the correlations between the total dataset and matched data with the unmatched data were lower (R values between 0.38 to 0.60). The rank order of functional groups by biomass landing and ex-vessel value was only partially in alignment between the matched and unmatched fish ticket data, but identical between the matched and total fish ticket data (Figure 7.6). Likewise, highest landings from unmatched fish ticket data were from Central California (Morro Bay, Avila/Port St. Luis), while the matched and total fish ticket data both showed the highest landings from two Northern California ports (Eureka, Fort Bragg) (Figure 7.7).

Table 7.2. Correlation coefficient of species and port composition of groundfish fisheries

R	Species: landing (n = 7)	Species: ex-vessel value (n = 7)	Port: landing (n = 85)	Port: ex-vessel value (n = 85)
All vs matched	0.997	0.98	0.998	0.99
All vs unmatched	0.57	0.55	0.65	0.71
Matched vs unmatched	0.51	0.38	0.60	0.58

This table presents the correlation coefficient I between two datasets from total groundfish fish tickets (all), fish tickets after matching with VMS data (matched), and fish tickets that had no match with VMS data (unmatched). Data points for each comparison were for species groups (n = 7) or ports (n = 85). For example, for 'Species: Landing all vs matched', the R was computed using the landing weights from all data and matched data for each of the seven species groups. For ports without any reported landings or ex-vessel value, the landings and ex-vessel value were set to zero.

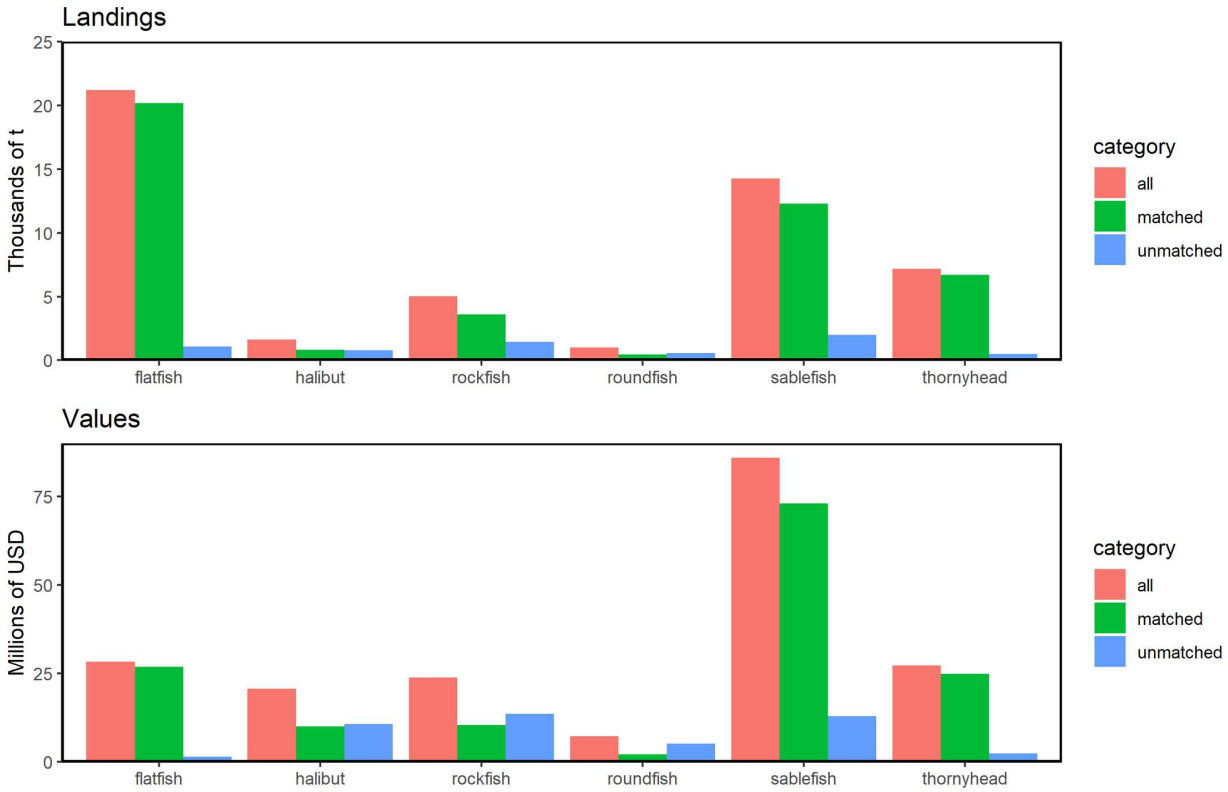

Figure 7.6. Landings and ex-vessel values of groundfish fisheries categorized by species.
Note: Landings (top, in metric tons, t) and ex-vessel values (bottom, in 2019 dollars) of all groundfish fisheries in California from 2010–2017, categorized into 7 species subsets, based on total fish tickets ('all'), fish tickets that

matched with VMS trips ('matched'), and fish tickets that did not match with VMS trips ('unmatched'). Species groups are ordered alphabetically. Note that 'other' is not shown because landings and ex-vessel values were too low to appear on the plot. For each group, 'all' is the sum of 'matched' and 'unmatched.'

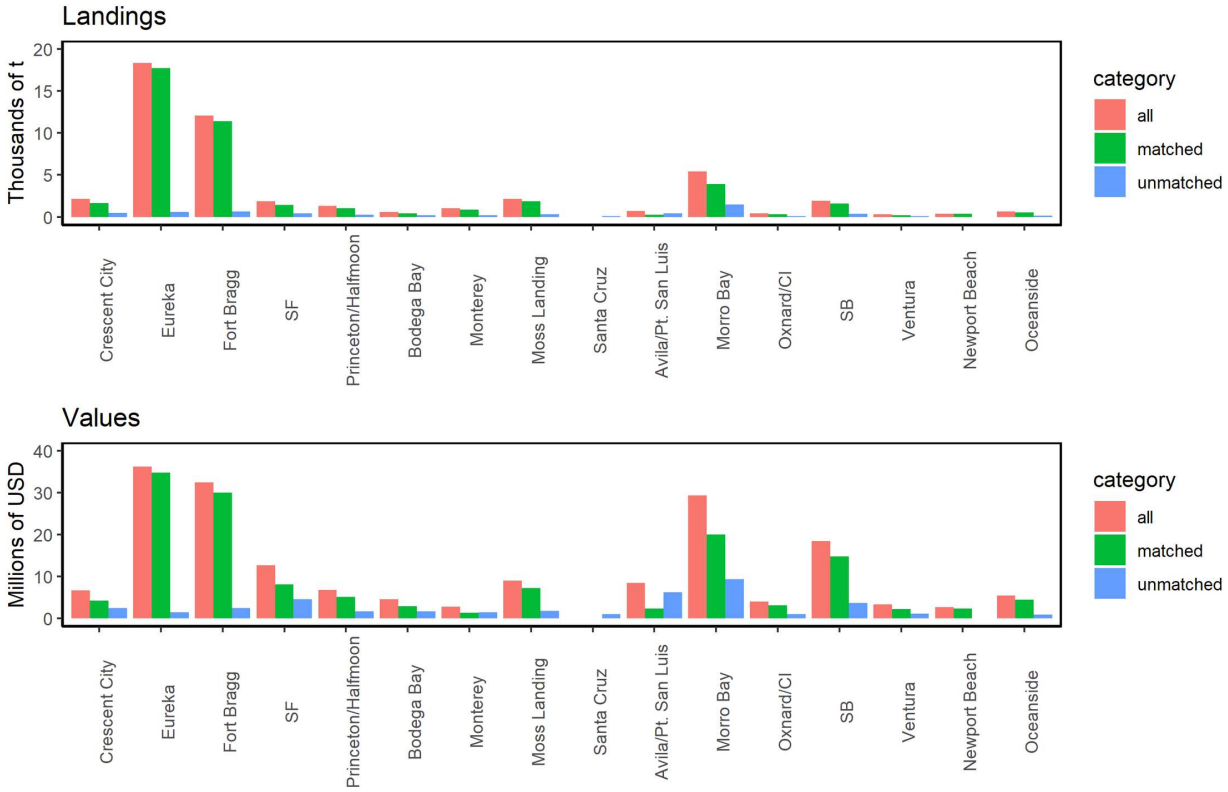

Figure 7.7. Landings and ex-vessel values of groundfish fisheries categorized by ports.
Note: Similar to Figure 7.6, but for the top 15 ports in California.

Groundfish fisheries effort was distributed unevenly latitudinally along the California coast (Figure 7.8), with a large hotspot in Northern California offshore of Humboldt County, and smaller hotspots along the Santa Barbara and Ventura County coasts, including the western Channel Islands. Landings and ex-vessel value spatial distributions showed similar trends to fisheries effort (Figures 7.9-7.10). These broad patterns generally matched those from previous work that examined spatial distribution of landings using only self-reported fishing block data from fish tickets (Wang et al. 2022). However, a more detailed analysis of individual trips from the matched dataset for groundfish found that 64% of the trips had no VMS polls recorded from the self-reported fishing block recorded in the fish ticket.

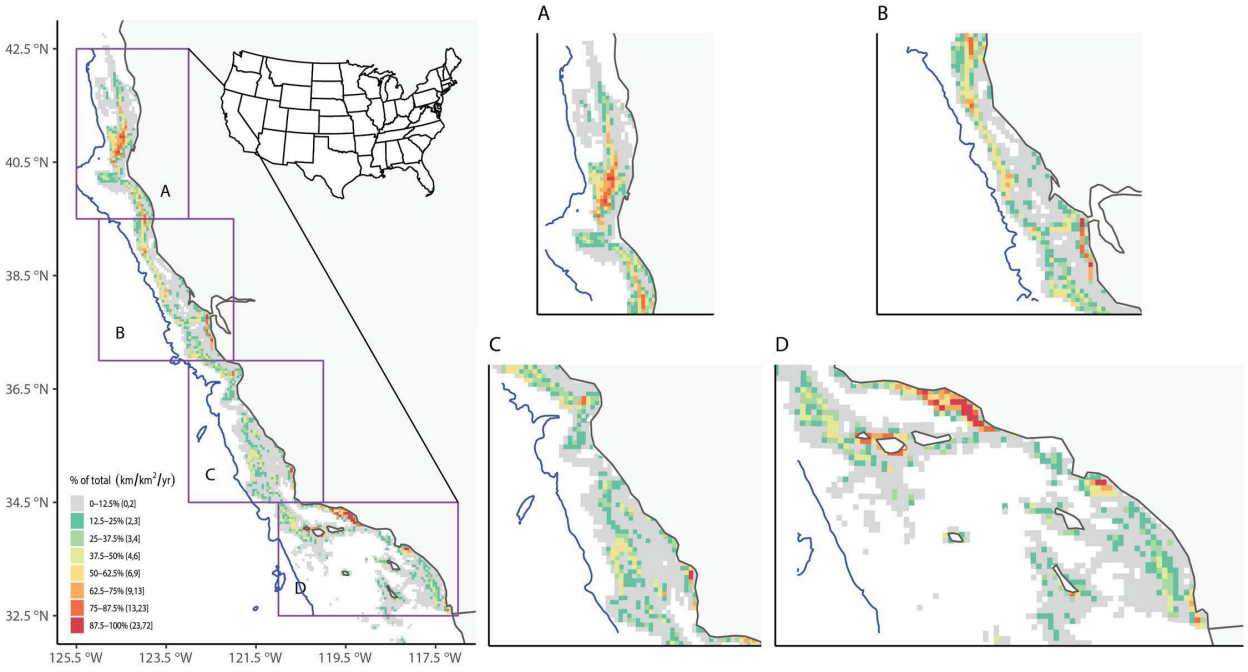

Figure 7.8. Annual-average fishing effort using matched VMS-landings data for groundfish.
Note: Left: Annual-average fishing effort (in km/km^2/yr) in BOEM lease blocks along the California coast over 2010–2017. The blue line is the 2700 m isobath, representing the maximum depth for all groundfish fisheries. Right: Same as left, but with regions magnified.

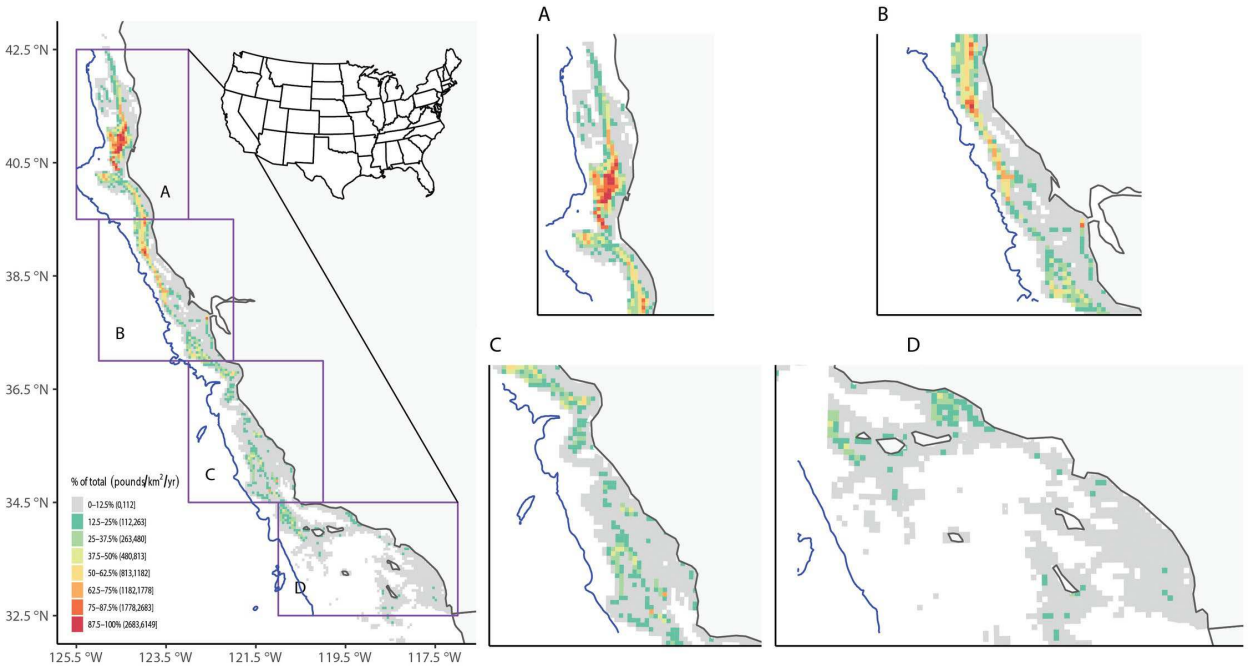

Figure 7.9. Annual-average landings using matched VMS-landings data for groundfish.
Note: Similar to Figure 7.8, except for annual-average landings (in lbs/km^2/yr).

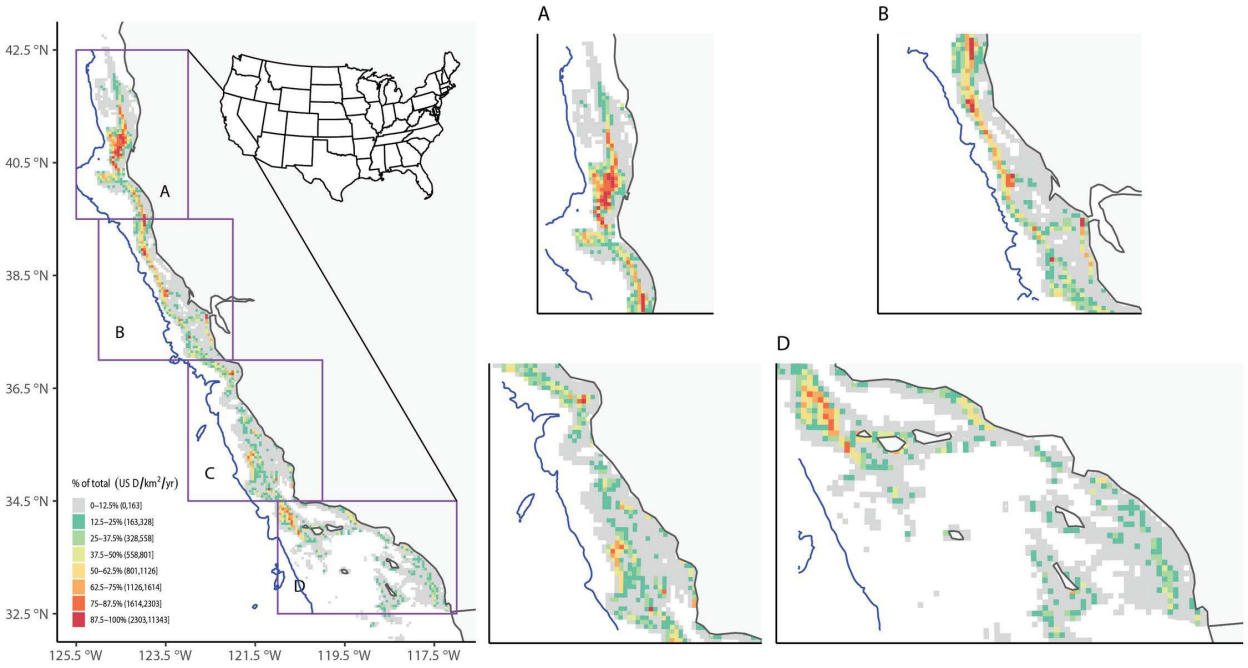

Figure 7.10. Annual-average ex-vessel value using matched VMS-landings data for groundfish.
Note: Similar to Figure 7.8, except for ex-vessel value (in 2019 dollars/km2/yr).

To gain a deeper insight into the temporal and spatial dynamics of fishing activities, we presented fishing effort, landings, and ex-vessel value for each year across depth ranges in Figure D27-D29. To create these figures, we first computed the mean ocean depth within each lease block. Then, for each year of matched groundfish fisheries data, we summed each of fishing effort, landing, and ex-vessel value over the lease blocks within the respective depth intervals. Averaged across the State of California, fishing effort by the matched groundfish fisheries data was found to be greatest closest to shore (< 100 m depth), with a second, much smaller maximum offshore at ~500-600 m depth (Figure D27). Fisheries landings and ex-vessel value also exhibited local maxima close to shore at < 100 m depth and at ~500-600 m depth (Figures D28-29). Fisheries effort, landings, and ex-vessel value all exhibited local minimums between these depths around ~200-300 m (Figures D28-29).

To understand interannual variability of fishing activities, the matched data were categorized on a yearly basis. Statewide groundfish fisheries activity varied substantially over the eight-year evaluation period, with an annual change as large as 30% (from 2011 to 2012) (Figure D30). Fishing effort, landings and ex-vessel value all declined precipitously from peak levels early in the time series (2010-11), followed by a further but much weaker decline in effort over the remainder of the time series, coincident with moderately variable but loosely stable landings and positive-trending ex-vessel value.

7.4 Discussion and conclusions

We used a combination of federally-managed spatial fisheries data (VMS) and state-managed landings data (fish tickets) to quantify spatial patterns in fisheries effort, catch, and ex-vessel value for the economically-important groundfish fisheries in California, as well as spatial patterns in effort across a range of other fisheries throughout the U.S. West Coast. As expected, the data revealed substantial spatial variability in fishing effort within and among different fisheries. Importantly, our estimates of effort generated using VMS data for certain groundfish fisheries matched closely with estimates for the same fisheries using NOAA Observer data. Since the NOAA Observer dataset has nearly complete coverage,

this provides evidence that our estimates of effort derived from VMS data accurately capture the spatial pattern of relative fishing activities. This is particularly true for U.S. West Coast groundfish fisheries, given that VMS is legally required and Observer datasets for groundfish fisheries have greater than 99% coverage (Somers et al. 2022). Additionally, the spatial patterns from VMS data for the Dungeness crab fishery, for which VMS is only required if they hold a permit or participate in groundfish fishing in that year (e.g., approximately 19-26% of the Dungeness crab fishery's vessels and 10-57% of its landings ; (Liu et al. 2023)), closely match the independently-generated estimates of effort from ODFW This suggests that VMS data may be useful for evaluating U.S. West Coast fisheries without high-coverage VMS data. This validation lends important credibility to the high-resolution estimates of catch and ex-vessel value generated here. As such, we expect these data to be highly useful in supporting fisheries management and marine spatial planning.

7.4.1 U.S. West Coast fisheries effort based on VMS data only

Since the VMS data primarily generates information on location only, vessel speed must be inferred from distance traveled between two points. Therefore, one of the most critical challenges is determining vessel activity (i.e., fishing or transit) from these data. Despite these challenges (see e.g., Watson et al. 2016), our estimates of the spatial distribution of relative fishing effort were largely insensitive to the assumed cutoff speed between fishing and transit, based on two methods of estimating cutoff speed, suggesting that our results are robust to underlying assumptions about vessel activity. Furthermore, our analyses of VMS data found that a much higher percentage of fishing effort occurred within the biological depth limits for a given species than the self-reported block data from fish ticket data alone (Wang et al. 2022). These findings, combined with the strong correlation between spatial patterns between VMS data and NOAA Observer data, highlight the reliability of our VMS-based estimates of spatial fisheries effort.

Estimates of fisheries effort based on fish ticket data alone found small but significant inaccuracies revealed by fish ticket reports of landings beyond the species' biological depth limit (Wang et al. 2022). Furthermore, we also examined the correspondence between reported fishing blocks from the fish ticket dataset and the track recorded from VMS data. This analysis found that 64% of the groundfish fishing trips from the matched dataset did not have a single VMS poll inside the fishing block reported in the fish ticket, suggesting that that self-reported fishing block data are highly unreliable. Combined with the reliability of VMS data in recording vessel location, these findings suggest that VMS data can more accurately map fisheries activities. In addition, this highlights the need to improve the reliability of self-reported fishing location information in fish tickets for that data stream to be useful in understanding the spatial distribution of fisheries. Our analyses revealed a number of noteworthy spatial patterns in effort across a range of fisheries (see Figures D5-D25 for fishing effort maps across all VMS declarations). Fishing effort is strongly heterogeneous along the U.S. West Coast, typically with greater effort in northern regions (Oregon and Washington) than further south (California). This pattern is especially clear for midwater trawl fisheries (Figures D7-D8) and HMS fisheries (Figure D23), both of which are concentrated in Oregon and Washington, with little activity in California. Several fisheries also clearly target specific depth bands, either nearshore (e.g., open access Dungeness crab, Figure 7.3) or offshore (e.g., trawl gear for pink shrimp, Figure D14; open access line gear for HMS, Figure D23; and fixed gear and trawl fisheries for groundfish, Figures 7.4 and 7.5). Other species appear to be highly concentrated either latitudinally or in relation to depth, or in very specific local areas. For example, ridgeback prawn and sea cucumber trawl fisheries are limited to the nearshore in the Southern California Bight (Figures D13 and D16), and open access trap fisheries for spot prawn are limited to offshore areas in northern Oregon (Figure D18). It is important to note that these non-groundfish fisheries do not require VMS, so estimates from VMS data alone likely do not capture the absolute magnitude of fishing effort. While the spatial patterns for selected bottom trawl and Dungeness crab fisheries in the VMS dataset generally matched those from other datasets, the spatial patterns revealed by the VMS dataset for each of these other fisheries may or may not be broadly representative of activity for that fishery.

7.4.2 California groundfish fisheries patterns using merged VMS-FT dataset

Based on fish tickets recording landings of groundfish, large vessels tend to generate more contribution to the overall landings (Figure D26). The matched VMS-FT dataset (see Method and Results details in sections 7.2.4 and 7.3.3) included a higher proportion of vessels with high total weight landings than the full fish ticket dataset, and therefore included fewer vessels that fished less and landed smaller quantities of fish in each trip. It is possible that many of the smaller vessels with fewer fish tickets and/or less total fish landed were fishing closer to shore, possibly only in state waters (< 3 nm [~5.6 km] from shore), such that VMS was not required. Since fish tickets from many of those vessels could not be matched to VMS trips, their activity was not included in the matched VMS-FT dataset. Nonetheless, the greatest amount of fishing effort recorded in the matched VMS-FT data occurred in depths of less than 100 m (Figure D27). In most locations in California, 100 m is well within state waters, indicating that a substantial proportion of the overall groundfish fishing activity is occurring in state waters by vessels with VMS. Consequently, the absence of data from small-vessel, state water-only fishing activity may not substantially impact the overall estimates of spatial and temporal patterns of the groundfish fishery. The absence of this information also should have virtually no impact on estimates of fishing activity occurring in federal waters.

Importantly, the matched dataset is very similar in a variety of attributes to the full fish ticket dataset: the relative contributions of different species and different ports for both landings and ex-vessel value are very similar in both datasets, and the matched dataset captures a large proportion of the landings and ex-vessel value in the full dataset (87% and 76%, respectively), even though the matched dataset includes only 39% of the groundfish fish tickets (Figures 7.6-7.7; Table 7.2). Overall, these findings suggest that the matched fish ticket dataset provides an excellent representation of the commercial groundfish fishery activity in federal waters of California. While the matched data also shows significant activity in state waters, it will be important to interpret these inshore patterns carefully if they are used for spatial management or planning purposes, since this combined dataset may be missing different components of groundfish fishing activity by vessels operating only in state waters.

For groundfish fisheries, both effort and ex-vessel value showed increasing intensity close to shore and again offshore at ~500-600 m depth, while landings peaked offshore at ~500-600 m depth without a second clear nearshore local maximum (Figures D27-29). Despite some differences, effort, landing, and ex-vessel value all showed a consistent presence of a local minimum at ~200-300 m depth occurring across the State and over the eight-year study period (Figures D27-29), which may be partly attributable to the boundaries of the Rockfish Conservation Areas (RCA) and other areas that limit groundfish trawling in that depth zone (Thompson et al. 2017; Keller et al. 2018). The RCAs in California have changed over time in response to changes in the status of stocks they are meant to protect. As certain stocks continue to recover, these closed areas for trawling have been reduced or removed over the last several years (NOAA Fisheries 2023), providing the opportunity to evaluate changes in fishing activity that may expand into the previously-closed 200-300m depth zone (Figures D27-29).

The groundfish fisheries in California target a range of different species with differing life histories, habitat requirements, and population dynamics in different regions of the State (e.g., Kolora et al. 2021). As a result, fisheries across the state target multiple high-value species. Fisheries activities fluctuated over time (Figure D30), including a noticeable drop in 2012 that may be linked to the implementation of trawl rationalization (i.e., IFQ program; CDFW). But the temporal changes in this eight-year study period were relatively small compared to changes observed over larger time scales (e.g., Miller et al. 2017; Wang et al. 2022).

7.4.3 Caveats and future research

As we demonstrate, VMS-based estimates of fisheries metrics are likely highly reliable, but there are still important limitations to these data. First, not all vessels are required to utilize VMS, so the actual absolute magnitude of a given metric (e.g., total effort, at any scale) may be underestimated for many declaration codes, with the possible exception of the commercial groundfish fisheries, for which VMS is required (see section 7.2.1). However, while it may be difficult to quantify the absolute magnitude of fishing intensity at a given location, the relative spatial patterns are likely representative, such that areas of high and low fishing intensity are generally accurately identified. Second, the fisheries effort metric of km/km^2 used here is likely more amenable for measuring mobile gear fisheries (such as trawls, that travel while fishing), and less ideal for measuring fixed gear fisheries (e.g., pots). Therefore, further validation is needed to allow direct comparisons of relative patterns of effort between fisheries. Third, we focused on commercial fisheries activity predominantly occurring in federal waters monitored with VMS, while recognizing that other fisheries outside the scope of this study contribute significant landings and substantial socioeconomic value to the U.S. West Coast. For example, recreational fisheries constitute a smaller but significant proportion of the total fisheries harvest in California, Oregon, and Washington, with disproportionate overall economic impact (Coleman et al. 2004), and subsistence fisheries support a diversity of communities and local economies across the U.S. West Coast (Poe et al. 2015). In addition, there are some fisheries that operate nearly-exclusively in state waters, such as the nearshore live-fish fisheries (CDFW 2009); because they are not operating in federal waters, they are not monitored by VMS. While the number of operators engaged in that fishery and landings have declined in recent years (CDFW), the data we present here will not capture any of that activity. An improved understanding of these fisheries alongside the results presented here for most California commercial fisheries is needed to develop a more holistic understanding of the spatial patterns and socioeconomic contributions to communities throughout the West Coast. Fourth, while most of the activity for a given fishery occurred within the biological limits of the target species, some activity for some fisheries occurred outside these limits (Table 7.1). Such activity is likely the result of misidentified declaration codes (e.g., a vessel trip declares a Dungeness crab code but is actually fishing offshore for HMS). While NOAA OLE attempts to correct these obvious errors in real-time, they are unable to fix all incorrect declaration codes (K. Spalding, pers. comm.). Despite these issues, in nearly all cases the likely erroneous declaration codes outside of the depth limits comprise less than 5% of the total effort for the fishery, such that the broad spatial patterns these data represent are likely accurate.

Integrating additional spatial fisheries datasets (e.g., NOAA Observer data, state-level Logbook data) with the data generated here could help validate and further calibrate our findings. Moreover, the matched VMS-FT groundfish dataset only included landings data from California. Future research could expand to include Oregon and Washington, which have similar landings receipt data systems, as well as incorporate NMFS Observer and Logbook datasets. These coast-wide datasets could be used to further assess spatial patterns, landings, and ex-vessel value across all federally-managed U.S. West Coast groundfish fisheries, all of which require VMS coverage. Such an expansion could support efforts to inform a range of important spatial and fishery management questions.

In this study, we developed methods to generate the combined VMS-FT data that, to our knowledge, is one of the highest spatial resolution and most accurate assessments of recent fishery activity along the entire U.S. West Coast (but see Feist et al. 2021; Watson et al. 2018; Samhouri et al. 2021 for recent applications of these approaches on select species). There are numerous potential future applications for these data in marine science and management, including spatially-explicit fishery stock assessments and ecosystem-based management, marine spatial planning of protected areas and new uses of ocean space such as offshore aquaculture and renewable energy (Magris 2021), assessing spatial human-wildlife conflicts (Feist et al. 2021; Samhouri et al. 2021), and supporting climate-change readiness and resilience planning (Fisher et al. 2021).

7.4.4 Conclusion

Fine-scale spatial characterization of fishery dynamics is increasingly important for supporting fisheries management, from regional stock assessment to ecosystem-based approaches to spatial regulation and planning (Berger et al. 2017). In addition, other uses of ocean space have intensified over the last few decades, including increased shipping activity, offshore aquaculture, and offshore renewable energy development. These uses may interact with fisheries in significant, new ways (Natale et al. 2013; Gill et al. 2020). Concurrently, advances in fisheries remote monitoring technology are generating a wealth of information on the movement, distribution, activities, and impacts of fishing vessels at unprecedented spatiotemporal scales (e.g., Kroodsma et al. 2018). This study demonstrates a process to obtain, process, integrate and analyze such data – fish ticket reports and VMS polls – to provide a more comprehensive and up-to-date understanding of commercial fisheries activities across the U.S. West Coast. Our hope is that the products generated here will provide valuable support for spatial fisheries assessment and management, including efforts in ecosystem-based fisheries science to sustainably integrate fisheries with new ocean uses along the U.S. West Coast.

8 References

Adams J, Kelsey EC, Felis JJ, Pereksta DM. 2017. Collision and displacement vulnerability among marine birds of the California Current System associated with offshore wind energy infrastructure. U.S. Geological Survey Report No.: 2016–1154.

Ainley D, Porzig E, Zajanc D, Spear LB. 2015. Seabird flight behavior and height in response to altered wind strength and direction. Marine Ornithology. 43:25–36.

Allen LG, Horn MH, editors. 2006. The Ecology of Marine Fishes: California and Adjacent Waters. University of California Press. [accessed 2023 Nov 9]. https://www.degruyter.com/document/doi/10.1525/9780520932470/html.

Alvarez I, Gomez-Gesteira M, deCastro M, Carvalho D. 2014. Comparison of different wind products and buoy wind data with seasonality and interannual climate variability in the southern Bay of Biscay (2000–2009). Deep Sea Research Part II: Topical Studies in Oceanography. 106:38–48. doi:10.1016/j.dsr2.2013.09.028.

Aquaculture Opportunity Areas. 2023. NOAA Fisheries. [accessed 2023 Jun 12]. https://www.fisheries.noaa.gov/national/aquaculture/aquaculture-opportunity-areas.

Arai T, Harino H, Ohji M, Langston WJ, editors. 2009. Ecotoxicology of antifouling biocides. 1. Aufl. Tokyo 102-0073: Springer Japan KK.

Arnett EB, Brown WK, Erickson WP, Fiedler JK, Hamilton BL, Henry TH, Jain A, Johnson GD, Kerns J, Koford RR, et al. 2008. Patterns of Bat Fatalities at Wind Energy Facilities in North America. J Wildl Manag. 72(1):61–78. doi:10.2193/2007-221.

Atlas R, Hoffman RN, Ardizzone J, Leidner SM, Jusem JC, Smith DK, Gombos D. 2011. A Cross-calibrated, Multiplatform Ocean Surface Wind Velocity Product for Meteorological and Oceanographic Applications. Bull Amer Meteor Soc. 92(2):157–174. doi:10.1175/2010BAMS2946.1.

Bahreinian, Aniss, Bailey, Stephanie, Bartridge, Jim, Brathwaite, Leon, Campagna, Jennifer, Crisostomo, Noel, Doughman, Pamela, Flynn, Tom, Franco, Guido, Grau, Judy, et al. 2017. 2017 Integrated Energy Policy Report. California Energy Commission (CEC) Report No.: CEC-100-2017-001-CMF.

Bang J-I, Ma C, Tarantino ECJ, Vela A, Yamane D. 2018. Life Cycle Assessment of Greenhouse Gas Emissions for Floating Offshore Wind Energy in California. University of California Santa Barbara.

Barbeaux SJ, Holsman K, Zador S. 2020. Marine Heatwave Stress Test of Ecosystem-Based Fisheries Management in the Gulf of Alaska Pacific Cod Fishery. Front Mar Sci. 7:703. doi:10.3389/fmars.2020.00703.

Barlow J, Cameron GA. 2003. FIELD EXPERIMENTS SHOW THAT ACOUSTIC PINGERS REDUCE MARINE MAMMAL BYCATCH IN THE CALIFORNIA DRIFT GILL NET FISHERY. Marine Mammal Sci. 19(2):265–283. doi:10.1111/j.1748-7692.2003.tb01108.x.

Barrios L, Rodríguez A. 2004. Behavioural and environmental correlates of soaring-bird mortality at on-shore wind turbines. Journal of Applied Ecology. 41(1):72–81. doi:10.1111/j.1365-2664.2004.00876.x.

Beiter P, Musial W, Duffy P, Cooperman A, Shields M, Heimiller D, Optis M. 2020. The Cost of Floating Offshore Wind Energy in California Between 2019 and 2032. Golden, CO: National Renewable Energy Laboratory Report No.: NREL/TP-5000-77384.

Beiter P, Musial W, Smith A, Kilcher L, Damiani R, Maness M, Sirnivas S, Stehly T, Gevorgian V, Mooney M, et al. 2016. A Spatial-Economic Cost-Reduction Pathway Analysis for U.S. Offshore Wind Energy Development from 2015–2030. Report No.: NREL/TP--6A20-66579, 1324526. [accessed 2023 Nov 8]. http://www.osti.gov/servlets/purl/1324526/.

Bejarano, Adriana C., Michel, Jacqueline, Rowe, Jill, Li, Zhengkai, French McCay,Deborah, Schmidt Etkin, Dagmar. 2013. Environmental Risks, Fate, and Effects of Chemicals Associated with Wind Turbines on the Atlantic Outer Continental Shelf. Herndon, VA: U.S. Department of the Interior, Bureau of Ocean Energy Management, Office of Renewable Energy Programs Report No.: BOEM 2013-213.

Benjamins S, Harnois V, Smith HCM, Johanning L, Greenhill L, Carter C, Wilson B. 2014. Understanding the potential for marine megafauna entanglement risk from marine renewable energy developments. Report No.: No. 791.

Bentamy A, Croize-Fillon D, Perigaud C. 2008. Characterization of ASCAT measurements based on buoy and QuikSCAT wind vector observations. Ocean Sci. 4(4):265–274. doi:10.5194/os-4-265-2008.

Berger AM, Goethel DR, Lynch PD. 2017. Introduction to "Space Oddity: Recent Advances Incorporating Spatial Processes in the Fishery Stock Assessment and Management Interface." Can J Fish Aquat Sci. 74(11):1693–1697. doi:10.1139/cjfas-2017-0296.

Bertrand S, Joo R, Arbulu Smet C, Tremblay Y, Barbraud C, Weimerskirch H. 2012. Local depletion by a fishery can affect seabird foraging. Frederiksen M, editor. Journal of Applied Ecology. 49(5):1168–1177. doi:10.1111/j.1365-2664.2012.02190.x.

Blaxter JHS. 1981. The Swimbladder and Hearing. In: Tavolga WN, Popper AN, Fay RR, editors. Hearing and Sound Communication in Fishes. New York, NY: Springer New York. (Proceedings in Life Sciences). p. 61–71. [accessed 2023 Nov 15]. http://link.springer.com/10.1007/978-1-4615-7186-5_3.

Boehlert G, Gill AB. 2010. Environmental and Ecological Effects of Ocean Renewable Energy Development – A Current Synthesis. Oceanography. 23. doi:10.5670/oceanog.2010.46.

BOEM_BSEE/MMC_Layers (MapServer). 2023.

Borg DA, Trombetta LD. 2010. Toxicity and bioaccumulation of the booster biocide copper pyrithione, copper 2-pyridinethiol-1-oxide, in gill tissues of *Salvelinus fontinalis* (brook trout). Toxicol Ind Health. 26(3):139–150. doi:10.1177/0748233710362381.

Brady RX, Alexander MA, Lovenduski NS, Rykaczewski RR. 2017. Emergent anthropogenic trends in California Current upwelling. Geophysical Research Letters. 44(10):5044–5052. doi:10.1002/2017GL072945.

Brandt MJ, Diederichs A, Betke K, Nehls G. 2011. Responses of harbour porpoises to pile driving at the Horns Rev II offshore wind farm in the Danish North Sea. Mar Ecol Prog Ser. 421:205–216. doi:10.3354/meps08888.

Brothers JR, Lohmann KJ. 2015. Evidence for Geomagnetic Imprinting and Magnetic Navigation in the Natal Homing of Sea Turtles. Current Biology. 25(3):392–396. doi:10.1016/j.cub.2014.12.035.

Brown T, Schlachtberger D, Kies A, Schramm S, Greiner M. 2018. Synergies of sector coupling and transmission reinforcement in a cost-optimised, highly renewable European energy system. Energy. 160:720–739. doi:10.1016/j.energy.2018.06.222.

Bryan GW, Gibbs PE, Hummerstone LG, Burt GR. 1986. The Decline of the Gastropod *Nucella Lapillus* Around South-West England: Evidence for the Effect of Tributyltin from Antifouling Paints. J Mar Biol Ass. 66(3):611–640. doi:10.1017/S0025315400042247.

Bulleri F, Airoldi L. 2005. Artificial marine structures facilitate the spread of a non-indigenous green alga, *Codium fragile* ssp. *tomentosoides* , in the north Adriatic Sea. Journal of Applied Ecology. 42(6):1063–1072. doi:10.1111/j.1365-2664.2005.01096.x.

Bylhouwer B, Ianson D, Kohfeld K. 2013. Changes in the onset and intensity of wind-driven upwelling and downwelling along the North American Pacific coast. JGR Oceans. 118(5):2565–2580. doi:10.1002/jgrc.20194.

Cai W, Wang G, Santoso A, McPhaden MJ, Wu L, Jin F-F, Timmermann A, Collins M, Vecchi G, Lengaigne M, et al. 2015. Increased frequency of extreme La Niña events under greenhouse warming. Nature Clim Change. 5(2):132–137. doi:10.1038/nclimate2492.

California Activities. 2019. Bureau of Ocean Energy Management (BOEM). [accessed 2019 Feb 4]. https://boem.gov/California/.

California Activities. 2022. BOEM. [accessed 2022 Mar 23]. https://www.boem.gov/renewable-energy/state-activities/california.

California Marine Protected Areas (MPAs). c2023. California Department of Fish and Wildlife. [accessed 2023 Jun 12]. https://wildlife.ca.gov/Conservation/Marine/MPAs.

Campbell MS, Stehfest KM, Votier SC, Hall-Spencer JM. 2014. Mapping fisheries for marine spatial planning: Gear-specific vessel monitoring system (VMS), marine conservation and offshore renewable energy. Marine Policy. 45:293–300. doi:10.1016/j.marpol.2013.09.015.

Capps SB, Zender CS. 2009. Global ocean wind power sensitivity to surface layer stability. Geophysical Research Letters. 36(9):2008GL037063. doi:10.1029/2008GL037063.

Carlström J, Berggren P, Tregenza NJC. 2009. Spatial and temporal impact of pingers on porpoises. Can J Fish Aquat Sci. 66(1):72–82. doi:10.1139/F08-186.

Carpenter JR, Merckelbach L, Callies U, Clark S, Gaslikova L, Baschek B. 2016. Potential Impacts of Offshore Wind Farms on North Sea Stratification. Álvarez I, editor. PLoS ONE. 11(8):e0160830. doi:10.1371/journal.pone.0160830.

Carter L, Burnett D, Drew S, Marle G, Hagadorn L, Bartlett-McNeil D, Irvine N. 2009. Submarine cables and the oceans: connecting the world. ICPC/UNEP/UNEP-WCMC UNEP-WCMC Biodiversity Series Report No.: No. 31.

Carvalho D, Rocha A, Gómez-Gesteira M, Santos C. 2012. A sensitivity study of the WRF model in wind simulation for an area of high wind energy. Environmental Modelling & Software. 33:23–34. doi:10.1016/j.envsoft.2012.01.019.

Carvalho D, Rocha A, Gómez-Gesteira M, Silva Santos C. 2014. Comparison of reanalyzed, analyzed, satellite-retrieved and NWP modelled winds with buoy data along the Iberian Peninsula coast. Remote Sensing of Environment. 152:480–492. doi:10.1016/j.rse.2014.07.017.

Carvalho D, Rocha A, Gómez-Gesteira M, Silva Santos C. 2017. Offshore winds and wind energy production estimates derived from ASCAT, OSCAT, numerical weather prediction models and buoys – A comparative study for the Iberian Peninsula Atlantic coast. Renewable Energy. 102:433–444. doi:10.1016/j.renene.2016.10.063.

Cassoff R, Moore K, McLellan W, Barco S, Rotstein D, Moore M. 2011. Lethal entanglement in baleen whales. Dis Aquat Org. 96(3):175–185. doi:10.3354/dao02385.

Castro JJ, Santiago JA, Santana-Ortega AT. 2001. A general theory on fish aggregation to floating objects: An alternative to the meeting point hypothesis. Reviews in Fish Biology and Fisheries. 11(3):255–277. doi:10.1023/A:1020302414472.

Cavole L, Demko A, Diner R, Giddings A, Koester I, Pagniello C, Paulsen M-L, Ramirez-Valdez A, Schwenck S, Yen N, et al. 2016. Biological Impacts of the 2013–2015 Warm-Water Anomaly in the Northeast Pacific: Winners, Losers, and the Future. Oceanog. 29(2). doi:10.5670/oceanog.2016.32. [accessed 2023 Nov 9]. https://tos.org/oceanography/article/biological-impacts-of-the-20132015-warm-water-anomaly-in-the-northeast-paci.

Cazenave PW, Torres R, Allen JI. 2016. Unstructured grid modelling of offshore wind farm impacts on seasonally stratified shelf seas. Progress in Oceanography. 145:25–41. doi:10.1016/j.pocean.2016.04.004.

CEC. 2019. https://www.energy.ca.gov/data-reports/energy-almanac/california-electricity-data/2019-total-system-electric- generation.

Central California Call Areas. 2018. https://www.boem.gov/sites/default/files/renewable-energy-program/State-Activities/CA/Central-California-Call-Areas-Map-NOAA.pdf.

Chambers LD, Stokes KR, Walsh FC, Wood RJK. 2006. Modern approaches to marine antifouling coatings. Surface and Coatings Technology. 201(6):3642–3652. doi:10.1016/j.surfcoat.2006.08.129.

Chaudhary C, Richardson AJ, Schoeman DS, Costello MJ. 2021. Global warming is causing a more pronounced dip in marine species richness around the equator. Proc Natl Acad Sci USA. 118(15):e2015094118. doi:10.1073/pnas.2015094118.

Chavez, F.P., Costello, C., Aseltine-Neilson, D., Doremus, H., Field, J.C., Gaines, S.D., Hall-Arber, M., Mantua, N.J., McCovey, B., Pomeroy, C., et al. 2017. Readying California Fisheries for Climate Change. California Ocean Protection Council Science Advisory Team Working Group.

Chavez FP, Ryan J, Lluch-Cota SE, Ñiquen C. M. 2003. From Anchovies to Sardines and Back: Multidecadal Change in the Pacific Ocean. Science. 299(5604):217–221. doi:10.1126/science.1075880.

Checkley DM, Barth JA. 2009. Patterns and processes in the California Current System. Progress in Oceanography. 83(1–4):49–64. doi:10.1016/j.pocean.2009.07.028.

Cheung WWL, Frölicher TL. 2020. Marine heatwaves exacerbate climate change impacts for fisheries in the northeast Pacific. Sci Rep. 10(1):6678. doi:10.1038/s41598-020-63650-z.

Cheung WWL, Lam VWY, Sarmiento JL, Kearney K, Watson R, Zeller D, Pauly D. 2010. Large-scale redistribution of maximum fisheries catch potential in the global ocean under climate change. Global Change Biology. 16(1):24–35. doi:10.1111/j.1365-2486.2009.01995.x.

Christensen ED, Johnson M, Sørensen OR, Hasager CB, Badger M, Larsen SE. 2013. Transmission of wave energy through an offshore wind turbine farm. Coastal Engineering. 82:25–46. doi:10.1016/j.coastaleng.2013.08.004.

Christiansen MB, Hasager CB. 2005. Wake effects of large offshore wind farms identified from satellite SAR. Remote Sensing of Environment. 98(2–3):251–268. doi:10.1016/j.rse.2005.07.009.

Ciriminna R, Bright FV, Pagliaro M. 2015. Ecofriendly Antifouling Marine Coatings. ACS Sustainable Chem Eng. 3(4):559–565. doi:10.1021/sc500845n.

Claisse JT, Pondella DJ, Love M, Zahn LA, Williams CM, Williams JP, Bull AS. 2014. Oil platforms off California are among the most productive marine fish habitats globally. Proc Natl Acad Sci USA. 111(43):15462–15467. doi:10.1073/pnas.1411477111.

Clark S, Schroeder F, Baschek B. 2014. The influence of large offshore wind farms on the North Sea and Baltic Sea - a comprehensive literature review. Report No.: 2014–6.

Cliff A, Ord J. 1982. Spatial Processes: Models & Applications. The Quarterly Review of Biology. 57(2):236–236. doi:10.1086/412797.

Coleman FC, Figueira WF, Ueland JS, Crowder LB. 2004. The Impact of United States Recreational Fisheries on Marine Fish Populations. Science. 305(5692):1958–1960. doi:10.1126/science.1100397.

Collier R. 2020. Deep water on the road to 100. How offshore wind power can help California meet its climate goals for clean energy. Environment California Research and Policy Center. Febuary 16, 2021.

Collier R, Hull S, Sawyerr O, Li S, Mogadali M, Mullen D, Olson A. 2019. California offshore wind: workforce impacts and grid integration. Center for Labor Research and Education, University of California, Berkeley. http://laborcenter.berkeley.edu/ offshore-wind-workforce-grid.

Copping A, Hanna L, Whiting J, Geerlofs S, Grear M, Blake K, Coffey A, Massaua M, Brown-Saracino J, Battey H. 2013. Environmental Effects of Marine Energy Development Around the World. Annex IV Final Report. Report No.: PNNL--22176, 1219898. [accessed 2023 Nov 17]. http://www.osti.gov/servlets/purl/1219898/.

Costoya X, deCastro M, Carvalho D, Gómez-Gesteira M. 2020. On the suitability of offshore wind energy resource in the United States of America for the 21st century. Applied Energy. 262:114537. doi:10.1016/j.apenergy.2020.114537.

Cox TM, Read AJ, Solow A, Tregenza N. 2023. Will harbour porpoises *(Phocoena phocoena*) habituate to pingers? jcrm. 3(1):81–86. doi:10.47536/jcrm.v3i1.904.

Cronin M, Gerritsen H, Reid D, Jessopp M. 2016. Spatial Overlap of Grey Seals and Fisheries in Irish Waters, Some New Insights Using Telemetry Technology and VMS. Hyrenbach D, editor. PLoS ONE. 11(9):e0160564. doi:10.1371/journal.pone.0160564.

Dawson SM, Northridge S, Waples D, Read A. 2013. To ping or not to ping: the use of active acoustic devices in mitigating interactions between small cetaceans and gillnet fisheries. Endang Species Res. 19(3):201–221. doi:10.3354/esr00464.

deCastro M, Salvador S, Gómez-Gesteira M, Costoya X, Carvalho D, Sanz-Larruga FJ, Gimeno L. 2019. Europe, China and the United States: Three different approaches to the development of offshore wind energy. Renewable and Sustainable Energy Reviews. 109:55–70. doi:10.1016/j.rser.2019.04.025.

Deng R, Dichmont C, Milton D, Haywood M, Vance D, Hall N, Die D. 2005. Can vessel monitoring system data also be used to study trawling intensity and population depletion? The example of Australia's northern prawn fishery. Can J Fish Aquat Sci. 62(3):611–622. doi:10.1139/f04-219.

Denholm P, O'Connell M, Brinkman G, Jorgenson J. 2015. Overgeneration from Solar Energy in California. A Field Guide to the Duck Chart. Report No.: NREL/TP--6A20-65023, 1226167. [accessed 2023 Nov 19]. http://www.osti.gov/servlets/purl/1226167/.

Desholm M, Kahlert J. 2005. Avian collision risk at an offshore wind farm. Biol Lett. 1(3):296–298. doi:10.1098/rsbl.2005.0336.

Dong C, Renault L, Zhang Y, Ma J, Cao Y. 2017. Expansion of West Coast Oceanographic Modeling Capability. Pacific: U.S. Department of the Interior, Bureau of Ocean Energy Management, Report No.: BOEM 2017-055.

Draxl Caroline, Clifton A, Hodge B-M, McCaa J. 2015. The Wind Integration National Dataset (WIND) Toolkit. Applied Energy. 151:355–366. doi:10.1016/j.apenergy.2015.03.121.

Draxl C., Hodge B-M, Clifton A, McCaa J. 2015. Overview and Meteorological Validation of the Wind Integration National Dataset toolkit. Report No.: NREL/TP--5000-61740, 1214985. [accessed 2023 Nov 9]. http://www.osti.gov/servlets/purl/1214985/.

Dundas SJ, Levine AS, Lewison RL, Doerr AN, White C, Galloway AWE, Garza C, Hazen EL, Padilla-Gamiño J, Samhouri JF, et al. 2020. Integrating oceans into climate policy: Any green new deal needs a splash of blue. CONSERVATION LETTERS. 13(5):e12716. doi:10.1111/conl.12716.

Dunlop ES, Reid SM, Murrant M. 2016. Limited influence of a wind power project submarine cable on a Laurentian Great Lakes fish community. J Appl Ichthyol. 32(1):18–31. doi:10.1111/jai.12940.

Dvorak MJ, Archer CL, Jacobson MZ. 2010. California offshore wind energy potential. Renewable Energy. 35(6):1244–1254. doi:10.1016/j.renene.2009.11.022.

Dvorak MJ, Stoutenburg ED, Archer CL, Kempton W, Jacobson MZ. 2012. Where is the ideal location for a U.S. East Coast offshore grid? Geophysical Research Letters. 39(6):2011GL050659. doi:10.1029/2011GL050659.

Ebuchi N. 2001. Evaluation of wind vectors observed by QuikSCAT/SeaWinds using ocean buoy data. In: IGARSS 2001. Scanning the Present and Resolving the Future. Proceedings. IEEE 2001 International Geoscience and Remote Sensing Symposium (Cat. No.01CH37217). Vol. 3. Sydney, NSW, Australia: IEEE. p. 1082–1085. [accessed 2023 Nov 9]. http://ieeexplore.ieee.org/document/976753/.

Erickson WP, Johnson GD, Young DP. 2005. A Summary and Comparison of Bird Mortality from Anthropogenic Causes with an Emphasis on Collisions. Albany, CA: U.S. Department of Agriculture, Forest Service, Pacific Southest Research Station: USDA Forest Service Report No.: PSW-GTR-191.

Farr H, Wang Y, Ruttenberg B, Walter R, White C. 2017. Environmental Impacts of Deepwater Floating Offshore Wind and Wave Energy Facilities.

Feist BE, Samhouri JF, Forney KA, Saez LE. 2021. Footprints of fixed-gear fisheries in relation to rising whale entanglements on the U.S. West Coast. Fisheries Management Eco. 28(3):283–294. doi:10.1111/fme.12478.

Fewings MR, Washburn L, Dorman CE, Gotschalk C, Lombardo K. 2016. Synoptic forcing of wind relaxations at Pt. Conception, California. JGR Oceans. 121(8):5711–5730. doi:10.1002/2016JC011699.

Fiedler B, Bukovsky M. 2011. The effect of a giant wind farm on precipitation in a regional climate model. Environ Res Lett. 6(4):045101. doi:10.1088/1748-9326/6/4/045101.

Field JC, Francis RC. 2006. Considering ecosystem-based fisheries management in the California Current. Marine Policy. 30(5):552–569. doi:10.1016/j.marpol.2005.07.004.

FishBase. 2023. [accessed 2023 Jun 12]. fishbase.org.

Fisher MC, Moore SK, Jardine SL, Watson JR, Samhouri JF. 2021. Climate shock effects and mediation in fisheries. Proc Natl Acad Sci USA. 118(2):e2014379117. doi:10.1073/pnas.2014379117.

Floeter J, Van Beusekom JEE, Auch D, Callies U, Carpenter J, Dudeck T, Eberle S, Eckhardt A, Gloe D, Hänselmann K, et al. 2017. Pelagic effects of offshore wind farm foundations in the stratified North Sea. Progress in Oceanography. 156:154–173. doi:10.1016/j.pocean.2017.07.003.

Fox AD, Desholm M, Kahlert J, Christensen TK, Petersen IK. 2006. Information needs to support environmental impact assessment of the effects of European marine offshore wind farms on birds. Ibis. 148(s1):129–144. doi:10.1111/j.1474-919X.2006.00510.x.

Frid C, Andonegi E, Depestele J, Judd A, Rihan D, Rogers SI, Kenchington E. 2012. The environmental interactions of tidal and wave energy generation devices. Environmental Impact Assessment Review. 32(1):133–139. doi:10.1016/j.eiar.2011.06.002.

Fripp M, Wiser R. 2008. Effects of Temporal Wind Patterns on the Value of Wind-Generated Electricity in California and the Northwest. IEEE Trans Power Syst. 23(2):477–485. doi:10.1109/TPWRS.2008.919427.

Frith J. 2017. The World's First Floating Wind Farm, Statoil's Hywind Project, Has Been Officially Opened by Scotland's First Minister Nicola Sturgeon. Maritime Journal. [accessed 2018 Mar 2]. http://www.maritimejournal.com/news101/ marine-renewable-energy/words-first-floating-offshore-wind-farm-now-open.

Frölicher TL, Fischer EM, Gruber N. 2018. Marine heatwaves under global warming. Nature. 560(7718):360–364. doi:10.1038/s41586-018-0383-9.

Garthe S, Hüppop O. 2004. Scaling possible adverse effects of marine wind farms on seabirds: developing and applying a vulnerability index. Journal of Applied Ecology. 41(4):724–734. doi:10.1111/j.0021-8901.2004.00918.x.

Gerritsen H, Lordan C. 2011. Integrating vessel monitoring systems (VMS) data with daily catch data from logbooks to explore the spatial distribution of catch and effort at high resolution. ICES Journal of Marine Science. 68(1):245–252. doi:10.1093/icesjms/fsq137.

Gill A, Degraer S, Lipsky A, Mavraki N, Methratta E, Brabant R. 2020. Setting the Context for Offshore Wind Development Effects on Fish and Fisheries. Oceanog. 33(4):118–127. doi:10.5670/oceanog.2020.411.

Gill AB, Gloyne-Philips I, Kimber J, Sigray P. 2014. Marine Renewable Energy, Electromagnetic (EM) Fields and EM-Sensitive Animals. In: Shields MA, Payne AIL, editors. Marine Renewable Energy Technology and Environmental Interactions. Dordrecht: Springer Netherlands. (Humanity and the Sea). p. 61–79. [accessed 2023 Nov 19]. https://link.springer.com/10.1007/978-94-017-8002-5_6.

Glenn S, Dunk R. 2015. Evaluation of New Jersey's Offshore Wind Resources. New Brunswick, New Jersey: Rutgers Marine and Coastal Sciences.

Global Wind Energy Report: Annual Market Update 2017. 2017. Global Wind Energy Council (GWEC).

Gobler CJ. 2020. Climate Change and Harmful Algal Blooms: Insights and perspective. Harmful Algae. 91:101731. doi:10.1016/j.hal.2019.101731.

Gomiero A, Volpato E, Nasci C, Perra G, Viarengo A, Dagnino A, Spagnolo A, Fabi G. 2015. Use of multiple cell and tissue-level biomarkers in mussels collected along two gas fields in the northern Adriatic Sea as a tool for long term environmental monitoring. Marine Pollution Bulletin. 93(1–2):228–244. doi:10.1016/j.marpolbul.2014.12.034.

Götz T, Hastie, G., Hatch, L., Raustein, O., Southall, B., Tasker, M., Thomsen, F., Campbell, J., Fredheim, B. 2009. Overview of the impacts of anthropogenic underwater sound in the marine environment. London: OSPAR Commission.

Graabak I, Korpås M. 2016. Variability Characteristics of European Wind and Solar Power Resources—A Review. Energies. 9(6):449. doi:10.3390/en9060449.

Grantham BA, Chan F, Nielsen KJ, Fox DS, Barth JA, Huyer A, Lubchenco J, Menge BA. 2004. Upwelling-driven nearshore hypoxia signals ecosystem and oceanographic changes in the northeast Pacific. Nature. 429(6993):749–754. doi:10.1038/nature02605.

Gruber N, Boyd PW, Frölicher TL, Vogt M. 2021. Biogeochemical extremes and compound events in the ocean. Nature. 600(7889):395–407. doi:10.1038/s41586-021-03981-7.

GWEC Globe Wind 2017 Report. 2018. GWEC (Global Wind Energy Council).

Hackett S, Hansen M, King D, Price E. 2009. The Economic Structure of California's Commercial Fisheries. California Department of Fish and Game.

Hammar L, Perry D, Gullström M. 2016. Offshore Wind Power for Marine Conservation. OJMS. 06(01):66–78. doi:10.4236/ojms.2016.61007.

Harcourt R, Pirotta V, Heller G, Peddemors V, Slip D. 2014. A whale alarm fails to deter migrating humpback whales: an empirical test. Endang Species Res. 25(1):35–42. doi:10.3354/esr00614.

Hart LC, Goodman MC, Walter RK, Rogers-Bennett L, Shum P, Garrett AD, Watanabe JM, O'Leary JK. 2020. Abalone Recruitment in Low-Density and Aggregated Populations Facing Climatic Stress. Journal of Shellfish Research. 39(2):359. doi:10.2983/035.039.0218.

Hazen EL, Jorgensen S, Rykaczewski RR, Bograd SJ, Foley DG, Jonsen ID, Shaffer SA, Dunne JP, Costa DP, Crowder LB, et al. 2013. Predicted habitat shifts of Pacific top predators in a changing climate. Nature Clim Change. 3(3):234–238. doi:10.1038/nclimate1686.

He G, Kammen DM. 2014. Where, when and how much wind is available? A provincial-scale wind resource assessment for China. Energy Policy. 74:116–122. doi:10.1016/j.enpol.2014.07.003.

Holbrook NJ, Scannell HA, Sen Gupta A, Benthuysen JA, Feng M, Oliver ECJ, Alexander LV, Burrows MT, Donat MG, Hobday AJ, et al. 2019. A global assessment of marine heatwaves and their drivers. Nat Commun. 10(1):2624. doi:10.1038/s41467-019-10206-z.

Holland DS, Abbott JK, Norman KE. 2020. Fishing to live or living to fish: Job satisfaction and identity of west coast fishermen. Ambio. 49(2):628–639. doi:10.1007/s13280-019-01206-w.

Holt E, Wang J. 2012. Trends in Wind Speed at Wind Turbine Height of 80 m over the Contiguous United States Using the North American Regional Reanalysis (NARR). Journal of Applied Meteorology and Climatology. 51(12):2188–2202. doi:10.1175/JAMC-D-11-0205.1.

Hong L, Möller B. 2011. Offshore wind energy potential in China: Under technical, spatial and economic constraints. Energy. 36(7):4482–4491. doi:10.1016/j.energy.2011.03.071.

Hüppop O, Dierschke J, Exo K, Fredrich E, Hill R. 2006. Bird migration studies and potential collision risk with offshore wind turbines. Ibis. 148(s1):90–109. doi:10.1111/j.1474-919X.2006.00536.x.

Hutchison ZP, Sigray P, He H, Gill A, King J, Gibson C. 2018. Electromagnetic Field (EMF) Impacts on Elasmobranch (shark, rays, and skates) and American Lobster Movement and Migration from Direct Current Cables. Sterling, VA: U.S. Department of the Interior, Bureau of Ocean Energy Management Report No.: BOEM 2018-003.

Hywind Scotland Pilot Park Offshore Wind Farm. 2018. 4C Offshore. [accessed 2018 Sep 11]. https://www.4coffshore.com/windfarms/hywind-scotland-pilot-park-united-kingdom-uk76.html.

ICF. 2020. Comparison of Environmental Effects from Different Offshore Wind Turbine Foundations. Sterling, VA: U.S. Department of the Interior, Bureau of Ocean Energy Management Report No.: BOEM 2020-041.

IRENA (International Renewable Energy Agency). 2016. Innovation Outlook: Offshore Wind. Abu Dhabi: International Renewable Energy Agency.

James R, Ros MC. 2015. Floating Offshore Wind: Market and Technology Review. United Kingdom: The Carbon Trust.

Jiang Q, Doyle JD, Haack T, Dvorak MJ, Archer CL, Jacobson MZ. 2008. Exploring wind energy potential off the California coast. Geophysical Research Letters. 35(20):2008GL034674. doi:10.1029/2008GL034674.

Johnson DH, Loss SR, Smallwood KS, Erickson WP. 2016. Avian Fatalities at Wind Energy Facilities in North America: A Comparison of Recent Approaches. Human-Wildlife Interactions. 10:7–18. doi:10.26077/A4EC-ED37.

Joo R, Salcedo O, Gutierrez M, Fablet R, Bertrand S. 2015. Defining fishing spatial strategies from VMS data: Insights from the world's largest monospecific fishery. Fisheries Research. 164:223–230. doi:10.1016/j.fishres.2014.12.004.

Kako S, Isobe A, Kubota M. 2011. High-resolution ASCAT wind vector data set gridded by applying an optimum interpolation method to the global ocean: ASCAT WIND VECTOR DATA SET. J Geophys Res. 116(D23):n/a-n/a. doi:10.1029/2010JD015484.

Karnauskas KB, Lundquist JK, Zhang L. 2018. Southward shift of the global wind energy resource under high carbon dioxide emissions. Nature Geosci. 11(1):38–43. doi:10.1038/s41561-017-0029-9.

Katz RS. 2015. Fisheries of the United States. Euro J Political Res Yrbk. 54(1):309–315. doi:10.1111/2047-8852.12112.

Keith DW, DeCarolis JF, Denkenberger DC, Lenschow DH, Malyshev SL, Pacala S, Rasch PJ. 2004. The influence of large-scale wind power on global climate. Proc Natl Acad Sci USA. 101(46):16115–16120. doi:10.1073/pnas.0406930101.

Keller A, Frey P, Wallace J, Head M, Wetzel C, Cope J, Harms J. 2018. Canary rockfishes Sebastes pinniger return from the brink: catch, distribution and life history along the US west coast (Washington to California). Mar Ecol Prog Ser. 599:181–200. doi:10.3354/meps12603.

King J, Clifton A, Hodge B. 2014. Validation of Power Output for the WIND Toolkit. Report No.: NREL/TP-5D00-61714, 1159354. [accessed 2023 Nov 19]. http://www.osti.gov/servlets/purl/1159354/.

Kirchgeorg T, Weinberg I, Hörnig M, Baier R, Schmid MJ, Brockmeyer B. 2018. Emissions from corrosion protection systems of offshore wind farms: Evaluation of the potential impact on the marine environment. Marine Pollution Bulletin. 136:257–268. doi:10.1016/j.marpolbul.2018.08.058.

Klimley AP, Wyman MT, Kavet R. 2017. Chinook salmon and green sturgeon migrate through San Francisco Estuary despite large distortions in the local magnetic field produced by bridges. Fine ML, editor. PLoS ONE. 12(6):e0169031. doi:10.1371/journal.pone.0169031.

Koivisto M, Maule P, Nuño E, Sørensen P, Cutululis N. 2018. Statistical Analysis of Offshore Wind and other VRE Generation to Estimate the Variability in Future Residual Load. J Phys: Conf Ser. 1104:012011. doi:10.1088/1742-6596/1104/1/012011.

Kolora SRR, Owens GL, Vazquez JM, Stubbs A, Chatla K, Jainese C, Seeto K, McCrea M, Sandel MW, Vianna JA, et al. 2021. Origins and evolution of extreme life span in Pacific Ocean rockfishes. Science. 374(6569):842–847. doi:10.1126/science.abg5332.

Konstantinou IK, Albanis TA. 2004. Worldwide occurrence and effects of antifouling paint booster biocides in the aquatic environment: a review. Environment International. 30(2):235–248. doi:10.1016/S0160-4120(03)00176-4.

Kot BW, Sears R, Anis A, Nowacek DP, Gedamke J, Marshall CD. 2012. Behavioral responses of minke whales (Balaenoptera acutorostrata) to experimental fishing gear in a coastal environment. Journal of Experimental Marine Biology and Ecology. 413:13–20. doi:10.1016/j.jembe.2011.11.018.

Kramer SH, Hamilton CD, Spencer GC, Ogston HO. 2015. Evaluating the Potential for Marine and Hydrokinetic Devices to Act as Artificial Reefs or Fish Aggregating Devices. Based on Analysis of Surrogates in Tropical, Subtropical, and Temperate U.S. West Coast and Hawaiian Coastal Waters. Report No.: DOE-HTH--0006389, 1179455. [accessed 2023 Nov 19]. http://www.osti.gov/servlets/purl/1179455/.

Kraus S, Fasick J, Werner T, McFarron P. 2014. Enhancing the visibility of fishing ropes to reduce right whale entanglements. National Marine Fisheries Service, Office of Sustainable Fisheries.

Krone R, Gutow L, Brey T, Dannheim J, Schröder A. 2013. Mobile demersal megafauna at artificial structures in the German Bight – Likely effects of offshore wind farm development. Estuarine, Coastal and Shelf Science. 125:1–9. doi:10.1016/j.ecss.2013.03.012.

Kroodsma DA, Mayorga J, Hochberg T, Miller NA, Boerder K, Ferretti F, Wilson A, Bergman B, White TD, Block BA, et al. 2018. Tracking the global footprint of fisheries. Science. 359(6378):904–908. doi:10.1126/science.aao5646.

Langhamer O. 2012. Artificial Reef Effect in relation to Offshore Renewable Energy Conversion: State of the Art. The Scientific World Journal. 2012:1–8. doi:10.1100/2012/386713.

Lee J, South AB, Jennings S. 2010. Developing reliable, repeatable, and accessible methods to provide high-resolution estimates of fishing-effort distributions from vessel monitoring system (VMS) data. ICES Journal of Marine Science. 67(6):1260–1271. doi:10.1093/icesjms/fsq010.

Lee JC-Y, Fields MJ, Lundquist JK, Lunacek M. 2018. Determining variabilities of non-Gaussian wind-speed distributions using different metrics and timescales. J Phys: Conf Ser. 1037:072038. doi:10.1088/1742-6596/1037/7/072038.

Legg M, Yücel MK, Garcia De Carellan I, Kappatos V, Selcuk C, Gan TH. 2015. Acoustic methods for biofouling control: A review. Ocean Engineering. 103:237–247. doi:10.1016/j.oceaneng.2015.04.070.

Lester SE, Costello C, Halpern BS, Gaines SD, White C, Barth JA. 2013. Evaluating tradeoffs among ecosystem services to inform marine spatial planning. Marine Policy. 38:80–89. doi:10.1016/j.marpol.2012.05.022.

Lester SE, Stevens JM, Gentry RR, Kappel CV, Bell TW, Costello CJ, Gaines SD, Kiefer DA, Maue CC, Rensel JE, et al. 2018. Marine spatial planning makes room for offshore aquaculture in crowded coastal waters. Nat Commun. 9(1):945. doi:10.1038/s41467-018-03249-1.

Li X, Zhong S, Bian X, Heilman WE. 2010. Climate and climate variability of the wind power resources in the Great Lakes region of the United States. J Geophys Res. 115(D18):2009JD013415. doi:10.1029/2009JD013415.

Li Y, Kalnay E, Motesharrei S, Rivas J, Kucharski F, Kirk-Davidoff D, Bach E, Zeng N. 2018. Climate model shows large-scale wind and solar farms in the Sahara increase rain and vegetation. Science. 361(6406):1019–1022. doi:10.1126/science.aar5629.

Liu OR, Fisher M, Feist BE, Abrahms B, Richerson K, Samhouri JF. 2022. Mobility and Flexibility Enable Resilience of Human Harvesters to Environmental Perturbation. SSRN Journal. doi:10.2139/ssrn.4004911. [accessed 2023 Nov 19]. https://www.ssrn.com/abstract=4004911.

Liu WT, Tang W. 1996. Equivalent Neutral Wind. JPL Publication.:17–96.

Liu WTL, Xie X. 2006. Measuring ocean surface wind from space. In: Remote Sensing of the Marine Environment: Manual of Remote Sensing. Vol. 6. p. 149–178.

Long M, Mooney T, Zakroff C. 2016. Extreme low oxygen and decreased pH conditions naturally occur within developing squid egg capsules. Mar Ecol Prog Ser. 550:111–119. doi:10.3354/meps11737.

Lonhart SI, Jeppesen R, Beas-Luna R, Crooks JA, Lorda J. 2019. Shifts in the distribution and abundance of coastal marine species along the eastern Pacific Ocean during marine heatwaves from 2013 to 2018. Mar Biodivers Rec. 12(1):13. doi:10.1186/s41200-019-0171-8.

Love M, York A. 2005. A comparison of the fish assemblages associated with an oil/gas pipeline and adjacent seafloor in the Santa Barbara Channel, Southern California Bight. Bulletin of Marine Science. 77:101–118.

Love MS, Bizzarro JJ, Cornthwaite AM, Frable BW, Maslenikov KP. 2021. Checklist of marine and estuarine fishes from the Alaska–Yukon Border, Beaufort Sea, to Cabo San Lucas, Mexico. Zootaxa. 5053(1):1–285. doi:10.11646/zootaxa.5053.1.1.

Love MS, Nishimoto MM, Clark S, Bull AS. 2015. Identical Response of Caged Rock Crabs (Genera Metacarcinus and Cancer) to Energized and Unenergized Undersea Power Cables in Southern California, USA. Bulletin, Southern California Academy of Sciences. 114(1):33–41. doi:10.3160/0038-3872-114.1.33.

Ludewig E. 2015. On the Effect of Offshore Wind Farms on the Atmosphere and Ocean Dynamics. Cham: Springer International Publishing (Hamburg Studies on Maritime Affairs). [accessed 2023 Nov 19]. https://link.springer.com/10.1007/978-3-319-08641-5.

Madsen P, Wahlberg M, Tougaard J, Lucke K, Tyack P. 2006. Wind turbine underwater noise and marine mammals: implications of current knowledge and data needs. Mar Ecol Prog Ser. 309:279–295. doi:10.3354/meps309279.

Magris RA. 2021. Effectiveness of Large-Scale Marine Protected Areas in the Atlantic Ocean for Reducing Fishing Activities. Front Mar Sci. 8:711011. doi:10.3389/fmars.2021.711011.

Mamula, Aaron, Kosaka, Rosemary. Community Sustainability Cooperatives in Central California: Continued fishery participation through quota share holdings in the Pacific Coast groundfish fishery. U.S. Department of Commerce Report No.: NMFS-SWFSC-620.

Mamula, Aaron, Thomas-Smyth, Alice, Speir, Cameron, Kosaka, Rosemary, Pearson, Don. 2020. Matching Vessel Monitoring System data to trawl logbook and fish ticket data for the Pacific groundfish fishery. National Marine Fisheries Service Report No.: NOAA-TM-NMFS-SWFSC-623.

Mantua NJ, Hare SR, Zhang Y, Wallace JM, Francis RC. 1997. A Pacific Interdecadal Climate Oscillation with Impacts on Salmon Production. Bull Amer Meteor Soc. 78(6):1069–1079. doi:10.1175/1520-0477(1997)078<1069:APICOW>2.0.CO;2.

Maria M, Jacobson M. 2009. Investigating the Effect of Large Wind Farms on Energy in the Atmosphere. Energies. 2(4):816–838. doi:10.3390/en20400816.

Markowitz H. 1952. PORTFOLIO SELECTION*. The Journal of Finance. 7(1):77–91. doi:10.1111/j.1540-6261.1952.tb01525.x.

Marmo, Brett, Roberts, Iain, Buckingham, Mark-Paul, King, Stephanie, Booth, Cormac. 2013. Modelling of noise effects of operational offshore wind turbines including noise transmission through various foundation types. Edinburgh: Scottish Government Report No.: MS-101-REP-F.

Marques AT, Batalha H, Rodrigues S, Costa H, Pereira MJR, Fonseca C, Mascarenhas M, Bernardino J. 2014. Understanding bird collisions at wind farms: An updated review on the causes and possible mitigation strategies. Biological Conservation. 179:40–52. doi:10.1016/j.biocon.2014.08.017.

Marshall KN, Kaplan IC, Hodgson EE, Hermann A, Busch DS, McElhany P, Essington TE, Harvey CJ, Fulton EA. 2017. Risks of ocean acidification in the California Current food web and fisheries: ecosystem model projections. Global Change Biology. 23(4):1525–1539. doi:10.1111/gcb.13594.

Masden EA, Haydon DT, Fox AD, Furness RW, Bullman R, Desholm M. 2009. Barriers to movement: impacts of wind farms on migrating birds. ICES Journal of Marine Science. 66(4):746–753. doi:10.1093/icesjms/fsp031.

Masden EA, Reeve R, Desholm M, Fox AD, Furness RW, Haydon DT. 2012. Assessing the impact of marine wind farms on birds through movement modelling. J R Soc Interface. 9(74):2120–2130. doi:10.1098/rsif.2012.0121.

Maxwell SM, Hazen EL, Lewison RL, Dunn DC, Bailey H, Bograd SJ, Briscoe DK, Fossette S, Hobday AJ, Bennett M, et al. 2015. Dynamic ocean management: Defining and conceptualizing real-time management of the ocean. Marine Policy. 58:42–50. doi:10.1016/j.marpol.2015.03.014.

McClatchie S. 2014. Regional Fisheries Oceanography of the California Current System: The CalCOFI program. Dordrecht: Springer Netherlands. [accessed 2023 Nov 9]. https://link.springer.com/10.1007/978-94-007-7223-6.

Mesinger F, DiMego G, Kalnay E, Mitchell K, Shafran PC, Ebisuzaki W, Jović D, Woollen J, Rogers E, Berbery EH, et al. 2006. North American Regional Reanalysis. Bull Amer Meteor Soc. 87(3):343–360. doi:10.1175/BAMS-87-3-343.

Methot RD, Wetzel CR. 2013. Stock synthesis: A biological and statistical framework for fish stock assessment and fishery management. Fisheries Research. 142:86–99. doi:10.1016/j.fishres.2012.10.012.

Miller RR, Field JC, Santora JA, Monk MH, Kosaka R, Thomson C. 2017. Spatial valuation of California marine fisheries as an ecosystem service. Can J Fish Aquat Sci. 74(11):1732–1748. doi:10.1139/cjfas-2016-0228.

Miller RR, Field JC, Santora JA, Schroeder ID, Huff DD, Key M, Pearson DE, MacCall AD. 2014. A Spatially Distinct History of the Development of California Groundfish Fisheries. Hyrenbach D, editor. PLoS ONE. 9(6):e99758. doi:10.1371/journal.pone.0099758.

Mills AD, Millstein D, Jeong S, Lavin L, Wiser R, Bolinger M. 2018. Estimating the value of offshore wind along the United States' Eastern Coast. Environ Res Lett. 13(9):094013. doi:10.1088/1748-9326/aada62.

MMS (Minerals Management Service). 2007. Programmatic Environmental Impact Statement for Alternative Energy Development and Production and Alternate Use of Facilities on the Outer Continental Shelf: Final Environmental Impact Statement. U.S. Department of the Interior Report No.: MMS 2007-046.

Molnar JL, Gamboa RL, Revenga C, Spalding MD. 2008. Assessing the global threat of invasive species to marine biodiversity. Frontiers in Ecol & Environ. 6(9):485–492. doi:10.1890/070064.

Montevecchi WA. 2006. Influences of Artificial Light on Marine Birds. In: C. Rich and T. Longcore (eds). Ecological Consequences of Artificial Night Lighting. Island Press.

Moore GWK, Pickart RS, Renfrew IA. 2008. Buoy observations from the windiest location in the world ocean, Cape Farewell, Greenland. Geophysical Research Letters. 35(18):2008GL034845. doi:10.1029/2008GL034845.

Murray S, Hee TT. 2019. A rising tide: California's ongoing commitment to monitoring, managing and enforcing its marine protected areas. Ocean & Coastal Management. 182:104920. doi:10.1016/j.ocecoaman.2019.104920.

Musial W, Beiter P, Nunemaker J, Heimiller D, Ahmann J, Busch J. 2019. Oregon Offshore Wind Site Feasibility and Cost Study. Golden, CO: National Renewable Energy Laboratory Report No.: NREL/TP-5000-74597.

Musial Walter, Beiter P, Tegen S, Smith A. 2016. Potential Offshore Wind Energy Areas in California: An Assessment of Locations, Technology, and Costs. Report No.: NREL/TP--5000-67414, 1338174. [accessed 2023 Nov 19]. http://www.osti.gov/servlets/purl/1338174/.

Musial W, Elliot D, Fields J, Parker Z, Scott G, Draxl C. 2013. Assessment of Offshore Wind Energy Leasing Areas for the BOEM New Jersey Wind Energy Area. Golden, CO: National Renewable Energy Laboratory Report No.: NREL/TP-5000-60403.

Musial Walt, Heimiller D, Beiter P, Scott G, Draxl C. 2016. 2016 Offshore Wind Energy Resource Assessment for the United States. Report No.: NREL/TP--5000-66599, 1324533. [accessed 2023 Nov 8]. http://www.osti.gov/servlets/purl/1324533/.

Musial W, Ram B. 2010. Large-Scale Offshore Wind Power in the United: Assessment of Opportunities and Barriers. National Renewable Energy Lab Report No.: NREL/TP-500-40745.

Nagel T, Chauchat J, Wirth A, Bonamy C. 2018. On the multi-scale interactions between an offshore-wind-turbine wake and the ocean-sediment dynamics in an idealized framework – A numerical investigation. Renewable Energy. 115:783–796. doi:10.1016/j.renene.2017.08.078.

Nakanishi M, Niino H. 2006. An Improved Mellor–Yamada Level-3 Model: Its Numerical Stability and Application to a Regional Prediction of Advection Fog. Boundary-Layer Meteorol. 119(2):397–407. doi:10.1007/s10546-005-9030-8.

Natale F, Hofherr J, Fiore G, Virtanen J. 2013. Interactions between aquaculture and fisheries. Marine Policy. 38:205–213. doi:10.1016/j.marpol.2012.05.037.

National Marine Fisheries Service. 2018. Fisheries Economics of the United States. Report No.: NMFS-F/SPO-187a.

National Marine Fisheries Service. 2019. Fisheries of the United States, 2019. https://www.fisheries.noaa.gov/national/sustainable-fisheries/fisheries-united-states.

New York State Offshore Wind Master Plan: Marine Mammals and Sea Turtles Study. 2017. NYSERDA (New York State Energy Research and Development Authority) Report No.: NYSERDA Report 17-25L.

NOAA. 2018. National report on large whale entanglement confirmed in the United States in 2017. NOAA Fisheries.

Norman K, Sepez J, Lazrus H, Milne N, Package C, Russell S, Grant K, Lewis R, Primo J, Springer E, et al. 2007. Community Profiles for West Coast and North Pacific Fisheries, Washington, Oregon, California, and other U.S. States. National Marine Fisheries Service Report No.: NMFS-NWFSC-85.

Nurioglu AG, Esteves ACC, De With G. 2015. Non-toxic, non-biocide-release antifouling coatings based on molecular structure design for marine applications. J Mater Chem B. 3(32):6547–6570. doi:10.1039/C5TB00232J.

Offshore wind outlook 2019. 2019. IEA. https://webstore.iea.org/offshore-wind-outlook-2019-world-energy-outlook-special-report.

Optis M, Rybchuk A, Heimiller D, Bodini N, Rossol M, Musial W. 2020. 2020 Offshore Wind Resource Assessment for the California Pacific Outer Continental Shelf. National Renewable Energy Laboratory.

Oregon Activities. 2023. Bureau of Ocean Energy Management (BOEM). [accessed 2023 Jun 12]. https://www.boem.gov/renewable-energy/state-activities/Oregon.

OSI SAF/EARS Winds Team. 2021. Advanced Retransmission Service ASCAT Wind Product User Manual. Royal Netherlands Meteorological Institute.

Pacific Coast Groundfish Fishery Vessel Monitoring Program Compliance Guide. 2020. National Marine Fisheries Service. https://media.fisheries.noaa.gov/dam-migration/vms_complianceguide_may2020.pdf.

Palmer MC, Wigley SE. 2009. Using Positional Data from Vessel Monitoring Systems to Validate the Logbook-Reported Area Fished and the Stock Allocation of Commercial Fisheries Landings. N American J Fish Manag. 29(4):928–942. doi:10.1577/M08-135.1.

Paré G, Trudel M-C, Jaana M, Kitsiou S. 2015. Synthesizing information systems knowledge: A typology of literature reviews. Information & Management. 52(2):183–199. doi:10.1016/j.im.2014.08.008.

Patel P. 2009. Floating Wind Turbines to Be Tested. IEEE Spectrum. [accessed 2018 Jul 30]. https://spectrum.ieee.org/green-tech/wind/floating-wind- turbines-to-be-tested.

Pensieri S, Bozzano R, Schiano ME. 2010. Comparison between QuikSCAT and buoy wind data in the Ligurian Sea. Journal of Marine Systems. 81(4):286–296. doi:10.1016/j.jmarsys.2010.01.004.

PG&E. [accessed 2020 Sep 1]. https://www.pge.com/en_US/safety/how-the-system-works/diablo-canyon-power-plant/about-the-diablo- canyon-power-plant.page#:~:text=The%20two%20units%20produce%20a,provides%20throughout%20its%20service%20area.

Physical Oceanography Distributed Active Archive Center. 2013. QuikSCAT Level 2B Version 3 Guide Document.

Pickett MH, Tang W, Rosenfeld LK, Wash CH. 2003. QuikSCAT Satellite Comparisons with Nearshore Buoy Wind Data off the U.S. West Coast. J Atmos Oceanic Technol. 20(12):1869–1879. doi:10.1175/1520-0426(2003)020<1869:QSCWNB>2.0.CO;2.

Poe MR, Levin PS, Tolimieri N, Norman K. 2015. Subsistence fishing in a 21st century capitalist society: From commodity to gift. Ecological Economics. 116:241–250. doi:10.1016/j.ecolecon.2015.05.003.

Poot H, Ens BJ, De Vries H, Donners MAH, Wernand MR, Marquenie JM. 2008. Green Light for Nocturnally Migrating Birds. E&S. 13(2):art47. doi:10.5751/ES-02720-130247.

Popper AN, Hawkins AD. 2019. An overview of fish bioacoustics and the impacts of anthropogenic sounds on fishes. Journal of Fish Biology. 94(5):692–713. doi:10.1111/jfb.13948.

Porté-Agel F, Wu Y-T, Chen C-H. 2013. A Numerical Study of the Effects of Wind Direction on Turbine Wakes and Power Losses in a Large Wind Farm. Energies. 6(10):5297–5313. doi:10.3390/en6105297.

Possner A, Caldeira K. 2017. Geophysical potential for wind energy over the open oceans. Proc Natl Acad Sci USA. 114(43):11338–11343. doi:10.1073/pnas.1705710114.

Power S, Delage F, Chung C, Kociuba G, Keay K. 2013. Robust twenty-first-century projections of El Niño and related precipitation variability. Nature. 502(7472):541–545. doi:10.1038/nature12580.

Pozo Buil M, Jacox MG, Fiechter J, Alexander MA, Bograd SJ, Curchitser EN, Edwards CA, Rykaczewski RR, Stock CA. 2021. A Dynamically Downscaled Ensemble of Future Projections for the California Current System. Front Mar Sci. 8:612874. doi:10.3389/fmars.2021.612874.

Price S, Figueira R. 2017. Corrosion Protection Systems and Fatigue Corrosion in Offshore Wind Structures: Current Status and Future Perspectives. Coatings. 7(2):25. doi:10.3390/coatings7020025.

Punt AE, Butterworth DS, De Moor CL, De Oliveira JAA, Haddon M. 2016. Management strategy evaluation: best practices. Fish and Fisheries. 17(2):303–334. doi:10.1111/faf.12104.

Regional Vessel Monitoring Information. 2023. NOAA Fisheries. [accessed 2023 Jun 12]. https://www.fisheries.noaa.gov/national/enforcement/regional-vessel-monitoring-information.

Renault L, Hall A, McWilliams JC. 2016. Orographic shaping of U.S. West Coast wind profiles during the upwelling season. Clim Dyn. 46(1–2):273–289. doi:10.1007/s00382-015-2583-4.

Reubens JT, Degraer S, Vincx M. 2014. The ecology of benthopelagic fishes at offshore wind farms: a synthesis of 4 years of research. Hydrobiologia. 727(1):121–136. doi:10.1007/s10750-013-1793-1.

Review Of Selected California Fisheries For 2009: Coastal Pelagic Finfish, Market Squid, Dungeness Crab, Pacific Herring, Groundfish/Nearshore Live-Fish, Highly Migratory Species, Kelp, California Halibut, and Sandbasses. 2009. California Department of Fish and Wildlife.

Review of Selected California Fisheries for 2012: Coastal Pelagic Finfish, Market Squid, Pacific Herring, Groundfish, Highly Migratory Specities, White Seabass, Pacific Halibut, Red Sea Urchin, and Sea Cucumber. 2013. California Department of Fish and Wildlife.

Richerson K, Holland DS. 2017. Quantifying and predicting responses to a US West Coast salmon fishery closure. Schmidt J, editor. ICES Journal of Marine Science. 74(9):2364–2378. doi:10.1093/icesjms/fsx093.

Richmond L, Dumouchel R, Pontarelli H, Casali L, Smith W, Gillick K, Godde P, Dowling M, Suarez A. 2019. Fishing Community Sustainability Planning: A Roadmap and Examples from the California Coast. Sustainability. 11(7):1904. doi:10.3390/su11071904.

Rienecker MM, Suarez MJ, Gelaro R, Todling R, Bacmeister J, Liu E, Bosilovich MG, Schubert SD, Takacs L, Kim G-K, et al. 2011. MERRA: NASA's Modern-Era Retrospective Analysis for Research and Applications. Journal of Climate. 24(14):3624–3648. doi:10.1175/JCLI-D-11-00015.1.

Rogers-Bennett L, Catton CA. 2019. Marine heat wave and multiple stressors tip bull kelp forest to sea urchin barrens. Sci Rep. 9(1):15050. doi:10.1038/s41598-019-51114-y.

Rogers-Bennett L, Haaker PL, Huff TO, Dayton PK. Estimating Baseline Abundances of Abalone in California for Restoration. Report No.: CalCOFI Rep. 43.

Russell DJF, Brasseur SMJM, Thompson D, Hastie GD, Janik VM, Aarts G, McClintock BT, Matthiopoulos J, Moss SEW, McConnell B. 2014. Marine mammals trace anthropogenic structures at sea. Current Biology. 24(14):R638–R639. doi:10.1016/j.cub.2014.06.033.

Russell DJF, Hastie GD, Thompson D, Janik VM, Hammond PS, Scott-Hayward LAS, Matthiopoulos J, Jones EL, McConnell BJ. 2016. Avoidance of wind farms by harbour seals is limited to pile driving activities. Votier S, editor. Journal of Applied Ecology. 53(6):1642–1652. doi:10.1111/1365-2664.12678.

Russo T, Morello EB, Parisi A, Scarcella G, Angelini S, Labanchi L, Martinelli M, D'Andrea L, Santojanni A, Arneri E, et al. 2018. A model combining landings and VMS data to estimate landings by fishing ground and harbor. Fisheries Research. 199:218–230. doi:10.1016/j.fishres.2017.11.002.

Samhouri JF, Feist BE, Fisher MC, Liu O, Woodman SM, Abrahms B, Forney KA, Hazen EL, Lawson D, Redfern J, et al. 2021. Marine heatwave challenges solutions to human–wildlife conflict. Proc R Soc B. 288(1964):20211607. doi:10.1098/rspb.2021.1607.

Samhouri JF, Ramanujam E, Bizzarro JJ, Carter H, Sayce K, Shen S. 2019. An ecosystem-based risk assessment for California fisheries co-developed by scientists, managers, and stakeholders. Biological Conservation. 231:103–121. doi:10.1016/j.biocon.2018.12.027.

Sanford E, Sones JL, García-Reyes M, Goddard JHR, Largier JL. 2019. Widespread shifts in the coastal biota of northern California during the 2014–2016 marine heatwaves. Sci Rep. 9(1):4216. doi:10.1038/s41598-019-40784-3.

Santora JA, Mantua NJ, Schroeder ID, Field JC, Hazen EL, Bograd SJ, Sydeman WJ, Wells BK, Calambokidis J, Saez L, et al. 2020. Habitat compression and ecosystem shifts as potential links between marine heatwave and record whale entanglements. Nat Commun. 11(1):536. doi:10.1038/s41467-019-14215-w.

Santora JA, Schroeder ID, Field JC, Wells BK, Sydeman WJ. 2014. Spatio-temporal dynamics of ocean conditions and forage taxa reveal regional structuring of seabird–prey relationships. Ecological Applications. 24(7):1730–1747. doi:10.1890/13-1605.1.

Scheidat M, Tougaard J, Brasseur S, Carstensen J, Van Polanen Petel T, Teilmann J, Reijnders P. 2011. Harbour porpoises (*Phocoena phocoena*) and wind farms: a case study in the Dutch North Sea. Environ Res Lett. 6(2):025102. doi:10.1088/1748-9326/6/2/025102.

Schill W-P. 2013. Residual Load, Renewable Surplus Generation and Storage Requirements in Germany. SSRN Journal. doi:10.2139/ssrn.2340904. [accessed 2023 Nov 19]. http://www.ssrn.com/abstract=2340904.

Scoping 'Areas of Search' Study for Offshore Wind Energy in Scottish Waters. 2018. Aberdeen, Scotland: Marine Scotland Science.

Selden RL, Thorson JT, Samhouri JF, Bograd SJ, Brodie S, Carroll G, Haltuch MA, Hazen EL, Holsman KK, Pinsky ML, et al. 2020. Coupled changes in biomass and distribution drive trends in availability of fish stocks to US West Coast ports. Browman H, editor. ICES Journal of Marine Science. 77(1):188–199. doi:10.1093/icesjms/fsz211.

Shaner MR, Davis SJ, Lewis NS, Caldeira K. 2018. Geophysical constraints on the reliability of solar and wind power in the United States. Energy Environ Sci. 11(4):914–925. doi:10.1039/C7EE03029K.

Sharp E, Dodds P, Barrett M, Spataru C. 2015. Evaluating the accuracy of CFSR reanalysis hourly wind speed forecasts for the UK, using in situ measurements and geographical information. Renewable Energy. 77:527–538. doi:10.1016/j.renene.2014.12.025.

Sinden G. 2007. Characteristics of the UK wind resource: Long-term patterns and relationship to electricity demand. Energy Policy. 35(1):112–127. doi:10.1016/j.enpol.2005.10.003.

Skamarock W, Klemp J, Dudhia J, Gill D, Barker D, Wang W. 2005. A Description of the Advanced Research WRF Version 2. UCAR/NCAR. [accessed 2023 Nov 9]. http://opensky.ucar.edu/islandora/object/technotes:479.

Skov H, Heinänen S, Norman T, Ward R, Méndez-Roldán S, Ellis I. 2018. ORJIP Bird Collision and Avoidance Study. United Kingdom: The Carbon Trust.

Smale DA, Wernberg T, Oliver ECJ, Thomsen M, Harvey BP, Straub SC, Burrows MT, Alexander LV, Benthuysen JA, Donat MG, et al. 2019. Marine heatwaves threaten global biodiversity and the provision of ecosystem services. Nat Clim Chang. 9(4):306–312. doi:10.1038/s41558-019-0412-1.

Somers K, Richerson K, Tuttle V, McVeigh J. 2022. Fisheries Observation Science Program Coverage Rates, 2002-21. U.S. Department of Commerce Report No.: NMFS-NWFSC-DR-2002-02. https://repository.library.noaa.gov/view/noaa/47111.

Somers K, Whitmire C, Richerson K. 2020. Fishing Effort in the 2002–17 Pacific Coast Groundfish Fisheries. U.S. Department of Commerce Report No.: NMFS-NWFSC-153. https://repository.library.noaa.gov/view/noaa/23712.

Southall BL, Finneran JJ, Reichmuth C, Nachtigall PE, Ketten DR, Bowles AE, Ellison WT, Nowacek DP, Tyack PL. 2019. Marine Mammal Noise Exposure Criteria: Updated Scientific Recommendations for Residual Hearing Effects. Aquat Mamm. 45(2):125–232. doi:10.1578/AM.45.2.2019.125.

Spalding K. 2017. NATIONAL MARINE FISHERIES SERVICE POLICY 06-101. National Marine Fisheries Service Report No.: NMFS Policy 06-101. media.fisheries.noaa.gov/dam-migration/06-101.pdf.

State Nuclear Profiles. 2012. U.S. Energy Information Administration. [accessed 2020 Sep 1]. https://www.eia.gov/nuclear/state/california/.

Stoutenburg ED, Jenkins N, Jacobson MZ. 2010. Power output variations of co-located offshore wind turbines and wave energy converters in California. Renewable Energy. 35(12):2781–2791. doi:10.1016/j.renene.2010.04.033.

Sun X, Huang D, Wu G. 2012. The current state of offshore wind energy technology development. Energy. 41(1):298–312. doi:10.1016/j.energy.2012.02.054.

Suryan RM, Arimitsu ML, Coletti HA, Hopcroft RR, Lindeberg MR, Barbeaux SJ, Batten SD, Burt WJ, Bishop MA, Bodkin JL, et al. 2021. Ecosystem response persists after a prolonged marine heatwave. Sci Rep. 11(1):6235. doi:10.1038/s41598-021-83818-5.

Tang W, Liu WT, Stiles BW. 2004. Evaluation of high-resolution ocean surface vector winds measured by QuikSCAT scatterometer in coastal regions. IEEE Trans Geosci Remote Sensing. 42(8):1762–1769. doi:10.1109/TGRS.2004.831685.

Taylor PK, Kent EC, Yelland MJ, Moat BI. 1999. The Accuracy of Marine Surface Winds From Ships and Buoys. :59–68.

Templier M, Paré G. 2015. A Framework for Guiding and Evaluating Literature Reviews. CAIS. 37. doi:10.17705/1CAIS.03706. [accessed 2023 Nov 19]. https://aisel.aisnet.org/cais/vol37/iss1/6/.

Thomas KV, Brooks S. 2010. The environmental fate and effects of antifouling paint biocides. Biofouling. 26(1):73–88. doi:10.1080/08927010903216564.

Thompson AR, Chen DC, Guo LW, Hyde JR, Watson W. 2017. Larval abundances of rockfishes that were historically targeted by fishing increased over 16 years in association with a large marine protected area. R Soc open sci. 4(9):170639. doi:10.1098/rsos.170639.

Thompson M, Beston JA, Etterson M, Diffendorfer JE, Loss SR. 2017. Factors associated with bat mortality at wind energy facilities in the United States. Biological Conservation. 215:241–245. doi:10.1016/j.biocon.2017.09.014.

Thomsen F, Gill A, Kosecka M, Andersson M, Andre M, Degraer S, Folegot T, Gabriel J, Judd A, Neumann T, et al. 2015. MaRVEN - Environmental Impacts of Noise, Vibrations and Electromagnetic Emissions from Marine Renewable Energy. Brussels: European Commission Report No.: RTD-KI-NA-27-738-EN-N.

Thomson CJ. 2017. California's Commercial Fisheries: 1981-2012. MFR. 77(3):48–72. doi:10.7755/MFR.77.3.5.

Timeline of Marine Planning. 2023. Oregon Ocean Information. [accessed 2023 Jun 12]. https://www.oregonocean.info/index.php/timeline.

Tougaard J, Carstensen J, Wisz MS, Jespersen M, Teilmann J, Bech NI, Skov H. 2006. Harbour Porpoises on Horns Reef Effects of the Horns Reef Wind Farm. Roskilde, Denmark Report No.: Final Report to Vattenfall A/S.

Tougaard J, Henriksen OD, Miller LA. 2009. Underwater noise from three types of offshore wind turbines: Estimation of impact zones for harbor porpoises and harbor seals. The Journal of the Acoustical Society of America. 125(6):3766–3773. doi:10.1121/1.3117444.

Trident Winds. 2016. Unsolicited Application for an Outer Continental Shelf Renewable Energy Commercial Lease Under 30 CFR 585.230.

Uman LS. 2011. Systematic reviews and meta-analyses. J Can Acad Child Adolesc Psychiatry. 20(1):57–59.

User Guide for Electronic Fish Ticket Submission. 2021. https://nrm.dfg.ca.gov/FileHandler.ashx?DocumentID=165689&inline.

Van Cleve F, Bargmann G, Culver M. 2023. Marine Protected Areas in Washington: Recommendations of the Marine Protected Areas Work Group to the Washington State Legislature. Washington Department of Fish and Wildlife. [accessed 2023 Jun 12]. https://wdfw.wa.gov/publications/00038.

Vautard R, Thais F, Tobin I, Bréon F-M, De Lavergne J-GD, Colette A, Yiou P, Ruti PM. 2014. Regional climate model simulations indicate limited climatic impacts by operational and planned European wind farms. Nat Commun. 5(1):3196. doi:10.1038/ncomms4196.

Verhoef, Anton, Stoffelen, Ad. 2013. Validation of ASCAT 12.5-km winds. Report No.: SAF/OSI/CDOP/KNMI/TEC/RP/147.

Vermeirssen ELM, Dietschweiler C, Werner I, Burkhardt M. 2017. Corrosion protection products as a source of bisphenol A and toxicity to the aquatic environment. Water Research. 123:586–593. doi:10.1016/j.watres.2017.07.006.

Vindeby Offshore Wind Farm. 2017. 4C Offshore. [accessed 2018 Sep 11]. https://www.4coffshore.com/windfarms/vindeby-denmark-dk06.html.

Wahlberg M, Westerberg H. 2005. Hearing in fish and their reactions to sounds from offshore wind farms. Mar Ecol Prog Ser. 288:295–309. doi:10.3354/meps288295.

Walter RK, Armenta KJ, Shearer B, Robbins I, Steinbeck J. 2018. Coastal upwelling seasonality and variability of temperature and chlorophyll in a small coastal embayment. Continental Shelf Research. 154:9–18. doi:10.1016/j.csr.2018.01.002.

Walter RK, Reid EC, Davis KA, Armenta KJ, Merhoff K, Nidzieko NJ. 2017. Local diurnal wind-driven variability and upwelling in a small coastal embayment. J Geophys Res Oceans. 122(2):955–972. doi:10.1002/2016JC012466.

Wang B, Luo X, Yang Y-M, Sun W, Cane MA, Cai W, Yeh S-W, Liu J. 2019. Historical change of El Niño properties sheds light on future changes of extreme El Niño. Proc Natl Acad Sci USA. 116(45):22512–22517. doi:10.1073/pnas.1911130116.

Wang Y, Walter RK, White C, Ruttenberg BI. 2022. Spatial and Temporal Characteristics of California Commercial Fisheries from 2005 to 2019 and Potential Overlap with Offshore Wind Energy Development. Mar Coast Fish. 14(4):e10215. doi:10.1002/mcf2.10215.

Wang Y-H, Walter Ryan K., White C, Farr H, Ruttenberg BI. 2019. Assessment of surface wind datasets for estimating offshore wind energy along the Central California Coast. Renewable Energy. 133:343–353. doi:10.1016/j.renene.2018.10.008.

Wang Y-H, Walter Ryan K, White C, Kehrli MD, Hamilton SF, Soper PH, Ruttenberg BI. 2019. Spatial and temporal variation of offshore wind power and its value along the Central California Coast. Environ Res Commun. 1(12):121001. doi:10.1088/2515-7620/ab4ee1.

Watson JR, Fuller EC, Castruccio FS, Samhouri JF. 2018. Fishermen Follow Fine-Scale Physical Ocean Features for Finance. Front Mar Sci. 5:46. doi:10.3389/fmars.2018.00046.

Watson JT, Haynie AC. 2016. Using Vessel Monitoring System Data to Identify and Characterize Trips Made by Fishing Vessels in the United States North Pacific. Tsikliras AC, editor. PLoS ONE. 11(10):e0165173. doi:10.1371/journal.pone.0165173.

Weissman DE, Bourassa MA, Tongue J. 2002. Effects of Rain Rate and Wind Magnitude on SeaWinds Scatterometer Wind Speed Errors. J Atmos Oceanic Technol. 19(5):738–746. doi:10.1175/1520-0426(2002)019<0738:EORRAW>2.0.CO;2.

West Coast Groundfish. 2023. NOAA Fisheries. [accessed 2023 Jun 14]. Available from: https://www.fisheries.noaa.gov/species/west-coast-groundfish.

West Coast Groundfish Closed Areas. NOAA Fisheries. [accessed 2023 Jun 12]. https://www.fisheries.noaa.gov/west-coast/sustainable-fisheries/west-coast-groundfish-closed-areas.

Westerberg H, Lagenfelt I. 2008. Sub-sea power cables and the migration behaviour of the European eel. Fisheries Management Eco. 15(5–6):369–375. doi:10.1111/j.1365-2400.2008.00630.x.

What is the vessel monitoring system? 2021. NOAA Fisheries. [accessed 2023 Jun 12]. https://www.fisheries.noaa.gov/node/696.

White C, Halpern BS, Kappel CV. 2012. Ecosystem service tradeoff analysis reveals the value of marine spatial planning for multiple ocean uses. Proc Natl Acad Sci USA. 109(12):4696–4701. doi:10.1073/pnas.1114215109.

Wilcox C, Heathcote G, Goldberg J, Gunn R, Peel D, Hardesty BD. 2015. Understanding the sources and effects of abandoned, lost, and discarded fishing gear on marine turtles in northern Australia. Conservation Biology. 29(1):198–206. doi:10.1111/cobi.12355.

Wilhelmsson D, Langhamer O. 2014. The Influence of Fisheries Exclusion and Addition of Hard Substrata on Fish and Crustaceans. In: Shields MA, Payne AIL, editors. Marine Renewable Energy Technology and Environmental Interactions. Dordrecht: Springer Netherlands. (Humanity and the Sea). p. 49–60. [accessed 2023 Nov 19]. http://link.springer.com/10.1007/978-94-017-8002-5_5.

Wilhelmsson D, Malm T, Öhman MC. 2006. The influence of offshore windpower on demersal fish. ICES Journal of Marine Science. 63(5):775–784. doi:10.1016/j.icesjms.2006.02.001.

Wind Turbines - Part 1: Design Requirements. 2005. Geneva, Switzerland: International Electrotechnical Commission: International Electrotechnical Commission (IEC) 3rd PPUB edn Report No.: IEC 61400-1.

WINDExchange. 2019. [accessed 2019 Sep 6]. https://windexchange.energy.gov/maps-data/12.

Wiser RH, Mills A, Seel J, Levin T, Botterud A. 2017. Impacts of Variable Renewable Energy on Bulk Power System Assets, Pricing, and Costs. Report No.: 1411668. [accessed 2023 Nov 19]. http://www.osti.gov/servlets/purl/1411668/.

Woo CK, Moore J, Schneiderman B, Ho T, Olson A, Alagappan L, Chawla K, Toyama N, Zarnikau J. 2016. Merit-order effects of renewable energy and price divergence in California's day-ahead and real-time electricity markets. Energy Policy. 92:299–312. doi:10.1016/j.enpol.2016.02.023.

Wood MP, Carter L. 2008. Whale Entanglements With Submarine Telecommunication Cables. IEEE J Oceanic Eng. 33(4):445–450. doi:10.1109/JOE.2008.2001638.

World class performance by world's first floating wind farm. 2018. Equinor. [accessed 2019 Feb 4]. https://equinor.com/en/news/15feb2018-world-class-performance.html.

Xiao Y, Watson M. 2019. Guidance on Conducting a Systematic Literature Review. Journal of Planning Education and Research. 39(1):93–112. doi:10.1177/0739456X17723971.

Xiu P, Chai F, Curchitser EN, Castruccio FS. 2018. Future changes in coastal upwelling ecosystems with global warming: The case of the California Current System. Sci Rep. 8(1):2866. doi:10.1038/s41598-018-21247-7.

Yates KL, Schoeman DS, Klein CJ. 2015. Ocean zoning for conservation, fisheries and marine renewable energy: Assessing trade-offs and co-location opportunities. Journal of Environmental Management. 152:201–209. doi:10.1016/j.jenvman.2015.01.045.

Zacherl D, Gaines SD, Lonhart SI. 2003. The limits to biogeographical distributions: insights from the northward range extension of the marine snail, *Kelletia kelletii* (Forbes, 1852). Journal of Biogeography. 30(6):913–924. doi:10.1046/j.1365-2699.2003.00899.x.

Zeidberg L, Hamner WM, Nezlin N, Henry A. 2006. The fishery for California market squid (*Loligo opalescens*) (Cephalopoda: Myopsida), from 1981 through 2003. Fishery Bulletin. 104:46–59.

Appendix A: Supplementary Materials for Spatial and Temporal Variation of Offshore Wind Power and its Value along the Central California Coast

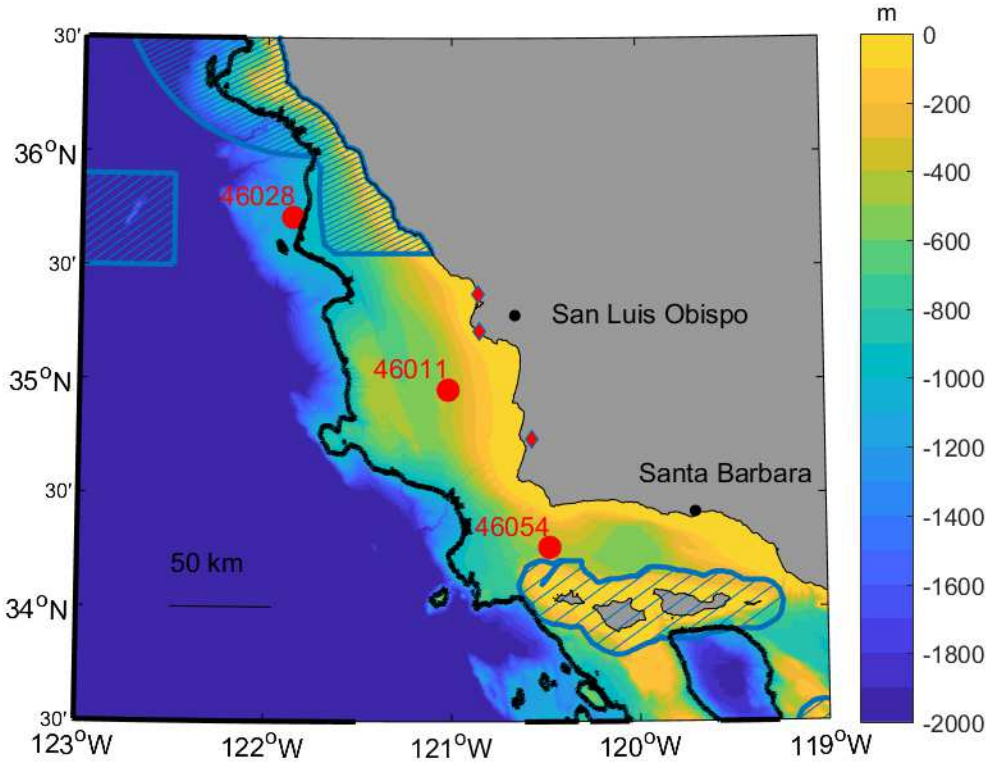

Figure A1. Bathymetry of the Central California Coast.
Note: Highlighting the locations of buoy platforms (red circles, representing buoys 46028, 46011, 46054 from north to south), existing state electrical grid connections (red diamonds), National Marine Sanctuaries (dashed blue lines; Monterey Bay Sanctuary to the north and Channel Islands Sanctuary to the south), and the 1000 m isobath (solid black line). The state electrical grid connections from north to south are the Morro Bay power plant, Diablo Canyon nuclear power plant, and Vandenberg Air Force Base. Reprinted from Wang et al., Copyright (2019), with permission from Elsevier.

A.1 CAISO data

CAISO data are available starting in April 2010 and measure approximately 80% of the power use in California, as well as a small part of Nevada. Although CAISO does not manage all electrical grids in California, its temporal variability in electricity demand is similar to the statewide demand measured by the Energy Information Administration (EIA). Unfortunately, since EIA does not provide hourly power generation data, the CAISO data is more useful for this study.

The renewable resources from CAISO for our analysis are solar and land-based wind. Other renewables like geothermal, biomass, and small hydro are not considered given their relatively small contribution to California's renewable energy portfolio and the low probability that these sources will increase dramatically in the future to meet renewable energy targets (CEC 2017).

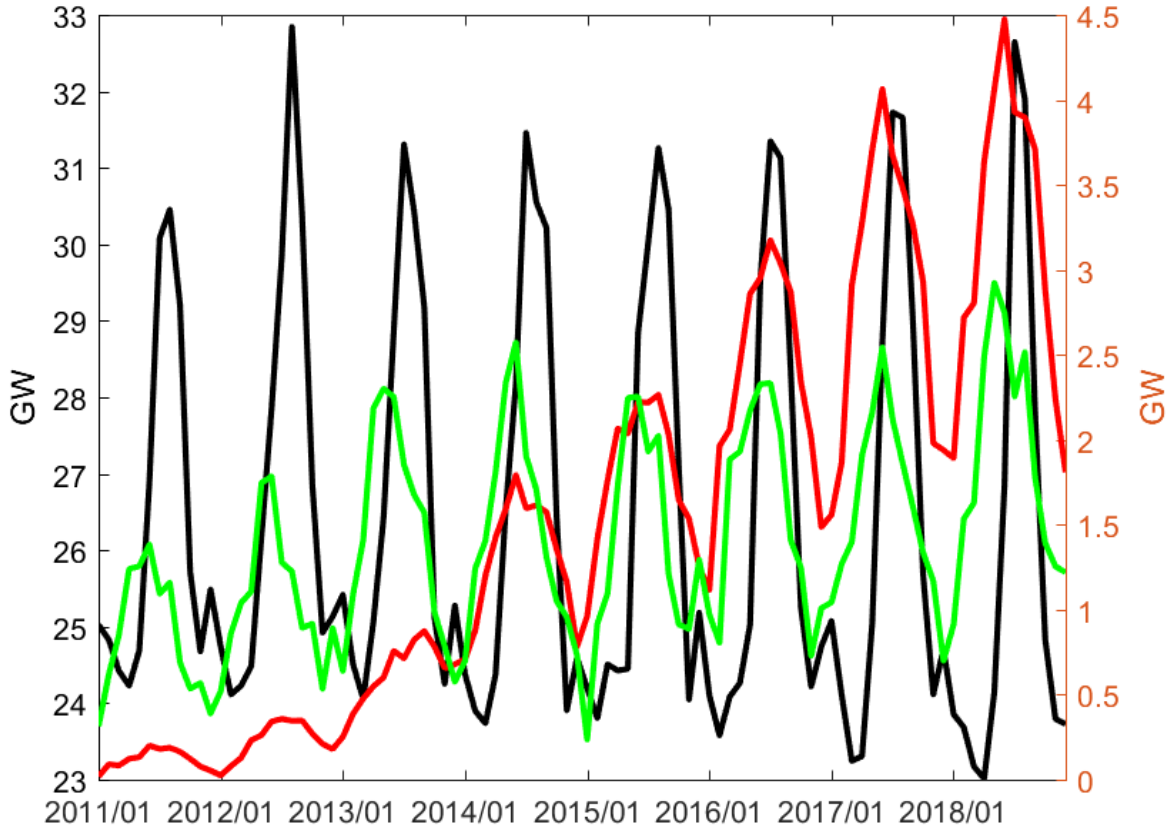

Figure A2. Monthly mean of statewide electricity demand (black, left axis), solar (red, right axis), and land-based wind production (green, right axis) in California from 2011 to 2018.

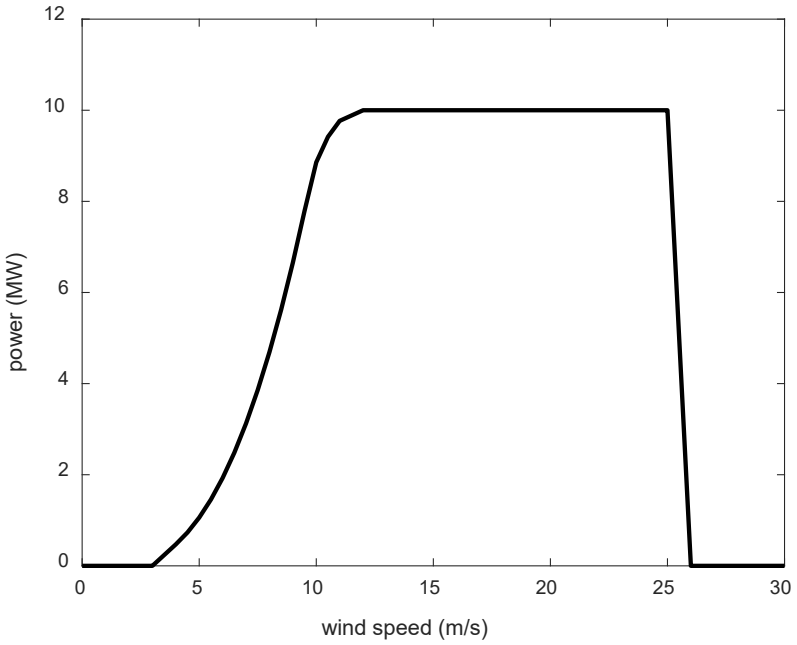

Figure A3. NREL 10 MW offshore wind turbine power curve (Musical et al., 2016).

A.2 Air density correction for wind power production calculation

Air density variations need to be considered in the calculation of power production, since wind power depends on the air density and the power curves are calculated using a standard reference density (1.225 kg/m^3) (Gipe 2016). In this study, we carried out air density corrections to estimate an effective wind speed at hub height (V_{effect}) at the turbine reference density (ρ_o = 1.225 kg/m^3) using the interpolated wind speed at hub height (V_{hub}) and air density at hub height (ρ_{hub}) (IEC, 2005):

$$V_{effect} = v_{hub} \cdot (\frac{\rho_{hub}}{\rho o})^{1/3}.$$

Since WIND Toolkit only provides air density at 2 m above the surface (ρ_{2m}), we estimated air density at hub height by applying the linear relationship between 2 m air density and hub-height air density, derived from all spatial points across the Central California Coast using the NARR data. Note that the linear relationship between air density at different altitudes varies with space. More than 80% of hourly air densities at hub height in this region over the seven-year period are slightly lower than the constant standard air density. Therefore, power estimates are slightly lower and more conservative with the air density correction. The effect of air density correction on power estimates is minimal that the mean of the difference in hourly power over seven years between using a variable density versus using the constant air density is approximately -0.01 MW.

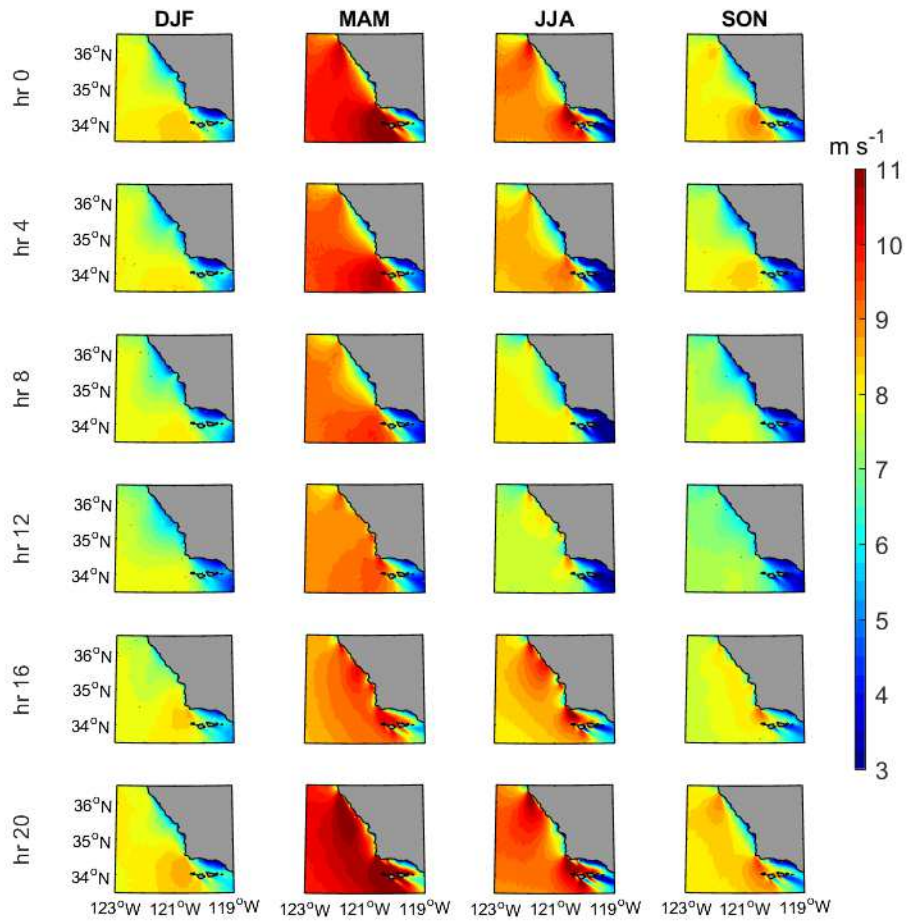

Figure A4. Averages of the hourly 125-m wind speed from WIND Toolkit over 2007-2013 at different hours and four seasons.

Note: Each column from the left to the right represents winter (December-January-February, DJF), spring (March-April-May, MAM), summer (June-July-August, JJA), and fall (September-October-November, SON). Each row from the top to the bottom represents 00 PST, 04 PST, 08 PST, 12 PST, 16 PST, and 20 PST.

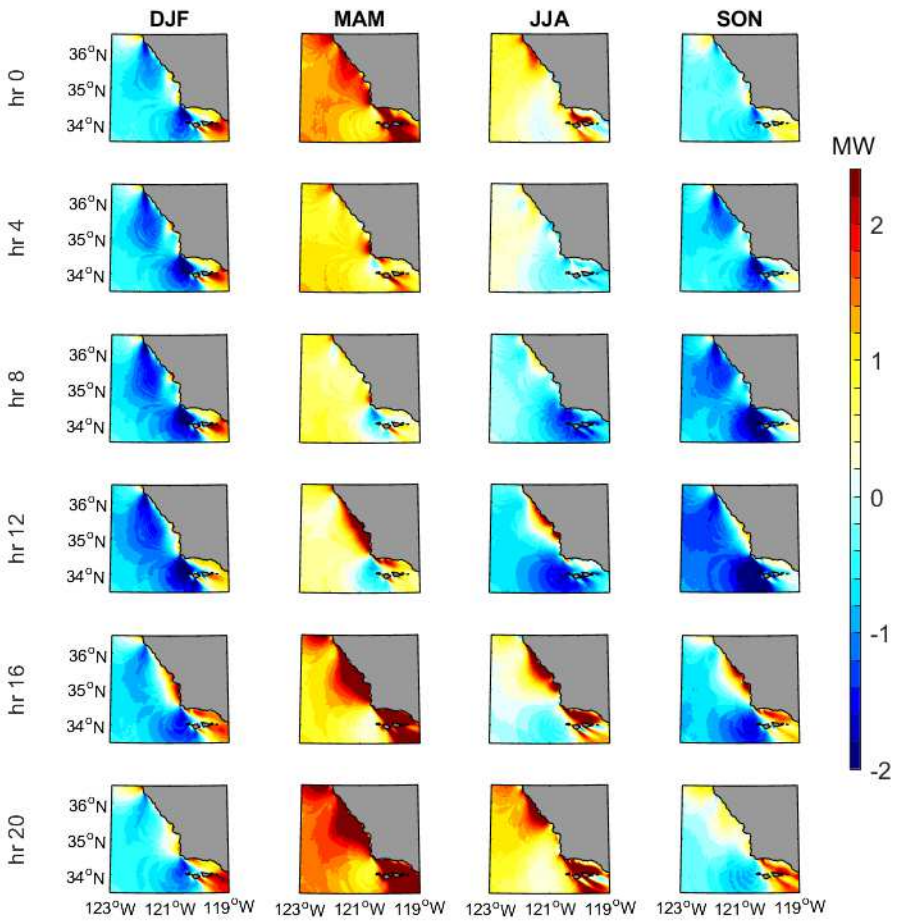

Figure A5. Same as Figure A4, but showing the difference between the average of hourly wind production and production estimated from annual mean wind speed over 2007-2013 at a particular hour of each respective season.

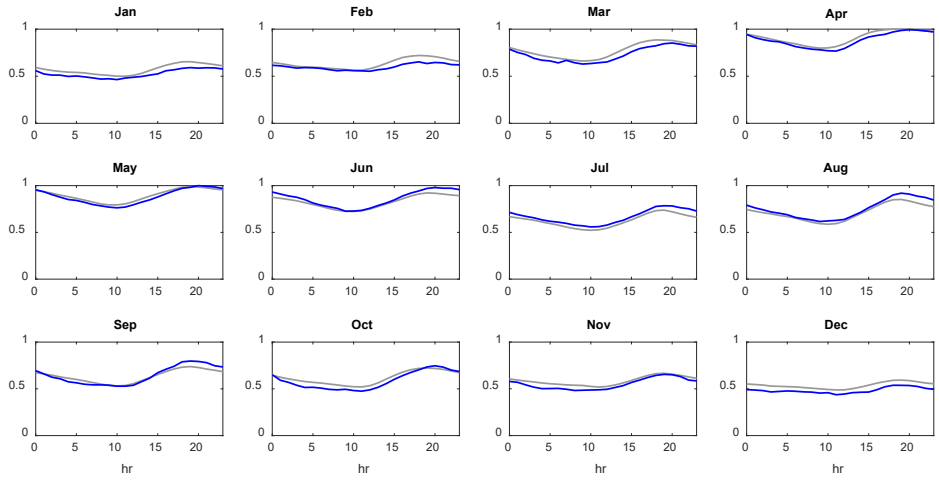

Figure A6. Daily composite averages of hourly offshore wind production near 46028.
Note: (Blue) and hourly offshore wind production aggregated over the entire study domain of interest (outside national marine sanctuaries, outside of state waters, shallower than depth limits of 1200 m, and north of Point Conception) (gray). Composite averages are normalized by the maximum over all months and hours of each respective curve.

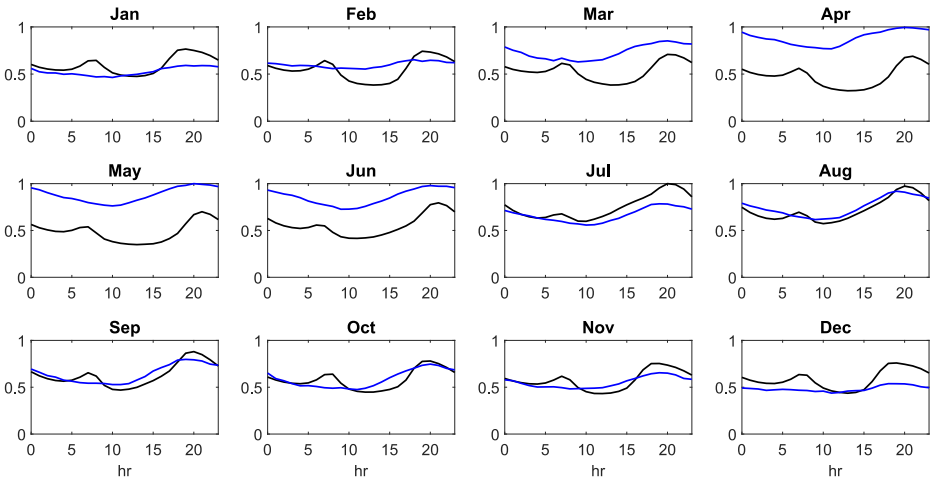

Figure A7. Daily composite averages of net demand.
Note: (demand minus solar generation and land-based wind generation; black), and offshore wind production near 46028 (blue) in each month. Composite averages are normalized by the maximum over all months and hours of each respective curve the maximum of composites.

A.3 Sensitivity of the wholesale value of offshore wind power production to time of pricing data

We used the pricing data in the most recent full year (2018) to calculate the wholesale value of offshore wind power production. However, there is a quantitative change (qualitative features remain robust year to year) in the diurnal and seasonal patterns of the wholesale value if we replaced the pricing data in 2018 by the pricing data in 2017. Readers should keep in mind that because of its volatile behavior, using a different time period of pricing data can result in different details in the wholesale value of offshore wind power production.

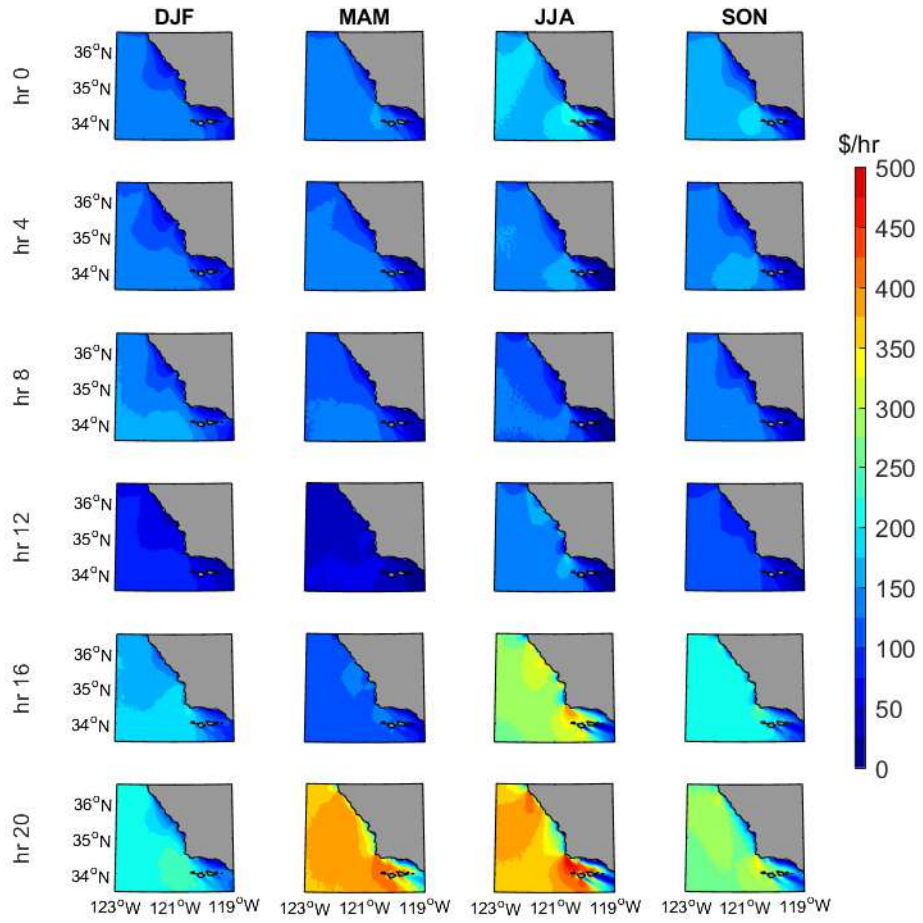

Figure A8. Averages of the hourly wholesale value of offshore wind power using the pricing data in 2017 at different hours and four seasons.

Appendix B: Supplementary Materials for Scenarios for Offshore Wind Power Production for Central California Call Areas

Table B1. Summary of rated power production for different wind farm size scenarios: a. 12 MW, b. 15 MW

a. 12 MW

Farm size (rated MW)	60	240	960
No. of turbines	5	20	80
7D x 7D footprint (km^2)	12.07	48.30	193.19
8D x 10D footprint (km^2)	19.71	78.85	315.42
Rated power relative to DCNPP (2200 MW)	2.73%	10.91%	43.64%

b. 15 MW

Farm size (MW)	60	240	960
No. of turbines	4	16	64
7D x 7D footprint (km^2)	12.05	48.22	192.88
8D x 10D footprint (km^2)	19.68	78.73	314.90
Rated power relative to DCNPP (2200 MW)	2.73%	10.91%	43.64%

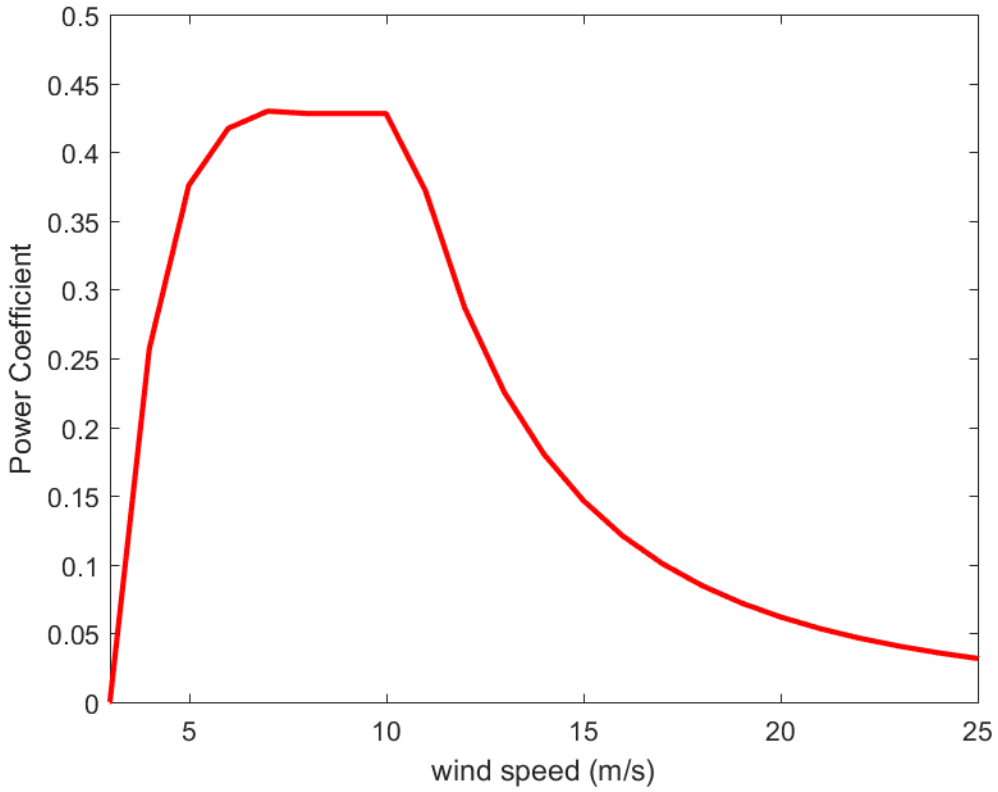

Figure B1. Power coefficient curve for the 15 MW wind turbine between the cut-in (3 m/s) and cut-out (25 m/s) wind speed. The power coefficient is zero beyond the cut-in and cut-out wind speeds.

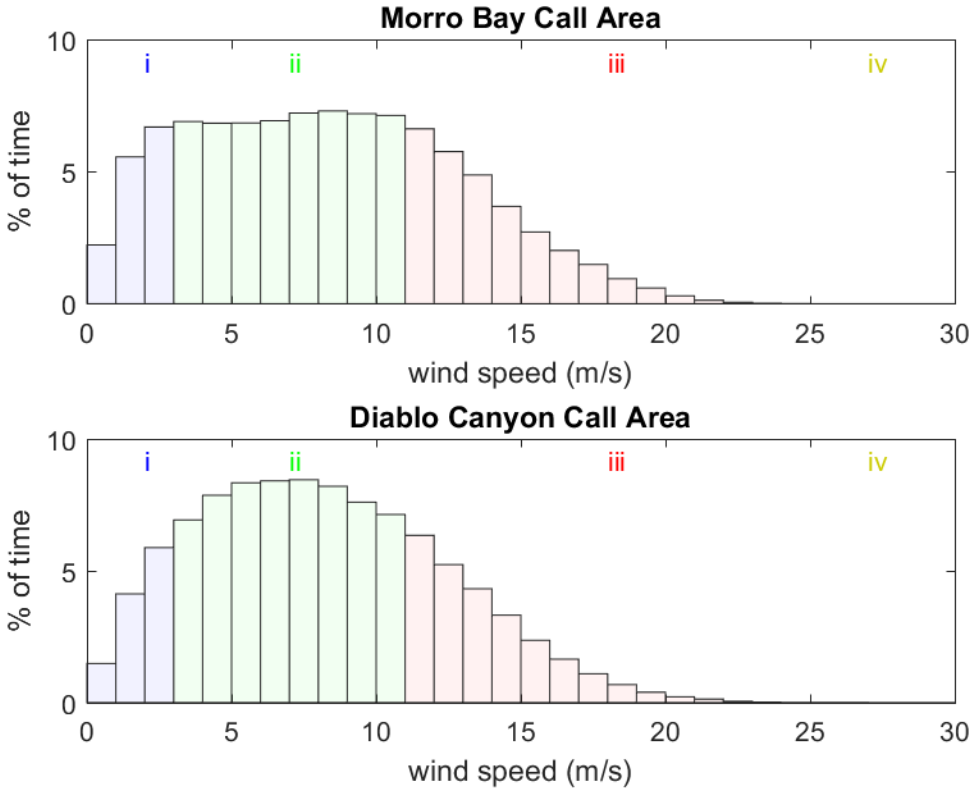

Figure B2. Frequency distribution of hourly hub-height wind speed (modeled for a 15 MW turbine) in each 2 km x 2 km grid cell within the Morro Bay Call Area (top) and the Diablo Canyon Call Area (bottom) over 2007-2013.

Note: Roman numerals and bar color corresponds with wind speed categories shown in Figure 1: (i) below cut-in wind speed (≤3 m/s), (ii) between cut-in and rated wind speed (> 3 m/s and < 11 m/s), (iii) between rated and cut-out wind speed (≥11 m/s and ≤25 m/s), and (iv) beyond cut-out wind speed.

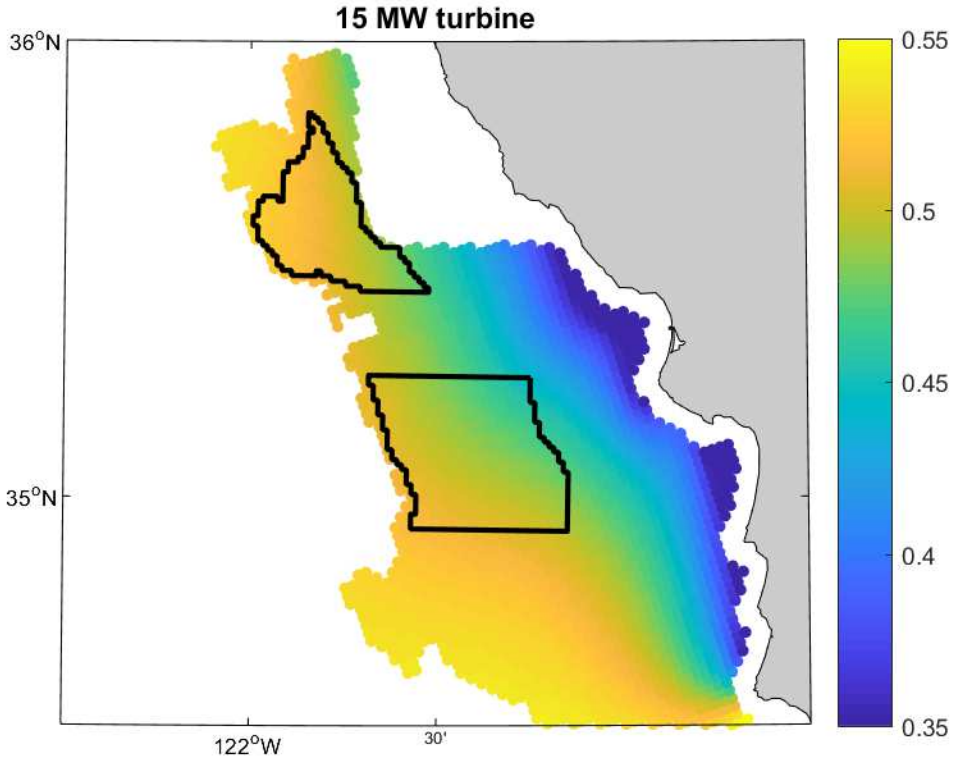

Figure B3. Capacity factor over 2007-2013 across the developable areas with one 15 MW turbine per grid cell. Call Areas are marked by black polygons.

Appendix C: Supplementary Materials for Spatial and temporal characteristics of California commercial fisheries from 2005 to 2019 and potential overlap with offshore wind energy development

Table C1. California commercial fisheries of nine taxonomic groups separated by assigned depth strata

Fishery types	Common name (Scientific name)	Depth strata
Coastal pelagic species	sardine (*Sardinops sagax*) (62%), northern anchovy (*Engraulis mordax*) (20%), Pacific mackerel (*Scomber japonicus*) and jack mackerel (*Trachurus symmetricus*) (16%)	
Salmonids	Chinook (*Oncorhynchus tshawytscha*) (99%), pink (*O. gorbuscha)* (~0%), coho (*O. kisutch*) (~0%), unspecified salmon (*O.* spp.)	
Groundfish	leopard shark (*Triakis semifasciata*), sanddabs, flounder - starry, unspecified (*Citharichthys* spp.); turbots (*Pleuronichthys* spp.), soles - bigmouth, rock, fantail, sand, English, butter, tongue (Pleuronectiformes), California halibut (*Paralichthys californicus*), cabezon (*Scorpaenichthys marmoratus*), scorpionfish (*Scorpaena* spp.), staghorn sculpin (*Leptocottus armatus*), yellowchin sculpin (*Icelinus* spp.)	0-200m
	Lingcod (*Ophiodon elongatus*), petrale sole (*Eopsetta jordani*), Pacific halibut (*Hippoglossus stenolepis*), North Pacific hake (*Merluccius productus*), flounder arrowtooth (*Atheresthes stomias*)	0-400m
	Rockfish (*Sebastes spp.*) (14%)	0-600m
	Sablefish (*Anoplopoma fimbria*) (39%), spiny dogfish (Squalidae spp.), soles - Dover, rex (*Microstomus pacificus*, *Glyptocephalus zachirus*), thornyheads (*Sebastolobus* spp.) (14%)	100-1200m
Game fish	Seabass (Serranidae, Epinephelinae) (60%), bonito (*Sarda chiliensis*) (21%), sheephead (*Semicossyphus pulcher*) (18%), barracuda (*Sphyraenidae*)	
Highly migratory species	Swordfish (*Xiphiidae gladius*) (55%), tunas (*Thunnus spp.*) (44%), thresher sharks (*Alopias* spp.) - shortfin mako (*Isurus oxyrinchus*), blue shark (*Prionace glauca*), hammerhead sharks (*Sphyrna* spp.)	
Market squid	California market squid (*Doryteuthis opalescens*)	0-100m
Echinoderms	Urchin (*Mesocentrotus franciscanus*, *Strongylocentrotus purpuratus*, *Lytechinus pictus*) (86%)	0-25m
	sea cucumber (*Parastichopus californicus*, *Parastichopus parvimensis*) (14%)	0-100m
Dungeness crab	Dungeness crab (*Metacarcinus magister*)	0-200m
Other crustaceans	rock crab (*Cancer antennarius*)	0-100m
	spiny lobster (*Panulirus interruptus*) (60%)	0-25m
	spot prawn (*Pandalus platyceros*) (24%), pink shrimp (*Pandalus jordani*) (11%)	50-300m

Note: The percentage of the revenue values relative to the whole group for the top three taxa during 2005-2019 is shown. This table was modified from Table 1 of Miller et al. (2017). Game fish refers to a group of species that are generally targeted by recreational anglers but are occasionally and legally captured by commercial fisheries.

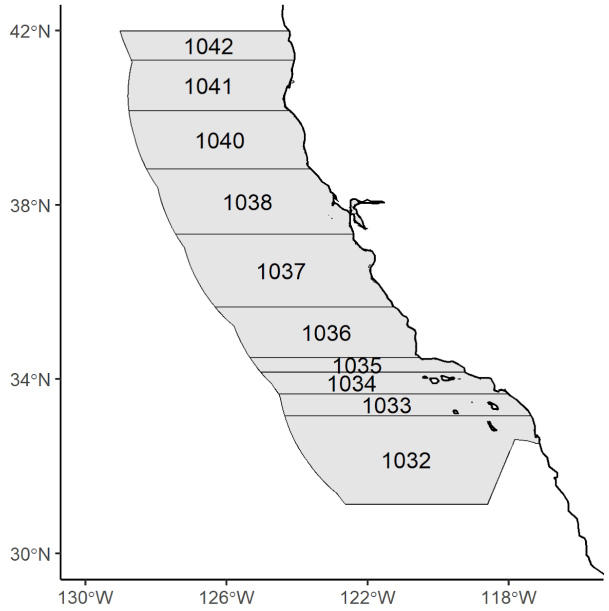

Figure C1. Map of four-digit fishing blocks in California.

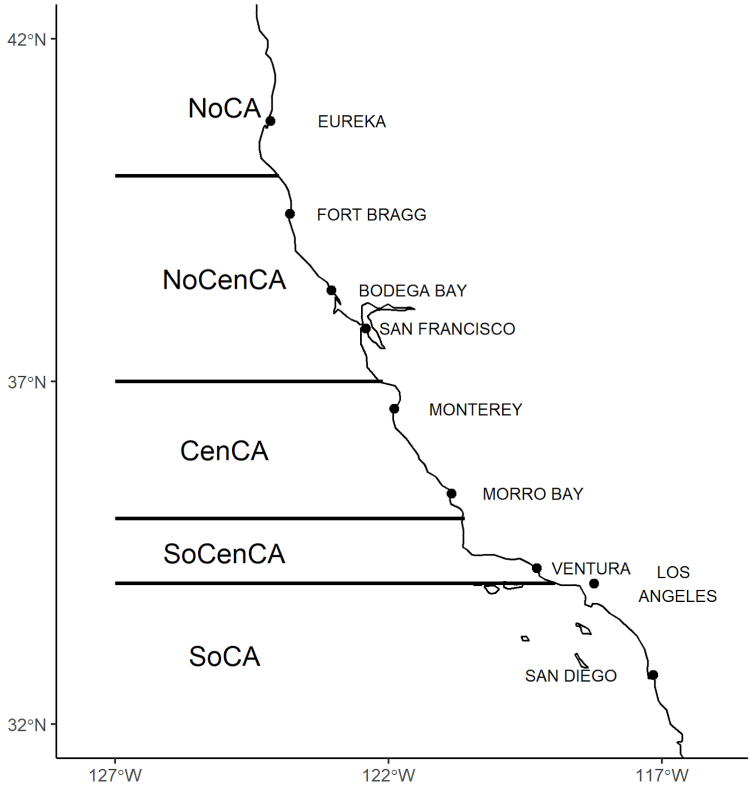

Figure C2. Major California fishing ports by region.
Note: Modified from Figure 8 of Thomson (2015).

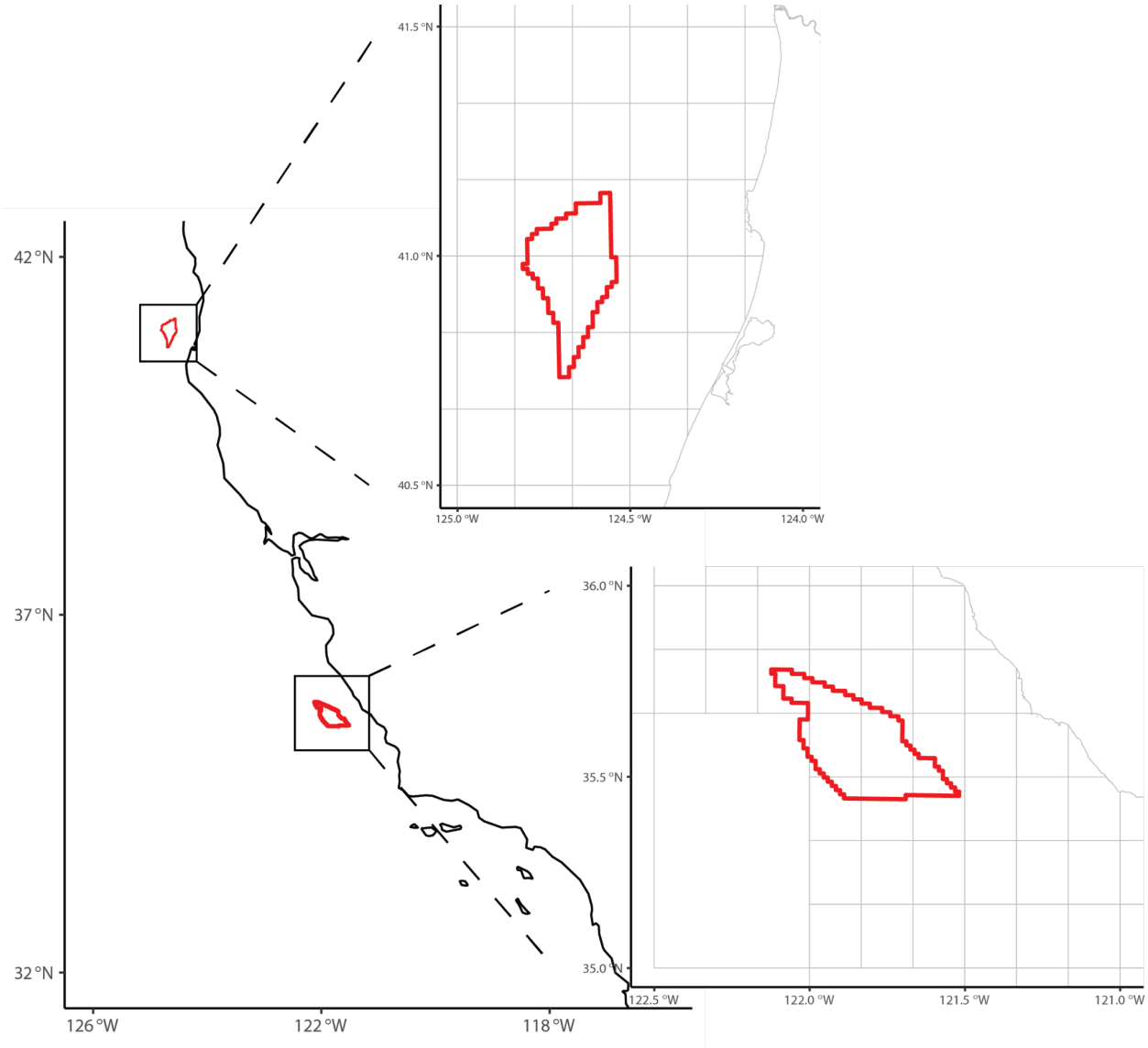

Figure C3. Map of WEAs in California for offshore wind development. (north) Humboldt WEA (south) Morro Bay WEA.

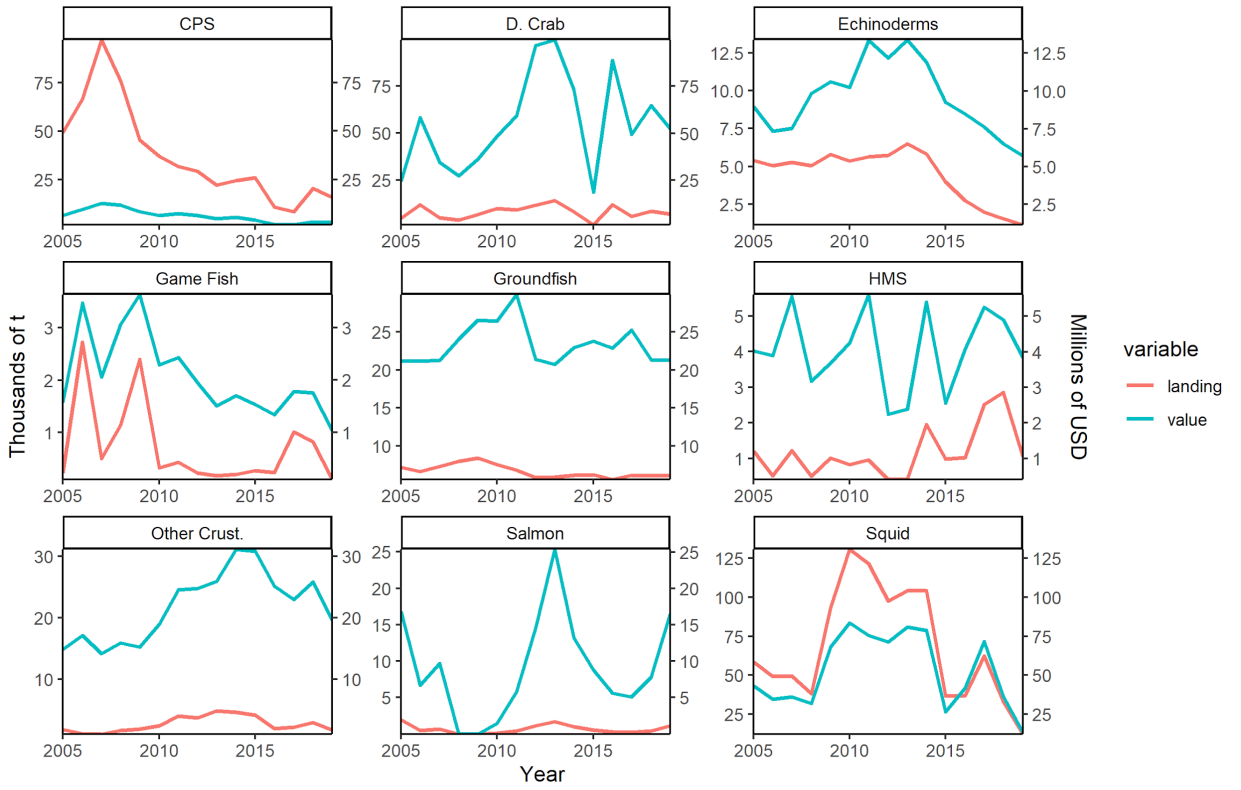

Figure C4. Annual landings (Thousand of t, left y-axis) and value (Millions of USD, right y-axis) for each fishery group.

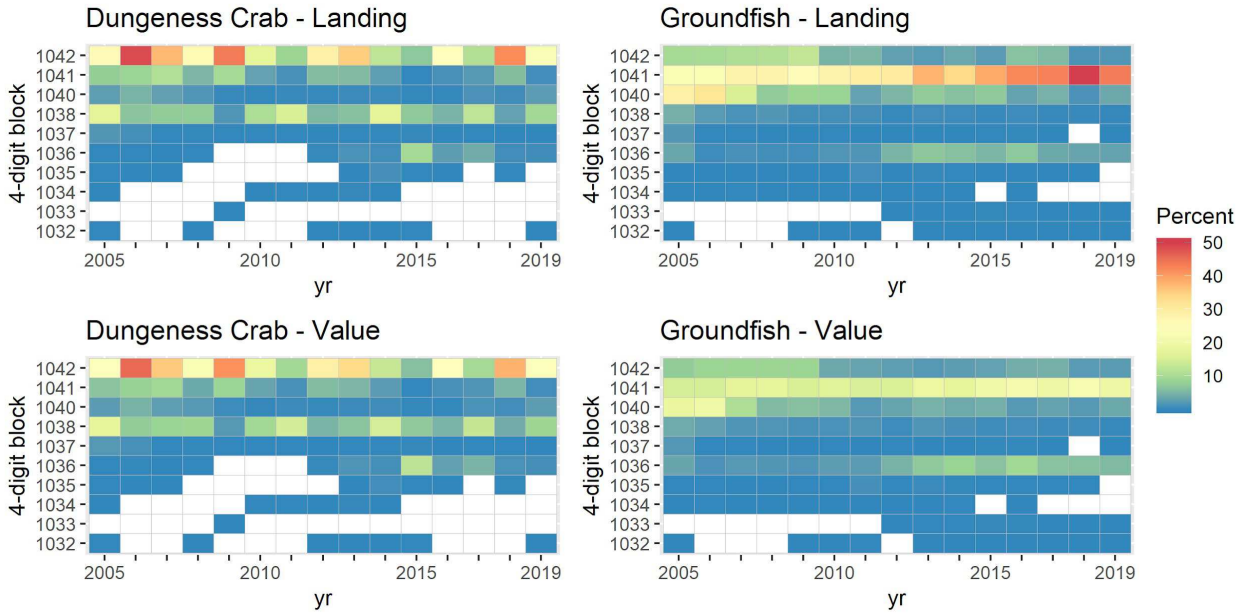

Figure C5. (top) Percentage of total landing in individual four-digit blocks relative to all blocks per year for Dungeness crab on the left and groundfish on the right. (bottom) Similar to the top panels but for total value. White represents a zero value, indicating no catch in the block during that year.

Appendix D: Supplementary Materials for High resolution assessment of commercial fisheries activity along the U.S. West Coast using Vessel Monitoring System data with a case study using California groundfish fisheries

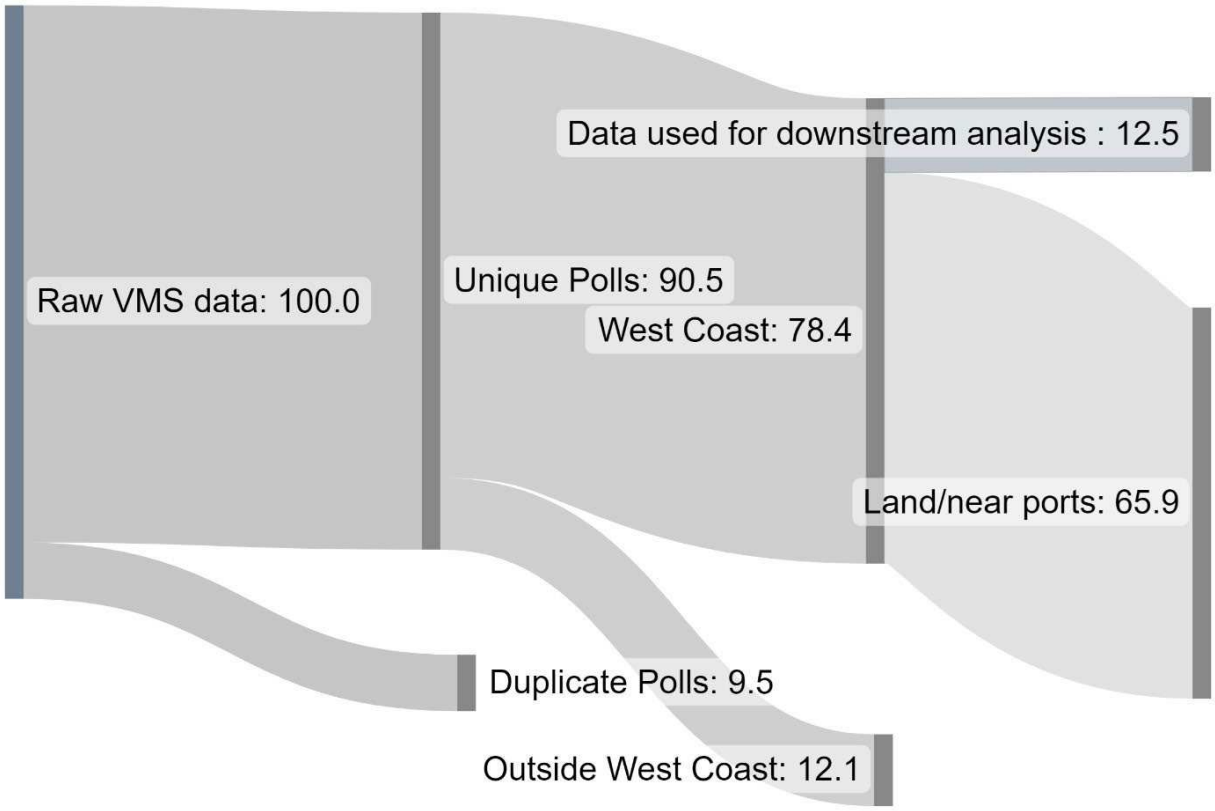

Figure D1. Sankey diagram representing VMS data loss in each step of processing.
Note: The starting point in the diagram is the raw data after correcting negative latitudes (0.39% of raw data). The percentage of data relative to the raw data for each step is provided. The raw data included over 50 million VMS polls, so the data for downstream analysis of fishing activity (12.5% of the VMS polls) still included over 6 million individual VMS polls.

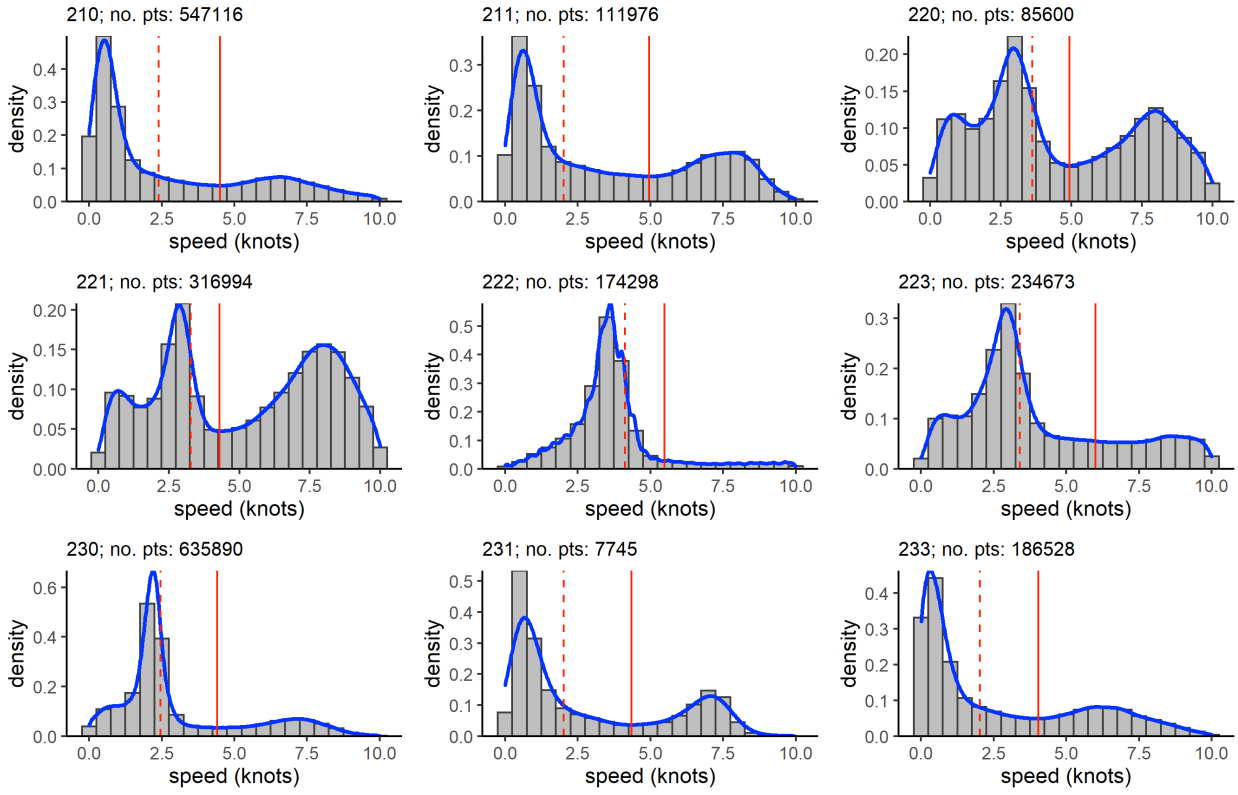

Figure D2. Distribution of vessel speed for Declaration Codes 210-233 using processed VMS data.
Note: The blue line represents a kernel density fit of the data. The red solid line shows the local minimum of the distribution, and the red dashed line shows the slope minimum between two and six knots. The number in the title for each subplot is the declaration code, and np. pts is the number of VMS polls included in each declaration code.

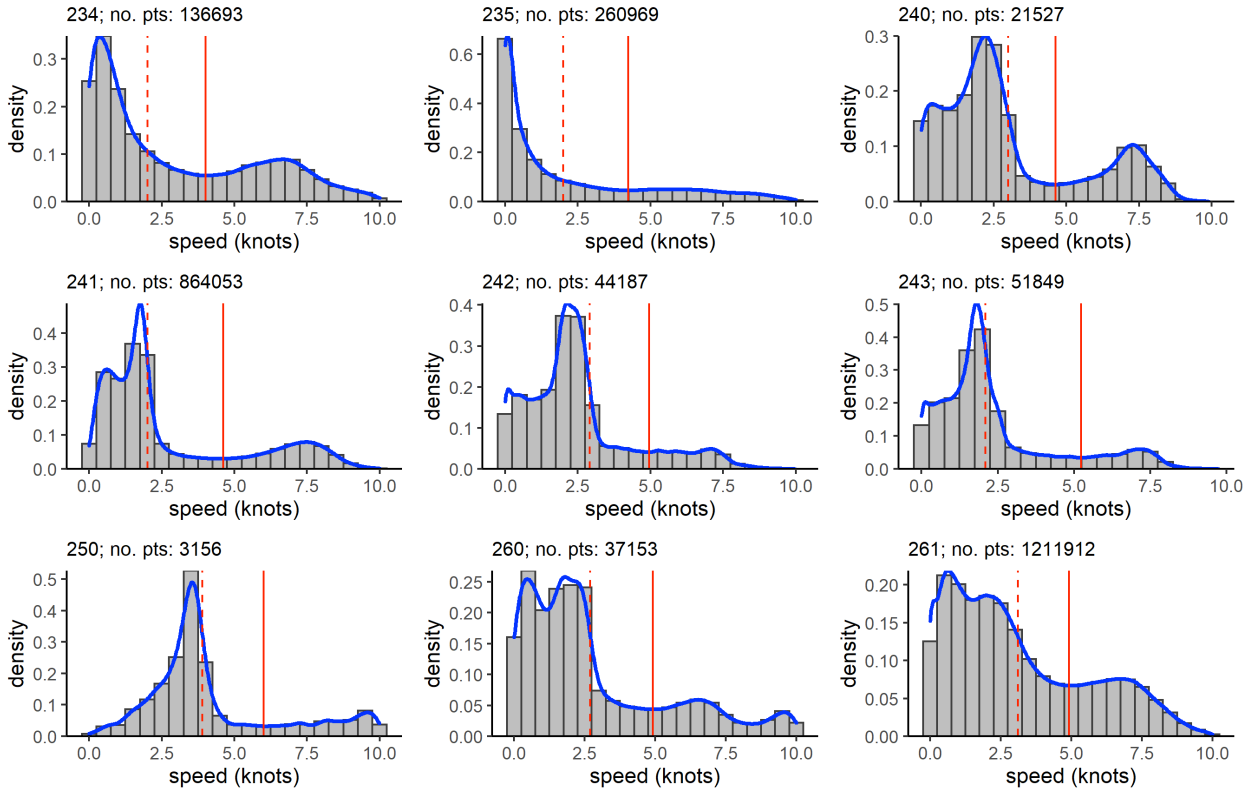

Figure D3. Distribution of vessel speed for Declaration Codes 234-261 using processed VMS data.
Note: Similar to Figure D2 but for Declaration Codes 234-261.

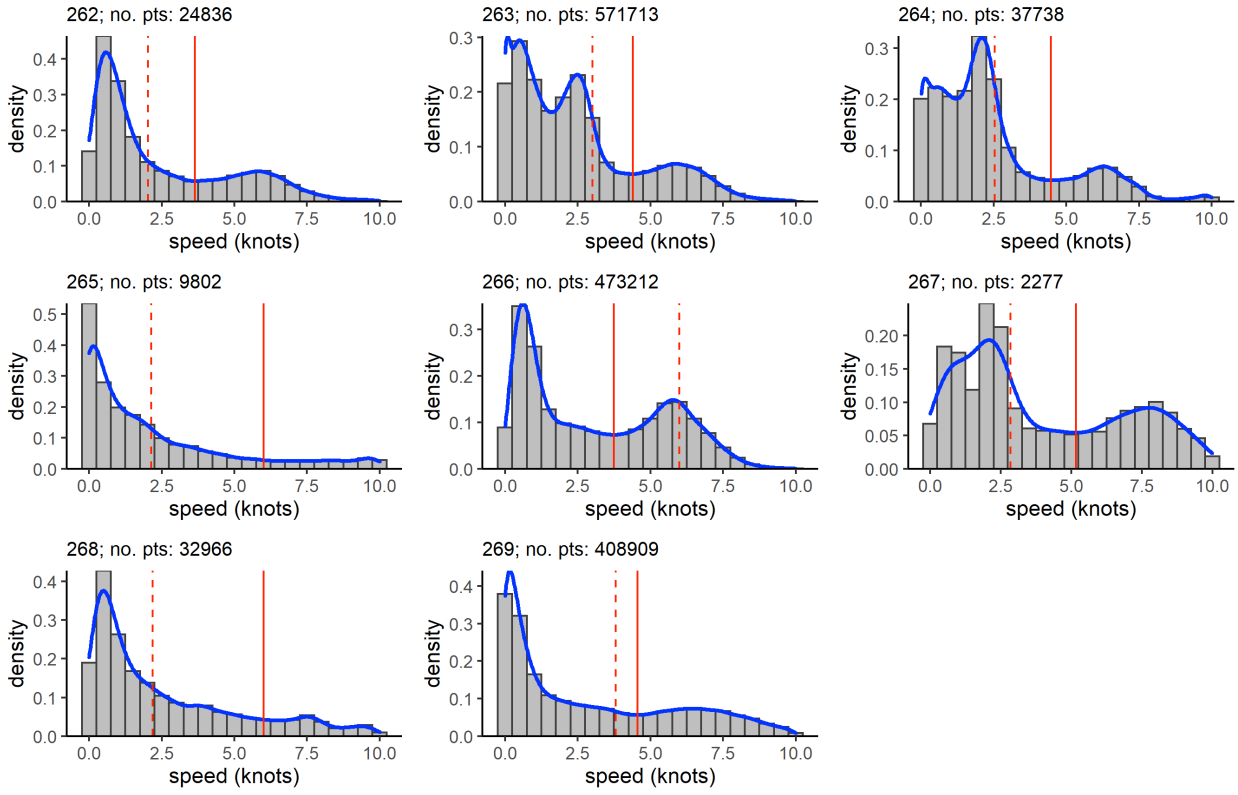

Figure D4. Distribution of vessel speed for Declaration Codes 262-269 using processed VMS data.
Note: Similar to Figure D2 but for Declaration Codes 262-269.

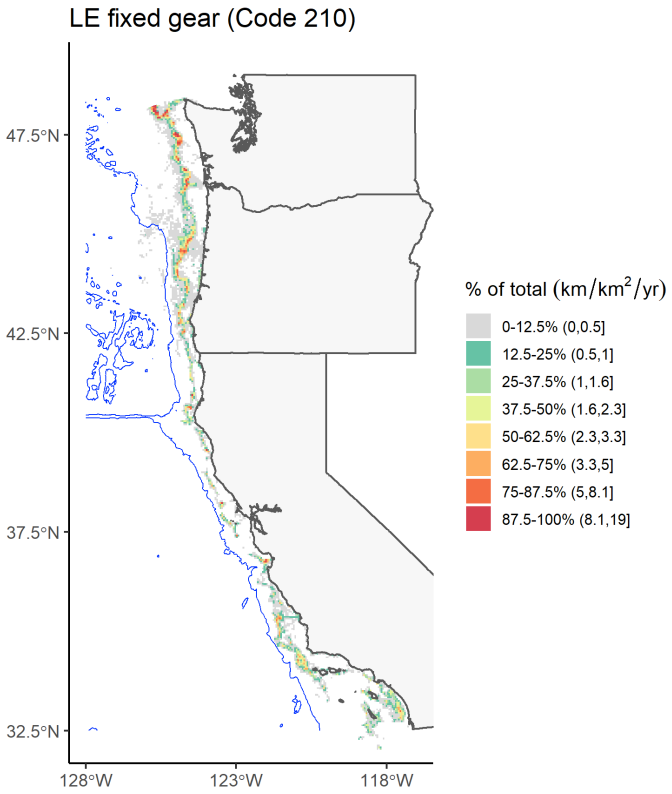

Figure D5. Annual-mean fishing effort per unit area (km fished/km^2/yr) across lease blocks for fixed limited entry (LE) fisheries not including shore-based IFQ (Declaration Code 210).
Note: The blue line is the 2700 m isobath, representing the maximum depth for all groundfish fisheries except for midwater trawl. The area outside of the biological depth limit may represent erroneous declaration codes, and only represent 2.6% of the total effort for the fishery.

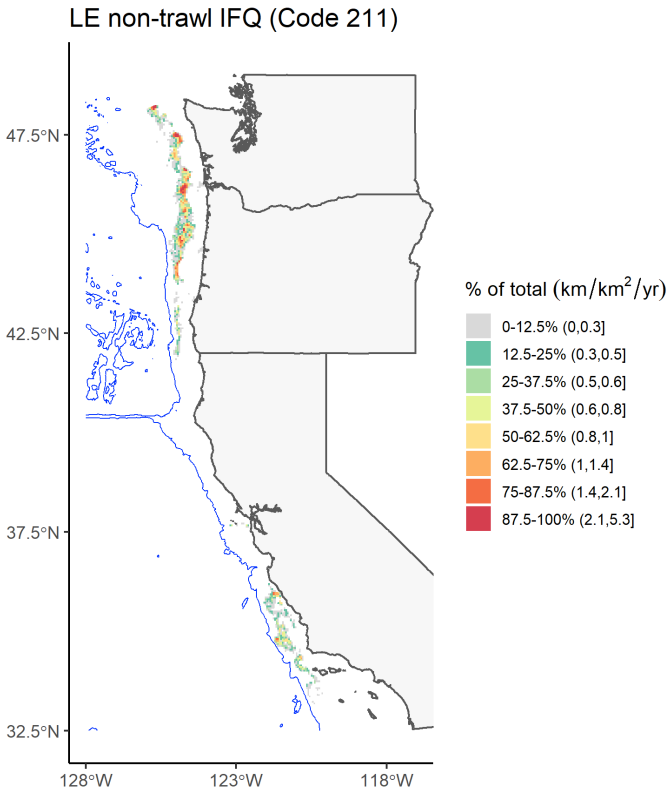

Figure D6. Annual-mean fishing effort per unit area (km fished/km²/yr) across lease blocks for limited entry groundfish non-trawl shore-based IFQ (Declaration Code 211).
Note: The area outside of the biological depth limit may represent erroneous declaration codes, and only represent 0.8% of the total effort for the fishery.

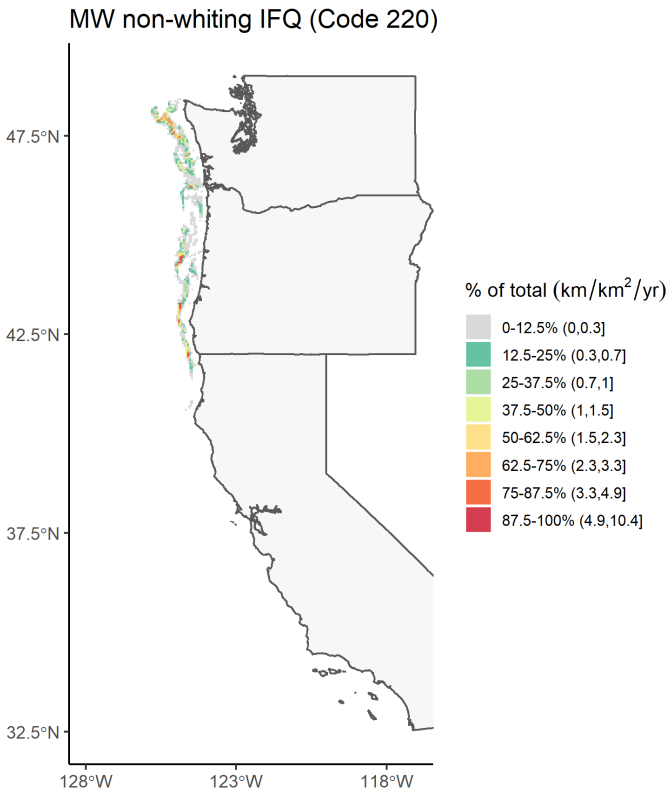

Figure D7. Annual-mean fishing effort per unit area (km fished/km^2/yr) across lease blocks for limited entry midwater trawl (MW) gear non-whiting shore-based IFQ (Declaration Code 220).
Note: An isobath line is not added since it is not applicable to the midwater trawl fishery.

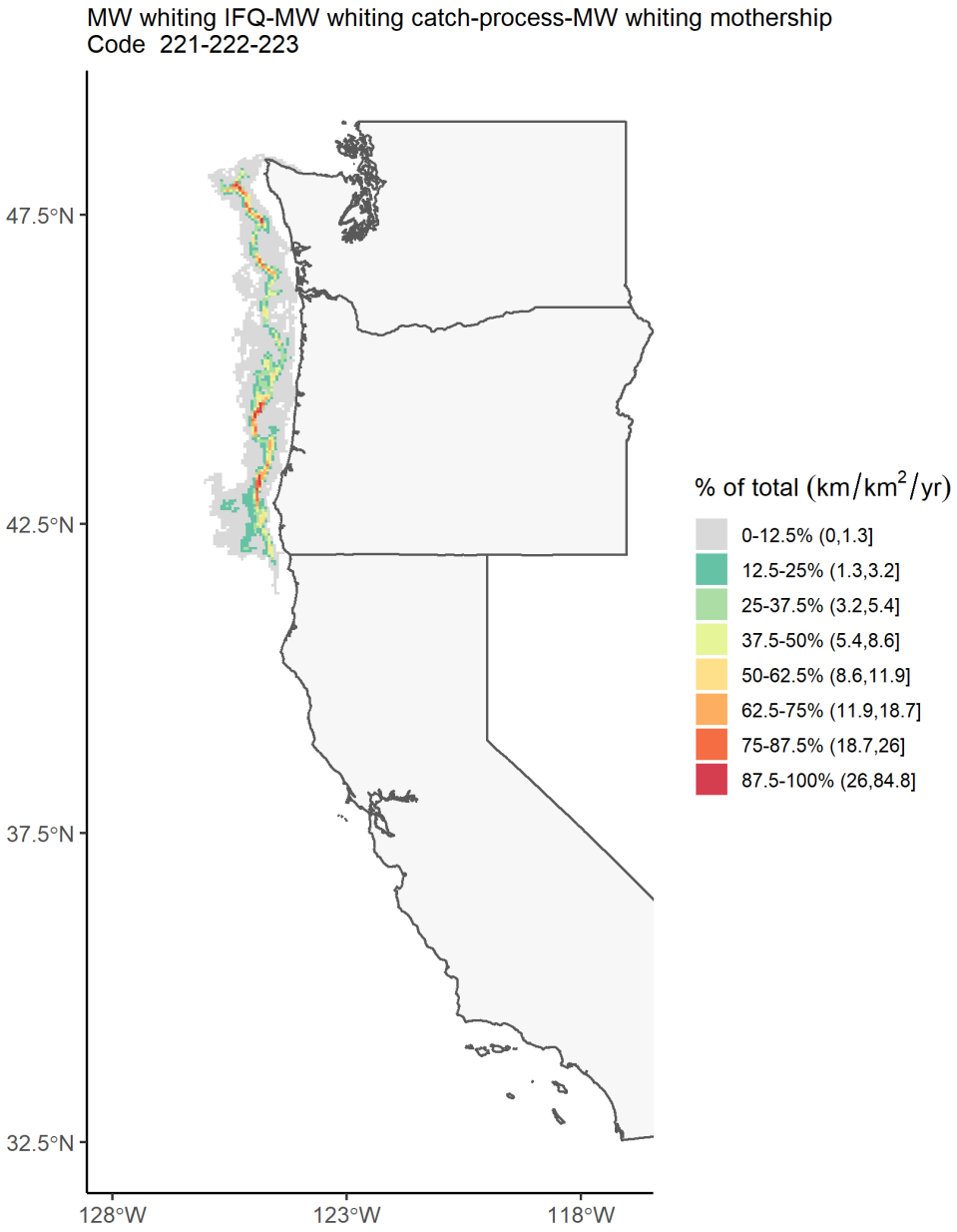

Figure D8. Annual-mean fishing effort per unit area (km fished/km^2/yr) across lease blocks for midwater trawl Pacific whiting, including whiting IFQ, whiting catcher-processor, and whiting mothership fisheries (Declaration Codes 221, 222, and 223).
Note: An isobath line is not including since depth limits are not applicable to the midwater trawl fisheries.

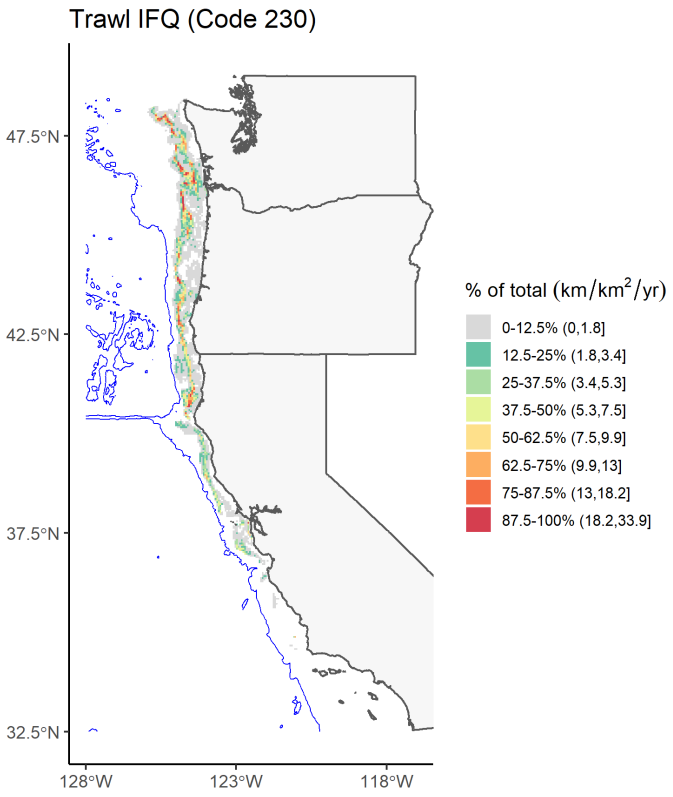

Figure D9. Annual-mean fishing effort per unit area (km fished/km^2/yr) across lease blocks for limited entry bottom trawl shore-based IFQ not including demersal trawl (Declaration Code 230).
Note: Almost all of the data (~100%) are inside the biological depth limit for the species.

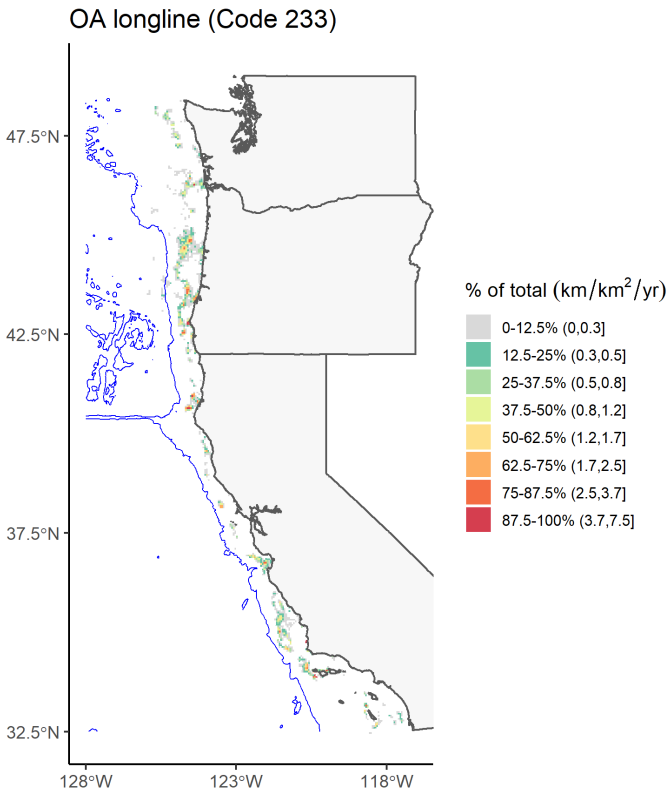

Figure D10. Annual-mean fishing effort per unit area (km fished/km^2/yr) across lease blocks for open access (OA) longline gear for groundfish (Declaration Code 233).
Note: The area outside of the biological depth limit may represent erroneous declaration codes, and only represent 2.7% of the total effort for the fishery.

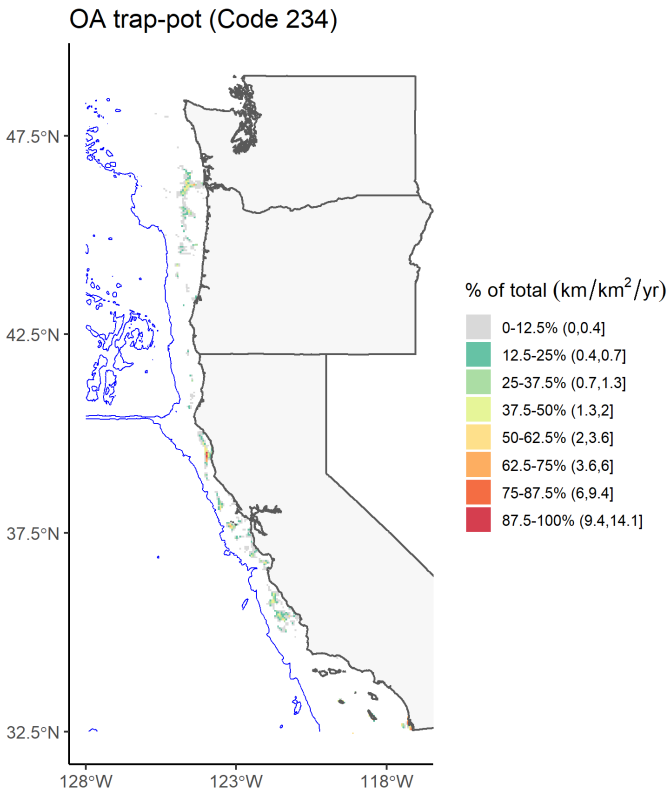

Figure D11. Annual-mean fishing effort per unit area (km fished/km²/yr) across lease blocks for open access (OA) groundfish trap or pot gear (Declaration Code 234).
Note: The area outside of the biological depth limit may represent erroneous declaration codes, and only represent 1.1% of the total effort for the fishery.

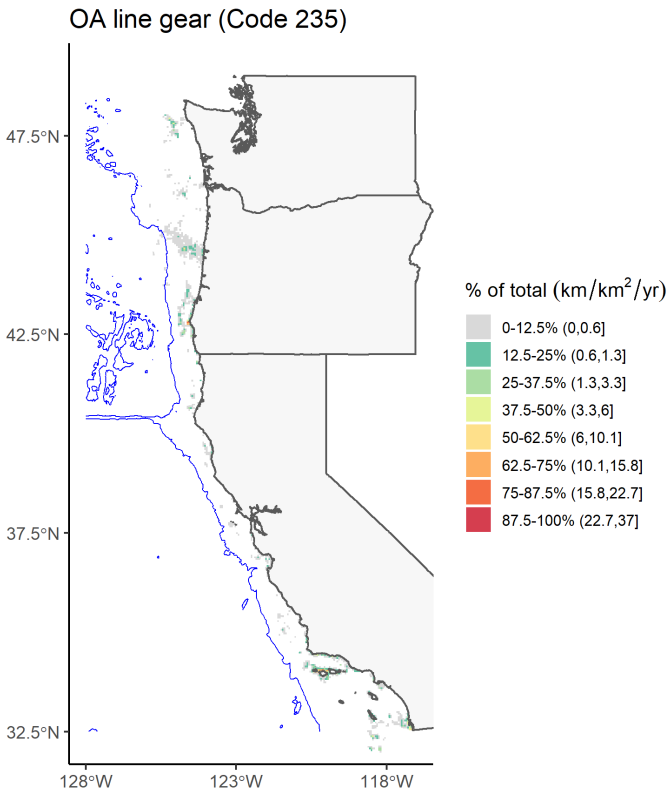

Figure D12. Annual-mean fishing effort per unit area (km fished/km^2/yr) across lease blocks for open access (OA) line gear for groundfish (Declaration Code 235).
Note: The area outside of the biological depth limit may represent erroneous declaration codes, and only represent 6% of the total effort for the fishery.

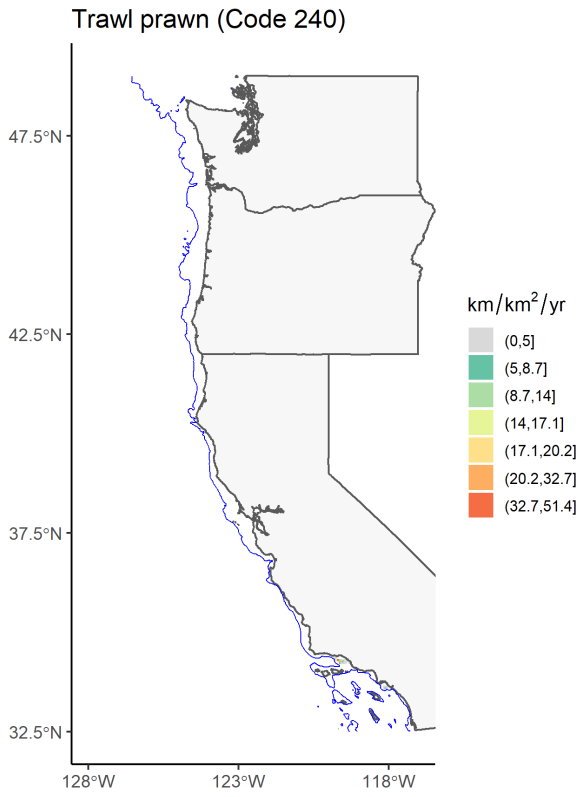

Figure D13. Annual-mean fishing effort per unit area (km fished/km^2/yr) across lease blocks for non-groundfish trawl gear for ridgeback prawn (Declaration Code 240).
Note: The blue line is the 300 m isobath, representing the maximum biological depth for the target species. The area outside of the biological depth limit may represent erroneous declaration codes, and only represent 0.4% of the total effort for the fishery. Data were too sparse to generate octiles as in the other plots.

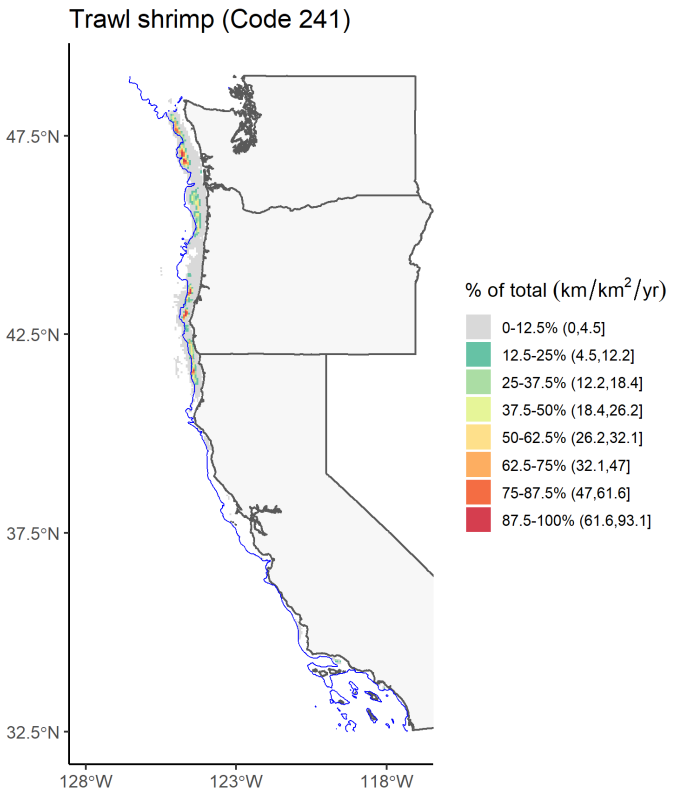

Figure D14. Annual-mean fishing effort per unit area (km fished/km^2/yr) across lease blocks for non-groundfish trawl gear for pink shrimp (Declaration Code 241).
Note: The blue line is the 300 m isobath, representing the maximum biological depth for the target species. The area outside of the biological depth limit may represent erroneous declaration codes, and only represent 1.7% of the total effort for the fishery.

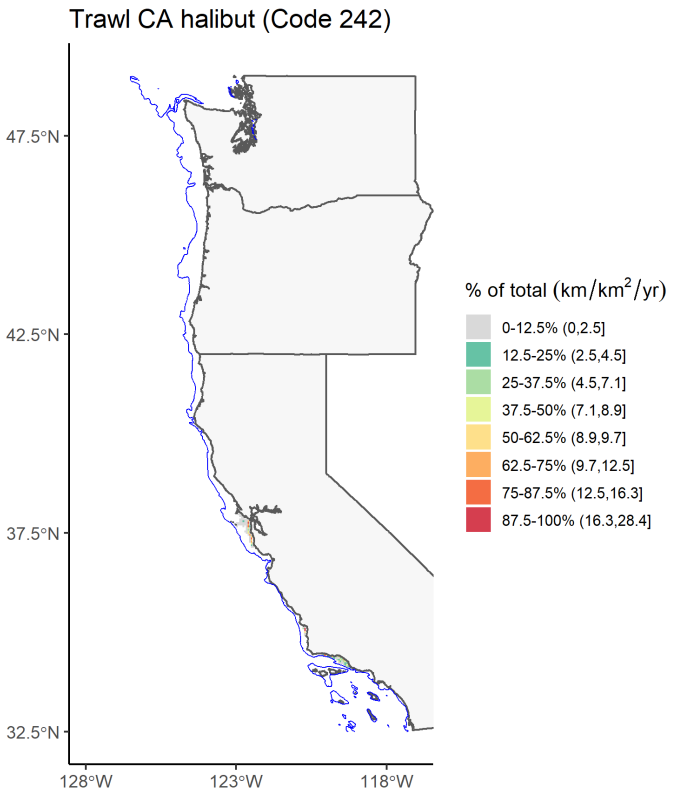

Figure D15. Annual-mean fishing effort per unit area (km fished/km^2/yr) across lease blocks for non-groundfish trawl gear for California halibut (Declaration Code 242).
Note: The blue line is the 200 m isobath, representing the maximum biological depth for the target species. The area outside of the biological depth limit may represent erroneous declaration codes, and only represent 0.4% of the total effort for the fishery.

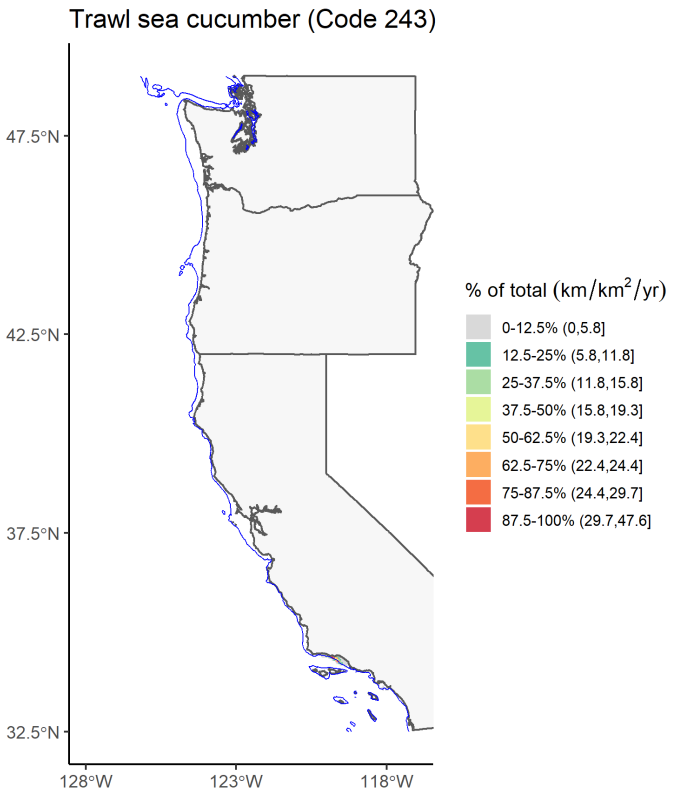

Figure D16. Annual-mean fishing effort per unit area (km fished/km²/yr) across lease blocks for non-groundfish trawl gear for sea cucumber (Declaration Code 243).
Note: The blue line is the 100 m isobath, representing the maximum biological depth for the target species. The area outside of the biological depth limit may represent erroneous declaration codes, and represent 10.3% of the total effort for the fishery.

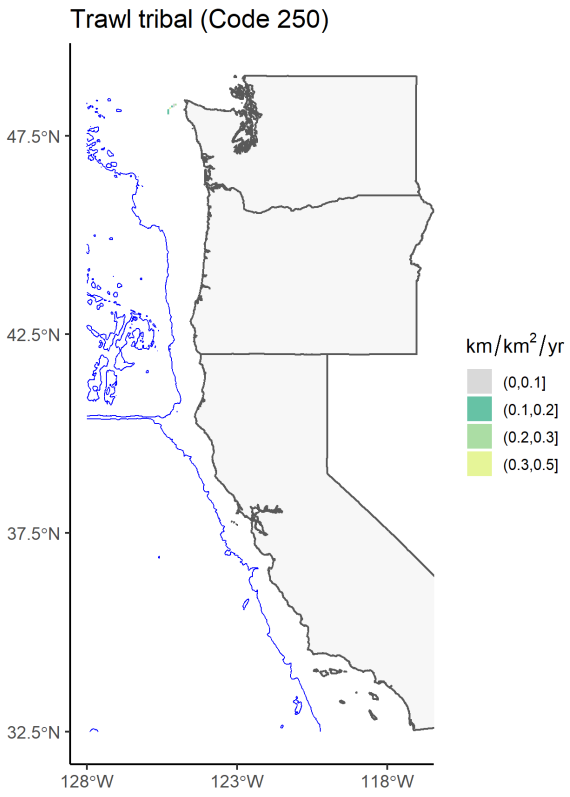

Figure D17. Annual-mean fishing effort per unit area (km fished/km^2/yr) across lease blocks for tribal trawl gear (Declaration Code 250).
Note: All of the data (100%) are inside the biological depth limit for the species. Data were too sparse to generate octiles as in the other plots.

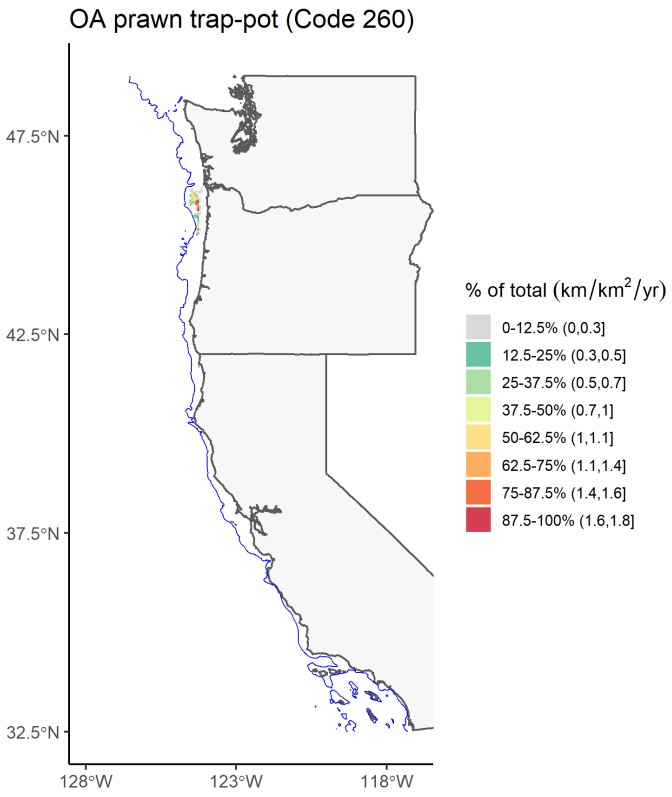

Figure D18. Annual-mean fishing effort per unit area (km fished/km^2/yr) across lease blocks for open access prawn trap or pot gear (Declaration Code 260).
Note: The blue line is the 300 m isobath, representing the maximum biological depth for the target species. The area outside of the biological depth limit may represent erroneous declaration codes, and only represent 3.2% of the total effort for the fishery.

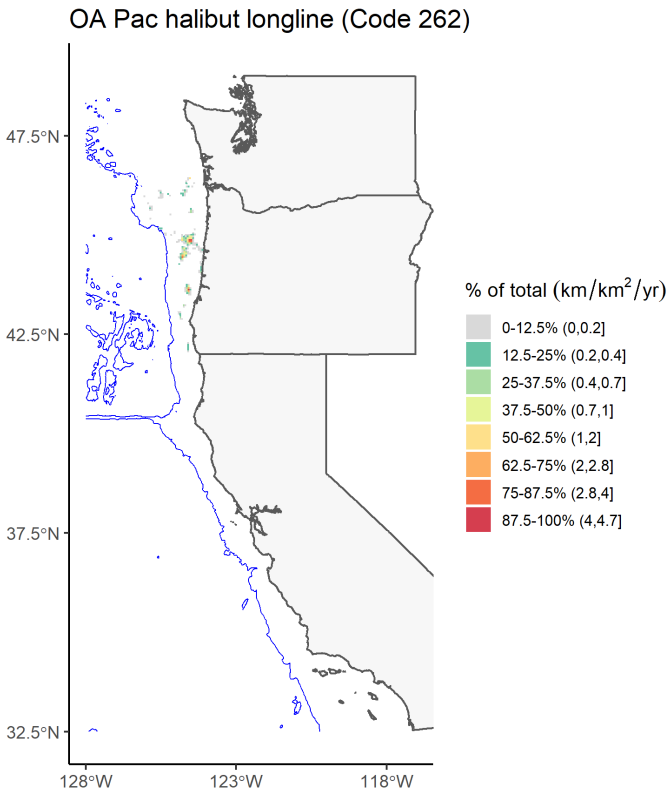

Figure D19. Annual-mean fishing effort per unit area (km fished/km²/yr) across lease blocks for open access Pacific Halibut longline gear (Declaration Code 262).
Note: The area outside of the biological depth limit may represent erroneous declaration codes and represent 4.9% of the total effort for the fishery.

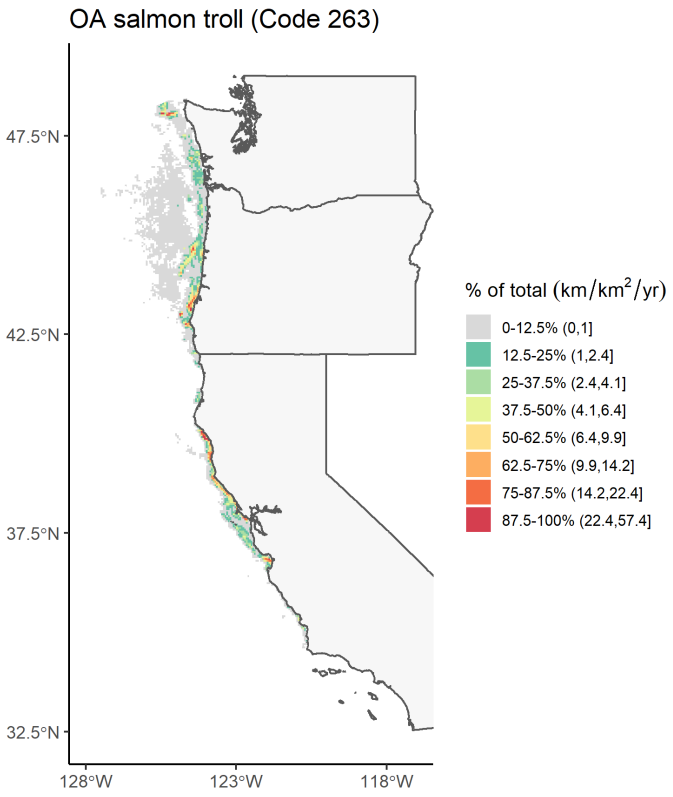

Figure D20. Annual-mean fishing effort per unit area (km fished/km²/yr) across lease blocks for open access salmon troll gear (Declaration Code 263).
Note: An isobath line is not added since it is not applicable to the salmon troll fishery.

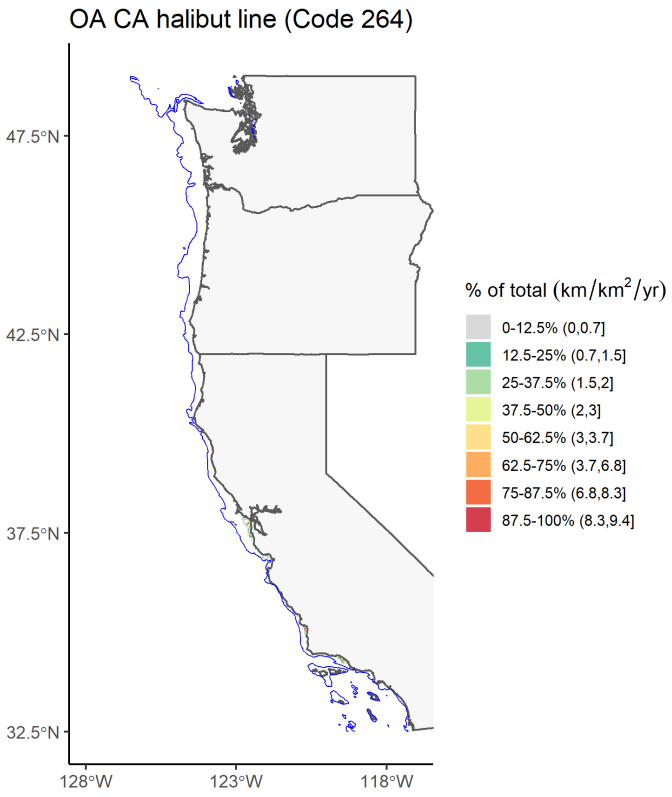

Figure D21. Annual-mean fishing effort per unit area (km fished/km²/yr) across lease blocks for open access California halibut line gear (Declaration Code 264).
Note: The blue line is the 200 m isobath, representing the maximum biological depth for the target species. The area outside of the biological depth limit may represent erroneous declaration codes, and only represent 6.3% of the total effort for the fishery.

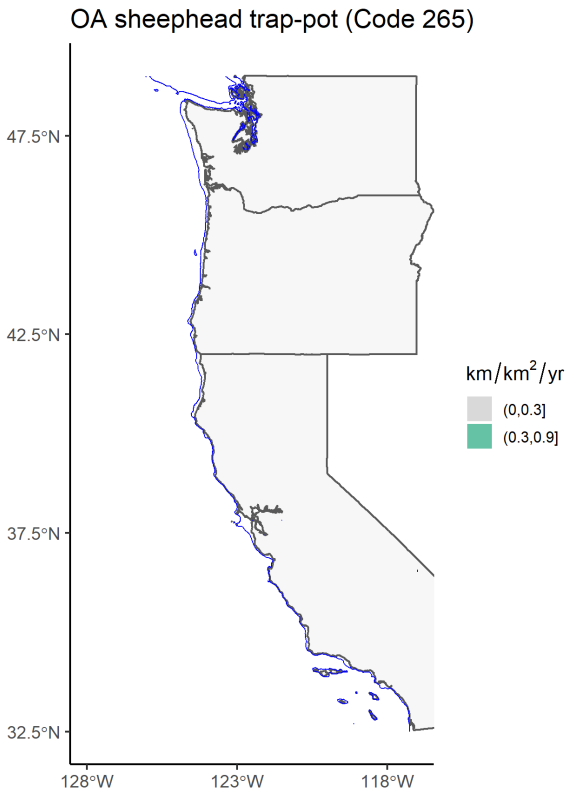

Figure D22. Annual-mean fishing effort per unit area (km fished/km^2/yr) across lease blocks open access for sheephead trap or pot gear (Declaration Code 265).
Note: The blue line is the 60 m isobath, representing the maximum biological depth for the target species. The area outside of the biological depth limit may represent erroneous declaration codes, and represent 26.2% of the total effort for the fishery. Data were too sparse to generate octiles as in the other plots.

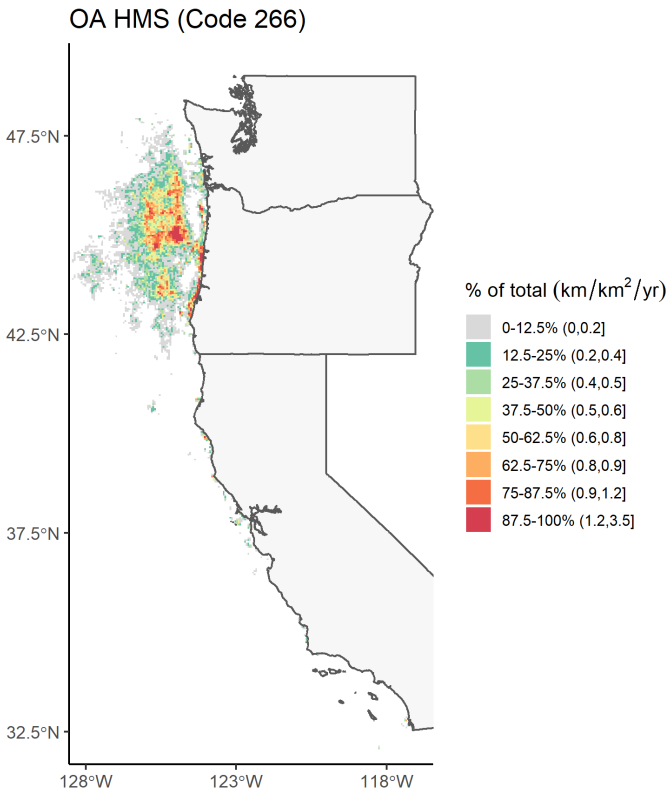

Figure D23. Annual-mean fishing effort per unit area (km fished/km²/yr) across lease blocks for open access Highly Migratory Species (HMS) line gear (Declaration Code 266).
Note: An isobath line is not added since it is not applicable to the HMS fishery.

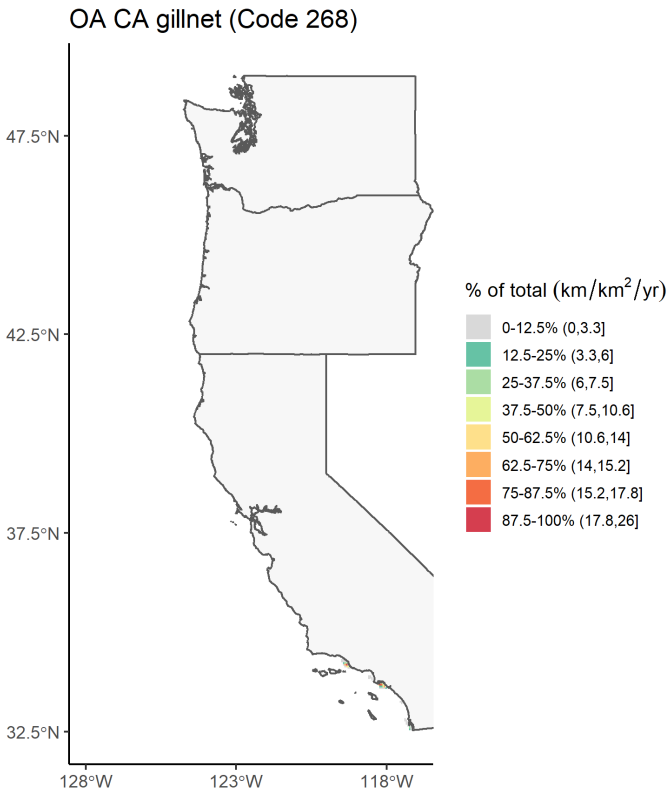

Figure D24. Annual-mean fishing effort per unit area (km fished/km²/yr) across lease blocks for open access California gillnet complex gear (Declaration Code 268).
Note: An isobath line is not added since it is not applicable to the gillnet fishery.

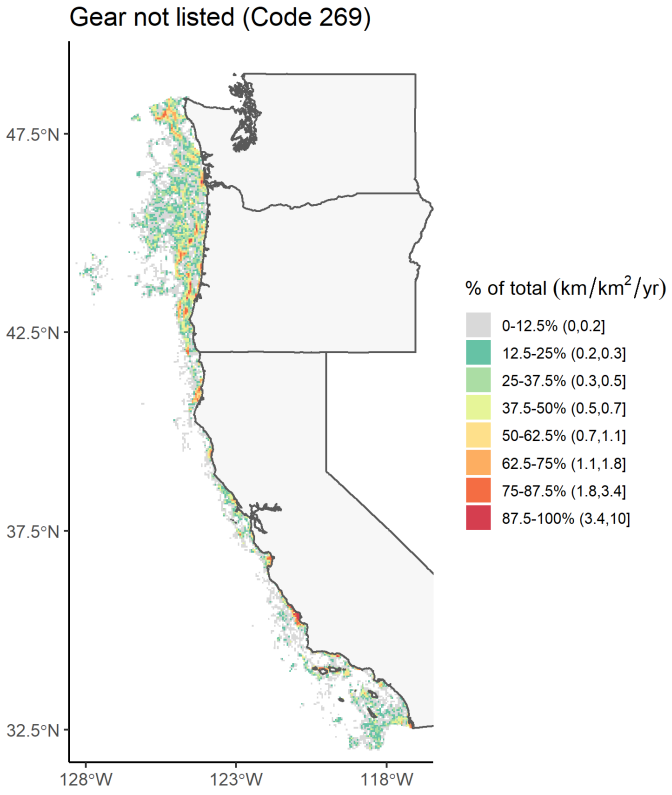

Figure D25. Annual-mean fishing effort per unit area (km fished/km²/yr) across lease blocks for gear not listed (Declaration Code 269).
Note: An isobath line is not added since it is unknown what species are captured with unlisted gear.

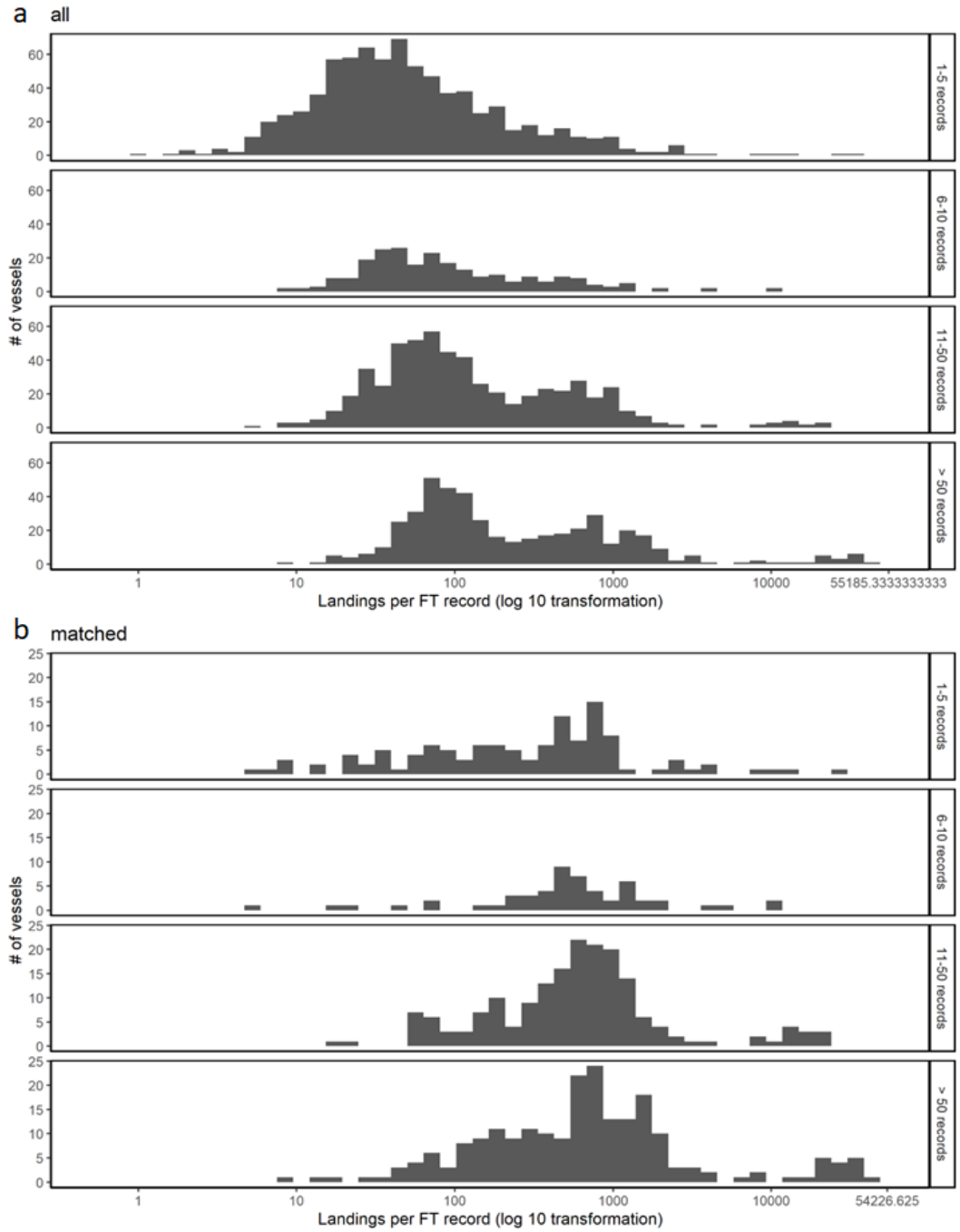

Figure D26. Frequency distribution of groundfish landings per fish ticket record for vessels with different numbers of fish ticket submission during 2010-2017.

Note: Panels from top to bottom represent vessels reporting fish total ticket records between 1 and 5, between 6 and 10, between 11 and 50, and greater than 50. (a) Total fish ticket records. (b) Fish ticket records that matched with VMS (matched). The unit of landings is pounds. Note that the vessels that reported 5 or fewer fish tickets also reported lower landings per fish ticket than those that reported > 50 fish tickets. That is, vessels that reported a relatively small number of fish tickets tended to also catch less fish per trip.

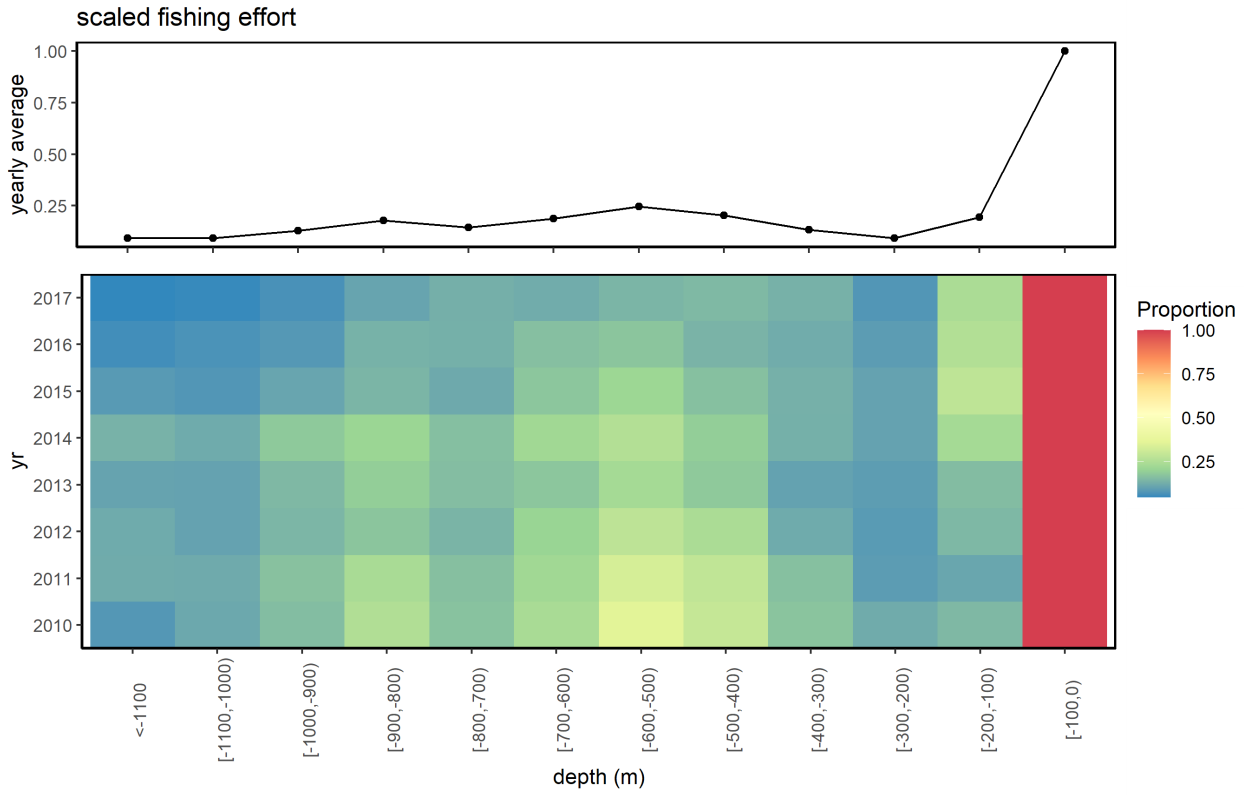

Figure D27. Fishing effort by year and depth ranges scaled by the maximum of the year based on VMS-FT data for groundfish.
Note: The top panel shows the average of the scaled fishing effort in the bottom panel over years.

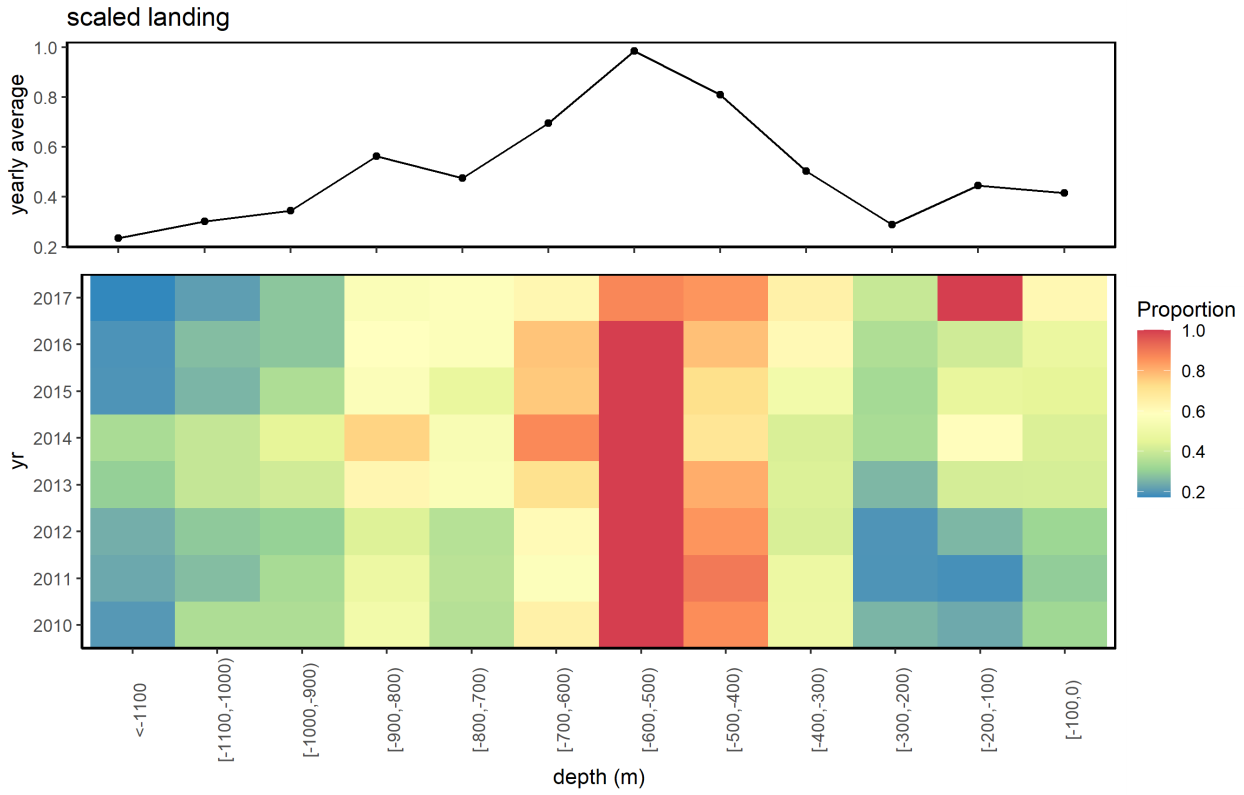

Figure D28. Landings by year and depth ranges scaled by the maximum of the year based on VMS-FT data for groundfish.

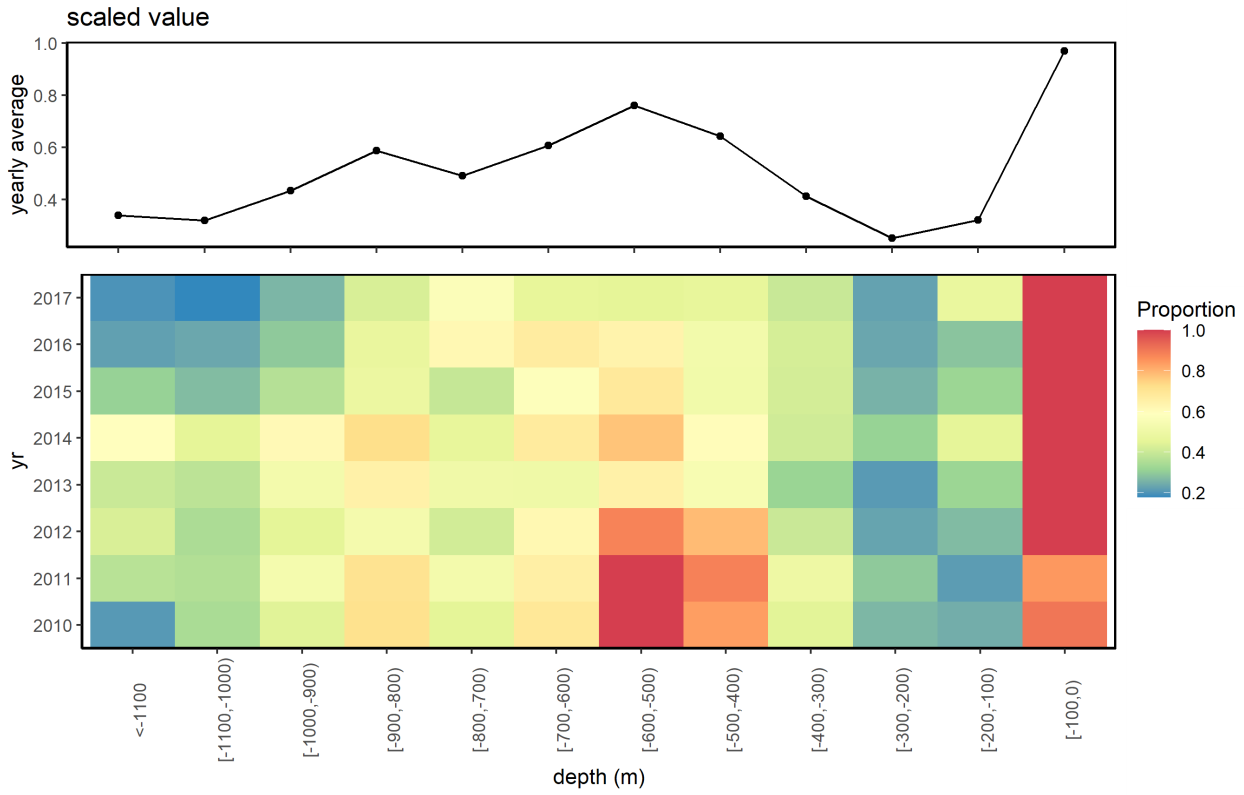

Figure D29. Ex-vessel value by year and depth ranges scaled by the maximum of the year based on VMS-FT data for groundfish.

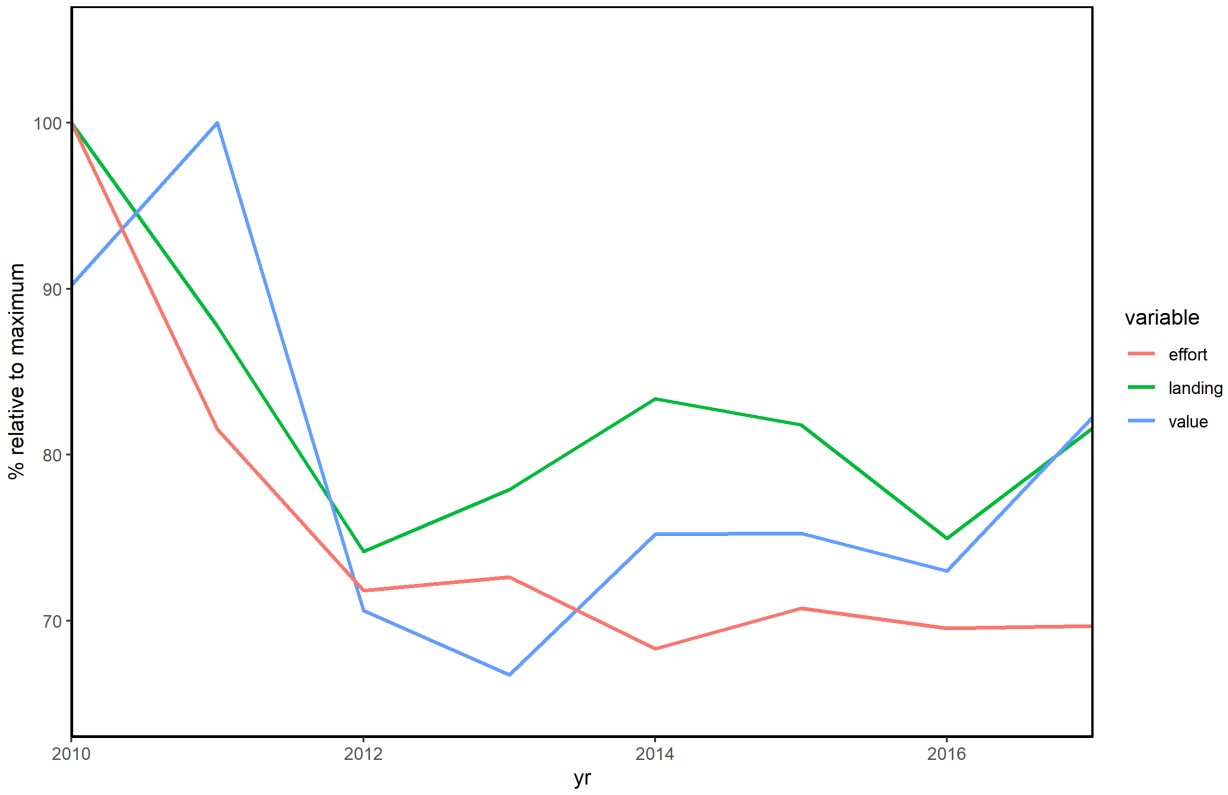

Figure D30. Annual fishing effort, landings, and ex-vessel value relative to respective maximum. Note: The maximum for effort (red) is 187.89 million km for effort in 2010. Based on VMS-FT data for groundfish, the maximum for landings (green) is 14.66 million pounds for landing in 2010. The maximum for ex-vessel value (blue) is $23.23 million in 2011.

U.S. Department of the Interior (DOI)
DOI protects and manages the Nation's natural resources and cultural heritage; provides scientific and other information about those resources; and honors the Nation's trust responsibilities or special commitments to American Indians, Alaska Natives, and affiliated island communities.

Bureau of Ocean Energy Management (BOEM)
BOEM's mission is to manage development of U.S. Outer Continental Shelf energy and mineral resources in an environmentally and economically responsible way.

BOEM Environmental Studies Program
The mission of the Environmental Studies Program is to provide the information needed to predict, assess, and manage impacts from offshore energy and marine mineral exploration, development, and production activities on human, marine, and coastal environments. The proposal, selection, research, review, collaboration, production, and dissemination of each of BOEM's Environmental Studies follows the DOI Code of Scientific and Scholarly Conduct, in support of a culture of scientific and professional integrity, as set out in the DOI Departmental Manual (305 DM 3).